RECTIFIED SOLAR WALL DEVELOPMENT

A thesis

submitted in fulfilment

of the requirements for the degree

of

Master of Engineering (Mechanical)

in the

University of Canterbury

by

A . NIMALENDRAN

Department of Mechanical Engineering

University of Canterbury

1995

CONTENTS

SUMMARY

Protection of our environment, and greater use of renewable energy are two major topics discussed throughout the world in recent years. It is imperative that every one understands the importance of leading a sustainable life-style. This project was aimed at utilising solar energy for domestic space heating.

A conceptual design of solar wall was proposed. It was suggested that the disadvantages of the Trombe wall could be largely overcome by using heat pipes as a thermal diodes between the solar energy source and the thermal mass of the wall. A computer model of such a wall was developed to predict its performance and this model was used to optimise the geometry and the materials in the design of the solar panel and the wall into which it was to be incorporated. A prototype panel of this design was manufactured and subjected to an experimental testing program.

In the first phase of the testing program the panel was heated by a hot water bath and the heat output was measured in another cold water tank. As a result of these first tests, some modifications were made to the panel which was then tested again to ensure that it would meet the design requirements.

In the second testing phase, the panel was subjected to solar radiation as the heat input, and its behaviour as a solar panel determined and compared with typical flat plate collectors.

After obtaining satisfactory results from these experiments, a prototype wall was constructed. To measure the useful space heating effect of the wall, a calorimeter box was constructed on the room side of the wall. Auxiliary equipment and instrumentation enabled monitoring of the net energy requirement of maintaining this box at the same temperature as the surrounding room. Time constraints required that the wall be tested during summer time, but the temperature distribution across the wall and the average energy output from the wall to the room was able to be obtained

under these conditions and compared with the predictions of the computer model.

From this comparison, the model was modified to match the actual results as closely as possible. The modified model then able to be used to predict the winter performance of the wall. Both quantitative and qualitative conclusions about the wall concept and its performance were able to be drawn, and some recommendations for further work made.

ACKNOWLEDGMENTS

I thank most sincerely my supervisor Dr A S Tucker for the advice and encouragement given throughout this project and finally for guidance in the thesis write-up itself.

I would also like to thank sincerely Prof. Arthur Williamson and the other staff of his company Thermocell Ltd, for their valuable suggestions throughout the project. Thermocell's prompt service towards panel manufacturing is also highly appreciated.

I thank Firth Industries Ltd for their generous financial support for the building of the prototype masonry wall. I gratefully acknowledge the help of Mr David Ashton of Firth in arranging this support.

I wish to extend my special thanks to Ron Tinker and Eric Cox for their willing support in constructing the experimental set-up and for the continuous help during the entire experimental work. Their valuable support during the solar wall construction are also much appreciated. I would also wish to thank Phillip Smith and Julian Murphy for their support from computer lab.

I wish to thank all work shop staff Otto Bolt, Ken Brown, and Scott Amies for their valuable support for manufacturing panels and parts for the experimental set-up. I thank Geoff Leathwick for his support from the stores and Bruce Sparks for his support during photographing the experimental set-up.

In general I would like to thank all Mechanical Engineering staff and fellow post-graduate students for their support during my stay in University.

Finally I would like to thank my wife for her full support and encouragement to finish up this project. I would also like to thank my little son for letting me work extra hours at nights during this period.

LIST OF SYMBOLS

Symbol	Description	Units
A	Cross-sectional area	m^2
B_i	Biot number	[0]
c	Specific heat	kJ/kg K
e	Energy stored	J
f	Fraction of the area occupied by the thermal bridge	[0]
F_o	Fourier number	[0]
F_R	Collector heat removal efficiency factor	[0]
h_c	Convective heat transfer coefficient	W/m^2 K
h_r	Radiative heat transfer coefficient	W/m^2 K
i	Angle of incidence of a solar radiation	degrees
I, I_T	Solar intensity	W/m^2
k	Thermal conductivity	W/m K
m	Mass flow rate	kg/s
Q, q	Heat flow rate	W
R_1,R_2	Thermal resistance of the other materials	m^2 K/W
R_L	Thermal resistance of the bridging material	m^2 K/W
T	Temperature	K
t	Temperature in	°C
U_L	Collector overall energy loss coefficient	W/m^2 °C
u_o	Internal energy	J
w	Work done	J
α	Thermal diffusivity (Chapter 2)	m^2/s
α	Absorptivity (Chapter 6,7 and Appendix A)	[0]
Δt	Temperature difference	K or °C
η	Efficiency	[0]
ρ	Mass density	kg/m^3
τ	Time	sec
τ_g	Transmissivity of glass	[0]

More list of symbols are presented in Appendix B.

LIST OF TABLES

LIST OF FIGURES

CHAPTER 1

1. INTRODUCTION

1.1 ENERGY

Energy flows constantly into and out of the earth's surface environment. As a result the material constituents of the earth's surface area are in a state of continuous or intermittent circulation. The energy available in the earth may be classified under two major categories:

1. Renewable energy : Solar, Wind, Tidal, Hydro energy etc.
2. Non-renewable energy : Fossil fuels and Nuclear energy.

Renewable energy sources were the first and until very recently on the human time scale, the only forms of energy used by humanity. With the start of the Industrial Revolution in the late eighteenth century, and the other technological advances, renewable resources began to be replaced by non-renewable resources, primarily in the form of coal. With the development of the internal combustion engine and the birth of the petrochemical industry in the late-nineteenth and into the twentieth century, there was a rapid growth in the demand for other non-renewable energy sources. Non-renewable energy is now the dominant energy supplier in the world. In 1990 the total amount of energy consumed worldwide from non-renewable energy sources was equivalent to the energy released from burning about 7.5 billion metric tons of oil (Golob and Brus - 1993). The limited resources of fossil fuel and its environmental damage, and the danger of using nuclear energy are now considered as serious issues by many countries. Some industrialised countries have embarked on ambitious programs to develop or improve renewable energy technologies and increase energy efficiency. Some others have largely ignored world-wide opposition to nuclear energy sources and launched large nuclear power programs: In 1990, France produced 75% of its electricity from nuclear power plant (Golob and Brus - 1993). New Zealand is unusual in comparison with most industrialised countries in that about 77% (ECNZ -1993) of its electrical generation is derived from renewable resources (dominantly hydro).

When we look for alternative sources of energy, the most logical first place to look is above us, at the sun. The sun is a small star in our galaxy, which produces energy by fusion reaction. It is estimated that the power radiated by the sun is 3.8×10^{26} W, of which about 1.7×10^{17} W is intercepted by earth (Kreith and Black - 1980). In one year this represents more than 16,000 times the total amount of energy used annually by all people on the planet (Golob and Brus - 1993). Out of this, New Zealand intercepts around 1.39×10^{21}J (4.21×10^{13} W) in one year with the average intensity of 14.1 MJ/m^2/day (Baines 1993).

However, this huge amount of solar energy available in the earth is not in a concentrated form like most other energy sources. The energy is everywhere in a 'diffused' form at the maximum intensity of about 1 kW/m^2. So that collecting and concentrating this energy on to a smaller area is necessary for high temperature applications. So far, this has been achieved world wide in only a few solar-thermal applications. In Daggett California USA the biggest solar-thermal plant "Solar one" produces 10 MW of power, and its central receiver receives solar energy from many reflectors to heat the steam to a 515°C (Golob and Brus -1993). In general, for day to day high temperature industrial applications, it is very difficult to concentrate this diluted solar heat. However, solar energy in its available dilute form could be very effectively used for any low temperature requirements (eg. water heating and space heating), provided appropriate thermal storage to overcome the intermittent nature of solar energy.

Solar energy equipment was very expensive in the earlier stages of its development but technological development has helped a lot to cut down the cost of solar installations to be almost equivalent with other sources of energy in some applications. For instance, the cost of photovoltaic cells has declined more than 95 percent since the early 1970's (Golob and Brus - 1993), opening up a variety of specialised commercial applications particularly in remote, low power applications and low powered electronic items. Solar-thermal electricity cost dropped from US$ 0.60 per kilowatt hour in 1983 to US$ 0.06-US$ 0.10 per kilowatt hour in 1990 (Kaneff - 1990). The interest in solar energy is growing all over the world, as increasingly it is seen as a means towards ensuring a sustainable future.

1.2 DOMESTIC SPACE HEATING

The energy base for space heating of buildings has traditionally been electricity and fossil fuels. The U.S. Department of energy estimates that USA use about twenty nine quads (30.56 EJ) of energy (36% of total primary energy consumption) each year to heat, cool, light and ventilate buildings at a cost of approximately US$ 200 billion (Carless - 1993). In New Zealand it has been noted that 37% of the national electric energy is used in domestic houses (Department of statistics - 1993). Of this about 40% is used for water heating, about 35% is used for space heating, and the balance of 25% is used for lighting and other applications (Breuer -1988). In New Zealand the space heating energy consumption varies from place to place, the north of the country consuming less energy while further south more energy is consumed for the same purpose. Furthermore the consumption depends on whether the house is insulated (NZS 4218P - 1977) or not. On average, in the Wellington climatic zone, an uninsulated house consumes about 3660 kWh/annum (32% of the total house hold energy use) while an insulated house consumes 2450 kWh/annum (21%) (Wright and Baines - 1986).

Electricity is the dominant energy source for domestic space heating in New Zealand, but considerable quantities of non-renewable energy resources (natural gas, coal and oil) are also consumed directly for this purpose (Watson and Noble - 1986). Wood is also extensively used for space heating and, although renewable in principle, it contributes net CO_2 emissions unless equivalent replacement forestation is undertaken. Wood does contribute other undesirable pollutants. It should be noted again that of New Zealand's electricity production, 23% is from non-renewable resources. So indirectly, electrical space heating is also partly a consumer of non-renewable energy.

The average standard comfortable temperature for a human body is considered as $\approx$20°C (Leslie - 1976) (it also depends on some other physical parameters like humidity, mean radiant temperature etc). However, a survey of New Zealand households suggest that houses are heated to a very low temperature ranging from 13.7°C to 16.3°C for economical reasons (Breuer -1988).

1.3 SOLAR ENERGY FOR SPACE HEATING

New Zealand interests in solar energy began as early as 1957 when Benseman conducted a series of studies in the course of assessing its potential utilisation in New Zealand. As a result of these studies, he established that both solar water and space heating are technically feasible throughout the country (Ward 1974). The importance of using solar energy in both of these applications is recognised throughout the world now and growing in public interest.

Solar space heating methods are normally classified under two categories :

1. Passive solar heating

   Passive solar design reduces the energy requirements of a building by meeting all or part of its daily heating needs with solar energy. The term "passive solar" refers to systems that absorb, store, and distribute the solar energy without relying on devices, such as pumps and fans, that require additional energy. Many passive solar heating systems make use of glass to transmit a required part of the solar energy. In passive solar buildings, incoming solar energy is typically stored in a thermal mass, such as a large amount of concrete, brick, rock, water, or a material that changes phases as the temperature changes. The three most common passive solar heating designs for homes are direct-gain, indirect-gain, and isolated gain systems. In a direct-gain system, sunlight passes directly through windows into the living space and is absorbed by the floor and walls. In an indirect-gain system a heat storage medium, such as wall, in one part of the building is used to absorb and store the heat. In an isolated-gain system, solar energy is absorbed and stored in a separate area, such as greenhouse or solarium, and then distributed to the living area through ducts. Nevertheless, passive solar systems are rarely sufficient to meet all of building's energy requirements so that some type of back-up heating system is required to maintain comfort conditions.

2. Active solar heating

   In active systems, solar collectors are used to convert the sun's energy into useful heat for hot water, space heating, or industrial processes. Flat plate collectors are

most often used to gather the sun's energy. The hot fluid is either used immediately for heating or stored for later use. Externally powered equipment, such as a fan or pump, is typically used to move the fluid and some form of control system must be provided to activate the fan or pump when appropriate.

Maintaining the low temperature of ≈20°C in the room is achievable by proper selection of solar heating methods. However, with present costing it may require governmental or other encouragement for this type of development to using freely available solar energy to achieve comfortable living conditions. This is because most of solar heating developments so far, have involved high capital cost (but very low or no running cost). The main emphasis in worldwide solar research is to reduce this initial capital cost to a minimum and make it affordable in comparison with traditional space heating installations.

A reduction in the use of fossil fuels for space heating would help to protect our environment. Recent International Energy Agency statistics shows that New Zealand is lagging behind the rest of the developed world in its efforts to cut greenhouse gas emissions. New Zealand's production of carbon dioxide is expected to grow 15.5% between 1990 and 2000, leaving it second only to Australia (16%), while other OECD countries showing reasonable improvement in their part (USA 2.7%, EC 2.5% and Japan 2.3%) and only Switzerland is on line to meet the target (Christchurch Press -14/3/1995).

Electrical energy saved by adopting the wide use of solar energy for space heating could be diverted to other industrial purposes where solar energy can not meet the requirements. In this way the need to construct new power stations could be delayed or postponed indefinitely.

1.3.1 Trombe wall

Professor Felix Trombe built his first prototype passive solar heating house in France in 1956 (Anderson and Riorder - 1976). Its south side (being in the Northern Hemisphere) was a 300 mm thick concrete wall, painted black and covered in front with a single pane of glass as shown in Fig 1.1. Solar heat was collected and distributed to the rooms without

using any pumps, fans, or blowers. Sunlight penetrating the glass was absorbed in the blackened wall, heating both the concrete and the air in the gap between glass and concrete. This heated air would expand, becoming lighter, rise, and flow through the top ducts into the rooms while the cooler return air passed through the bottom ducts. Such a process of gravity convection or thermosyphoning, carried most of the absorbed solar energy into the house during the day. The rest of the heat migrated through the concrete, with the time delay of 6 to 8 hours. At night, the interior was warmed by thermal radiation from the inner surface.

A disadvantage of this arrangement, however, is that much of the heat which enters the wall is lost through the glass during day and night. There is no simple, effective, and inexpensive way to interpose, between the wall and the glass, a thick insulation layer that will stop heat loss at least during night time, but some devices have been proposed and trialed. One such development was the "Beadwall" system in which polystyrene beads were blown in between the glass and the wall and left there as an insulation during night time. The beads were sucked back in the morning and stored in a storage box. A disadvantage was that because of the static charges between the beads and the glass, some of the beads stuck to the glass during day time, reducing the transmissivity of the glass. Furthermore, the box and blower unit utilised valuable floor space in the room.

A new technology recently developed in insulating materials is "Transparent Insulation (TI)" (Baker and dijk - 1994), which can transfer solar radiation very effectively. TI has a low thermal conductivity which minimises any heat losses by conduction but has good transmissivity to incident solar radiation. TI could be used with a Trombe wall to overcome its main disadvantage of losing heat to the outside during day and night. Presently TI is still in its teething stage of development and economically it is very expensive for wide application.

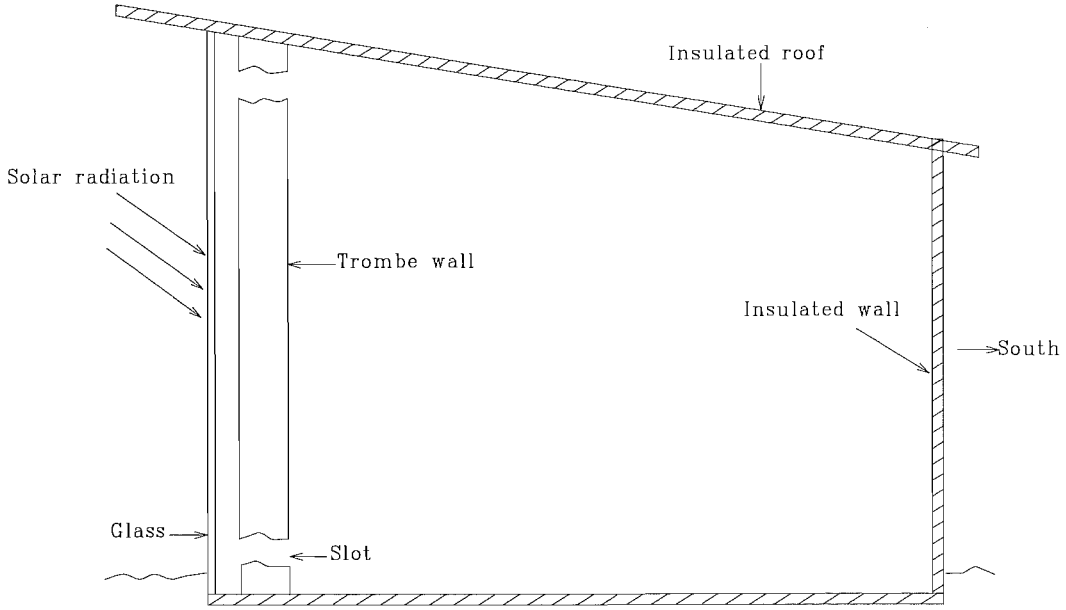

Figure 1.1 Vertical cross section of a Trombe wall

1.4 HEAT PIPE PRINCIPLES AND APPLICATIONS

A heat pipe is a very simple device of very high thermal conductivity, that can transfer large quantities of heat through a small cross-sectional area to another location. The idea of the heat pipe was first suggested by R.S.Gauger of the General Motors Corporation Ohio, USA in 1942 and patented from June 1944. It was not, however, until its independent invention by G.M.Grover in the early 1960's that the remarkable properties of the heat pipe became appreciated and serious development work took place (Dunn and Reay -1994).

The method of operation of a fundamental heat pipe is shown schematically in Fig 1.2. The device consists of a pipe, usually circular in section, with an annular layer of wicking material covering the inside. The core of the system is hollow in the center to permit the working fluid to pass freely from the heat addition end (*evaporator*) to the heat rejection end (*Condenser*). The condenser and the evaporator are connected by an insulated section. The liquid permeates the wicking material by capillary action and when heat is added to the evaporator end of the heat pipe, liquid is vaporised in the wick and moves through central core to the condenser end where heat is removed. Then the vapour condenses back into the wick and the cycle repeats. There are many different working fluids and wick

materials used for different applications. In recent years it is widely used in nuclear power plants to transfer heat between emitters and collectors at very high temperature of 1600°C -1800°C, and in heat pipe heat exchangers (Dunn and Reay -1994). At the other extreme, very small heat pipes are marketed for inserting into roasts of meat to ensure more uniform cooking throughout the meat volume.

In another development by NASA, a rotating heat pipe in which the wick is omitted utilises centrifugal acceleration to transfer liquid from the condenser to the evaporator and can be used for cooling motor rotors and turbine blade rotors (Dunn and Reay -1994). As another development if a wick-less heat pipe is tilted to a near vertical angle with the condenser on top, then gravity would transfer the condensed fluid back to the evaporator. Such a system still very effectively transfers the heat from the evaporator to the condenser but because gravity is returning the condensed fluid, the heat pipe will transfer the heat only when the evaporator is below the condenser (Fig 1.3a). In the opposite direction heat can only flow through the pipe by conduction (Fig 1.3b), and since this amount is negligible, a heat pipe of this type acts as a very effective thermal diode.

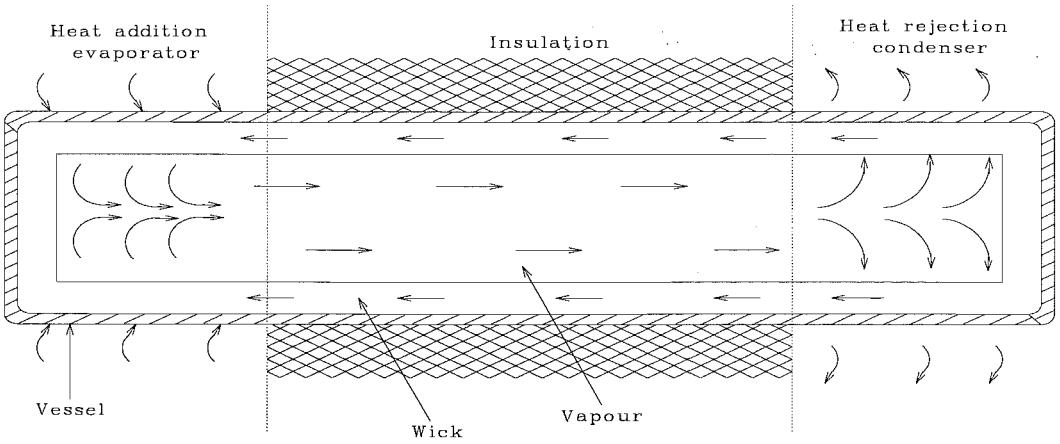

Figure 1.2 Schematic diagram of a wicked heat pipe capable of bi-directional heat flow.

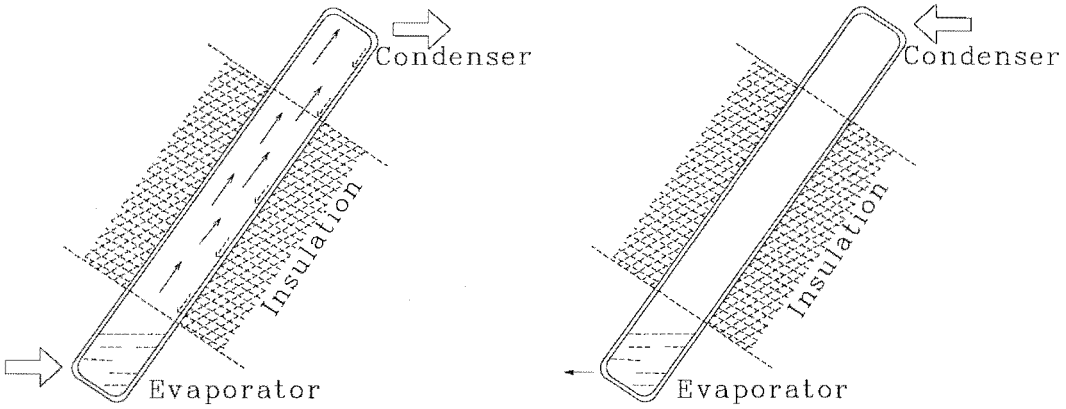

Fig 1.3 Gravitational heat pipe acting as a thermal diode.

1.4.1 'Thermocell Heatsheet'

Thermocell New Zealand Ltd a Christchurch-based company, patented the idea of using heat pipes to make in a unique design of water heating solar panel marketed under the tradename of "Heatsheet". They used the same principle of a gravitational heat pipe tilted to an angle to let the condensed fluid flow back from evaporator to the condenser. In effect the "Heatsheet" is a 2-dimensional form of heat pipe in which the evaporator section is effectively flattened so as to present a large, almost isothermal, solar collection area. Solar energy is absorbed over about 80% of the panel area (evaporator) and the collected energy removed over the remaining 20% panel area (condenser). The back side of the area is traversed by a 3-pass copper tube through which cold water passes. The heat gained by the water in the condenser is passed on into the hot water cylinder via a pumped circuit. The organic working fluid inside the "Heatsheet" having lost heat in the condenser, flows back as condensed liquid to the evaporator by gravity. This design gives the same performance as the best copper tube and plate collectors but at a fraction of the material cost since all of the "Heatsheet" is made out of steel except for the copper water circuit.

1.4.2 Conceptual design of a proposed panel

The "Heatsheet" concept of collecting solar energy and effectively transferring it into another region was considered as a very useful way of overcoming the main disadvantage

of the Trombe wall explained in Section 1.3.1. This idea was first suggested as a conceptual design of a vacuum panel heat exchanger (VPHE) by Robert K. Prudhoe of Australia as shown on Fig 1.4 (Prudhoe - 1991). However, there was not any detailed design and method for practically implementing the concept were not suggested.

Fundamentally the panel proposed for the present experimental investigation is also an off-set VPHE, but instead of locating the condenser directly in the room, the condenser was to be placed inside a masonry wall to achieve the additional requirement of storing energy. The front of the panel which collects solar radiation is called the *evaporator* and the other one releasing heat into the wall is called the *condenser*. Part of the space between those two planes would require insulation to minimise the heat losses to outside and to traverse this gap the evaporator and the condenser would require connection by an angled tube to ensure free gravity flow of the working fluid. The conceptual design of the proposed panel fixed in the solar wall is shown in Fig 1.5.

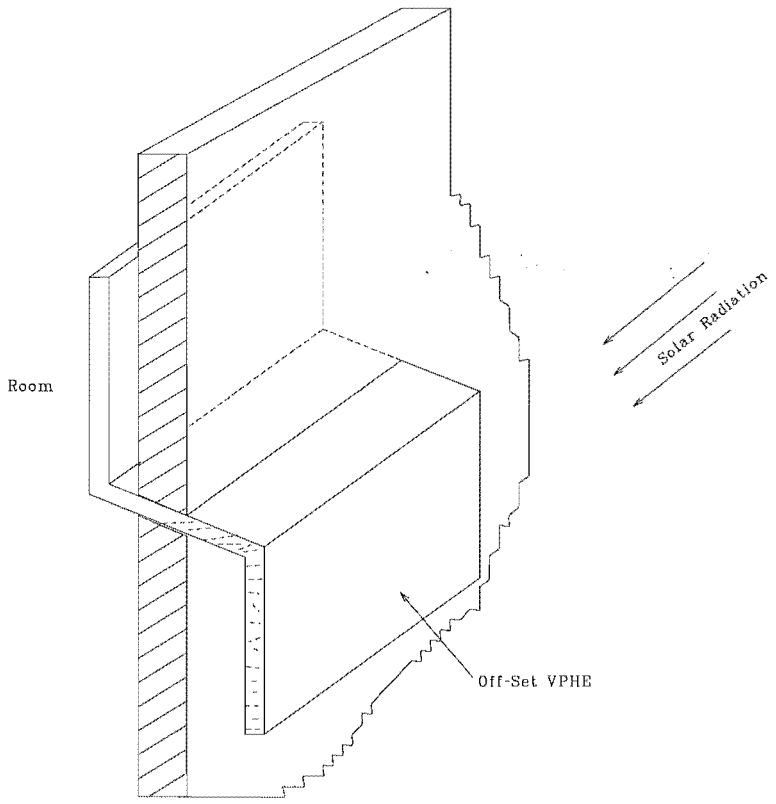

Figure 1.4 Conceptual design of the VPHE.

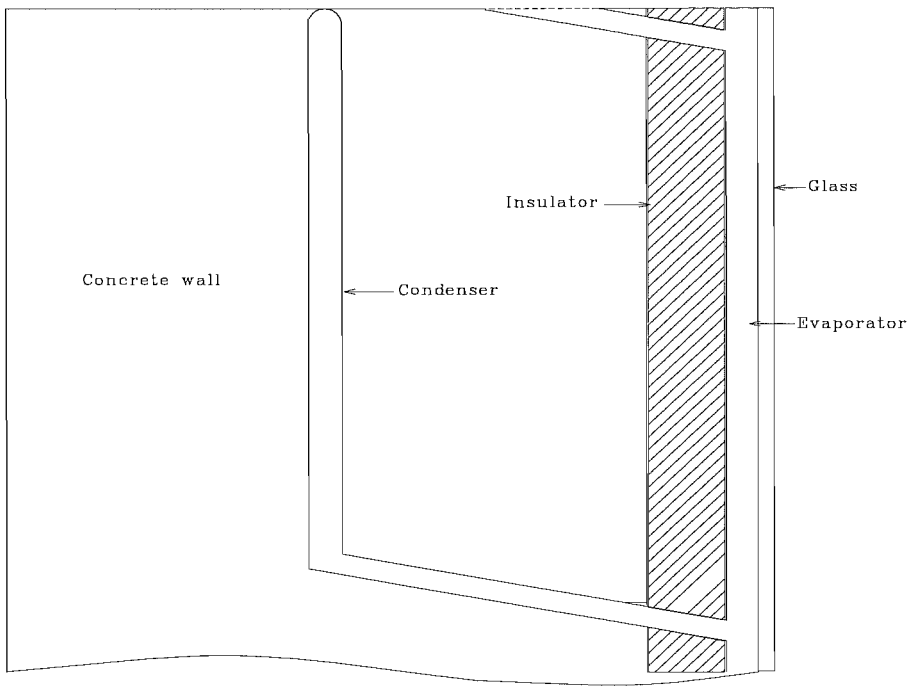

Figure 1.5 Conceptual design of the solar panel.

1.5 SCOPE AND OUTLINE OF THE PROJECT

As explained earlier in the previous Sections, more use of renewable energy and energy savings are very important to protect our environment. Some meaningful ways have to be developed and people have to be encouraged to use these systems widely. The main aim of the project was to find an alternate renewable energy source for domestic space heating.

Prior to the publication of Prudhoe's patented concept, some preliminary experimental work, based on heat pipes, had been carried out on a "rectified solar wall" at the University of Canterbury (Major - 1978). However it was the advent of the "Thermocell Heatsheet" which provided the key to implementing a practicably workable version of using heat pipe principles to achieve the desired "rectifying" effect. It was this conceptual design, proposed by Dr A S Tucker and explained in Section 1.4.2, which was the starting point for the present investigation.

It was recognised at the outset that it would be desirable to set up an approximate mathematical model of the proposed system to enable estimates to be made of the performance that might be able to be achieved, and to make soundly-based decisions on

same aspects of the proposed panel/wall design. The setting up of this model, and results obtained from it are covered in Chapters 2 and 3.

The proposed approach to a systematic testing program can be summarised as follows:

1. A prototype panel, designed using results for the mathematical model, was to be constructed and its performance tested (without solar input) by immersing the evaporator and the condenser in separate calorimeter water baths, to be run over a range of test temperatures. The design and construction of this panel are described in Chapter 4, and its testing in Chapter 5.
2. With satisfactory test performance having been achieved, the test panel was to be subjected to solar input to the evaporator with the condenser output being dissipated into a water calorimeter again. Chapter 6 describes this testing program.
3. The final stage of the experimental program was to consist of the construction of a substantial prototype wall, incorporating several panels of the design already tested. The overall performance of this completed wall would have two areas of particular interest:
   (a) The variation in temperature throughout the wall in response to varying ambient solar and temperature conditions.
   (b) The net energy contribution from the wall into the room over a significant test period.

   The construction of this wall (and its associated testing equipment), and the results obtained from it are described in Chapter 7.

The experimental results obtained in this way would represent a basis for comparing with the predictions of the mathematical model, and modifying the model if appropriate. If a reasonable match could be obtained between model and experiment during the test period, the model could then be used with responsible confidence for predicting performance at other times of the year. Chapter 8 outlines these comparisons, modifications, and predictions.

To complete the thesis, conclusions are drawn and recommendations for future work are made in Chapter 9.

CHAPTER 2

2. MODELLING OF THE SOLAR WALL

2.1 METHOD OF ANALYSIS

There is a variety of methods available to analyse unsteady state heat transfer problems, including numerical, analytical, analog and graphical. Techniques vary for the situation involved due to the limiting factors of the particular method, geometric shape of the body, the transient boundary conditions and the number or complexity of equations involved.

A numerical analysis was thought to be ideal for modelling this situation for two reasons:

1. the possibility of including the complexities of time-dependent and/or temperature dependent boundary conditions.
2. adaptability to solution by computer.

There are two broad numerical methods which will now be explained briefly.

2.1.1 Finite Element Method (FEM)

This method is a very versatile and powerful numerical technique. It is possible to write a very general finite element program that can be applied to a wide variety of heat transfer problems. Multi-purpose FEM software packages (ALGOR for example) include unsteady heat transfer problem solving capability but accommodating the variable solar inputs, and the unusual characteristics of a heat pipe would have been very difficult. Custom-written software would therefore be required and the finite difference method (below) was considered to be more suited to this particular problem.

2.1.2 Finite Difference Method

This method is based on the simultaneous solution of a set of equations, one for each elemental node of a body divided into equal increments in x, y and z directions (if the

problem is three dimensional). One such set of equations is required to be solved at each point in time, and the solution "marched" forward in time through the whole period of interest. An energy balance is applied to each node, which results in an algebraic equation for the temperature of each node. If the number of nodes in the solid is relatively small, some standard mathematical techniques to solve the resulting algebraic equations may be able to be used. As the number of nodes increases, the time required to achieve an acceptably exact solution becomes unreasonable. In these kinds of situation a problem is most easily solved by computer.

The equations of the finite difference method can be developed on the basis of either explicit or implicit formulations. The explicit technique involves expressing the temperature of a node at a future time in terms of the surrounding nodal temperatures at the beginning of the time increment. The method is limited in that the solution becomes numerically unstable if too large a time step interval is used.

The implicit formulation for the future temperatures in a transient analysis expresses each new nodal temperature in terms of the new (and unknown) temperatures of adjacent nodes. There is no limit to time or distance steps as for the explicit formulation but the disadvantage of the implicit method is the necessity of simultaneously solving a large set of algebraic equations at each time step.

The direct calculation of future nodal temperatures by explicit means is relatively easily understood, and the limits to stability were not anticipated to be unduly restrictive in this application. It was therefore decided to use the explicit method to solve this particular problem.

2.2 BASIC EQUATIONS

2.2.1 Heat flow fundamental equation

The thermal response of the concrete wall of a building is essentially a one dimensional heat flow situation. The general equation for heat conduction can be derived by using the First Law of Thermodynamics.

RATE OF ENERGY CONDUCTED INTO A CONTROL VOLUME	+	RATE OF ENERGY GENERATED INSIDE THE CONTROL VOLUME	=	RATE OF ENERGY CONDUCTED OUT OF THE CONTROL VOLUME	+	RATE OF ENERGY STORED IN SIDE THE CONTROL VOLUME

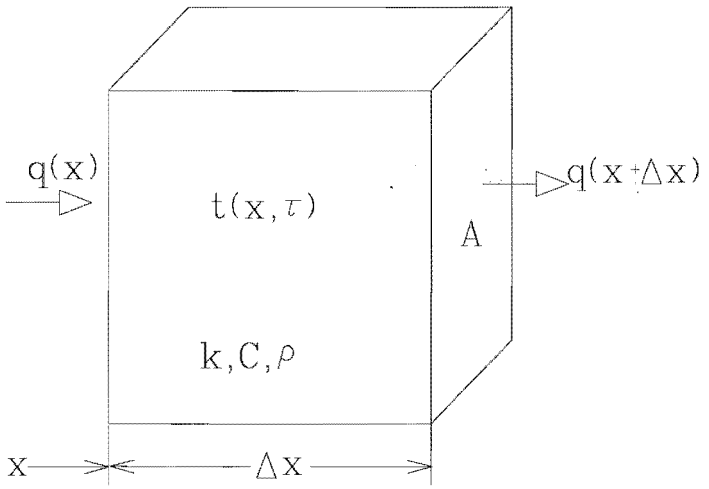

For the case of no internal heat generation, and material properties which are independent of temperatures, it can easily be shown that the governing equation for this case of one dimensional heat flow is :

$$\frac{\partial^2 t}{\partial x^2} = \frac{1}{\alpha}\frac{\partial t}{\partial \tau}$$

where $\alpha = k / \rho c$ is called the thermal diffusivity of the material (m^2/s).

k = thermal conductivity in W/m K

ρ = mass density in kg/m^3

c = specific heat J/kg K

τ = Time in seconds

x = distance in x direction.

2.2.2 Heat flow equation for the internal nodes

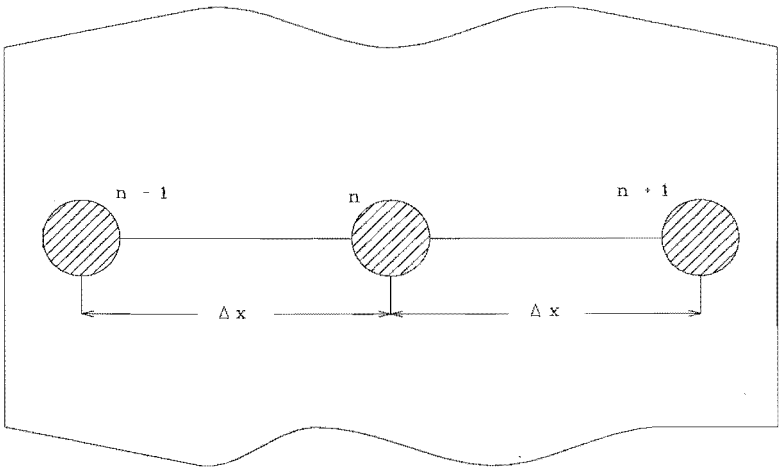

An energy balance on node n requires that

$$\Sigma_{i=n-1}^{i=n+1} \dot{q}_{i \to n} = \frac{\partial u_o}{\partial \tau}$$

where u_o = internal energy of node n.

$$\dot{q}_{n-1 \to n} + \dot{q}_{n+1 \to n} = \frac{\partial u_o}{\partial \tau}$$

The conductive heat flows $\dot{q}_{n-1 \to n}$ and $\dot{q}_{n+1 \to n}$ can be expressed by a finite difference form of Fourier's Law , i.e.

$$\frac{kA(t_{n-1}^{old} - t_n^{old})}{\Delta x} + \frac{kA(t_{n+1}^{old} - t_n^{old})}{\Delta x} = \frac{mc(t_n^{new} - t_n^{old})}{\Delta \tau}$$

$$t_n^{new} = F_o(t_{n-1}^{old} + t_{n+1}^{old}) + (1 - 2F_o)t_n^{old} \qquad (2.1)$$

where F_o = Fourier number = $\alpha\Delta\tau / \Delta x^2$

For one dimensional unsteady state heat flow it can be shown that the condition for numerical stability is

$$F_o \leq 1/2 \tag{2.2}$$

Thus, if temperatures of the various nodes are known at any particular time, the temperature after a time increment may be calculated by writing an equation like Eqn.2.1 for each of the internal nodes.

2.2.3 Heat flow equation for the boundary nodes

At the boundaries of the wall, radiation and convection also have a part in heat transfer and the general situation for a boundary node will be :

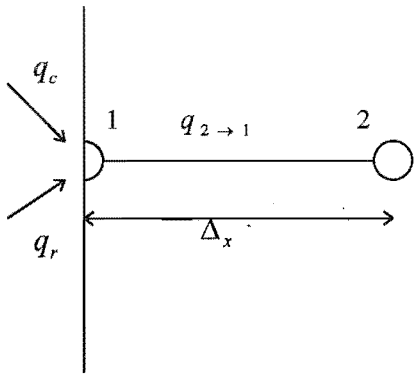

Applying an energy balance equation at node 1

$$\dot{q}_{2\to 1} + \dot{q}_c + \dot{q}_r = \frac{\partial u_o}{\partial \tau}$$

$$\frac{kA(t_2^{old} - t_1^{old})}{\Delta x} + h_c A(t_{air} - t_1^{old}) + h_r A(t_{air} - t_1^{old}) = \frac{\rho A \Delta x}{2\Delta\tau} c(t_1^{new} - t_1^{old})$$

where h_c = convective heat transfer coefficient in W/m^2 K

$h_r = \sigma \varepsilon \dfrac{(T_{air}^4 - T_1^4)}{(T_{air} - T_1)}$ is the radiative heat transfer coefficient in W/m^{2}K

Re - arranging:

$$t_1^{new} = t_1^{old} + 2F_o(t_2^{old} - t_1^{old}) + 2F_o B_i(t_{air} - t_1^{old}) \tag{2.3}$$

where

B_i = Biot number = $\frac{(h_r + h_c)\Delta x}{k}$

For boundary nodes, the numerical stability condition is

$$F_o(1+B_i) \leq 1/2 \qquad (2.4)$$

Which in comparison with Eqn.2.2, is more demanding , i.e. smaller time steps can be tolerated.

To analyse the performance of the wall, the wall has to be divided into 'n' nodes in a direction perpendicular to the wall. An energy balance equation can be written for each node, giving 'n' equations, each containing one unknown temperature. At each time step, these equations may be solved sequentially.

2.3 MATERIAL PROPERTIES

To build a model, it is essential to know more about the materials to be used in the proposed solar wall. The properties of the following materials are briefly explained below.

2.3.1 Glass

Glass is an item widely used in buildings to bring light and solar radiation inside the building and also it very effectively stops the wind. The following equation gives the value of the direct solar radiation which is normally incident upon a surface:

$$I_\delta = I \, Cos \, i$$

where I = solar intensity in W/m^2

i = angle of incidence.

This equation does not indicate how much of the quantity I_δ actually enters the surface to cause heat gain or, in the case of glass, how much is transmitted through the glass. Of the

energy which is incident upon the glass, some is reflected and lost, some is transmitted through the glass, and some is absorbed by the glass as the energy passes through it. This small amount of absorbed energy raises the temperature of the glass, and the glass eventually transmits this heat by convection, partly to the room and partly to the exterior.

Table 2.1 gives values for the transmissivity and absorptivity of glass but, in round figures, for angles of incidence between 60° and 0°, ordinary single window glass transmits about 85 per cent of the energy incident upon it. About 6 per cent is absorbed and the remaining 9 per cent is reflected. As the angle of incidence increases beyond 60°, the transmitted radiation falls off towards zero, the reflected amount increasing. The absorption figure remains fairly constant at about 6 percent for angles of incidence up to 80°(A.S.H.R.A.E Handbook - 1989)

For modelling purposes the absorptivity for the indirect component of solar radiation is taken as 0.06 and the transmissivity is taken as 0.79, regardless of the angle of incidence (A.S.H.R.A.E handbook - 1989).

For double glazing the picture is more complicated but, in approximate terms, only about 90 per cent of what passes through single glazing is transmitted. Thus the transmitted percentage for double glazing is about 76 per cent of the incident energy.

Table 2.1 Properties of glass at different angles of solar incidience.

	Angle of incidence							
	0°	20°	40°	50°	60°	70°	80°	90°
Transmissivity	o.87	0.87	0.86	0.84	0.79	0.67	0.42	0
Absorptivity	0.05	0.05	0.06	0.06	0.06	0.06	0.06	0

The thermal conductivity of glass is 0.81 W/m K

2.3.2 Concrete block

The high specific heat (950 J/kg.K) and high density (~ 2350 kg/m^2) of concrete makes it one of the best materials for storing heat in buildings. Concrete blocks are widely used in New Zealand buildings as a construction material rather than as a heat storage medium. The characteristics and shape of the concrete block was found to be very useful for this particular modelling.

As the equation of Section 2.2 shows, the thermal conductivity, k, of a material plays an important role in unsteady state heat transfer through a solid. For concrete, k can vary widely in value depending on the characteristics of the rock type from which the aggregate is obtained. In the Canterbury region, aggregates are obtained from greywacke rock and the thermal conductivity for such concrete is typically in a range from 2 to 2.5 W/m K (Wood and Adams - 1978).

2.3.3 Insulation

Insulation materials are very commonly used in New Zealand buildings to increase the thermal resistance of the wall. Materials having low thermal conductivity are considered to be good insulators. The following materials are used generally in buildings as an insulation.

FibreGlass - Thermal conductivity is 0.05 W/m.K
Expanded Polystyrene (EPS) - Thermal conductivity is 0.035 W/m.K
Foamed Polyurethane - Thermal conductivity is 0.025 W/m.K

In this particular application the panel's evaporator has to be supported from behind by the insulator. The non-rigid characteristics of fibreglass were not in its favour in this application and furthermore, if water gets into fibreglass, it becomes soaked and loses its insulating properties. Finally, fibreglass has a comparatively high thermal conductivity among these three insulators. Because of these characteristics, it was decided not to use fibreglass in this particular application.

The relative merits of other two possible insulants in this application were to be investigated in the modelling.

2.3.4 Panel and condenser pipe material

Two candidate materials were to be considered in this modelling :

Steel (1 % c) --------Thermal conductivity is 45 W/m K
Copper ----------Thermal conductivity is 400 W/m K

Solar water heating panels very frequently are made from copper, steel is generally being unsuitable because of its rusting characteristics as well as its low thermal conductivity. But for this modelling it was decided to compare both steel and copper as a panel and condenser pipe material, because water was unlikely to be present and the special characteristics of the heat pipe meant that low thermal conductivity might not be a disadvantage.

2.4 NODAL EQUATIONS

As shown in Fig 2.1 below, the wall is first subdivided in to a number of sections. A fictitious node is placed at the centre of each section. The figure also shows the cross section of the solar wall and the nodal positions. The 200 mm wide concrete block was divided into 7 nodes; node 1 was placed at the room side boundary, and node 7 was placed at outer surface of the wall. The other nodes from 2 to 5 were evenly separated and placed inside the block boundaries. Node 8 was at the evaporator, and the node 9 was located at the outside glass.

Every node was considered independently, and an energy balance performed on each node, resulting in an algebraic equation for the temperature of each node in terms of neighbouring nodal temperatures and thermal properties of the material. More detailed nodal equations are presented in Appendix A.

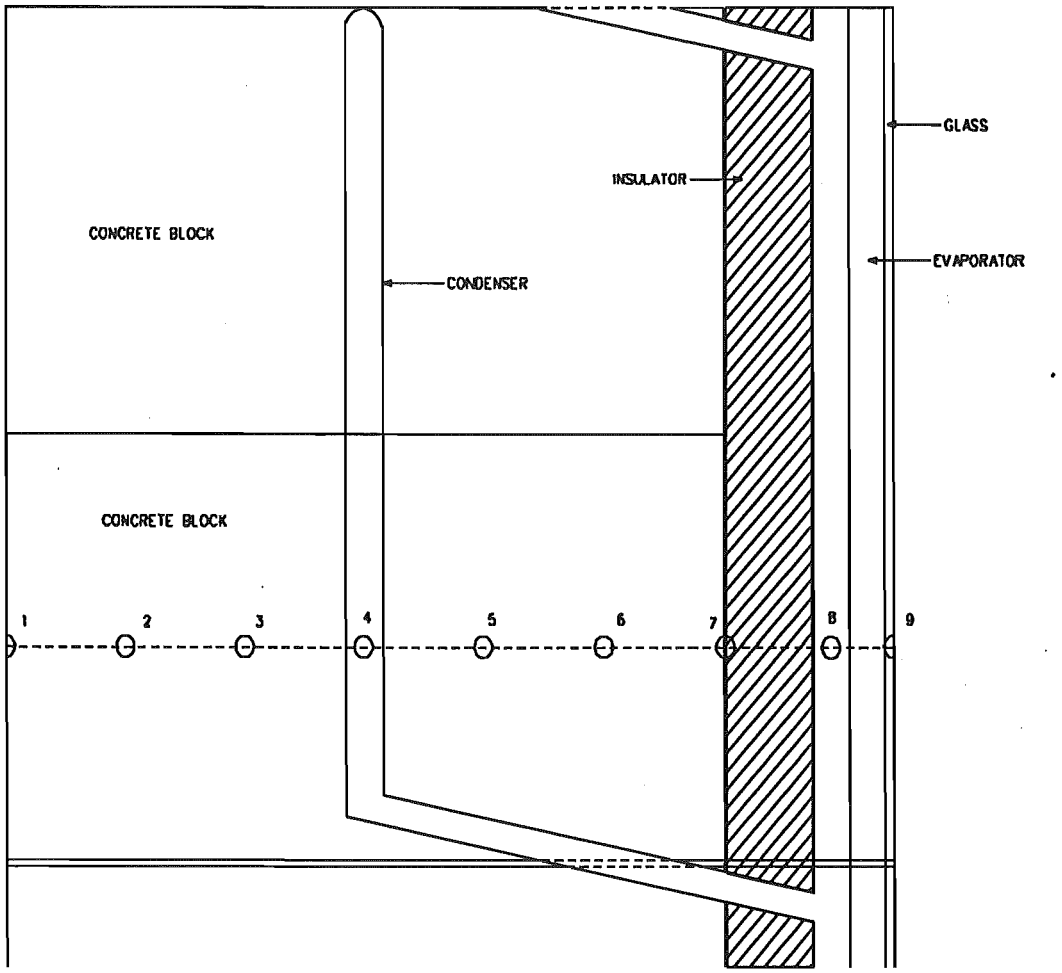

Figure 2.1 Nodal positions across the wall

The following assumptions were made while writing the nodal equations:

(i) For nodes other than the one at which the condenser is located, the thermal capacity of the condenser tubing is neglected in comparison with that of the concrete.

(ii) Horizontal thermal bridging due to the horizontal portion of the condenser tube is only taken into account across the insulation. It is neglected between nodes within the wall, because the thermal resistances of the condenser tube and the surrounding material (concrete) are not so dramatically different there.

In support of assumption (ii), consider the following:

The thermal resistance in the bridging situation can be calculated by the following equation (NZS 4214, 1977)

$$\frac{1}{R_L} = \frac{f}{R_1} + \frac{1-f}{R_2}$$

where R_L = Thermal resistance of the bridging material.

R_1 = Thermal resistance of the first material

R_2 = Thermal resistance of the second material and

f = fraction of the area occupied by the thermal bridge.

For example, steel tubing and polyurethane insulation :

f/R_L component for steel is 1.93 and for insulation is 0.49 (in the insulated area), while the f/R_L component for steel is 2.93 and for insulation is 60.48 (in the concrete area - between nodes). When comparing these numerical values, the bridging component of the steel in the first case clearly could not be neglected, whereas in the second case it could be neglected without introducing serious inaccuracy. More detailed calculations are given in the later part of Appendix A.

2.5 DEVELOPMENT OF THE PROGRAM

The computer language FORTRAN 77 was considered to be a suitable programming tool to solve this mathematical representation.

2.5.1 Flow chart

Flow charts are intended to be a formal way of describing the algorithms; they are informal ways of easily describing the steps in the algorithm without worrying about the syntax of a specific computer language. A detailed flow chart was prepared for this problem and given below (Fig 2.2).

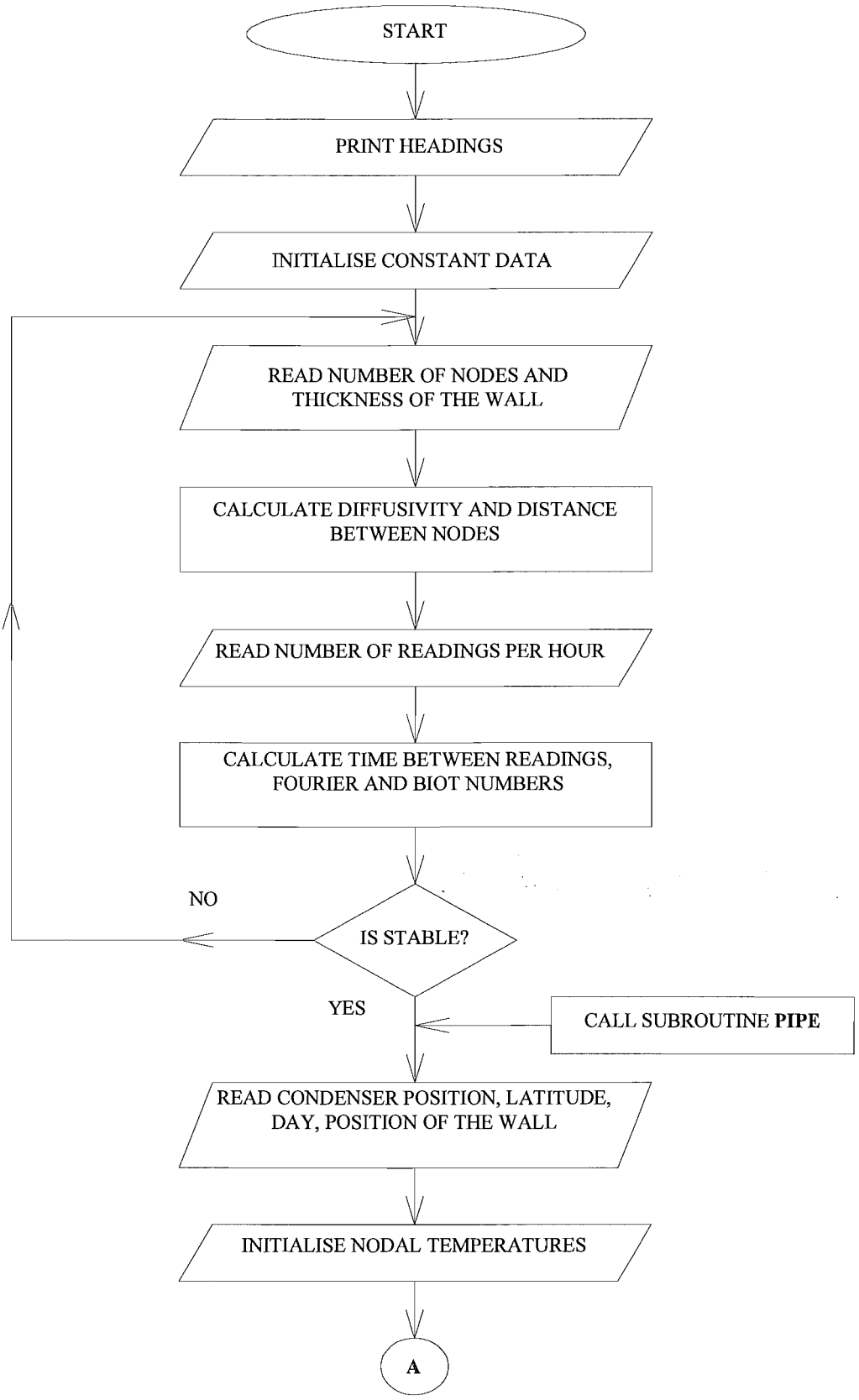

Figure 2.2 Flow Chart (Continued in next page)

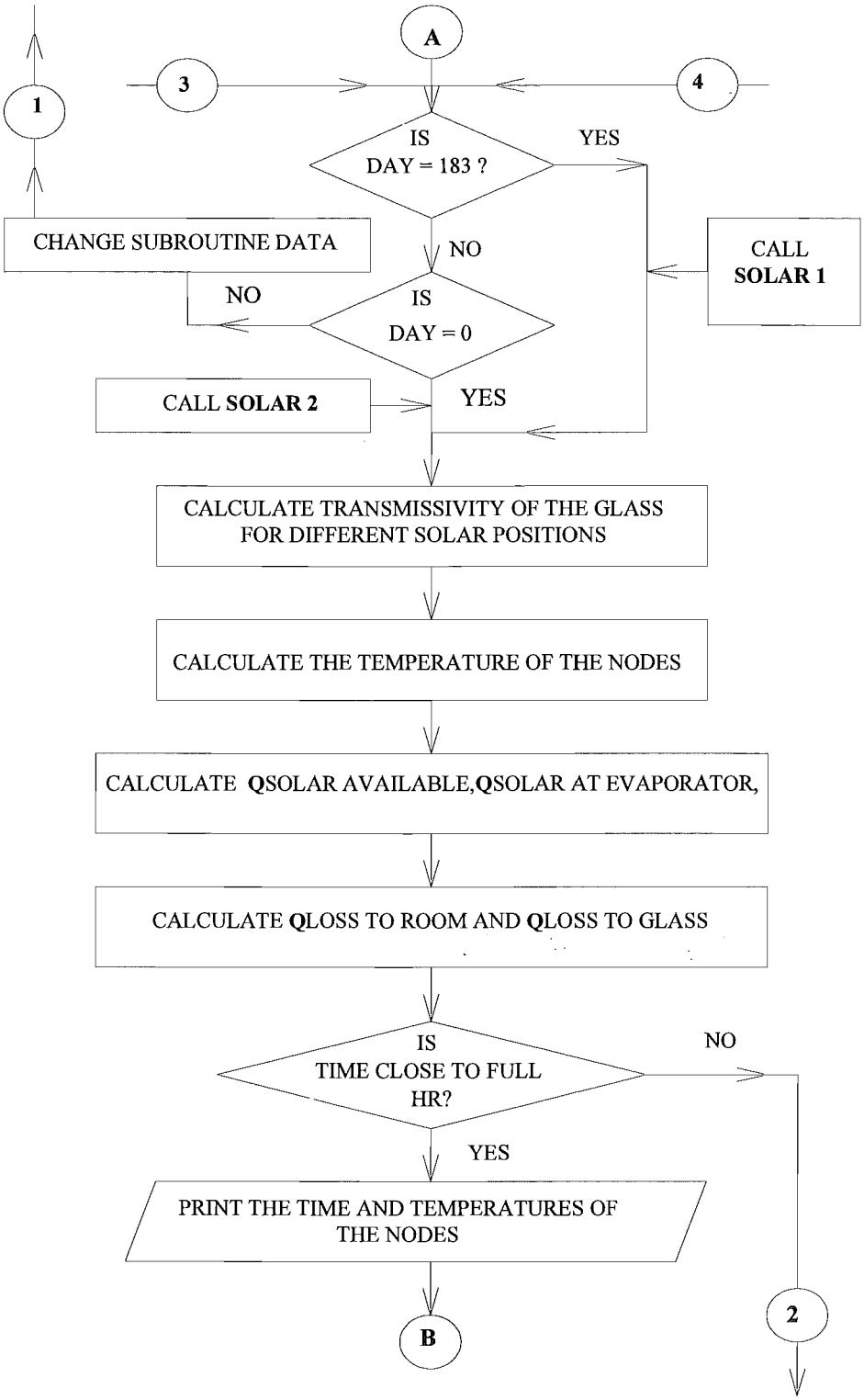

Figure 2.2 Flow Chart (Cont... from previous page)

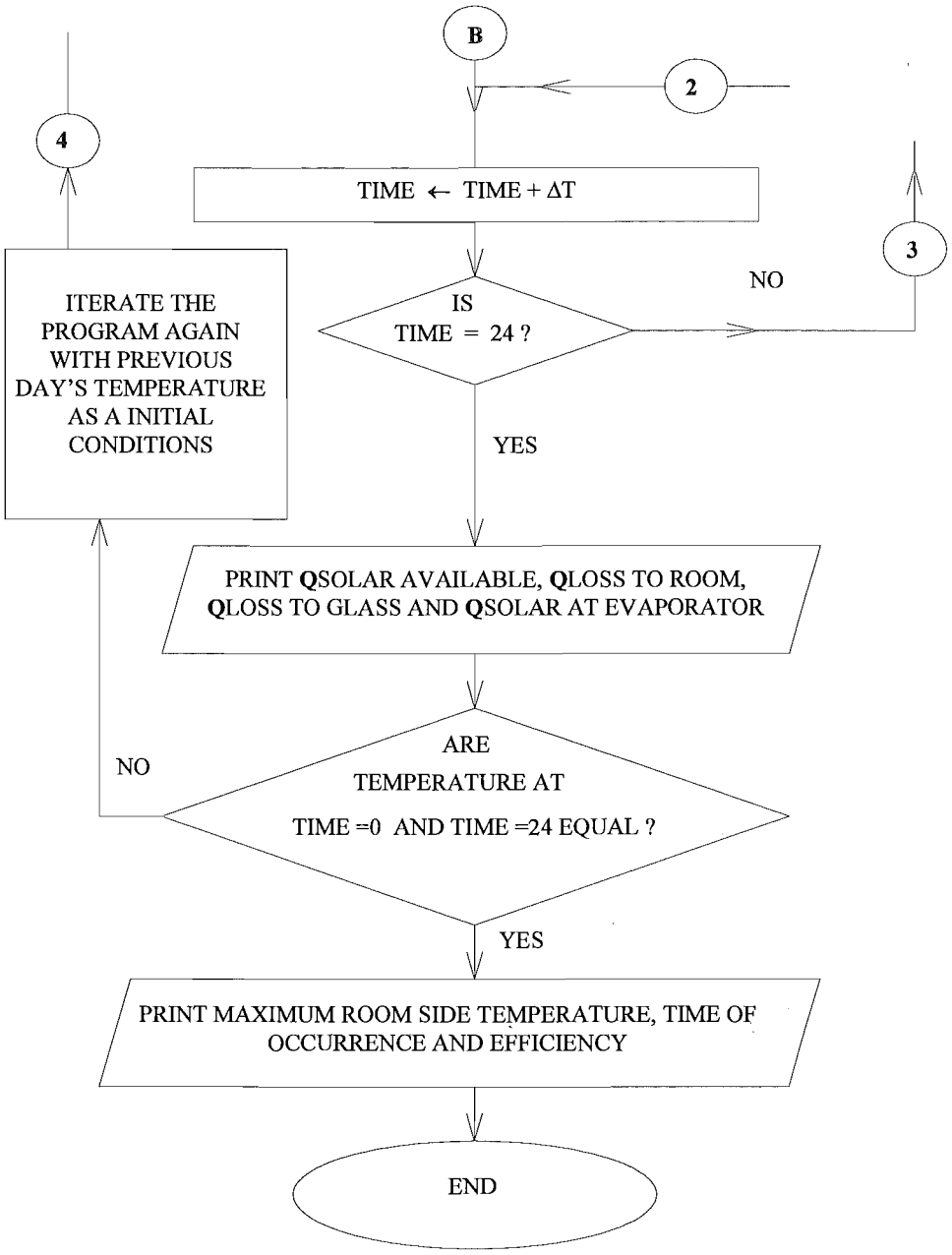

Figure 2.2 Flow Chart (Cont... from previous page)

2.5.2 Program listing

The statements written in FORTRAN to implement the steps set out in the program flow chart have been included as Appendix B. A brief description of how the program function is given in the next sub-section.

2.5.3 Description of the program

The numerical analysis of the thermal responses of the solar wall developed in the Fortran 77 language is basically in the form of an iterative loop structure and consists of a main program and subroutines.

All the thermal and the physical properties of the concrete, evaporator material, condenser tube material, glass and insulation were given under the DATA command. The stability conditions for F_o (Fourier Number) and B_i (Biot Number) were tested and the program was only allowed to run when it satisfied the stability conditions by making use of IF(....) THEN statements.

The transmissivity of the glass for different angles of incidence was calculated by linear interpolation between values of data available.

Iteration is necessary due to the nature of the explicit technique which requires an initial temperature profile through the wall at time = 0.0 in order to calculate temperatures in the following time steps. An estimate of this profile must be made and specified as temperatures of nodes 1 to 9. As this initial profile (T_{amb}) is but an estimate, and all temperatures at successive time increments are based on this estimate, it is generally necessary to iterate through the same day several times, replacing the initial profile with the final profile, before an acceptable level of equilibrium has been established. The confirmation or otherwise of equilibrium is determined at the end of each day (24 hours) by the comparison of the differences between initial and final temperatures with a permissible maximum tolerance. In this program this was achieved through the use of an IF(.....) THEN statement.

Calculation of the 'new' temperatures for the nodes through the wall is performed by a DO loop and an IF(....) THEN statements, using all the nodal equations which have been derived in the previous section 2.4.

After calculating the 'new' temperatures, the program calculates the following in each time step.

(i) Solar energy available.

(ii) Solar energy available at the evaporator.

(iii) Heat loss to room

(iv) Heat loss to glass.

All these four items are totalled for each hour and finally totalled for the full 24 hour day by an IF(....)THEN statement and a DO Loop.

2.5.4 Description of the subroutines

(a) Subroutines SOLAR1 and SOLAR2

Total solar radiation consists of the sum of the direct, indirect and the reflected components. At the time of this modelling, the reflected components were not considered. The other two components are found by interpolation between values of a data file within the subroutine (CIBSE Guide - 1986). This total solar radiation available will vary throughout the year. From these values the solar intensity incident upon a vertical wall was calculated separately for the direct and the indirect components and marked as I_{vert} and I_s respectively. One clear summer day readings were calculated by 'SOLAR 1', and one clear winter day readings were calculated by 'SOLAR 2'.

The ambient air temperatures were estimated by a sinusoidal equation representative of December temperatures for the summer, and June temperatures for the winter. These values are based on long-term average values from Christchurch meteorological records.

$$t_{air} = (16.5 + 3.5 \cos(Hour - \frac{\pi}{4})$$

$$t_{air} = (6.45 + 3.15 \cos(Hour - \frac{\pi}{4})$$

These three values of I_{vert} , I_s and t_{air} were calculated for every time steps and transferred to the main program whenever the main program call subroutines SOLAR1 or SOLAR 2.

(b) Subroutine PIPE

It is important to calculate appropriate equivalent dimensions wherever the wall material is non-homogeneous. This situation occurs at some places in the model, two assumptions were made and explained in Section 2.4. The appropriate equivalent dimensions were calculated wherever its effect could not be neglected.

At the condenser position, the tubes were not uniformly distributed in the cross-section of the wall. This subroutine calculates the equivalent thickness of the steel pipe (THICKP), and the equivalent outer diameter of the steel pipe (R) at condenser node.

Between node 7 and node 8, thermal bridging by the condenser tubing caused a reasonable effect in the model. This subroutine also calculates the total area of the condenser pipe (A) which is conducting heat between nodes 7 and 8, for unit cross sectional area of the wall. The formulation used to calculate these equivalent dimensions are detailed in Appendix A.

2.6 RUNNING THE PROGRAM

Inputs required by the program are :

(i) Number of nodes desired[♥].

(ii) Number of readings per hour.

[♥] This model was designed to work for any number of nodes, but this particular solar wall this value was fixed as 9.

At this stage the program checks the stability condition for the given input values. If the given inputs does not satisfy the stability condition a message will advise that the input values must be changed. Otherwise the program will ask for further inputs.

(iii) Condenser position - Node 3 or 4 or 5.

At this point it compares the values of calculated equivalent pipe thickness R, node separation DELX. If the value of 2R is greater than DELX, this will affect the energy balance of adjacent nodes. This would require that the nodal equations be re-written for those nodes. These facilities were not included in the model, so the program will run only if the value of 2R is less than DELX.

(iv) Latitude of the location (For Christchurch -43.5).

(v) Number of days since June 22nd (For winter 0 and for the summer 183).

(vi) Position of the wall - degrees east of north (0.0 for north facing wall).

At this stage the program starts to calculate the nodal temperatures of nodes 1 to 8 for the first time step. After it calculates the evaporator (node 8) temperature, the programme compares the evaporator temperature with the condenser temperature. If the evaporator temperature exceeds the condenser temperature :

(i) The heat flow path opens, and the concrete wall start to receive heat from the evaporator.

(ii) Under this condition the evaporator gains access to an additional heat loss path. (The evaporator loses heat to nodes 3 or 4 or 5 according to the condenser position.) Thus a new equation must be used to calculate the evaporator temperature, and the new results will replace the previous evaporator temperature.

(iii) The temperature of the condenser will be replaced by the evaporator temperature (assuming the heat pipe operates as a perfectly isothermal device when it is in "conducting " mode).

On the other hand if the evaporator temperature is less than the condenser temperature, this heat flow path will be closed. The program no longer replaces the condenser temperature with evaporator temperature.

The program moves to the next step, and calculates the following :

(a) The glass (node 9) temperature.

(b) The solar energy available at the outside wall.

(c) The solar energy available at the evaporator.

(d) The energy loss to the room.

(e) The energy loss from the glass.

(f) The efficiency. (= Energy loss to the room x 100 / Solar energy available at the outside wall)

The calculations are repeated at each increment of time until a total period of 24 hours has been covered.

The output from the program is an array of temperatures, each node being represented across the screen from 1 to 9 , and vertically from time = 0 at the top to time = 24 at the bottom, in intervals of one hour. The output concludes with a set of results, totalled over the 24 hours as given below.

(i) Solar energy available at the outside wall.

(ii) Solar energy available at the evaporator.

(iii) Energy loss to the room.

(iv) Energy loss from glass.

(v) Efficiency.

CHAPTER 3

3. RESULTS FROM MODELLING THE SOLAR WALL

The numerical results from the finite difference modelling of the solar wall are presented in this chapter. The main reason for doing this was to identify the most suitable materials for the wall design, optimise some dimensional decisions and also to get some insight into the performance of the wall. The mathematical model developed in the previous chapter was simulated for the winter day conditions. It should be noted that there were some probable deficiencies in the model at this stage of its development.

(a) The ground-reflected portion of the solar radiation was not considered for this simulation, leading to a significant drop in the values of available solar energy, energy loss into the room and the temperatures of the nodes.

(b) The air gap between the evaporator and the glass was very simply modelled.

(c) The heat pipe was assumed truly isothermal.

It is believed that the effect of these deficiencies on the efficiency value and the shape of the temperature profile should be small so that the design decisions being sought would be basically unaffected.

A number of materials and different situations were tested in the model by running the program with appropriate input values. The main concerns were :

(i) How much energy is flowing into the room during the 24 - hour test day ?

(ii) What is the maximum temperature on the room side of the wall and the time of its occurrence ?

(iii) What is the overall efficiency ? (i.e. energy input to room divided by solar energy incident on the external surface of the wall)

The different possibilities were tested in the mathematical model and the results are tabulated in Tables 3.1, 3.2 and 3.3. The numerical values are compared and discussed in the following Sections 3.1 to 3.4.

Table 3.1 Results for plane of condenser located at Node 3 and condenser pipes made of copper (Table 3.1 a) and steel (Table 3.1 b).

Table 3.1 a

	TEMP MAX (°C)	TIME OF DAY (H)	QSOLAR AVAILABLE (MJ)	QSOLAR AT EVAP (MJ)	QLOSS TO ROOM (MJ)	QLOSS TO GLASS (MJ)	EFFICE (%)
COPPER PIPE IS CONDUCTING							
INSULATOR POLYSTYRENE 50mm							
SINGLE GLAZE	30.6	1500	13.17	10.28	4.44	8.75	33.7
DOUBLE GLAZE	31.3	1506	13.17	8.97	5.41	7.78	41.0
INSULATOR POLYURETHANE 50mm							
SINGLE GLAZE	30.6	1500	13.17	10.28	4.44	8.75	33.7
DOUBLE GLAZE	31.3	1506	13.17	8.97	5.41	7.78	41.0
INSULATOR POLYSTYRENE 100mm							
SINGLE GLAZE	30.9	1454	13.17	10.28	4.77	8.42	36.2
DOUBLE GLAZE	31.5	1500	13.17	8.97	5.59	7.58	42.4

Table 3.1 b

STEEL PIPE IS CONDUCTING							
INSULATOR POLYSTYRENE 50mm							
SINGLE GLAZE	31.8	1448	13.17	10.28	5.70	7.53	43.3
DOUBLE GLAZE	32.1	1454	13.17	8.97	6.15	7.05	46.7
INSULATOR POLYURETHANE 50mm							
SINGLE GLAZE	31.8	1448	13.17	10.28	5.75	7.46	43.7
DOUBLE GLAZE	32.1	1454	13.17	8.97	6.17	7.01	46.9
INSULATOR POLYSTYRENE 100mm							
SINGLE GLAZE	32.2	1448	13.17	10.28	6.20	6.97	47.0
DOUBLE GLAZE	32.4	1454	13.17	8.97	6.49	6.68	49.3

Table 3.2 Results for plane of condenser located at Node 4 and condenser pipes made of copper (Table 3.2 a) and steel (Table 3.2 b).

Table 3.2 a

	TEMP MAX (°C)	TIME OF DAY (H)	QSOLAR AVAILABLE (MJ)	QSOLAR AT EVAP (MJ)	QLOSS TO ROOM (MJ)	QLOSS TO GLASS (MJ)	EFFICIE (%)
COPPER PIPE IS CONDUCTING							
INSULATOR POLYSTYRENE 50mm							
SINGLE GLAZE	29.8	1542	13.17	10.28	4.26	8.92	32.3
DOUBLE GLAZE	30.6	1548	13.17	8.97	5.30	7.89	40.2
INSULATOR POLYURETHANE 50mm							
SINGLE GLAZE	29.8	1542	13.17	10.28	4.26	8.91	32.4
DOUBLE GLAZE	30.6	1548	13.17	8.97	5.30	7.89	40.3
INSULATOR POLYSTYRENE 100mm							
SINGLE GLAZE	30.1	1536	13.17	10.28	4.61	8.58	35.0
DOUBLE GLAZE	30.7	1554	13.17	8.97	5.49	7.71	41.7

Table 3.2 b

STEEL PIPE IS CONDUCTING							
INSULATOR POLYSTYRENE 50mm							
SINGLE GLAZE	30.8	1530	13.17	10.28	5.56	7.66	42.2
DOUBLE GLAZE	31.1	1536	13.17	8.97	6.03	7.16	45.8
INSULATOR POLYURETHANE 50mm							
SINGLE GLAZE	30.8	1530	13.17	10.28	5.61	7.59	42.6
DOUBLE GLAZE	31.2	1536	13.17	8.97	6.10	7.12	46.3
INSULATOR POLYSTYRENE 100mm							
SINGLE GLAZE	31.2	1530	13.17	10.28	6.11	7.11	46.4
DOUBLE GLAZE	31.5	1536	13.17	8.97	6.44	6.79	48.8

Table 3.3 Results for plane of condenser located at Node 5 and condenser pipes made of copper (Table 3.3 a) and steel (Table 3.3 b).

Table 3.3 a

	TEMP MAX (°C)	TIME OF DAY (H)	QSOLAR AVAILABLE (MJ)	QSOLAR AT EVAP (MJ)	QLOSS TO ROOM (MJ)	QLOSS TO GLASS (MJ)	EFFICIE (%)
COPPER PIPE IS CONDUCTING							
INSULATOR POLYSTYRENE 50mm							
SINGLE GLAZE	29.3	1618	13.17	10.28	4.06	9.11	30.8
DOUBLE GLAZE	30.1	1624	13.17	8.97	5.15	8.03	39.1
INSULATOR POLYURETHANE 50mm							
SINGLE GLAZE	29.3	1618	13.17	10.28	4.08	9.12	30.9
DOUBLE GLAZE	30.1	1624	13.17	8.97	5.15	8.03	39.1
INSULATOR POLYSTYRENE 100mm							
SINGLE GLAZE	29.5	1618	13.17	10.28	4.41	8.77	33.4
DOUBLE GLAZE	30.2	1624	13.17	8.97	5.33	7.85	40.4

Table 3.3 b

STEEL PIPE IS CONDUCTING							
INSULATOR POLYSTYRENE 50mm							
SINGLE GLAZE	30.2	1612	13.17	10.28	5.37	7.84	40.8
DOUBLE GLAZE	30.6	1618	13.17	8.97	5.89	7.29	44.7
INSULATOR POLYURETHANE 50mm							
SINGLE GLAZE	30.2	1612	13.17	10.28	5.43	7.77	41.2
DOUBLE GLAZE	30.7	1618	13.17	8.97	5.96	7.26	45.3
INSULATOR POLYSTYRENE 100mm							
SINGLE GLAZE	30.5	1606	13.17	10.28	5.93	7.28	45.0
DOUBLE GLAZE	30.9	1618	13.17	8.97	6.30	6.91	47.8

3.1 CONDENSER POSITION

Three possibilities for the condenser location were tested in the model.

(i) At node 3 --- Towards interior side of wall centre.

(ii) At node 4 --- At centre of the wall.

(iii) At node 5 --- Towards exterior side of wall centre.

When the condenser was placed at node 3, both the efficiency and the temperature of the room side wall were found to be a maximum. However it was noted that the temperature of the room side wall reached its maximum value a few minutes earlier than the other two. When compared with the other two, the temperature of the room side wall was lower in the time between 1700 and 2200 hours (when the domestic house would require evening comfort).

For case (iii), the room side wall temperature was found to be higher than that for case (i) between 1700 and 2200 hours. Also the average temperature of the room side wall surface was found to be better than case (i). But its efficiency and maximum wall temperature were found to be lower than case(i).

After comparing all the advantages and disadvantages of the above condenser positions, it was hard to decide which position would be the best because the differences were quite minor. Hence the "compromise location", node 4 (i.e. centre of the wall) was selected to place the condenser.

3.2 THICKNESS AND QUALITY OF THE INSULATOR

Three different type of insulators were tested in the program :

(i) 50mm thick polyurethane.

(ii) 50mm thick polystyrene.

(iii) 100mm thick polystyrene.

Three points were analysed to choose the insulator :

(i) Thermal conductivity

Lower thermal conductivity is always good for an insulator. Polyurethane was the better of selected two materials in this respect. The simulation results also proves that the efficiency of the system is marginally better for a 50 mm polyurethane (42.6 %) than a same thickness of polystyrene (42.2 %) (for the condenser position at node 4 and for a single glazed glass).

(ii) Thickness of the insulator

Greater thickness of the material always give better performance as an insulator. It means 100mm thick polystyrene would be the best among them. The 100 mm polystyrene gave better efficiency (46.4 %) than low conductive 50 mm polyurethane (42.2 %) (for the condenser position at node 4 and for a single glazed glass). But as a disadvantage, 100mm thick insulation would reduce the available floor area for the same roof size.

(iii) Cost.

The cost of polystyrene was found to be cheaper than polyurethane (2400 x 1200 x 50 mm standard sheet of polyurethane cost NZ$ 38.90 and the same size polystyrene cost NZ$ 25.90). However, considering the total cost of a completed wall, this price difference was not significant so, 50mm of polyurethane was selected as the insulator for the prototype wall.

3.3 QUALITY OF THE CONDENSER PIPE

Two type of tubes were tested in the program :

(i) Steel tube of 19 mm outside diameter, 1.0 mm tube wall thickness

(ii) Copper tube of 21 mm outside diameter, 1.02 mm tube wall thickness.

Three points were considered to choose the tube for the condenser :

(i) Thermal conductivity.

The thermal conductivity of the copper (386 W/m K) is almost an order of magnitude higher than that of a typical low carbon steel (~ 40 W/m K).The condenser tube material does not take any major part in transferring the heat from evaporator to condenser, because this particular panel was designed to transfer the heat through the working fluid. But as a reverse, when the evaporator temperature drops below the condenser temperature, the condenser tube takes a major part in transferring the heat from the condenser to the evaporator and this is considered as a heat loss from the wall. This loss has to be kept at minimum to get a higher efficiency. The simulation results clearly shows the difference in efficiency. (For example to place the condenser at node 4 with 50 mm polyurethane and single glazed glass, the efficiency for the copper tube is 32.4 % while for the steel tube is 42.6 %). Because of this, the lower the thermal conductivity of the condenser material, the better the performance, and therefore steel tube was found to be more suitable for this application.

(ii) Cost

Copper is much more expensive than steel and this comparison also favours the decision of selecting steel pipe as the condenser tubing.

(iii) Rust

The panel should have good durability because once the panels were placed inside the wall they can not be replaced or repaired for a long period. If steel pipes were selected as a material, then rust may be a major problem to overcome. However rusting requires the following to be present :

a) steel

b) water

c) oxygen

Once the masonry wall was constructed and cured there is no possibility of water contacting the steel. In fact the situation would be no different from the common situation of reinforcing steel inside concrete.

After considering all these points, steel tube was considered as the most suitable material for the condenser but as an added precaution, it was decided to give two coats of paint to the panels to minimise any chance of rust..

3.4 TYPE OF GLASS IN THE EVAPORATOR

Two glazing systems were considered :

(i) Single glazed glass.

(ii) Double glazed glass* .

The heat loss to the outside from the double glazed glass was found to be less than single glazed glass, as expected. On the other hand double glazing also reduces the solar radiation available to the evaporator. Even so, double glazed glass gave better performance (efficiency 46.3 %) than single glazed glass (efficiency 42.6 %) (for the condenser position at node 4 and for a 50 mm polyurethane insulator). This comparatively small advantage in efficiency of double glazing glass was not considered sufficient enough to justify the clearly greater cost of double glazing.

3.5 SUMMARY OF DESIGN DECISIONS

(i) Condenser position ---- At node 4. (i.e. centre of the concrete wall)

(ii) Insulator ---- 50mm polyurethane.

(iii) Condenser ---- Steel pipe.

(iv) Glass at the evaporator ---Single glazed glass.

These final decisions were used as the input to the model and the resulting temperature distribution is tabulated (Table 3.4) and the temperature profile is plotted as a graph (Figure 3.1) below.

---

* Although not analysed, a "Twinwall" polycarbonate glazing system could be expected to give performance comparable with that of double glazing.

Table 3.4 Model predictions of the temperatures of all the nodes for a 24 hour period in the winter (in °C).

Time (Hours)	t_1 (Internal wall surface)	t_2	t_3	t_4 (Condenser position)	t_5	t_6	t_7 (External concrete surface)	t_8 (Evaporator position)	t_9 (Glass surface)	t_{air}
0000	25.2	26.1	26.7	27.1	27.3	27.1	26.7	12.7	6.4	4.2
0100	24.7	25.5	26.1	26.4	26.5	26.3	25.9	12.1	5.9	3.7
0200	24.2	24.9	25.4	25.7	25.8	25.6	25.2	11.5	5.5	3.4
0300	23.7	24.4	24.8	25.0	25.1	24.9	24.5	11.2	5.3	3.3
0400	23.3	23.9	24.2	24.4	24.4	24.2	23.8	11.0	5.3	3.4
0500	22.9	23.4	23.7	23.9	23.9	23.6	23.2	10.9	5.5	3.7
0600	22.6	23.0	23.3	23.4	23.3	23.1	22.7	11.0	5.9	4.2
0700	22.2	22.6	22.8	22.9	22.8	22.6	22.3	11.2	6.4	4.9
0800	21.9	22.2	22.4	22.5	22.4	22.2	22.0	17.4	8.1	5.6
0900	21.9	22.3	23.0	24.1	23.1	22.7	22.6	24.1	11.5	6.5
1000	22.8	23.6	25.0	27.1	25.3	24.3	24.1	27.1	13.3	7.3
1100	24.5	25.7	27.6	30.3	28.1	26.8	26.5	30.3	14.9	8.0
1200	26.4	28.0	30.3	33.3	31.1	29.7	29.4	33.3	16.3	8.7
1300	28.3	30.1	32.6	35.7	33.8	32.5	32.2	35.7	17.2	9.2
1400	29.8	31.8	34.3	37.1	35.8	34.8	34.6	37.1	17.6	9.5
1500	30.7	32.8	34.9	37.0	36.6	36.2	36.1	37.0	17.3	9.6
1600	30.7	32.6	34.2	35.2	36.0	36.3	36.3	35.2	16.3	9.5
1700	29.9	31.6	33.0	34.1	34.7	34.9	34.6	19.2	11.8	9.2
1800	29.2	30.8	32.0	32.9	33.4	33.5	33.1	17.9	11.1	8.7
1900	28.4	29.9	31.0	31.8	32.2	32.2	31.8	17.0	10.3	8.0
2000	27.7	29.0	30.0	30.7	31.0	31.0	30.6	16.1	9.6	7.3
2100	27.0	28.2	29.1	29.7	30.0	30.0	29.6	15.2	8.7	6.5
2200	26.4	27.5	28.3	28.8	29.0	29.0	28.6	14.3	7.9	5.6
2300	25.8	26.7	27.5	27.9	28.1	28.0	27.6	13.5	7.1	4.9
2400	25.2	26.1	26.7	27.1	27.3	27.1	26.7	12.7	6.4	4.2

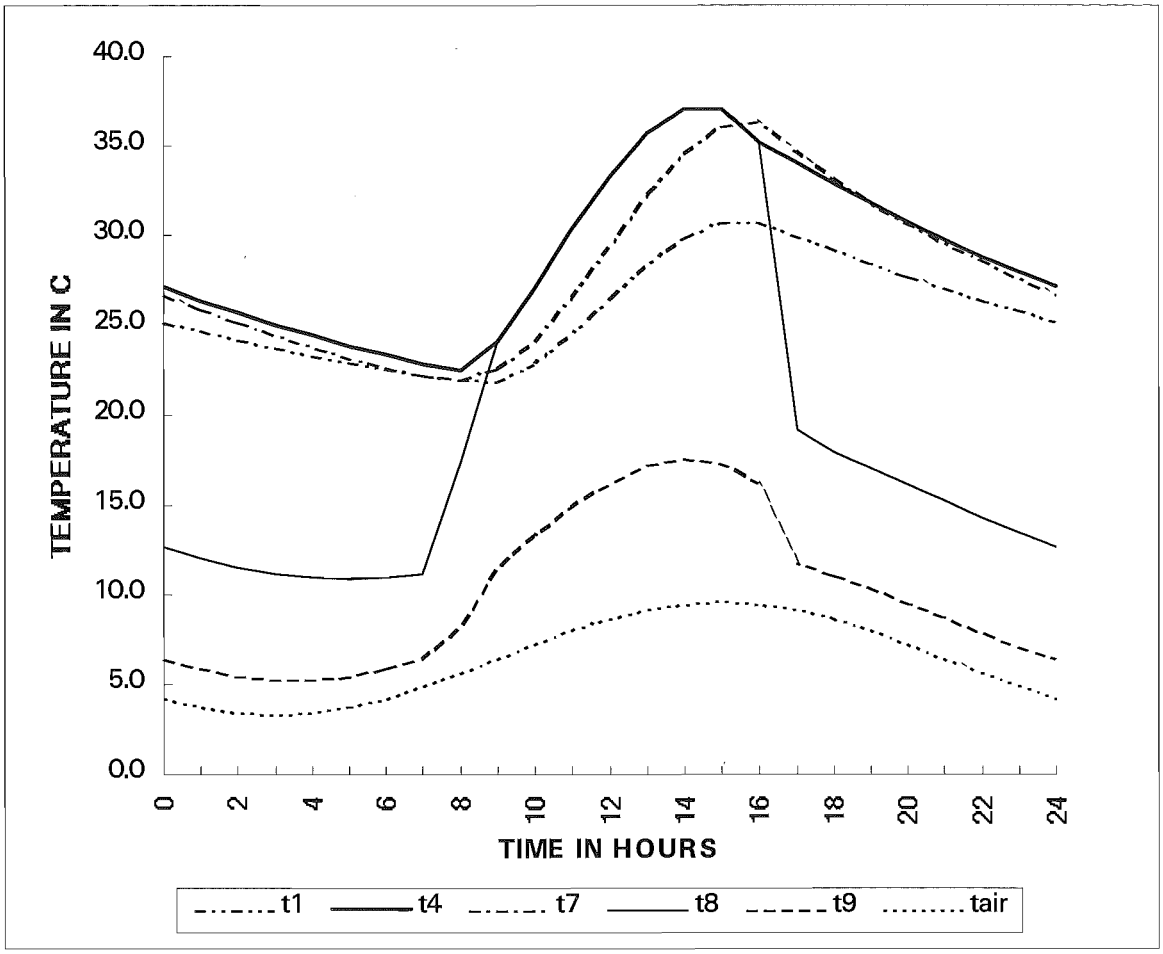

Figure 3.1 The temperature variations at different nodes in the modelled solar wall.

The temperature prediction show that the evaporator temperature t_8 starts at 12.7°C at midnight, and reduces to its lowest value of 10.9°C at 0500 hours, and from there onwards it climbs up to its maximum value of 37.1°C at 1400 hours. Meanwhile the room side wall temperature t_1 starts at 25.4°C at midnight, and reduces to its lowest value of 21.9°C at 0900 hours and from their onwards it climbs up to its maximum value of 30.8 °C at 1530 hours.

The panel is in transferring mode only between 0900 hours and 1600 hours. It is clearly seen in Fig. 3.1 as the t_8 and t_4 curves coincide during that period.

CHAPTER 4

4. SOLAR PANEL DESIGNING AND MANUFACTURING

Because of the accessibility of a local company (Thermocell Ltd.) with experience in manufacturing solar water heating panels operating on the same principle as the proposed wall panels, it was decided to make use of their expertise and facilities for the fabrication of the wall panels. Because of some limitations in those facilities it was decided to manufacture both the evaporator and the condenser separately and join both together by TIG welding. Design details, other than those arrived at by the modelling described in Chapter 3, will now be described.

4.1 SIZE OF THE PANEL

The size of the panel is very critical and should have two main characteristics :

1. It should be capable of functioning as a two-phase, gravity return heat pipe.

2. It should be easy to handle for installation into a wall at a construction site.

Before deciding the size of the panel, the available concrete blocks were checked. After looked through the blocks from the Firth* product range, a very commonly used block (20 series model 20.16C) was selected. The size of this block is 390 x 190 mm and 190 mm thickness. But when these blocks are laid as a wall, each block covers 400 x 200 mm face area including mortar thickness. The block has two cavities, one being closed and the other open (see Fig 4.1).

The area of the evaporator could be as small as one block size of 400 x 200 mm or it could cover several blocks. As a reasonable compromise, the area of the evaporator was selected as 800 x 400 mm (2 x 2 block area). The condenser, comprising a set of steel

* Firth Industries Ltd., New Zealand's largest manufacturer and supplier of concrete building products.

tubes extended from the top of the evaporator, would therefore have to match up with the cavities of another 2 x 2 block size (see Figure 4.2). The panels could be laid easily by one above the other and side by side to cover the required wall area.

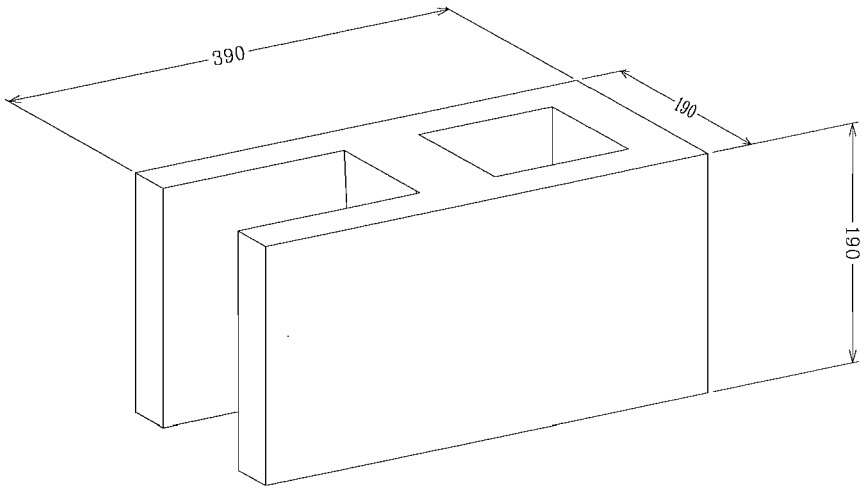

Figure 4.1 The concrete block used in the solar wall

4.2 EVAPORATOR DESIGN

The evaporator is the part of a heat pipe which collects heat from the surroundings or from an external heat source. To get the maximum efficiency from the panel the evaporator should be designed to collect the maximum possible solar radiation from the sun. According to the basic panel pattern explained in previous chapters, the evaporator should be a thin tank, sealed all over its edges. The condenser pipes should be connected from the top of the evaporator and extended upwards. The whole system should be sealed, evacuated and partially filled with the working fluid. (see Fig 4.3).

If it is an ordinary flat tank the working fluid will sit on the bottom of the evaporator as shown in the Fig 4.3. The solar radiation on the area of BC would not give an immediate effect on the working fluid. This would decrease the efficiency of the panel. By some means the liquid should be spread all over the panel to get maximum gain by the evaporator. The idea behind Thermocell's water heating panel is used to spread the working fluid across the panel area. Many kidney shaped dents are placed all over the

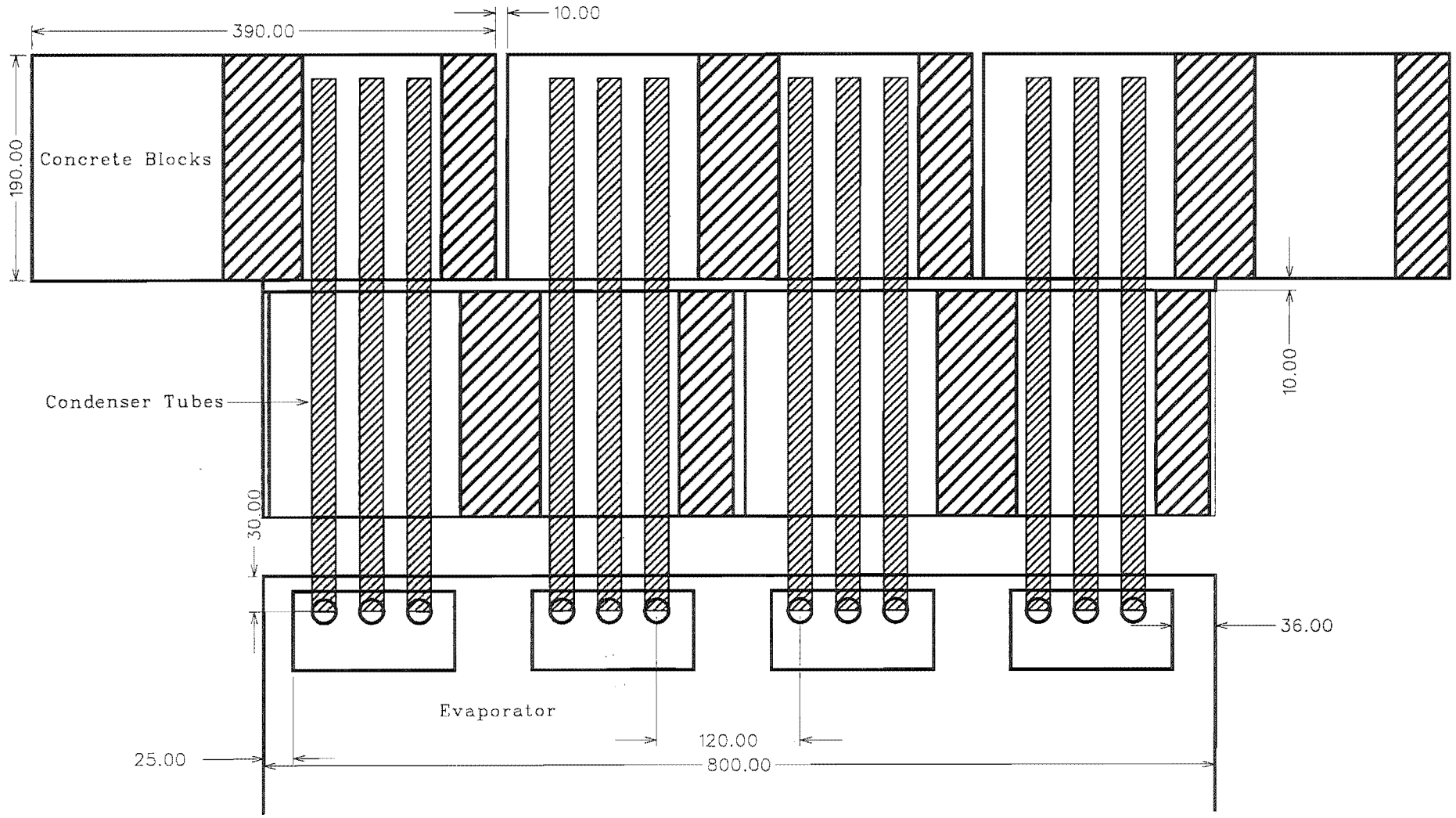

Figure 4.2 Cross section of the wall design after the blocks are laid

front panel to spread the working fluid and also fulfil the important function of maintaining separation between the two sheets which contain the working fluid at sub-atmospheric pressure. The back side of the evaporator is almost a flat plate except four bulges in the top to connect to the condenser. The bulges are placed in such a way that they would match up with the concrete block cavity holes. The bulges are extended 10 to 12 mm from the evaporator plane and have an angle of 30 degrees to take the condenser pipes perpendicularly from the angled surface of the evaporator bulge.

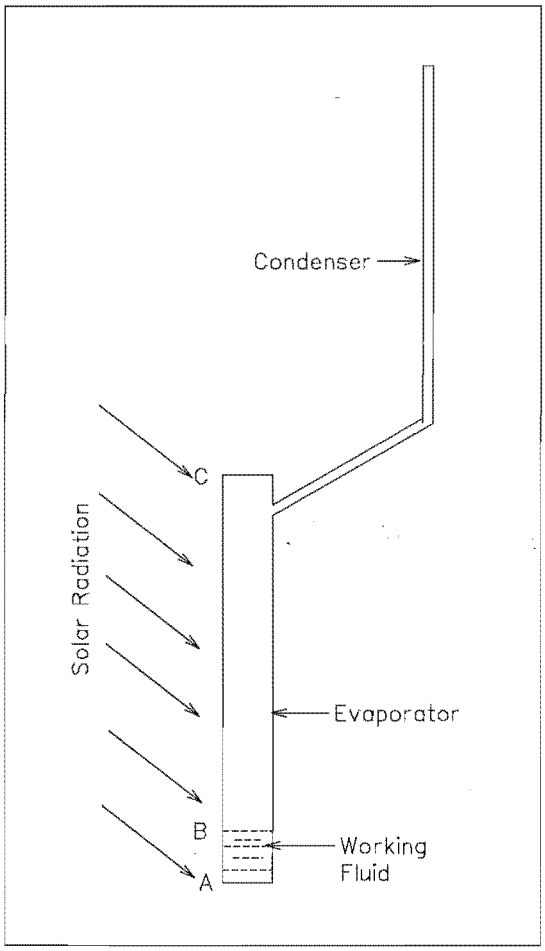

Figure 4.3 Basic solar panel.

4.2.1 Evaporator die designing and manufacturing

A die was designed using the CAD software package "Microstation" to make a mould of this evaporator incorporating all the kidney shaped dents in the front, and four bulges on the back. Appendix C contains detailed calculations, drawings and dimensions of the evaporator die. The designed die was then transferred to a Computer Aided Manufacturing (CAM) software package called "Mastercam" to enable a Fanuc milling machine (Tape Center model - D , Type A04B-0015-A003) to be used to make the die. Proper selection of tool and tool paths were defined in "Mastercam", which automatically wrote a numerical program and fed it into the CNC milling machine to mill out the particular die from 20 mm thick Customwood.

This manufactured die was given to Thermocell Ltd. for them to make the evaporator to our specifications, using the same basic manufacturing sequence that they use for their "Heatsheet" solar water heating panels.

4.3 CONDENSER DESIGN

As the concrete blocks were already selected, the condenser design was also be required to match the shape and dimensions of these blocks. The condenser could not cover the whole 800 mm of the panel length, as the concrete blocks have only four cavities in that portion. The condenser was designed in such a way that it would fill the cavities of the top two courses of the four course of concrete blocks that a single panel would involve. According to the simulation results, steel pipes of 19 mm diameter and 1 mm wall thickness were selected as a condenser pipe. Each cavity would be filled with three individual pipes, extended from one bulge of the evaporator. The four bulges of each evaporator panels therefore carried twelve condenser pipes in total. Each pipe was bent to 60 degrees at 160 mm from one end, making them parallel to the evaporator panel after assembly. The other ends were pressed flat and brazed. Appendix C contains full detailed calculations and dimensions of the condenser pipe design.

4.4 PANEL ASSEMBLY

As mentioned earlier the separately-made evaporator and condenser tubes needed to be joined together to make a complete panel. The four bulges of the evaporator back were drilled to make three holes of 19.5 mm diameter according to the designed dimensions (see Appendix C). The evaporator and all the condenser pipes were placed in a jig in which the evaporator and condenser planes were aligned parallel to each other and separated by 145 mm (since from the simulation results, the condenser should be placed on the middle of the cavities, i.e. 95 mm and another 50 mm insulation). The open edge of each pipe was passed inside its hole for 5 mm and TIG welded to the evaporator around the perimeter of the condenser tube.

4.5 SELECTION OF WORKING FLUID

The proper selection of working fluid is essential to get maximum efficiency from the solar panel. The experience of Thermocell Ltd., in optimising working fluids suitable for their "Heatsheet" solar panels was heavily drawn on in deciding which fluids might be suitable in this application. It was obvious at an early stage that the working fluid would almost certainly be organic, and specific points to be considered in this particular application were:

1. Anti-rust characteristics

   As the whole panel was made out of steel, it was important to select a working fluid which would not encourage any corrosion of the steel. Most organic fluids will satisfy this requirement.

2. Desired boiling point

   Simulation results from Chapter 3 showed that, the maximum temperature of the evaporator could go up to 60°C at Christchurch. Therefore the organic fluid's boiling point at atmospheric pressure should not be less than 60°C to ensure that a sub-atmospheric internal pressure is always maintained, thereby guarding against the possibility of the panel bulging and distorting. The solar inputs on the vertical

plane will change with location on the planet and it may be that different fluids are the most suitable at different location.

3. Desired freezing point

In very cold situations, such as early mornings in winter months, the temperature of the air may drop very low. The working fluid should not freeze under such conditions as this may damage the panel and also may inhibit panel start-up. As explained in the previous section this possibility also changes with the location at which the panel is to be installed.

4. Cost

The cost of this fluid should not play a major role in the total cost of the panel. The fluid must also be easily available.

Consideration of those points narrowed the range of likely working fluids to those shown in Table 4.1 (Liley, Makita and Tanaka - 1988).

Table 4.1 Potential working fluids for the panels.

Name	Boiling point at 1 atm (°C)	Freezing point at 1 atm (°C)	Cost per litre ($)
Toluene(C_7H_8)	110.65	-94.95	2.10
N-Hexane (C_6H_{14})	68.75	-95.80	2.20
Methanol (CH_3OH)	64.55	-97.55	2.20
N-Heptane (C_7H_{16})	98.45	-90.55	2.30
N-Octane(C_8H_{18})	125.67	-56.78	10.20
Ethanol (C_2H_5OH)	78.25	-114.65	2.25

Toluene, with which Thermocell Ltd. had had considerable experience, was selected as the working fluid for initial panel testing. One of the more volatile (lower boiling point) alternatives could be considered later, depending on initial test results.

4.6 FINAL PANEL MANUFACTURING

The evacuation and subsequent filling of the panels with working fluid was carried out by Thermocell Ltd. The panel was heated up to 200°C to vaporise any volatile impurities inside the panel while it was connected to a vacuum pump. Pumping continued until a pressure of 0.5 microns was achieved. In this connected position the panel was allowed to cool down to room temperature and 200 ml of degassed working fluid was drawn in. Initially just one toluene filled panel was made is shown photographically in Fig 4.4.

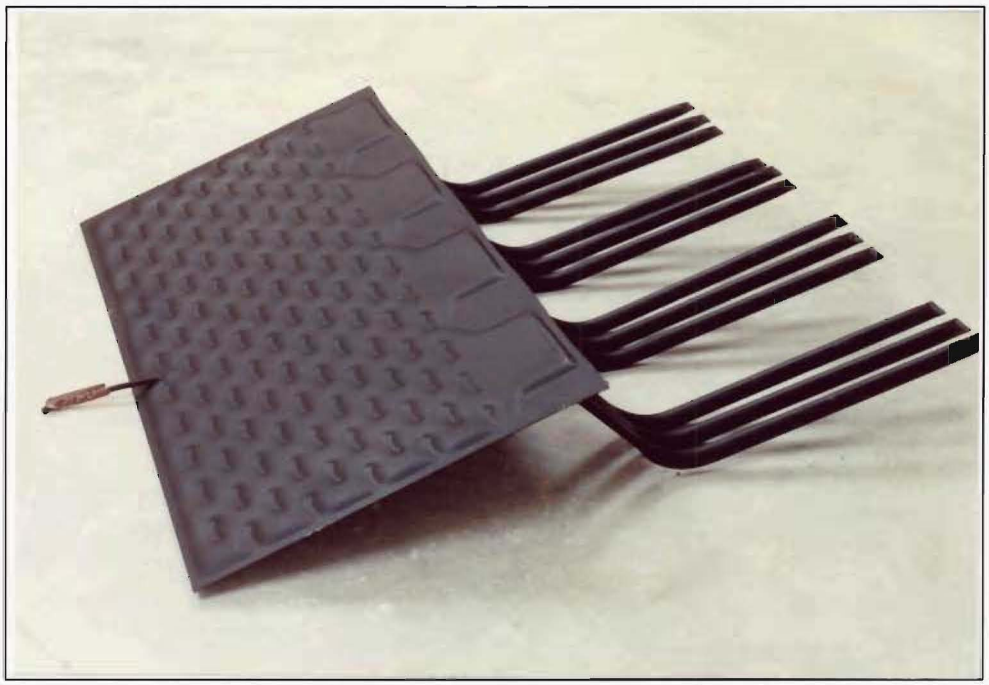

Figure 4.4 Solar panel (small tube in the bottom is used to evacuate the panel and to pump the working fluid)

CHAPTER 5

5. PANEL GENERAL PERFORMANCE TEST

Prior to testing the panel with a solar input, it was considered essential to test the panel's performance in an experiment in which the heat transfer rates at both evaporator and condenser, and any relevant panel temperatures could be easily measured. The outcome of the experiment would produce numbers from which the performance would be easily understood and any alterations or major changes (such as changing the working fluid) could be easily done to the system.

5.1 SET UP

The experiment was carried out in a temperature-controlled laboratory maintained at 20±1.5°C to find the panel's performance for different heat inputs. The experimental set up was arranged as shown in Fig 5.1.

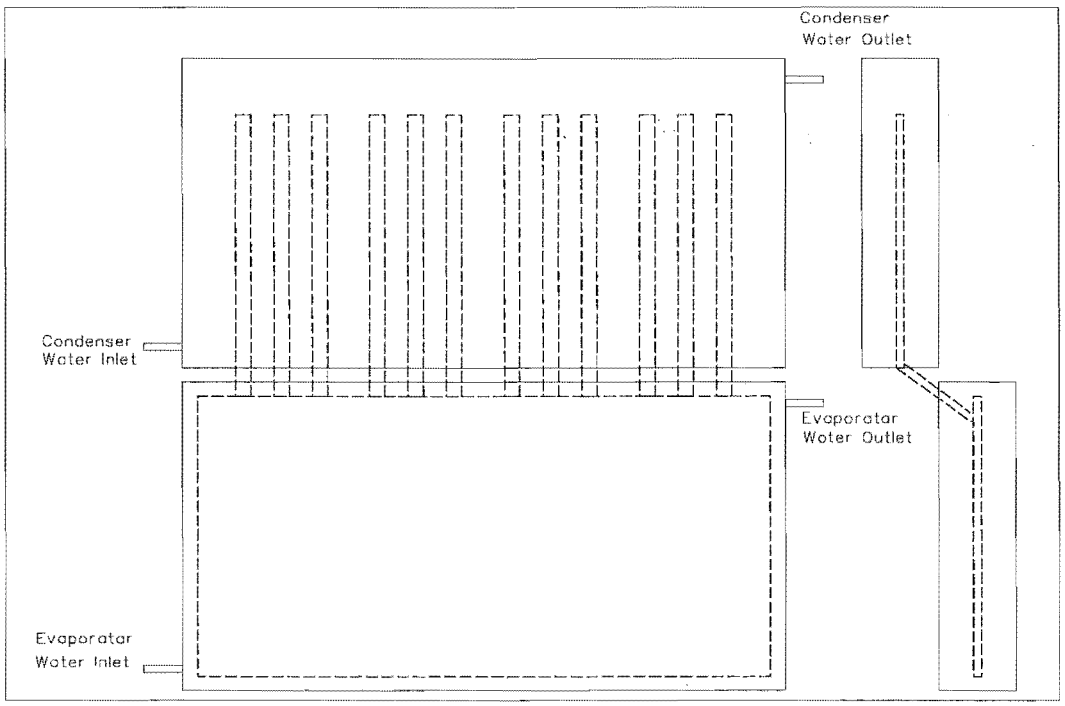

Figure 5.1 Panel placement for general performance test.

The experimental set up consisted of two water tanks, one of which surrounded the evaporator and the other the condenser. 'K-type' thermocouples were soldered to the top and bottom parts of the evaporator and also to the top and bottom parts of one condenser tube to measure the temperature distribution. Both tanks were insulated with 50 mm polystyrene sheets to reduce heat loss or gain to/from the room to negligible levels. The heat loss/gain to/from room, for both tanks were calculated for different temperature conditions and given in Table 5.1.

Table 5.1 Estimated heat loss/gain to/from room to the water tanks.
(Assuming a room temperature of 20°C)

Evaporator temperature (°C)	Heat loss to the room (W)
25	4
30	8
35	13
40	17
45	21
50	25

The experimental set-up is schematically presented in Fig 5.2. The evaporator tank was connected to a Haake FS 2 thermostated water circulator. The inlet water was pumped from the bottom right hand corner of the tank and taken out from the top left hand corner of the tank to avoid short circuiting. All the connections were made with PVC hoses. The flow of the water could be controlled by an adjustable hose clamp in the inlet line. The water was heated by a built-in heater, the output of which could be controlled up to a maximum of 1000 W. For a desired temperature set on the control thermostat, the power output of the heating element could be adjusted so that it was ON and OFF for reasonably equal time intervals to maintain the evaporator water inlet temperature at a set level, within a tolerance of ±0.5 °C. "K-type" thermocouples were connected in the inlet and outlet water lines of the evaporator tank to measure the inlet and outlet temperatures.

The well-insulated condenser tank water inlet temperature also needed to be maintained at a particular value. The way in which was done is shown in Fig 5.2. The water was

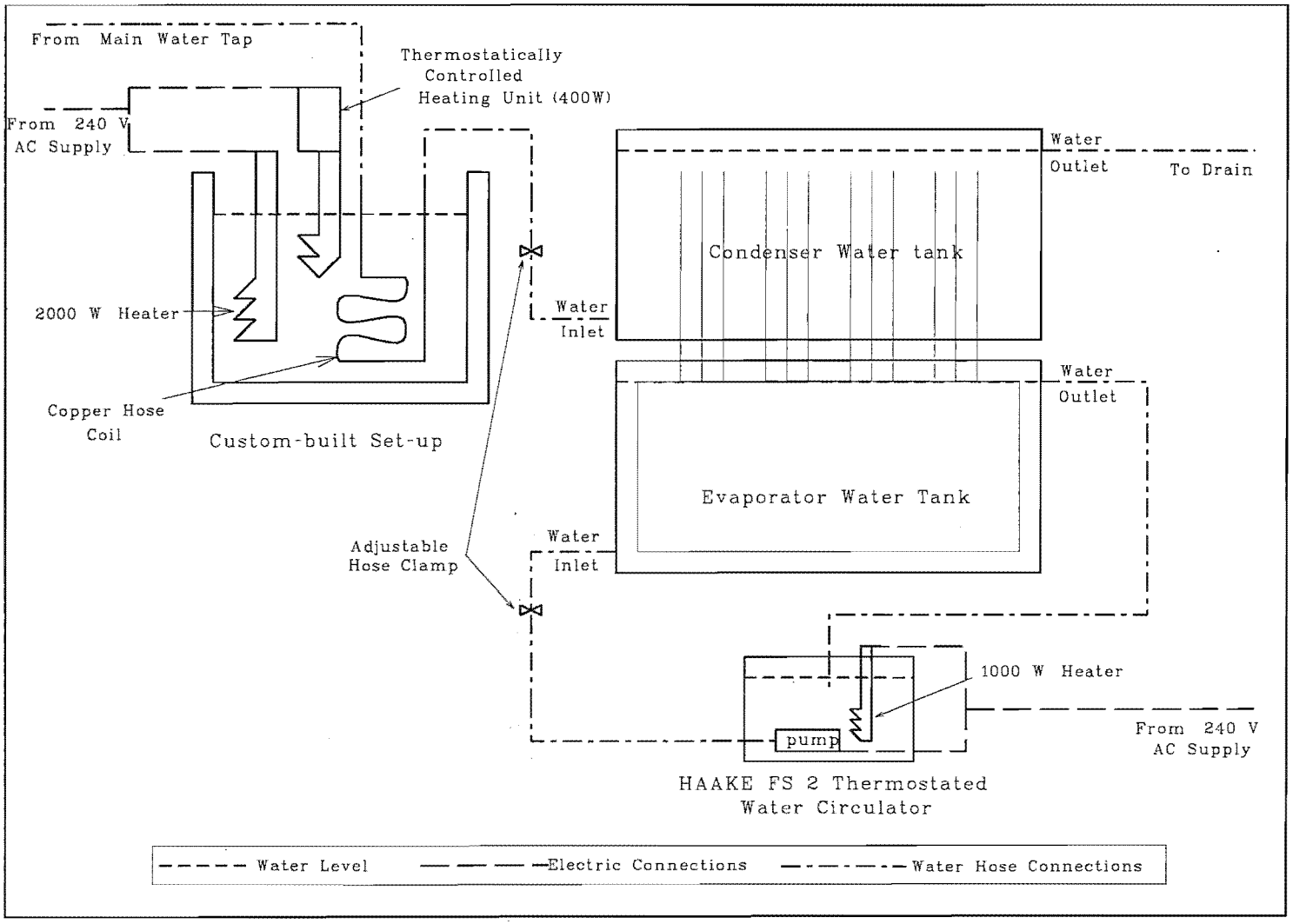

Figure 5.2 Schematic diagram of the general performance test

drawn directly from the water tap through a piece of PVC hose, connected through a copper tube coil, to the bottom left hand corner of the condenser water tank. The inlet line of the PVC hose was connected with the adjustable hose clamp to control the water flow rate. A separate water tank was placed next to the condenser tank and the water was heated by a 2000W immersion heater. The heater was connected through a separate variac to control its power output. Another thermostatically controlled 400 W heater was also immersed in the water and turned on and off to control the water temperature to a fixed value within a tolerance of ±1°C. The copper coil was mounted on an adjustable stand and immersed in the water. By changing the number of turns immersed in the hot water, the inlet water temperature could be changed. In this way the inlet temperature of the condenser tank was easily set at a required level. The outlet water was taken out from the top right hand corner of the tank, to avoid short circuiting. 'K-type' thermocouples were connected in the inlet and outlet water lines of the condenser tank to measure the inlet and outlet temperatures.

All the thermocouples were labelled and connected to a multiple switch unit, and its output was connected to a Yokogawa Model 2455 'K-type' digital readout instrument, resolving to 0.1°, and capable of storing and recalling maximum and minimum temperature values.

Room temperature was maintained by an installed air-conditioning system controlled by a wall-mounted thermostat. Room temperature was continuously monitored by using a Micromech MM-01 Hygrothermograph which was calibrated against a Platinum Resistance Thermometer (PRT) prior to the tests.

A measuring cylinder and stop watch were used to measure the water flow rate of the evaporator and condenser tanks from their outlet lines.

5.2 TOLUENE PANEL TEST

The toluene filled panel was placed in the experimental set up as explained in the previous Section 5.1. The experiment was divided into two major series of tests :

1. The evaporator tank temperature was increased from 25°C to 50°C at intervals of 5°, and also at 60°C, while the average temperature of the condenser tank was maintained at 20°C.
2. The evaporator tank temperature was increased from 30°C to 50°C at intervals of 5°, while the average temperature of the condenser tank was maintained at 25°C.

To maintain the average water temperature of the condenser tank at a certain level, for example at 20°C, by changing the water flow rate (adjusting the hose clamp) the inlet water temperature was supplied approximately 1° *lower* (say at 19°C) and the outlet water temperature approximately 1° higher (say at 21°C). For the evaporator tank, the flow was controlled so that the inlet temperature was 1° *higher* than the nominal temperature required and the outlet 1° lower.

5.2.1 Readings and calculations

The water flow rates were measured independently for the evaporator tank and the condenser tank. Three readings were taken for every situation and the average of those values in ml/sec was converted to kg/sec. The room temperature was maintained at 20°C to a tolerance of ± 1.5°. The inlet and the outlet water temperatures of the tanks were noted after the system had settled down to a particular set temperature. The experimental readings were used to calculate the total rate of heat gain in the evaporator ($\dot{Q}_{evap}$) and the total rate of heat loss from the condenser ($\dot{Q}_{cond}$) by using the following formulas :

$$\dot{Q}_{evap} = \dot{m}_E C_p \Delta t_E$$

and

$$\dot{Q}_{cond} = \dot{m}_C C_p \Delta t_C$$

where

$\dot{m}_E$ – Mass flow rate in the evaporator tank. (kg/s)

$\dot{m}_C$ – Mass flow rate in the condenser tank. (kg/s)

C_p – Specific heat of the water. (kJ/kg K)

Δt_E – Temperature difference between inlet and the outlet of the evaporator tank. (K)

Δt_C – Temperature difference between inlet and the outlet of the condenser tank. (K)

All the summarised experimental and calculated values are tabulated below. The detailed experimental data are given in Appendix D (Test series 1 and Test series 2).

Table 5.2 Summarised results from Test series 1

Condenser water tank nominal temperature : 20 °C

Working fluid : Toluene

Nominal evaporator water tank temperature (°C)	$\dot{Q}_{evap}$ (W)	$\dot{Q}_{cond}$ (W)	$\dot{Q}_{loss}$ (W)
25	42	40	2
30	136	130	6
35	273 *	223 *	50 *
	240 *	220 *	20 *
40	350 *	316 *	34 *
	343 *	310 *	33 *
45	944	937	7
50	1220 *	1208 *	12 *
	1456 *	1246 *	210 *
60	1650	1599	51

* Averages of two separate experimental runs have been carried into Table 5.4 and plotted in Fig 5.3.

Table 5.3 Summarised results from Test series 2

Condenser water tank nominal temperature : 25 °C

Working fluid : Toluene

Nominal evaporator water tank temperature (°C)	$\dot{Q}_{evap}$ (W)	$\dot{Q}_{Cond}$ (W)	$\dot{Q}_{loss}$ (W)
30	80	35	45
35	154	137	17
40	321	232	89
45	494	398	96
50	630	566	64

$\dot{Q}_{cond}$ values have been carried into Table 5.4 and plotted in Fig 5.3.

Table 5.4 Summary of data from Table 5.2 and 5.3 for different nominal evaporator - water tank temperatures.

t_{evap} (W)	$\dot{Q}_{cond}$ 20 (°C)	$\dot{Q}_{cond}$ 25 (°C)
25	40	
30	130	35
35	222	137
40	313	232
45	937	398
50	1227	566
55	1403	
60	1599	

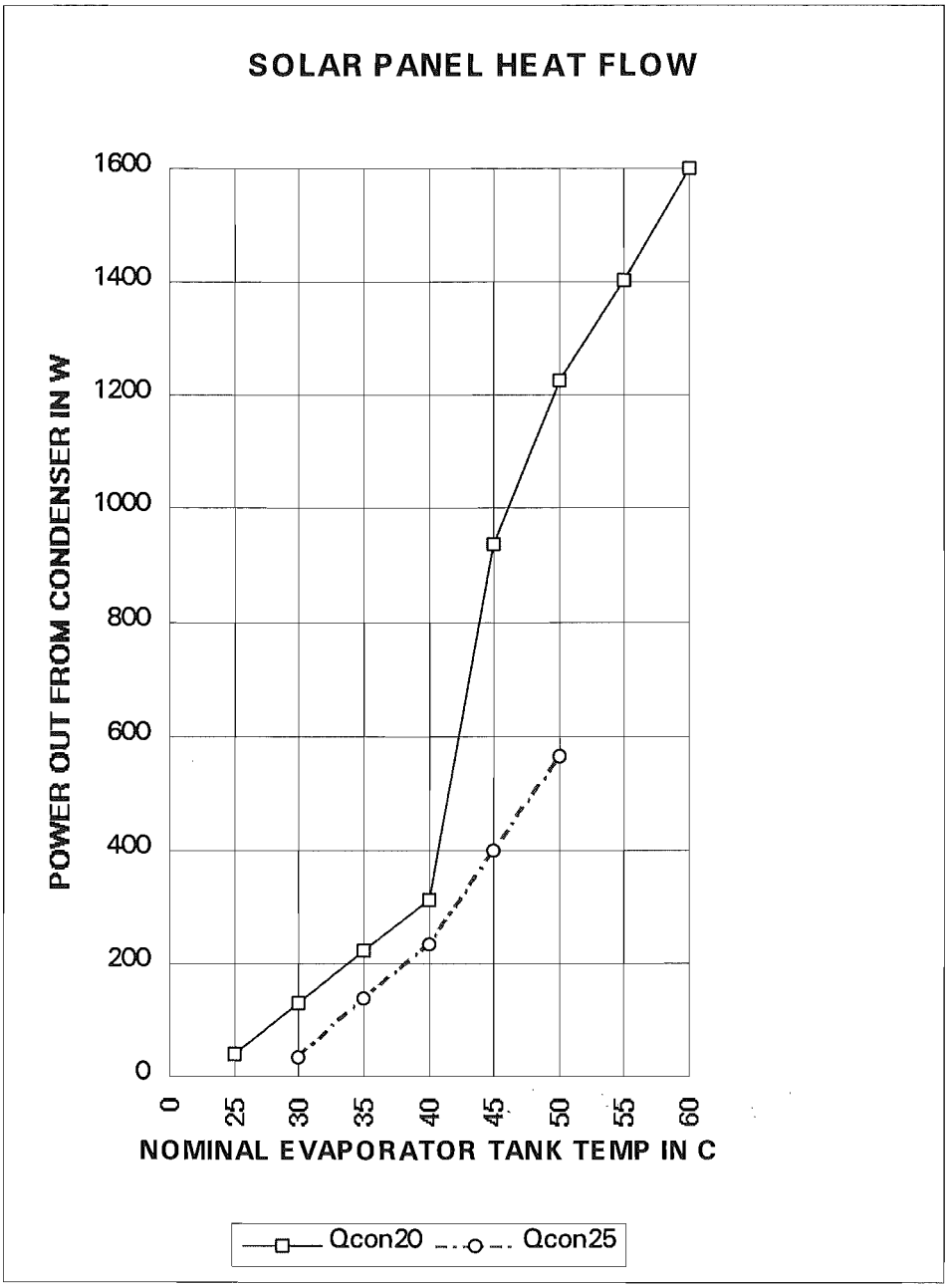

Figure 5.4 Comparison of panel performance for different condenser temperatures.

5.2.2 Analysis of the Toluene panel results.

From Fig 5.4 it is very clear that the panel was capable of transferring a large quantity of heat. However, for a 20°C condenser temperature, the panel's heat transferring mode suddenly changed to a high rate when the evaporator temperature reached about 42°C, suggesting a change in the boiling regime. For 25°C condenser temperature, there is some evidence of similar change at about 45°C, but experimental limitations on power input to the evaporator meant, that this characteristic could not be exlored at evaporator temperatures above 50°C. Referring to the wall simulation results in Chapter 3, the prediction there was that the evaporator temperature would vary between 30°C and 45°C for most of the sunny hours. This comparison suggests that the panel would be in moderate heat transferring mode for most of the working time.

The panel's consistency was also observed from repeated test values (Table 5.2).

It would therefore be desirable if the mode-changing temperature of the evaporator could be reduced to near 30°C to get a better performance for this particular situation. Re-examining toluene's properties, (Table 4.1) it is suggested that its high boiling point of 110°C may be the reason for this type of behaviour. Thus other organic fluids with similar properties and having a lower boiling point were considered, and it was decided to test the performance of the panel charged with normal-hexane (C_6H_{14}) which has a boiling point of 68.9°C still in excess of the model's predicted maximum panel temperature of 60°C.

5.3 N-HEXANE PANEL TEST

The re-charged panel was placed in the experimental set up as explained in the previous section 5.1. The experiment was divided into three major test series :

1. The evaporator tank temperature was increased from 25°C to 45°C at intervals of 5°, while the average temperature of the condenser tank was maintained at 20°C.
2. The evaporator tank temperature was increased from 30°C to 45°C at intervals of 5°, while the average temperature of the condenser tank was maintained at 25 °C.

3. The evaporator tank temperature was maintained at 20°C, while the average temperature of the condenser tank was maintained at 40°C, to find the amount of reverse heat flow.

5.3.1 Readings and calculations

The same previous experimental procedures were carried out for n-hexane panel and the results are tabulated below. The results from the first two series of tests on the n-hexane panel are presented in Table 5.5 and 5.6 and the important values summarised in Table 5.7 and plotted in Fig 5.5 (with the corresponding data for toluene added for comparison). The detailed experimental data are again included in Appendix D (Test series 3 and Test series 4).

Table 5.5 Summarised results from Test series 3

Condenser water tank nominal temperature : 20 °C

Working fluid : n-hexane

Nominal evaporator water tank temperature (°C)	Q_{evap} (W)	Q_{Cond} (W)	Q_{loss} (W)
25	50	36	14
30	128 *	117 *	11 *
	127 *	113 *	14 *
35	328	298	30
40	776 *	643 *	133 *
	767 *	636 *	131 *
45	1115	850	265

* Averages of two separate experimental runs have been carried into Table 5.7 and plotted in Fig 5.5.

Table 5.6 Summarised results from Test series 4

Condenser water tank nominal temperature : 25 °C

Working fluid : n-hexane

Nominal evaporator water tank temperature (°C)	$\dot{Q}_{evap}$ (W)	$\dot{Q}_{Cond}$ (W)	$\dot{Q}_{loss}$ (W)
30	50	37	13
35	138	114	24
40	230 *	201 *	29 *
	480 *	428 *	52 *
	508 *	446 *	62 *
45	827	712	115

* Averages of three separate experimental runs have been carried into Table 5.7 and plotted in Fig 5.5.

$\dot{Q}_{cond}$ values have been carried into Table 5.7 and plotted in Fig 5.5.

Table 5.7 Summary of data from Table 5.5 and 5.6 for different nominal evaporator - water tank temperatures.

t_{evap} (°C)	Toluene 20 (W)	Toluene 25 (W)	Hexane 20 (W)	Hexane 25 (W)
25	40		36	
30	130	35	115	37
35	222	137	298	114
40	313	232	640	358
45	937	398	850	712
50	1227	566		
55	1403			
60	1599			

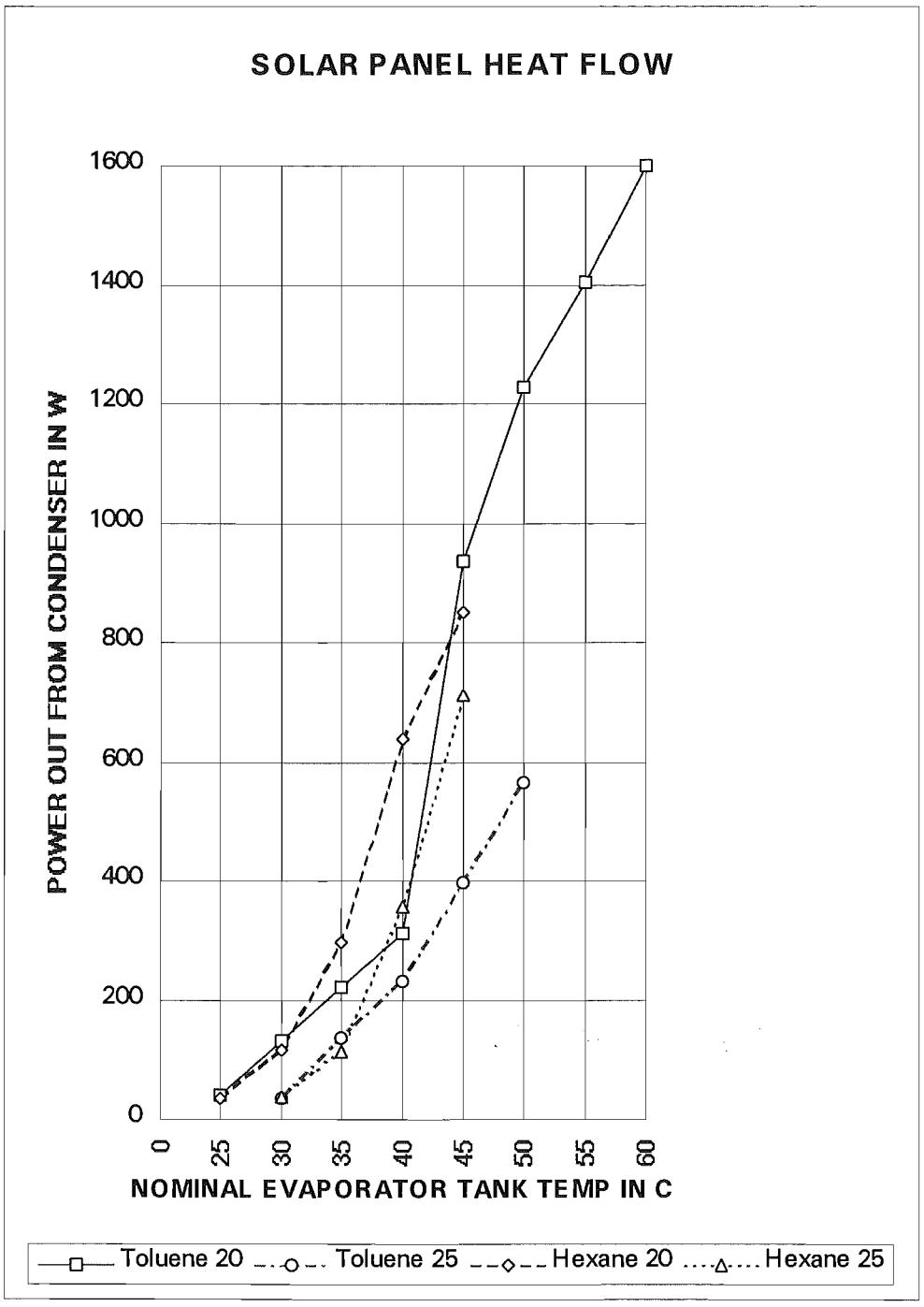

Figure 5.5 Comparison of panel performance for different condenser temperatures and for different working fluids.

5.3.2 Analysis of the n-hexane panel results

The n-hexane results also showed a similar pattern to that noted in the toluene panel results. But, as expected, the heat transferring mode was changed to a high rate at lower temperature than occurred with the toluene panel. The heat transferring mode changed to a high rate when the evaporator tank temperature was between 35°C and 40°C (for 20°C condenser tank temperature) and the evaporator tank temperature between 40°C and 45°C (for 25 °C condenser tank temperature). It was also noted that even at same temperature the n-hexane panel transferred more heat than the toluene panel. Since the simulation in Chapter 3 showed that the evaporator temperature would vary between 30°C and 45°C for most of the sunny hours, the n-hexane panel would be in reasonably good heat transferring mode when the sun was shining.

It was also noted that for a fixed evaporator temperature, the panel transferred the heat effectively if the test was conducted immediately after a high temperature test. This is most obvious in the second and third sets of results at an evaporator tank temperature of 40°C in Table 5.6. This result suggested that the panel would perform better after solar noon than before solar noon even for the same solar intensity.

Any further search for a different working fluid with lower boiling point, lower than that of n-hexane (68.9°C) was considered unwarranted, because that could cause an irreversible panel bulging if the evaporator temperature were to exceed the boiling point during operation. The simulation results showed that in Christchurch the evaporator temperature would go up to 50°C in July, but meteorological data for Christchurch shows that the solar intensity for a vertical wall is even higher in August-September and April-May period. It was predicted the evaporator temperature would go up to 60°C in these periods. So that any other fluid with a lower boiling point could be unsuited to use in Christchurch. For the subsequent prototype testing under Christchurch conditions, n-hexane was therefore selected as being the most suitable.

At the same time, n-hexane may not be the most suitable fluid to use in other locations. The meteorological data of any other particular place would need to be checked and the

maximum possible evaporator temperature calculated prior to selecting the working fluid.

5.4 REVERSE HEAT FLOW TEST

The same experimental set-up was used to test the panel's thermal diode characteristics. To proof this panel effectively transfer heat only in one direction, the condenser tank was heated to 40°C while the evaporator tank was maintained at 20°C. Two set of readings were taken and tabulated in Test series 5 in Appendix D.

Table 5.8 Summarised results from Test series 5.

	Evaporator tank temperature (°C)	Condenser tank temperature (°C)	$\dot{Q}_{evap}$ (W)	$\dot{Q}_{cond}$ (W)
Run 1	20.0	40.0	9.1	47.0
Run 2	20.0	40.0	9.9	46.1

These reverse heat transfer tests prove that the panel very effectively transferred heat in only one direction. For the same temperature difference of 20° between the condenser tank and the evaporator tank, in the intended conducting mode it transferred 643W while in the opposite direction it transferred only 9W. This occurs because in the reverse direction the heat is only able to be transferred by conduction along the walls of the condenser tubes.

This results was encouraging because it showed conclusively that the panel exhibited the thermal diode behaviour which was the fundamental principle on which the wall design was based.

CHAPTER 6

6. PANEL PERFORMANCE TEST IN THE SUN

With the behaviour of the panel under different evaporator /condenser temperatures now understood, the next step was to check the performance of the panel in a real working situation with the solar input. However, if the panel was to built into a concrete wall it would be very difficult to measure the actual power output from the condenser. Hence a 'compromise' test set-up was used in which the evaporator received a solar input and the previous arrangement of flowing water over the condenser tubes was used to measure the power output from the condenser.

6.1 EXPERIMENTAL SET-UP

The experimental set-up was arranged as shown photographically in Fig 6.1 and schematically in Fig 6.2.

Figure 6.1 Photographic view of the experimental set-up.

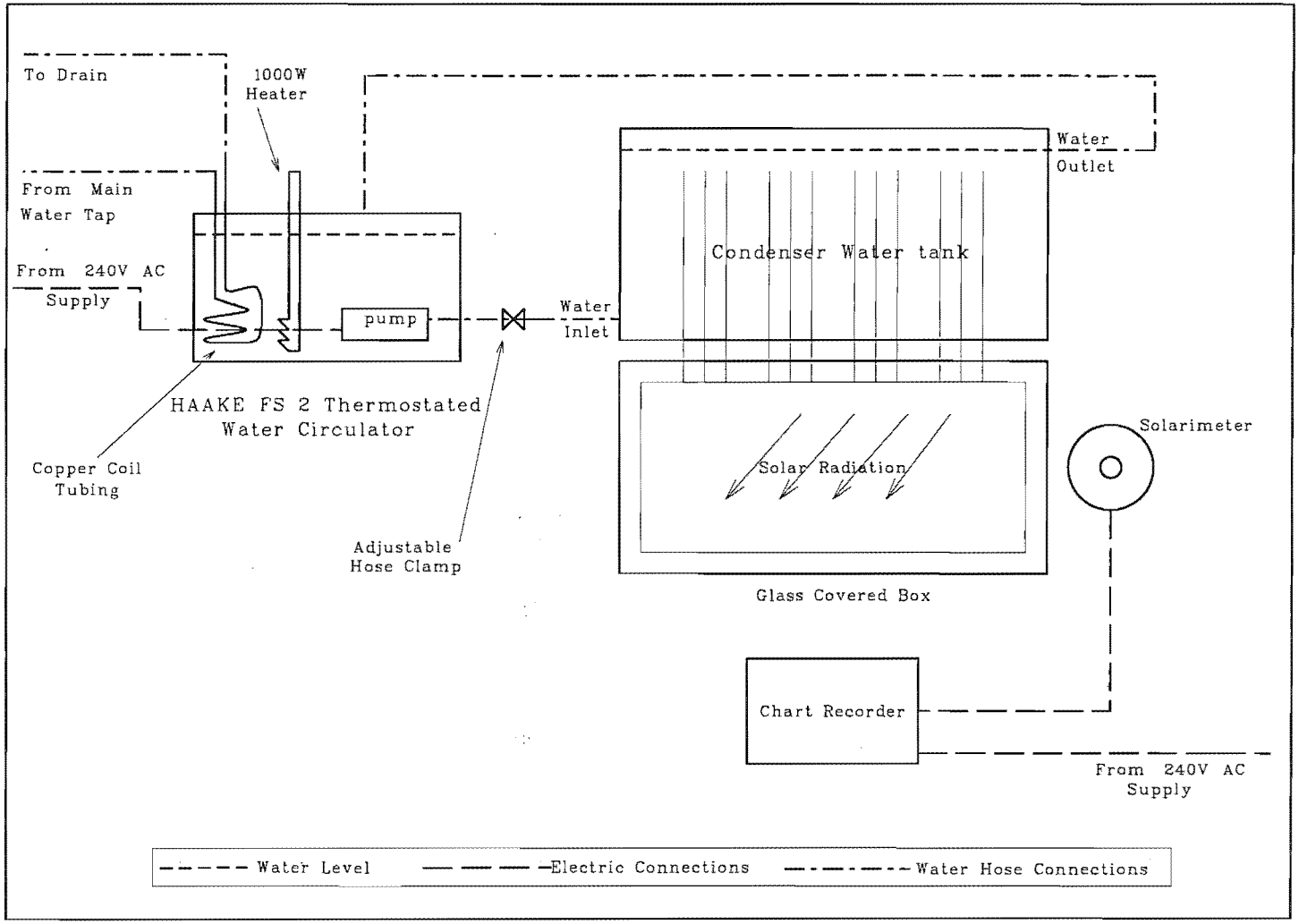

Figure 6.1 Schematic diagram of the panel's performance test in the sun

A support stand was made from mild steel angles to arrange the experimental set-up on a roof deck which has full north-facing solar exposure. K-type thermocouples were soldered on the top and bottom part of the evaporator and also on the top and bottom part of one condenser tube to measure the temperature distribution among them. A water tank was placed in such a way that it covered the condenser, and this tank was insulated with 50 mm polystyrene sheets to minimise heat loss or gain to/from the surroundings. An open rectangular box was made from galvanised steel sheet, and the evaporator was placed in it. All five sides except the open front were insulated with 50 mm polystyrene sheets. Ordinary window glass, 4 mm thick, placed in the front and sealed air tight with RTV.

The whole assembly was placed on the steel stand and bolted to the roof deck to prevent movement from wind. The whole set-up was placed in such a way that the evaporator was placed vertically and facing north. The Haake FS 2 thermostated water circulator was located inside the adjacent room and connected to the condenser tank. All the water line connections were made with PVC hoses insulated with expanded polyethylene flexible pipe insulation. The inlet water was pumped to the bottom right hand corner of the tank and taken out from the top left hand corner of the tank to ensure good mixing. The flow of the water was controlled by an adjustable hose clamp in the inlet line. In this situation, due to the solar input, the water returning to the thermostated water circulator was at a temperature higher than the supply temperature so the water in the thermostated water circulator was required to be cooled down. For this purpose a coil of copper tubing was connected with the main cold water supply and immersed in the tank. Although the inlet water temperature in the copper coil varied with time, it was always at least 5° below the maximum desired thermostated water circulator temperature of 20°C. The copper coil was also supported on an adjustable height stand which could be used to change the cooling rate of the water by varying the immersion depth. This cooling set-up continuously removed heat from the water of thermostated water circulator while the thermostatically controlled heater cycled on and off to maintain the thermostated water circulator at the set temperature value. As in previous test, the heater power output was controlled in such a way that the heating element cycled on and off in reasonably equal time intervals. In this way the water temperature was controlled

to a tolerance of ±0.1°C. The K type thermocouples were located within the inlet and outlet water lines of the condenser tank to measure the inlet and outlet temperatures.

To allow checking of the thermocouple readings, platinum resistance thermometer (PRT) probes were also located in the inlet and the outlet lines of the condenser tank. These probes could be connected one at a time to a Crison T637 digital read-out instrument to read the temperature, resolving to 0.1°. The calibration of these probes was checked against the boiling point of the water and in the melting ice prior to the tests.

To measure the ambient air temperature, a thermocouple was also placed in a louvred meteorological box, and this was placed adjacent to the experimental set up.

Each thermocouple was connected to a multiple switch unit, and its output was plugged in, to a Yokogawa Model 2455 'K Type' digital readout instrument.

A Kipp and Zonen solarimeter was positioned in a plane parallel to the evaporator (and on the same level) to measure the solar radiation available to the evaporator. The solarimeter was connected to a Yokogawa Electric Company F type - 3052 chart recorder located in the room adjacent to the roof deck. According to the calibration certificate the solarimeter produced 11.3 mV for a solar intensity of 1000 W/m^2. The chart recorder was first calibrated to zero point without any voltage supply and then the amplifier gain was checked using an external millivolt source.

A measuring cylinder and the stop watch were used as before to measure the water flow rate of the water returning from the condenser tank.

6.2 READINGS AND CALCULATIONS

The experiment was conducted for four different nominal condenser tank temperatures, varying from 20°C to 35°C in 5° steps. The experiments were carried out on reasonably cloud-free days during the August - September 1994 period. The experiment started each day between 0900 hours and 0930 hours and left to settle down at the desired

condition. The first reading started at 1000 hours and continued till 1600 hours with readings taken every 30 minutes. Temperatures were recorded from seven different points. The temperature difference between inlet and outlet of condenser tank water were calculated ($\Delta t = t_2 - t_1$).

Even though the condenser tank was insulated, the water in the tank lost heat to the surroundings. This value is dependent on the condenser tank water temperature, ambient air temperature and speed of air flow around the tank. It is hard to determine how the air speed affect the heat loss. The following example explains the steps to estimate the heat loss from the condenser tank, neglecting the convective resistance between the ambient air and the external surface of the insulated tank.

Condenser tank nominal temperature $t_{tank} = 30°C$
Ambient air temperature at 1200 hours on 3rd September 1994 $t_{air} = 13.0°C$
The total surface area of the condenser tank $A = 1.22\ m^2$
Thermal conductivity of the insulator (Polystyrene) $k = 0.035$ W/m K
Thickness of the insulator $\Delta x = 0.05$ m

$$\dot{Q}_{loss} = k A (t_{tank} - t_{air}) / \Delta x$$

$$\dot{Q}_{loss} \approx 15 \text{ W}$$

The flow rate in the condenser tank was adjusted for each time because of the variation in solar input. Basically a 2° temperature difference in Δt value was maintained by changing the flow rate to the condenser tank because the temperature read out instrument was resolved to 0.1° would give less than 10 % error in measured temperatures. The flow rate of water was measured for each time at the condenser tank outlet line in ml/sec and converted to kg/sec. As before the following formula was used to calculate the heat gained in the condenser tank ($\dot{Q}_{Calculated}$).

$$\dot{Q}_{Calculated} = \dot{m} C_p \Delta t$$

This value of $\dot{Q}_{Calculated}$ is not the true value of heat released by the condenser ($\dot{Q}_{cond}$) because of the heat loss from the tank (as estimated above). For this particular analysis, however, the $\dot{Q}_{Calculated}$ value was considered to be the heat released by the condenser since $\dot{Q}_{loss}$ could be estimated but not measured.

The total time required to replace the whole tank full of water, with a particular flow rate was calculated to find the time lag. The effect of the solar input in the evaporator would show up in the measured outlet temperature after this time lag. The time lag calculations were performed as follows :

Total Volume of the water = 19.3×10^3 ml^3

Flow rate at 1200 hours on 3rd September 1994 = 16.2 ml/sec

$\therefore$ Time required to replace this volume with the flow rate of 16.2 ml/s $\approx$ 20 min.

Flow rate at 1500 hours on 3rd September 1994 = 9.3 ml/sec

$\therefore$ Time required to replace this volume with the flow rate of 9.3 ml/s $\approx$ 35 min.

On average this time lag was taken as 30 minutes, and a 30 minutes earlier solar intensity (I) reading was tabulated against $\dot{Q}_{Calculated}$ value.

The following formulae was used to calculate the available solar power per panel.

$$\dot{Q}_{solar} = I_{Chart} \times 88.49 \times 0.32$$

where I_{Chart} is the chart reading in cm ; the value of 88.49 W/m^2/cm represents the chart recorder calibration constant determined from the initial calibration test and the value 0.32 is the evaporator area of one panel in m^2.

The following formula was used to calculate the efficiency of the panel as a device for converting externally available solar energy to useable energy at the condenser.

$$\eta = \frac{\dot{Q}_{calculated}}{\dot{Q}_{solar}} \times 100$$

All the experimental readings and calculated values are tabulated in the following Tables 6.1 to 6.4.

Table 6.1 Experiment with solar input and condenser tank at 20 °C (nominal) . (Conducted on 23rd August 1994)

Time of day NZST)	Temperature (°C)								Condenser Water Flow Rate		Heat Collected At Condenser Tank $Q_{collected}$ (W)	Available Solar Heat		Efficiency η
	t_1	t_2	t_3	t_4	t_5	t_6	t_{air}	$\Delta t = t_2 - t_1$	ml/sec	kg/sec (m)		Intensity (W/m^2)	For Panel Q_{solar} (W)	
1030	19.0	21.4	31.0	38.2	24.6	21.9	12.0	2.4	9.97	9.95×10^{-3}	100	655	210	47.6
1100	19.0	21.9	31.4	39.2	25.0	22.2	12.9	2.9	10.40	10.39×10^{-3}	126	717	229	54.9
1130	19.0	21.9	31.4	40.8	24.8	22.2	13.2	2.9	12.72	12.69×10^{-3}	154	779	249	61.9
1200	19.0	20.8	30.4	39.7	22.2	20.9	13.1	1.8	25.09	25.05×10^{-3}	189	814	261	72.4
1230	18.9	21.7	31.2	41.1	23.6	22.0	13.9	2.8	16.90	16.87×10^{-3}	198	827	265	74.6
1300	18.9	21.5	31.1	40.5	22.9	21.8	13.4	2.6	18.08	18.03×10^{-3}	196	823	263	74.4
1330	18.8	21.3	31.0	39.8	22.7	21.7	13.9	2.5	17.98	17.95×10^{-3}	188	810	259	72.4
1400	18.7	21.2	30.6	38.9	22.6	21.7	13.7	2.5	17.21	17.18×10^{-3}	180	779	249	72.1
1430	18.8	21.2	30.1	38.1	22.9	21.7	13.2	2.4	16.64	16.61×10^{-3}	167	726	232	71.8
1500	18.9	21.0	29.4	35.6	22.2	21.5	13.1	2.1	16.10	16.07×10^{-3}	141	659	211	66.8
1530	19.0	21.1	28.1	34.3	22.9	21.6	12.7	2.1	11.76	11.74×10^{-3}	103	584	187	55.2
1600	19.0	20.8	27.0	31.7	22.5	21.1	12.6	1.8	11.63	11.61×10^{-3}	87	495	159	55.1

t_1 - Inlet Water Temperature (PRT).

t_2 - Outlet Water Temperature (PRT).

t_3 - Evaporator Bottom Temperature (Thermocouple).

t_4 - Evaporator Top Temperature (Thermocouple).

t_5 - Condenser Bottom Temperature (Thermocouple).

t_8 - Condenser Top Temperature (Thermocouple).

Table 6.2 Experiment with solar input and condenser tank at 25 °C (nominal) . (Conducted on 21st September 1994)

Time of day NZST)	Temperature (°C)								Condenser Water Flow Rate		Heat Collected At Condenser Tank	Available Solar Heat		Efficiency
	t_1	t_2	t_3	t_4	t_5	t_6	t_{air}	$\Delta t = t_2 - t_1$	ml/sec	kg/sec (m)	$Q_{collected}$ (W)	Intensity (W/m^2)	For Panel Q_{solar} (W)	η
1030	24.0	26.8	33.5	43.3	30.4	27.5	16.4	2.8	8.34	8.32×10^{-3}	97	672	215	45.2
1100	24.0	27.7	33.5	45.9	31.1	28.5	16.3	3.7	7.35	7.33×10^{-3}	110	726	232	47.5
1130	24.1	27.2	32.6	45.5	30.0	28.1	17.8	3.1	12.21	12.18×10^{-3}	153	761	243	62.7
1200	24.1	27.1	32.4	46.5	29.7	28.0	15.2	3.0	14.14	14.11×10^{-3}	171	783	251	68.3
1230	24.0	27.1	32.9	45.1	29.4	27.8	17.0	3.1	13.80	13.78×10^{-3}	173	792	253	68.2
1300	23.9	27.1	33.3	46.2	29.7	27.9	18.0	3.2	13.32	13.30×10^{-3}	172	788	252	68.4
1330	23.9	27.1	33.5	48.0	30.2	28.0	19.0	3.2	12.86	12.84×10^{-3}	166	761	243	68.3
1400	23.9	27.0	33.0	46.1	28.0	27.5	17.5	3.1	12.43	12.40×10^{-3}	156	726	232	67.0
1430	23.9	27.0	32.2	45.2	27.8	27.3	17.6	3.1	11.82	11.80×10^{-3}	148	699	224	66.2
1500	24.0	27.0	32.0	42.1	27.7	27.2	17.7	3.0	10.85	10.83×10^{-3}	131	637	204	64.4
1530	24.0	26.5	31.8	41.3	26.9	26.8	15.0	2.5	8.26	8.24×10^{-3}	86	540	172	49.9
1600	24.0	26.0	31.6	36.0	26.5	26.2	14.2	2.0	8.26	8.24×10^{-3}	69	469	150	45.9

t_1 - Inlet Water Temperature (PRT).

t_2 - Outlet Water Temperature (PRT).

t_3 - Evaporator Bottom Temperature (Thermocouple).

t_4 - Evaporator Top Temperature (Thermocouple).

t_5 - Condenser Bottom Temperature (Thermocouple).

t_8 - Condenser Top Temperature (Thermocouple).

Table 6.3 Experiment with solar input and condenser tank at 30 °C (nominal) . (Conducted on 3rd September 1994)

Time of day	Temperature (°C)								Condenser Water Flow Rate		Heat Collected At	Available Solar Heat		Efficiency
NZST)	t_1	t_2	t_3	t_4	t_5	t_6	t_{air}	$\Delta t = t_2 - t_1$	ml/sec	kg/sec (m)	Condenser Tank $Q_{collected}$ (W)	Intensity (W/m^2)	For Panel Q_{solar} (W)	η
1030	29.1	30.3	37.5	47.5	32.8	30.7	12.5	1.2	7.79	7.77×10^{-3}	39	664	212	18.3
1100	29.0	31.4	38.6	48.9	33.6	31.9	14.4	2.4	9.25	9.24×10^{-3}	93	726	232	39.9
1130	28.9	31.7	39.1	49.8	33.8	32.5	14.0	2.8	11.75	11.73×10^{-3}	137	774	248	55.4
1200	29.0	31.4	40.7	50.0	33.9	31.9	13.0	2.4	16.21	16.18×10^{-3}	162	805	258	63.0
1230	28.9	31.5	40.2	49.9	33.8	31.9	13.9	2.6	15.02	14.99×10^{-3}	163	814	261	62.5
1300	28.9	31.7	40.4	49.6	34.1	31.9	13.0	2.8	12.65	12.62×10^{-3}	148	805	258	57.3
1330	28.9	31.7	40.6	49.2	33.8	32.1	12.0	2.8	11.97	11.95×10^{-3}	140	788	252	55.4
1400	28.8	31.4	39.7	47.1	33.0	31.9	12.4	2.6	11.61	11.59×10^{-3}	127	752	241	52.6
1430	28.8	31.1	38.3	45.9	32.8	31.6	12.4	2.3	11.61	11.59×10^{-3}	111	699	224	49.8
1500	28.8	30.7	38.9	43.4	32.6	31.2	12.1	1.9	9.25	9.24×10^{-3}	73	633	202	36.2
1530	28.9	30.5	37.9	41.0	31.8	30.9	11.2	1.6	6.72	6.70×10^{-3}	45	540	173	25.9
1600	28.8	30.0	35.5	38.2	31.1	30.3	11.0	1.2	6.48	6.47×10^{-3}	32	447	143	22.7

t_1 - Inlet Water Temperature (PRT).

t_2 - Outlet Water Temperature (PRT).

t_3 - Evaporator Bottom Temperature (Thermocouple).

t_4 - Evaporator Top Temperature (Thermocouple).

t_5 - Condenser Bottom Temperature (Thermocouple).

t_8 - Condenser Top Temperature (Thermocouple).

Table 6.4 Experiment with solar input and condenser tank at 35 °C (nominal) . (Conducted on 27 th September 1994)

Time of day	Temperature (°C)								Condenser Water Flow Rate		Heat Collected At Condenser Tank	Available Solar Heat		Efficiency
NZST)	t_1	t_2	t_3	t_4	t_5	t_6	t_{air}	$\Delta t = t_2 - t_1$	ml/sec	kg/sec (m)	$Q_{collected}$ (W)	Intensity (W/m^2)	For Panel Q_{solar} (W)	η
1030	33.8	34.1	44.0	49.2	37.0	34.4	11.0	0.3	7.86	7.84×10^{-3}	10	637	204	4.8
1100	33.8	34.9	43.7	51.4	38.7	35.9	11.1	1.1	8.05	8.04×10^{-3}	37	690	221	16.7
1130	33.9	35.8	44.7	52.7	39.5	36.7	13.2	1.9	7.93	7.91×10^{-3}	63	730	234	26.9
1200	34.0	36.1	44.4	52.1	39.3	36.9	14.0	2.1	9.52	9.50×10^{-3}	83	757	242	34.4
1230	33.9	36.3	46.2	53.1	39.0	37.1	12.3	2.4	11.69	11.67×10^{-3}	117	770	246	47.5
1300	34.0	36.0	45.7	52.5	38.5	36.7	12.2	2.0	11.58	11.56×10^{-3}	97	770	246	39.2
1330	34.1	35.7	45.1	51.1	38.0	36.4	12.3	1.6	10.89	10.87×10^{-3}	73	748	239	30.4
1400	34.0	35.5	44.6	49.9	37.5	36.1	11.4	1.5	9.60	9.60×10^{-3}	60	712	228	26.3
1430	34.0	35.3	43.9	48.3	37.2	35.9	11.3	1.3	9.68	9.66×10^{-3}	52	664	211	24.7
1500	33.8	34.8	42.2	46.0	36.7	35.5	10.1	1.0	9.43	9.41×10^{-3}	39	606	194	20.3
1530	33.9	34.2	40.3	42.8	36.2	35.0	10.1	0.3	5.11	5.10×10^{-3}	6	544	174	3.7
1600	34.6	34.6	40.0	41.0	34.7	34.5	10.0	0.0	5.11	5.10×10^{-3}	0	522	167	0.0

t_1 - Inlet Water Temperature (PRT).

t_2 - Outlet Water Temperature (PRT).

t_3 - Evaporator Bottom Temperature (Thermocouple).

t_4 - Evaporator Top Temperature (Thermocouple).

t_5 - Condenser Bottom Temperature (Thermocouple).

t_8 - Condenser Top Temperature (Thermocouple).

6.3 ANALYSIS OF THE RESULTS

The experimental results clearly show that the panel continued to transfer heat very effectively. The important data from the experimental results are summarised in Tables 6.5 to 6.8 and are plotted in Figs 6.3 to 6.6.

The power output from the condenser peaked at 1230 hours NZST in all four situations, corresponding to solar noon for Christchurch. The highest value was 198 W (when the condenser tank was maintained at 20°C) and gradually decreased to 117 W (when the condenser tank temperature was at 35°C). Now in the model predictions in Chapter 3, the condenser temperature was predicted to be around 20°C at sunrise, rising to more than 30°C at times of peak solar intensity. This comparison suggests that on a normal day the wall should start with the characteristics of Fig 6.3 and slowly change to the characteristics of Fig 6.4, 6.5 and 6.6 as solar noon approaches. The efficiency of the panel also decreases with increasing condenser temperature.

All four tests exhibited the same characteristic that the power output from the condenser followed a high rate of increase in the morning but lower rate of decrease in the afternoon.

Table 6.5 Summarised data from an experiment of condenser tank at 20 °C nominal temperature conducted on 23rd August 1994

Time of day (NZST)	Solar Intensity (W/m^2)	Solar power / panel (W)	Power output measured from condenser tank (W)	Air Temp (°C)	Energy gain from condenser tank (Wh) *
1030	656	210	100	12.0	
1100	716	229	126	12.9	56.5
1130	779	249	154	13.2	70.0
1200	814	260	189	13.1	85.8
1230	827	265	198	13.9	96.8
1300	823	263	196	13.4	98.5
1330	809	259	188	13.9	96.0
1400	779	249	180	13.7	92.0
1430	726	232	167	13.2	86.8
1500	659	211	141	13.1	77.0
1530	584	187	103	12.7	61.0
1600	495	159	87	12.6	47.5
		Total heat gain from condenser =			2.71 kWh

* Energy gained during preceding 30 minutes, obtained from the mean of initial and final power values for that period.

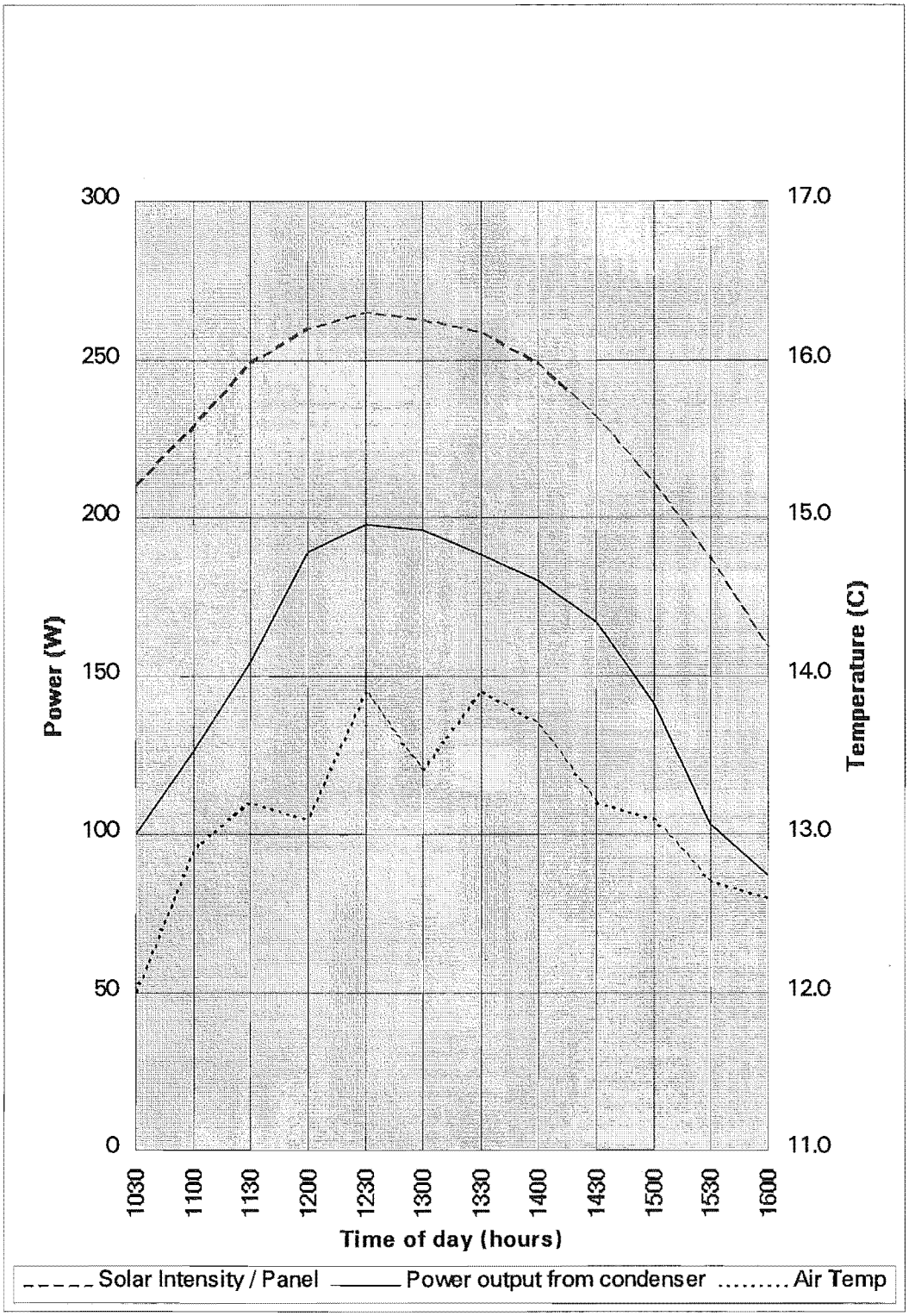

Figure 6.3 Graph for the data from an experiment of condenser tank at 20 °C nominal temperature, conducted on 23rd August 1994.

Table 6.6 Summarised data from an experiment of condenser tank at 25 °C nominal temperature conducted on 21st September 1994

Time of day (NZST)	Solar Intensity (W/m^2)	Solar power / panel (W)	Power output measured from condenser tank (W)	Air Temp (°C)	Energy gain from condenser tank (Wh) *
1030	672	215	97	16.4	
1100	726	232	110	16.3	51.8
1130	761	244	153	17.8	65.8
1200	783	251	171	15.2	81.0
1230	792	253	173	17.0	86.0
1300	788	252	172	18.0	86.3
1330	761	244	166	19.0	84.5
1400	726	232	156	17.5	80.5
1430	699	224	148	17.6	76.0
1500	637	204	131	17.7	69.8
1530	541	173	86	15.0	54.3
1600	469	150	69	14.2	38.8
			Total heat gain in condenser =		2.42 kWh

* Energy gained during preceding 30 minutes, obtained from the mean of initial and final power values for that period.

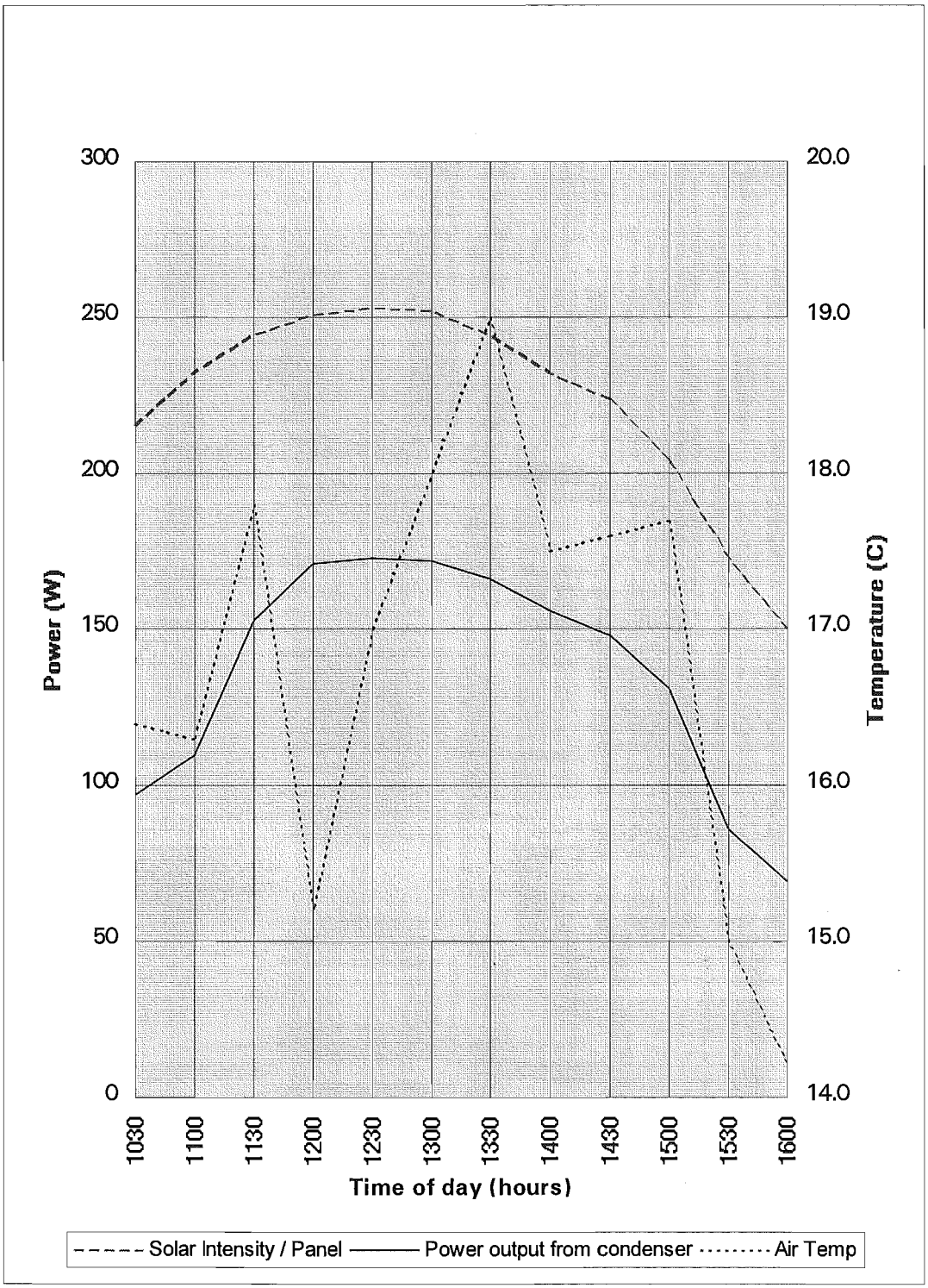

Figure 6.4 Graph for the data from an experiment of condenser tank at 25 °C nominal temperature, conducted on 21st September 1994.

Table 6.7 Summarised data from an experiment of condenser tank at 30 °C nominal temperature conducted on 3rd September 1994

Time of day (NZST)	Solar Intensity (W/m^2)	Solar power / panel (W)	Power output measured from condenser tank (W)	Air Temp (°C)	Energy gain from condenser tank (Wh) *
1030	664	212	39	12.5	
1100	726	232	93	14.4	33.0
1130	774	248	137	14.0	57.5
1200	805	258	162	13.0	74.8
1230	814	261	163	13.9	81.3
1300	805	258	148	13.0	77.8
1330	788	252	140	12.0	72.0
1400	752	241	127	12.4	66.8
1430	699	224	111	12.4	59.5
1500	633	202	73	12.1	46.0
1530	540	173	45	11.2	29.5
1600	447	143	32	11.0	19.3
			Total heat gain in condenser =		1.93 kWh

* Energy gained during preceding 30 minutes, obtained from the mean of initial and final power values for that period.

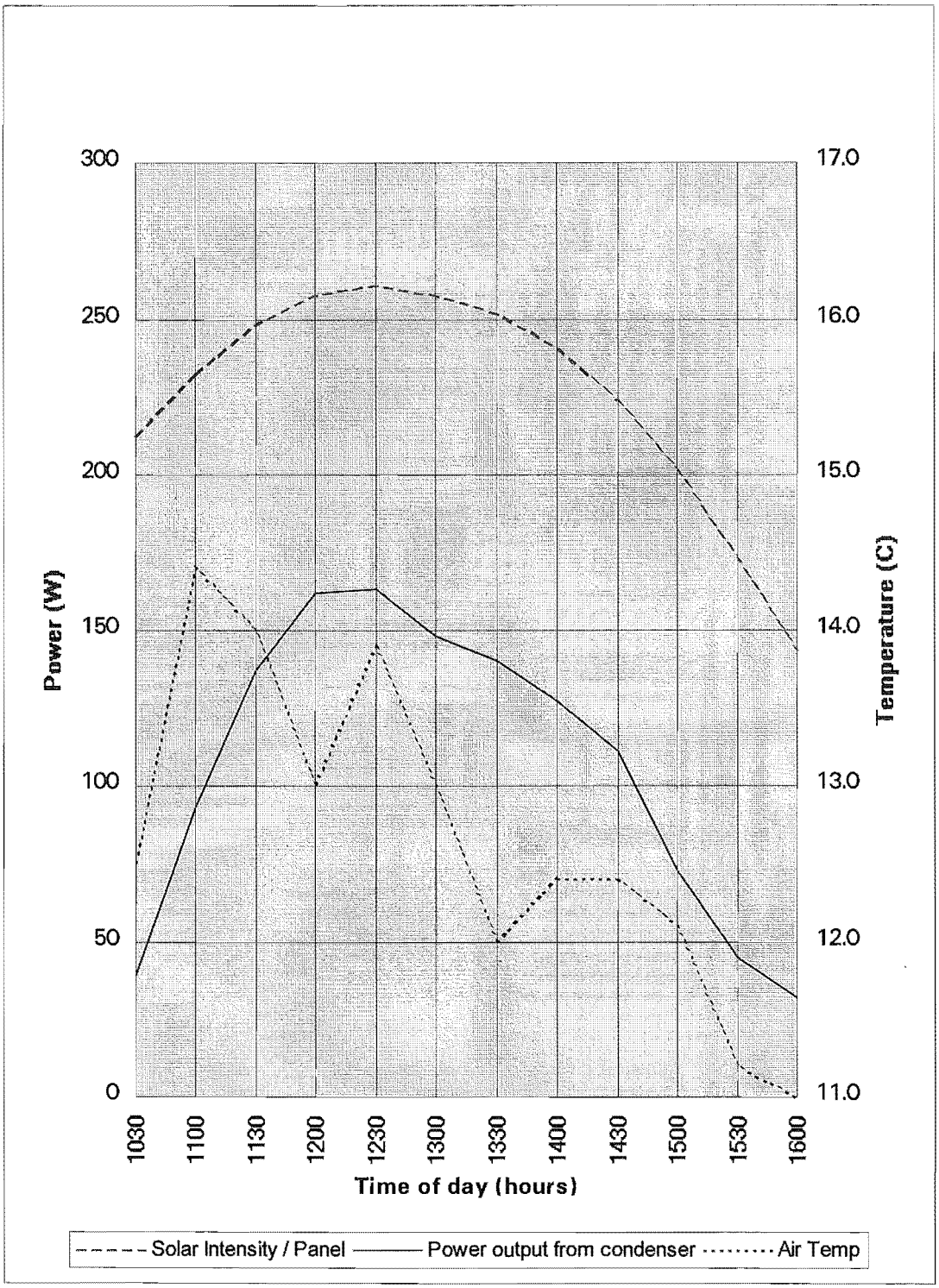

Figure 6.5 Graph for the data from an experiment of condenser tank at 30 °C nominal temperature, conducted on 3rd September 1994.

Table 6.8 Summarised data from an experiment of condenser tank at 35 °C nominal temperature conducted on 27th September 1994

Time of day (NZST)	Solar Intensity (W/m^2)	Solar power / panel (W)	Power output measured from condenser tank (W)	Air Temp (°C)	Energy gain from condenser tank (Wh) *
1030	637	204	10	11.0	11.8
1100	691	221	37	11.1	25.0
1130	731	234	63	13.2	36.5
1200	756	242	83	14.0	50.0
1230	769	246	117	12.3	53.5
1300	769	246	97	12.2	42.5
1330	747	239	73	12.3	33.3
1400	712	228	60	11.4	28.3
1430	662	212	53	11.3	23.0
1500	606	194	39	10.1	11.3
1530	544	174	6	10.1	1.5
1600	447	143	0	10.0	
			Total heat gain in condenser =		0.99 kWh

* Energy gained during preceding 30 minutes, obtained from the mean of initial and final power values for that period.

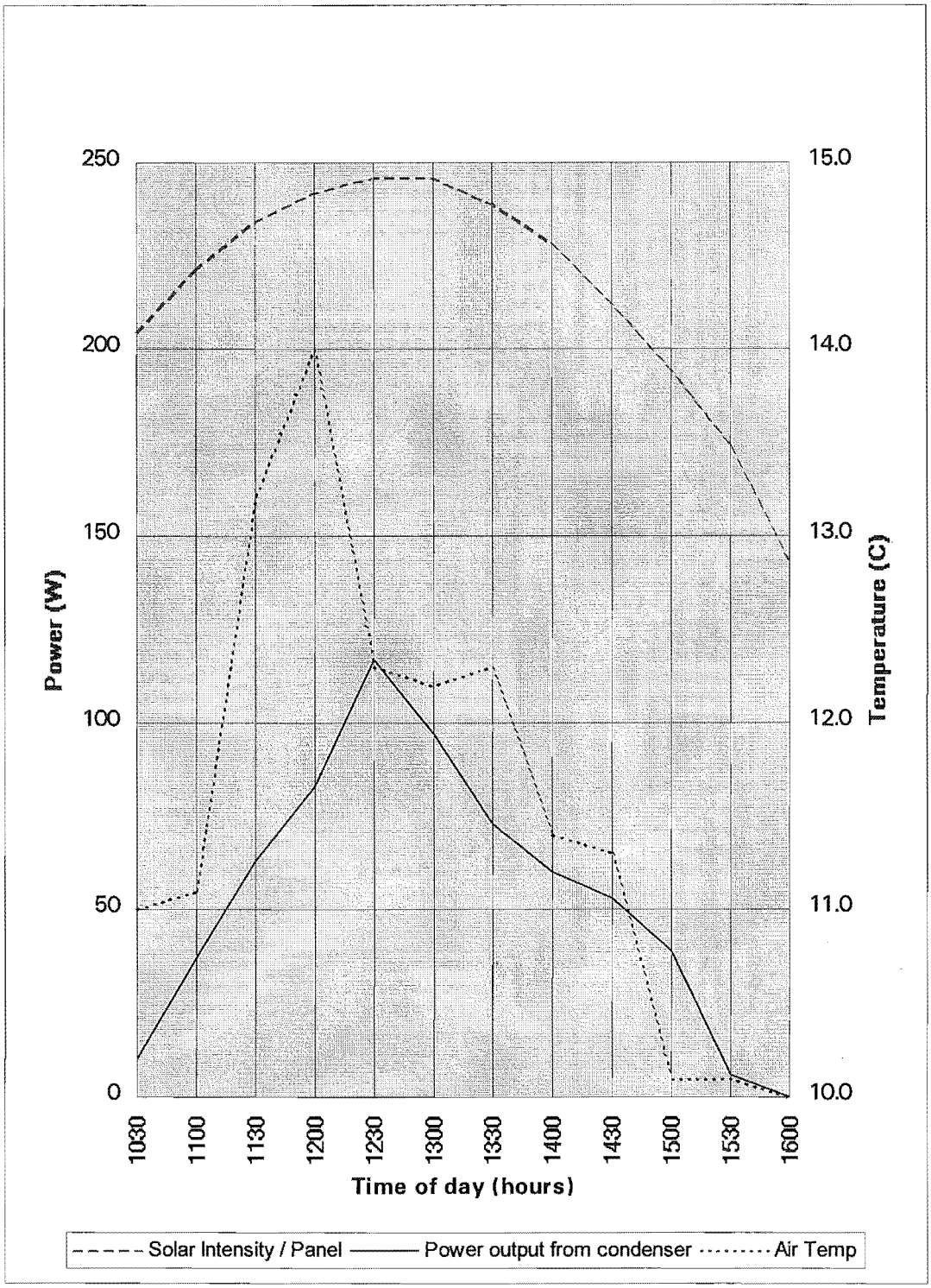

Figure 6.6 Graph for the data from an experiment of condenser tank at 35 °C nominal temperature, conducted on 27th September 1994.

6.4 GENERAL COMPARISON WITH OTHER FLAT PLATE SOLAR COLLECTORS

Flat plate solar collectors are often tested by the procedure recommended by the National Bureau of Standards. (Hillet et al.(1976) ; Beckman - 1977). The procedure is to operate the collector on a test stand under steady conditions, i.e., the solar radiation, wind speed, and the ambient and inlet fluid temperatures are essentially constant for a period such that the fluid outlet temperature and the useful energy gain do not change appreciably with time.

The useful energy gain from the collector at a given time is the difference between the amount of solar energy absorbed by the absorber plate and the energy lost to the surroundings. An equation which adequately describes the characteristics of almost all practical flat plate collector designs is (Beckman - 1977):

$$\dot{Q}_u = F_R\, A\, [I_T\, (\tau_g \alpha) - U_L\, (t_i - t_a)] \tag{6.1}$$

where

$\dot{Q}_u$ is the rate at which useful energy is collected in (W)

A is the collector area (m^2)

F_R is the collector heat removal efficiency factor

I_T is the rate at which solar radiation is incident on the collector surface per area (W/m^2)

τ_g is the solar transmittance of the glass cover

α is the solar absorptivity of the collector plate

U_L is the collector overall energy loss coefficient (W/m^2 °C)

t_i is the temperature of the fluid entering the collector (°C)

t_a is the outside ambient temperature (°C)

The result of collector tests is usually given in terms of collector efficiency, η, defined as :

$$\eta = \frac{\dot{Q}_u}{AI_T} = F_R(\tau_g \alpha) - F_R U_L \frac{(t_i - t_a)}{I_T} \qquad (6.2)$$

The results of collector tests are best presented as a plot of instantaneous efficiency η versus $(t_i - t_a)/ I_T$. This plot is commonly known as an HWB plot (Hottel, Whiller and Bliss Plot). If U_L is assumed to be constant, the plot results in a straight line having a slope equal to $F_R(\tau_g \alpha)$.

However the experiments described in this chapter were not conducted under steady state conditions to measure the instantaneous efficiency. Even so, it is considered to be worthwhile to compare the experimental results with those of other flat plate collectors. This particular solar panel is slightly different from other flat plate collectors in that heat losses occur from not just the solar panel itself but from the thermally-connected condenser as well. Therefore, a small modification to the equation is required to allow meaningful comparison of its performance with that of other conventional flat plate collectors. The equation that applies to this particular solar panel is :

$$\eta = F_R(\tau_g \alpha) - F_R U_L \frac{(t_e + t_{avg} - 2t_a)}{I_T} \qquad (6.3)$$

$$\downarrow \quad \downarrow \quad \downarrow \quad \downarrow$$

$$Y = \quad C \quad - \quad m \quad X$$

(Appendix E contains the derivation of this equation)

The relevant experimental data and derived values for Eqn 6.3 are tabulated in Table E.1 in Appendix E, and the graph of a best-fit line through these data is shown in Fig. 6.7. In Fig 6.8, this best-fit line is plotted together with the characteristic line for a typical flat plate solar collector fitted with single glazing and with a conventional (i.e. non-selective) absorber coating.

Slope =	-840.15
Y Intercept =	98.92

The best fit line coordinates	(0.118,0) and (0,98.92)

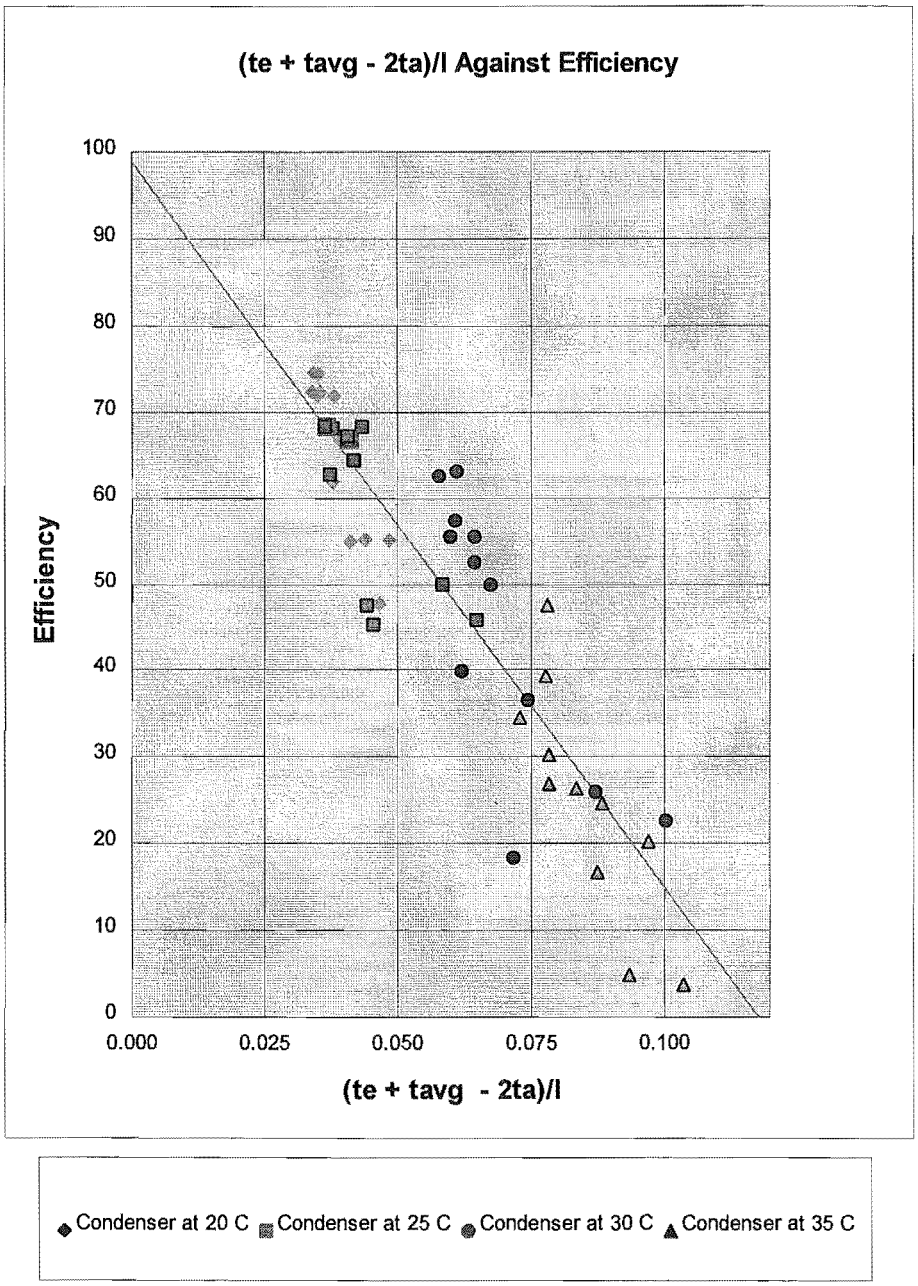

Figure 6.7 Plot of $(t_e + t_{avg} - 2t_a) / I$ versus efficiency

	$(t_e + t_{avg} - 2t_a)/I$	Efficiency
For tested solar panel	0.032	71.0
	0.105	10
For conventional flat plate collector (Ref : W. Beckman (1977)	0	77.24
	0.115	0

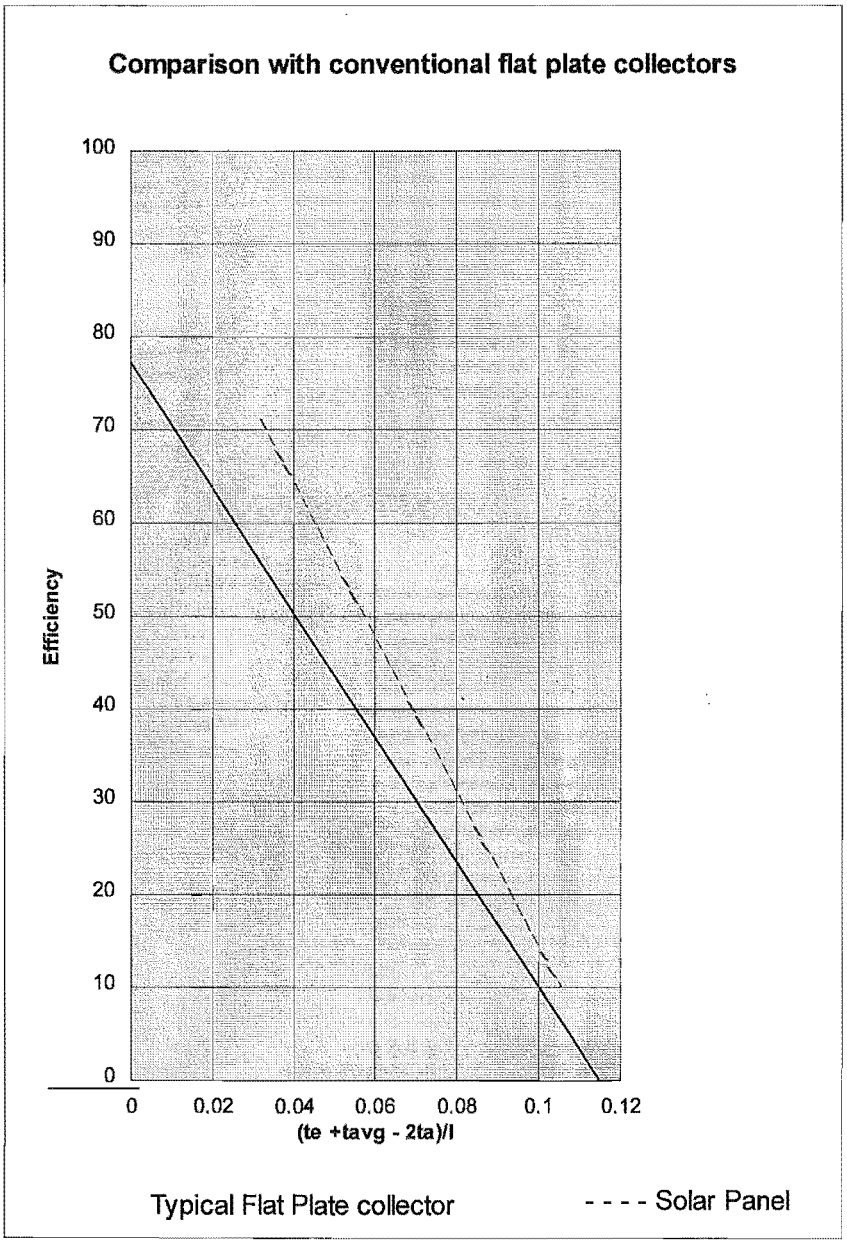

Figure 6.8 Comparison with conventional flat plate collector

Since a modified form of the HWB equation was used here (because of the additional heat loss opportunities in the experimental set-up), not too much significance can be placed on the actual numerical differences between the lines plotted in Fig 6.8. It should also be noted that the experimental data for the panel was obtained over a large range of solar and ambient conditions on each day, with significant departures from the steady state conditions which form the basis of HWB plots.

Overall, however, the panel's characteristics conform to the general trend of conventional flat plate collectors with efficiency decreasing more or less linearly as the temperature of the collector surface increases (thereby increasing heat losses to the surroundings).

Extrapolation of the test panel characteristic beyond the range shown in Fig 6.6 should not be attempted since there is no experimental data available outside this range.

CHAPTER 7

7. SOLAR WALL CONSTRUCTION AND TESTING

After getting a successful results from the tests described in the Chapters 5 and 6, it was decided to go ahead and build a prototype model wall. Six more panels were ordered to be manufactured. Unfortunately, pure n-hexane which was used in the first test panel was not readily available on the local market and the remaining stock at Thermocell Ltd was sufficient to fill only three panels. The local market did sell an alternative commercial grade hexane marketed as 'Pegasol 1516' which has almost the same physical and chemical characteristics except for having a small fraction of impurities. This was used to fill the remaining three panels. It was decided to build a wall in the north facing side of the testing room, the area of the test wall to be 1600 x 1600 mm corresponding to laying two 800 x 400 mm panels horizontally by 3 panels vertically. An experimental set-up was arranged inside the testing room to measure the heat output from one square metre area of the completed wall.

7.1 CONSTRUCTION OF THE PROTOTYPE WALL

Foamed polyurethane sheet of 50 mm thickness was cut to the right size and glued on the back side of each of the six panels. K-type thermocouples were soldered on to the evaporator and condenser of two panels (on one panel filled with n-hexane and on one panel filled with Pegasol 1516). The north wall of the temperature controlled test room included a large area (4.8 m wide by 2.4 m high) of removable 'Rudnev' panels consisting of 100 mm of expanded polystyrene (EPS) sandwiched between two facing sheets of painted steel. Two of these four wall panels were removed to leave a clear 2.4 m x 2.4 m opening in which to construct the prototype wall and its surroundings.

A local firm Firth Industries Ltd was very helpful for the building of this wall, and supplied all the necessary masonry materials and arranging a block-layer to construct the wall. The first two courses of blocks in the bottom part of the wall were only required to support the thermal storage blocks above and were covered by the evaporators of the bottom set of panels. For this particular purpose Firth Industries

supplied some of their patented 'Hot Blocks', which are a new type of block which they have developed recently to provide much improved insulative performance. These blocks are manufactured from a pumice-based aggregate (having lower thermal conductivity as well as density) and the block cavities, plus the outer 'leaf ' contains EPS plugs.

It was decided to build the wall with one side fitted with the three n-hexane panels and the other with the three Pegasol 1516 panels. Two courses of 'Hot Blocks' were laid and first two panels were placed against them. Clamps were used to hold the panels firmly in place against the blocks (see Fig 7.1). Another two courses of standard blocks were carefully positioned by lowering them over the projecting condenser tubes (see Fig 7.2). The third and fourth panels were placed in position against the front faces of the just laid blocks and firmly clamped (see Fig 7.3). The fifth course of blocks was lowered over the condenser tubes, and then, in mid-wall, seven K-type thermocouples were placed across the wall (one in each nodal position corresponding to the nodal positions in the model in Chapter 3) to measure the temperature profile through the wall (these thermocouple wires are visible in Fig 7.4). The sixth course of blocks were laid and final set of panels were placed in position before the seventh and eighth courses were laid to complete all block laying (Fig 7.5).

After a curing time of 24 hours, the wall's cavities were filled from the top with a concrete mixture (Fig 7.6). The wall was then left for two days for curing. The top two courses of blocks were exposed without an evaporator and that area was then also covered with a 50 mm polyurethane sheet (Fig 7.7), the front of which was covered with thin aluminium sheet and painted black to give a uniform appearance and insulative performance.

The gaps around the wall were framed with 100 mm x 50 mm timber and covered with 'Hardiesheet' from both sides, the cavities having been insulated with 100 mm fibreglass. Two more K-type thermocouples were placed as one in the air gap (between glass and evaporator) and another one on the glass (glued to the inside glass surface and covered with aluminium foil as a radiation shield) to measure the air gap temperature and the glass temperature respectively. A timber frame was constructed around the

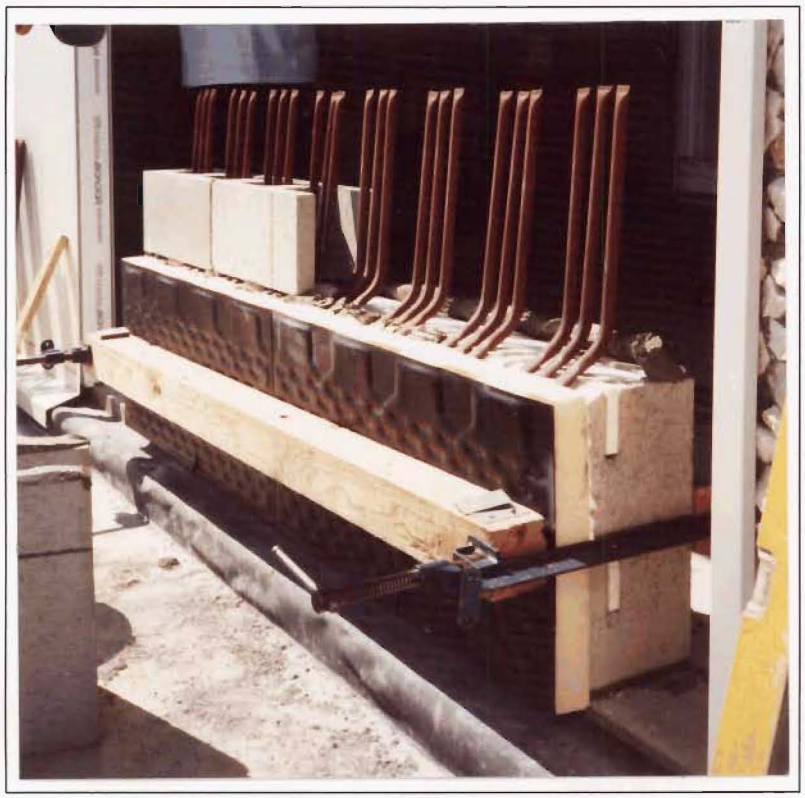

Figure 7.1 Solar wall after two courses of hot blocks and first set of panels had been laid

Figure 7.2 Solar wall after third course of blocks had been laid

Figure 7.3 Solar wall after second set of panels had been laid

Figure 7.4 Solar wall with thermocouples

Figure 7.5 Solar wall after all the courses of blocks had been laid

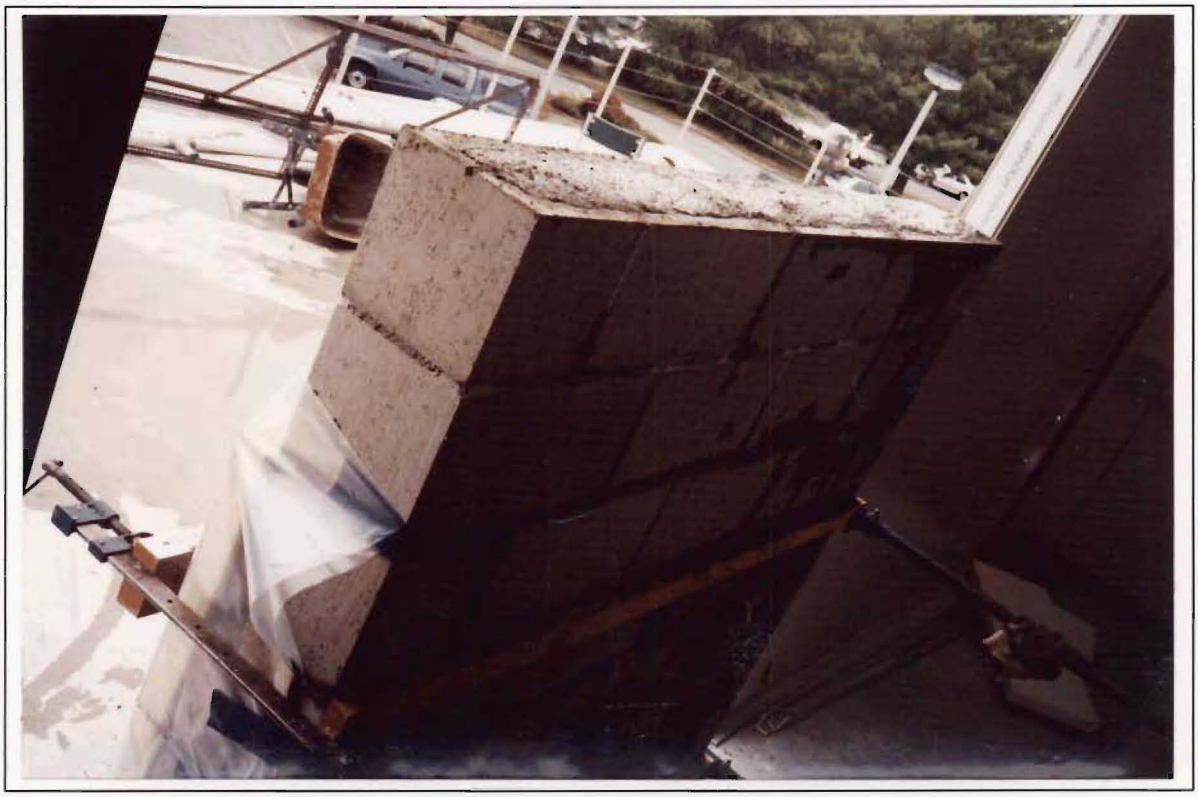

Figure 7.6 Solar wall after the cavities had been filled

Figure 7.7 Polyurethane sheets are covering the top two courses

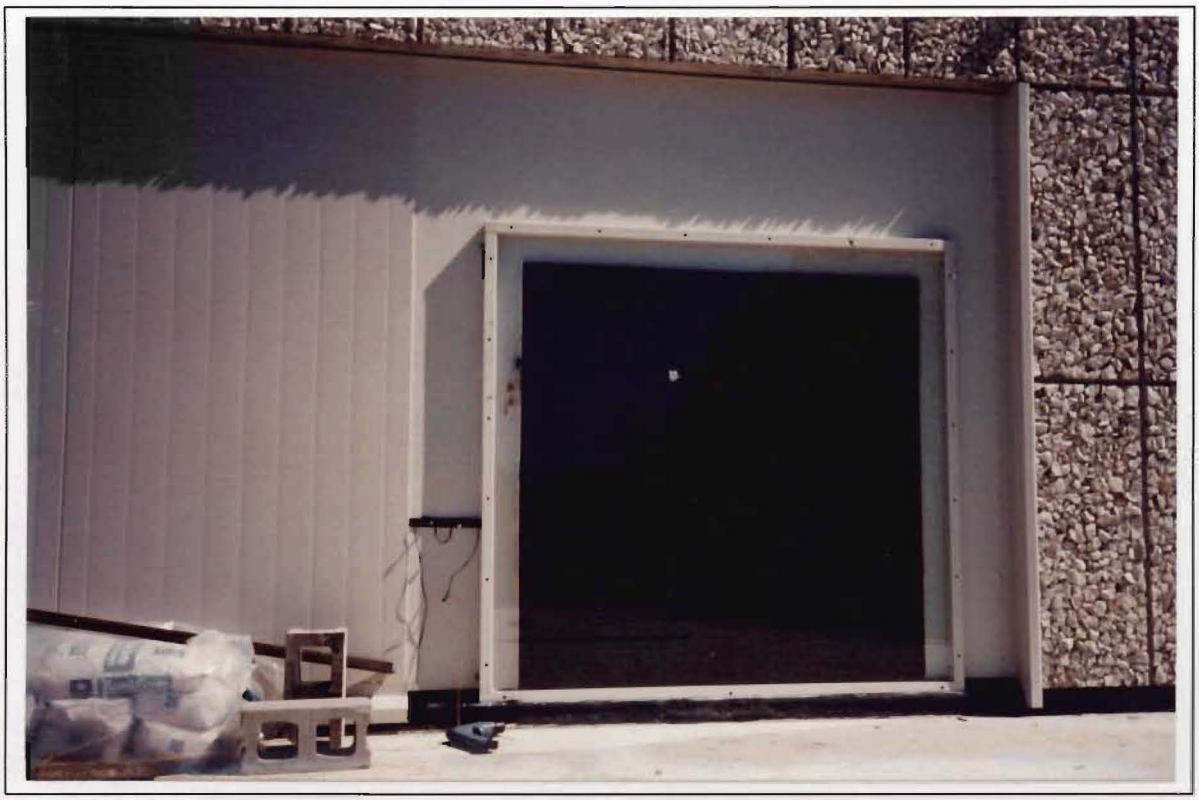

Figure 7.8 The finished solar wall covered by a 4 mm glass sheet

panel area and a single 4 mm glass sheet was fixed to cover the panels (Fig 7.8). Any gaps around the glass and its frame were sealed air tight with RTV, but four holes (two on top, two at bottom) were drilled and plugged with corks so that air could be allowed to circulate as the wall completed its initial heating up and drying out.

To measure the ambient air temperature, a thermocouple was also placed in louvred meteorological box, and this was fixed next to the built wall.

Each thermocouple was connected to a multiple switch unit, and its output was connected in, to a Yokogawa Model 2455 'K-type' digital readout instrument.

The Kipp and Zonan solarimeter (as used in the tests described in Chapter 6) was positioned in a plane parallel to the evaporator (and on the mid-panel level) to measure the average solar radiation available to the evaporators. The solarimeter was connected to the YEW chart recorder located in the room (as used before in Chapter 6).

7.2 CONSTRUCTION OF A CALORIMETER BOX

It was necessary to measure the heat flow from the wall accurately to show quantitatively the performance of the solar wall. Cromarty (1993) had designed a calorimeter box to conduct a similar type of experiment as his final year BE project. The calorimeter box was built according to his basic design with a few minor modifications.

7.2.1 Calorimeter box operating principle

The principle behind the operation of the calorimeter box is explained using the First Law of Thermodynamics for a closed system executing a non-cyclic process :

$$\int (\delta q - \delta w)_{net} = e_2 - e_1 \qquad (7.1)$$

where

q Heat transfer (J) (into system positive)

w Work done (J) (by system positive)

e Energy stored in system (J)

1, 2 Denotes initial and final states respectively

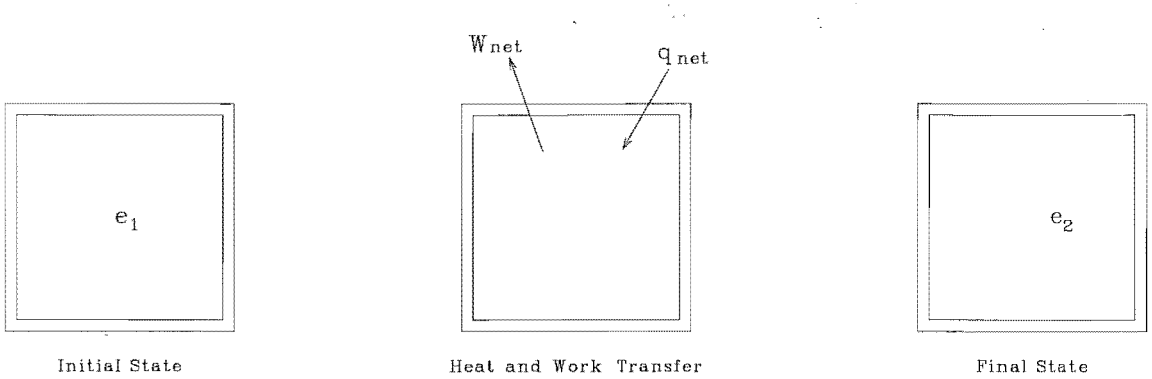

Figure 7.9 Closed system executing a non-cyclic process

In the case of the calorimeter box shown in Fig 7.9, there is no work done either by the system or on the system* , thus $w_{net} = 0$. Similarly, over the duration of sufficiently

* The fact that heat and work inputs of equal magnitude produce indistinguishable effects on a system mean that the work input via the electric fan (which will be described later) could be treated as an equivalent heat input.

long term testing, any instantaneous heat gains which are stored in the test cell fabric will eventually be removed as heat, therefore $(e_2-e_1) = 0$. So, the Eqn 7.1 reduces to :

$$\int \delta q_{net} = 0 \qquad (7.2)$$

This forms the basis of the calorimeter operation, where the heating and /or cooling requirements are measured in order to determine the loss/gain through the test cell envelope.

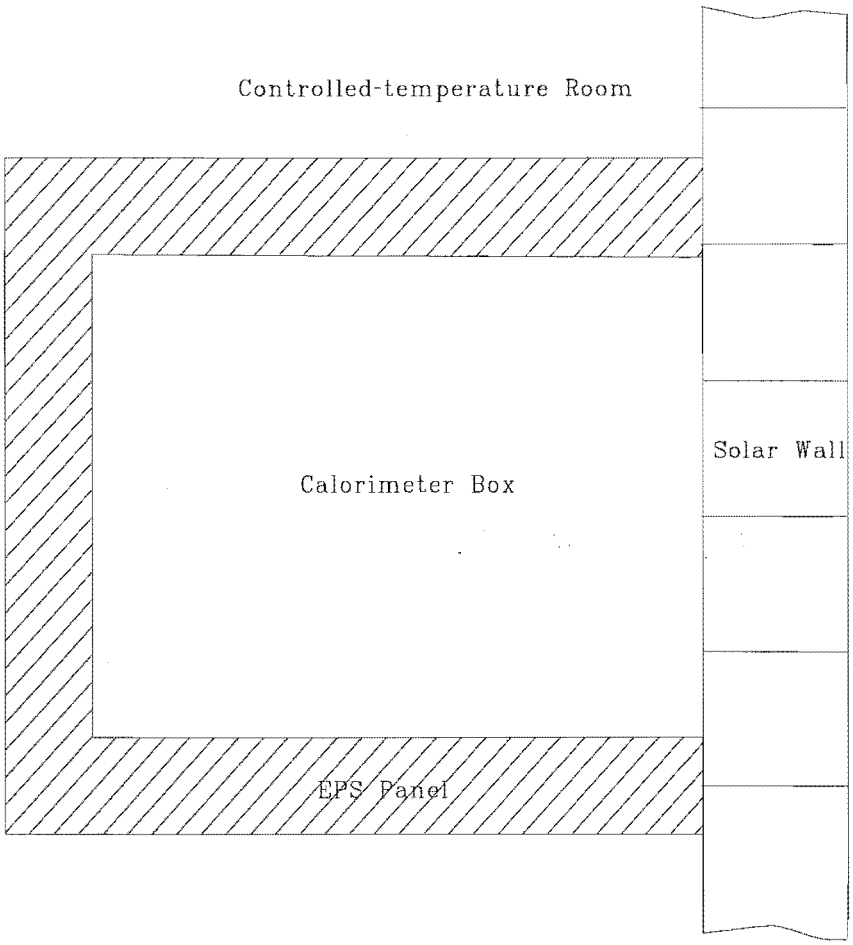

Figure 7.10 Calorimeter box with testing element

The test element (solar wall) had been constructed as an integral part of the north-facing wall of the temperature-controlled test room. The open fronted calorimeter box was to be placed against the solar wall as shown in Fig 7.10. The design goal was to achieve perfectly adiabatic boundaries on all surfaces other than the solar wall itself. This

would be achieved if no temperature difference ever occurred across these boundaries but the temperature control systems, particularly on the room side, were such that this condition would be unlikely to be achieved. Consequently, it was necessary to construct the box of sufficiently insulative materials that the small interior-exterior temperature differences which might exist across the box walls would result in heat flows negligibly small compared with those through the solar wall being tested. With near-adiabatic conditions ensured in this way, the operating principle of the box was reduced to one of continuously monitoring the necessary rate of heat supply to and/or heat removed from the calorimeter box to keep the box interior at the same nominal temperature as that of the surrounding room (20°C). This net heat transfer could then be interpreted to be equivalent to the rate at which the solar wall under test was introducing heat into (or removing heat from) the box.

7.2.2 Construction

A base frame of the calorimeter box was made from mild steel angles and mounted on four castor wheels for free manoeuvrability. The calorimeter box was assembled on top of the base. An open fronted box built from pre-cut 150 mm 'Rudnev' pre-finished structural insulation panels was designed and purchased. The bottom and back sides of the calorimeter box were fixed to the mild steel frame. Modified air duct-work was also assembled and attached inside the same unit as shown in Fig 7.11. Air flow from the standard fan heater to be used in the temperature control system had been measured to be around 1.8 m/s and, through increasing the cross-sectional area of ducting on either side of the heater, the air velocities at entry to and exit from the ductwork were reduced to around 0.3 m/s. In an attempt to ensure that the temperature of processed air passing back into the box was at a temperature very close to 20°C (so that temperature differentials across the box walls would be minimised), a secondary flow of box air was induced into the primary flow and mixed prior to final discharge. In this way, the temperature-changing effects of the cooling coil and heater element were only significant within the primary ductwork itself and had been diluted appreciably at points where the air might contact the box boundaries.

The other insulation panels were assembled separately to cover two sides and the top of the calorimeter box, as shown in Figure 7.12. This unit was pushed into the other unit and all the joints were tightened by toggle clamps. This cover assembly could be easily removed by releasing the ten toggle clamps. In addition all joints were sealed by masking tape to prevent any air movement through them. The completed calorimeter box is shown in Fig 7.13

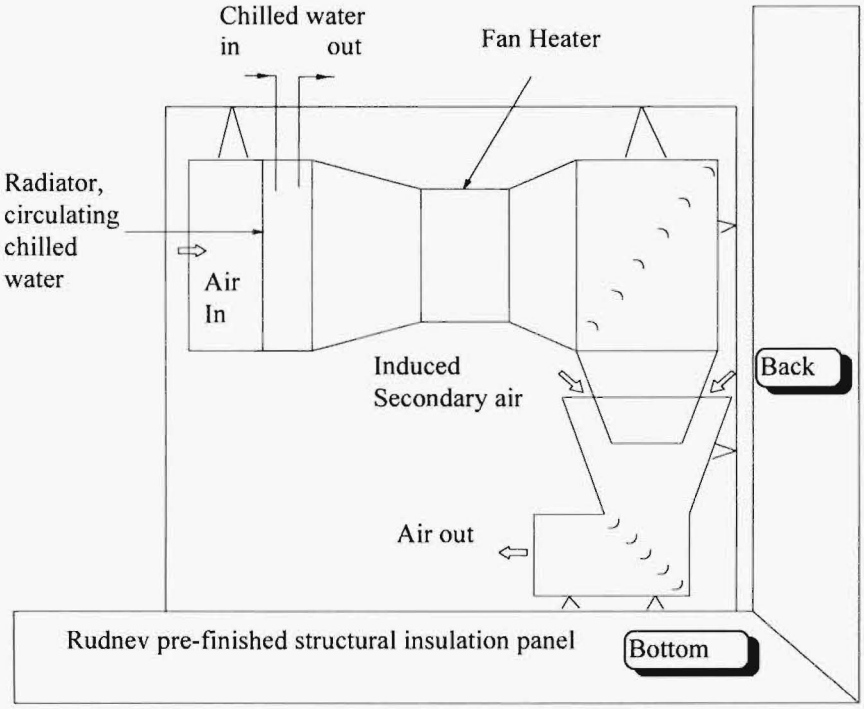

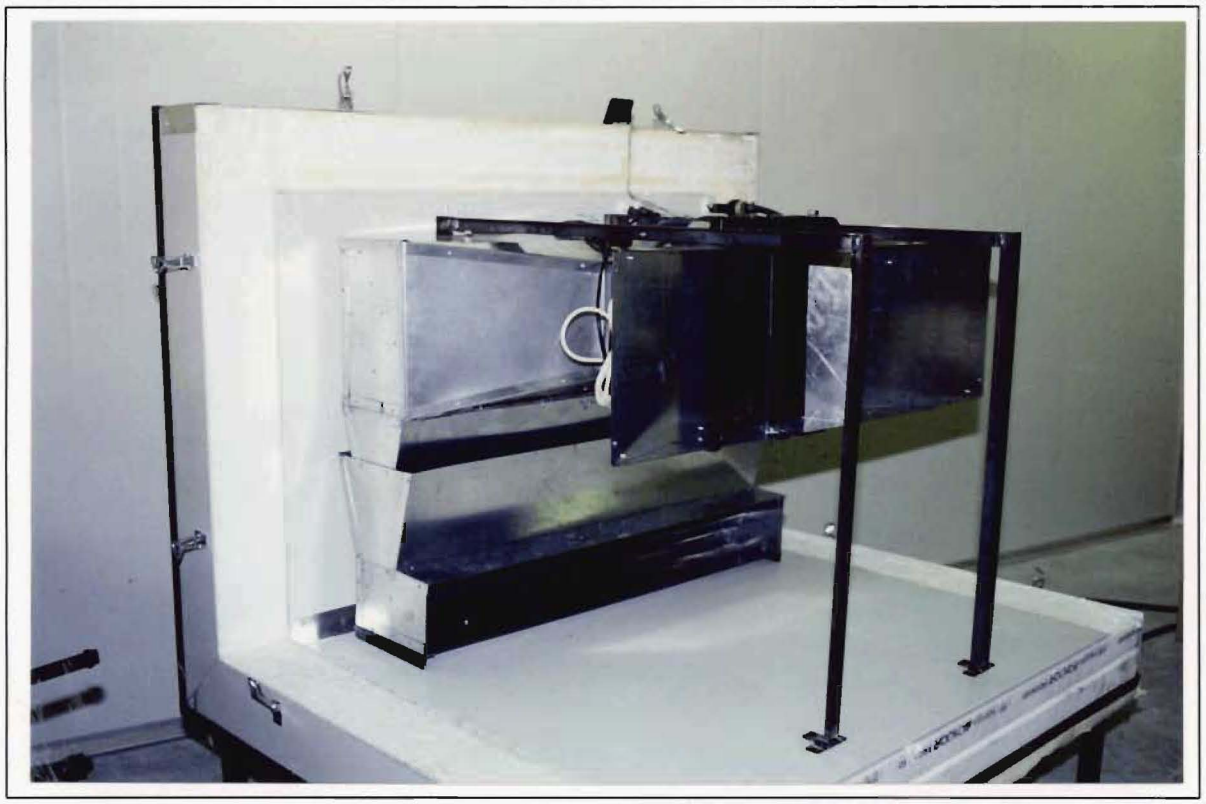

Figure 7.11 Part of calorimeter box with air duct-work

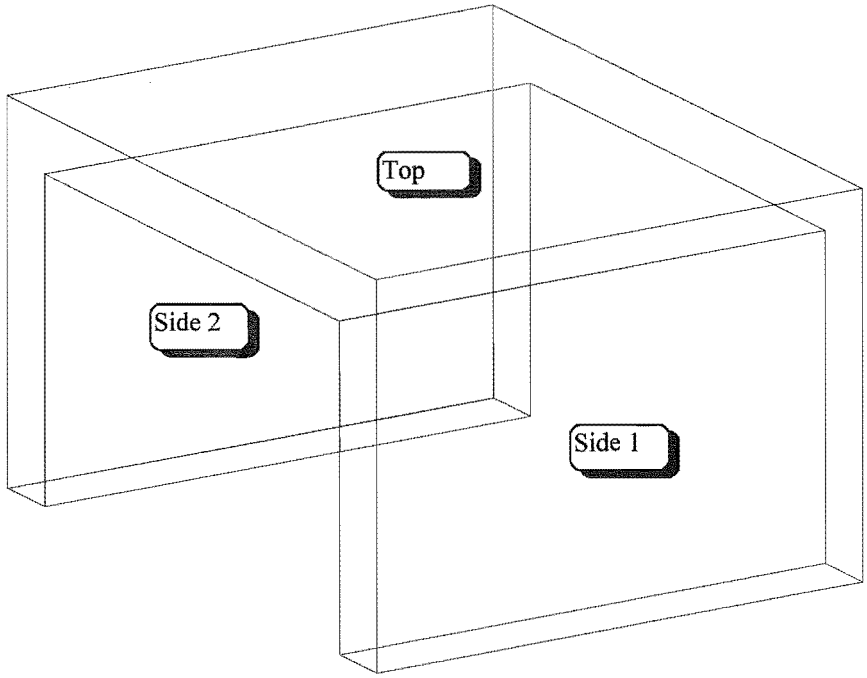

Figure 7.12 Part of calorimeter box

7.3 EXPERIMENTAL SET-UP

The experimental set-up was arranged as shown photographically in Fig 7.14 and schematically in Fig 7.15. Appropriate instrumentation was arranged for the calorimeter box. The temperature sensor of the fan heater was placed in the calorimeter box air space and it was surrounded by a chrome-plated pipe as a radiation shield. The electronic control for the fan heater element was also placed within the box and its control knobs were separated from the thermostat unit and placed outside the calorimeter box for ready access and adjustment. An 'English Electric Type C31 B/M Kilowatt-hour Meter' (300 disk revolutions per kWh) was connected in series between the 240 VAC single-phase supply and the fan heater to measure the total electrical energy used to heat the calorimeter box and circulate the air. One PRT probe was placed next to the temperature sensor of the fan heater (inside the chromed pipe) to measure the box temperature accurately. It was realised that if the assumption of the insulated walls of the box behaving adiabatically was to be valid, it would be necessary to minimise temperature gradients through the insulation, including those points where the box would be in contact with the solar heated wall. For this reason a 50 mm wide

Figure 7.13 Complete construction of the calorimeter shell

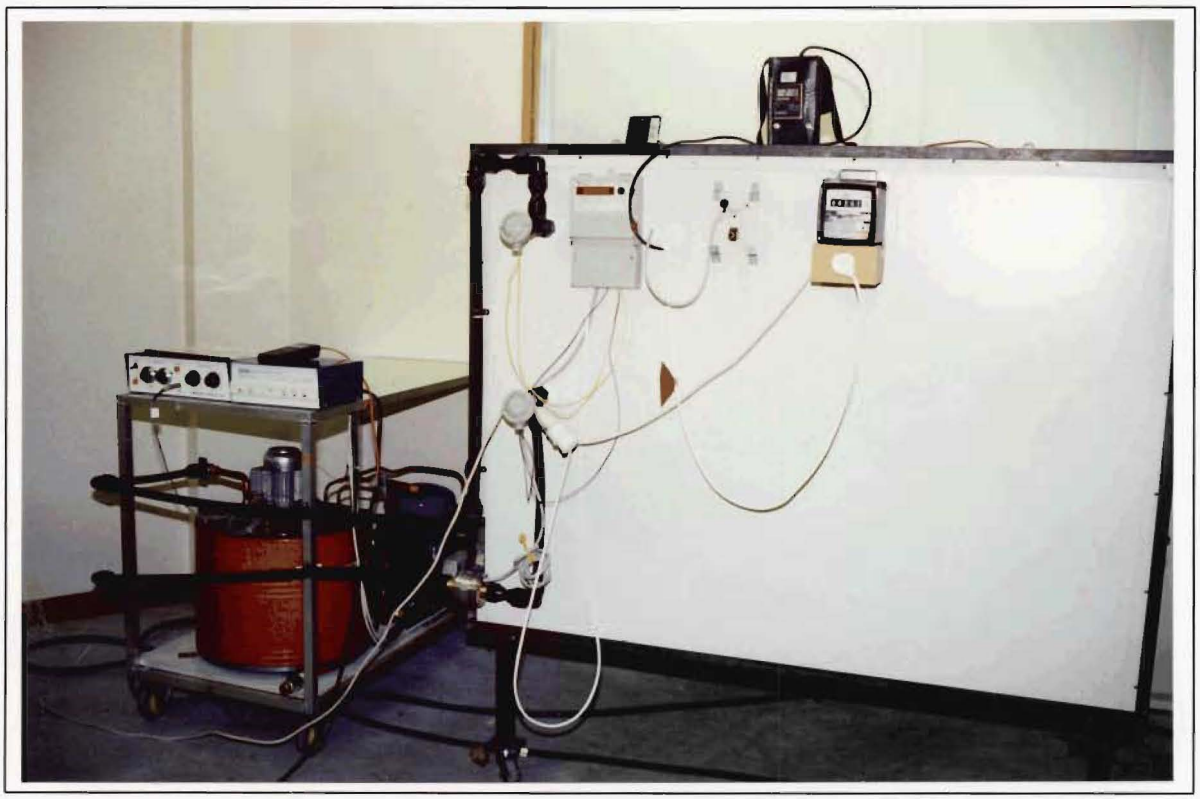

Figure 7.14 Calorimeter box in operation

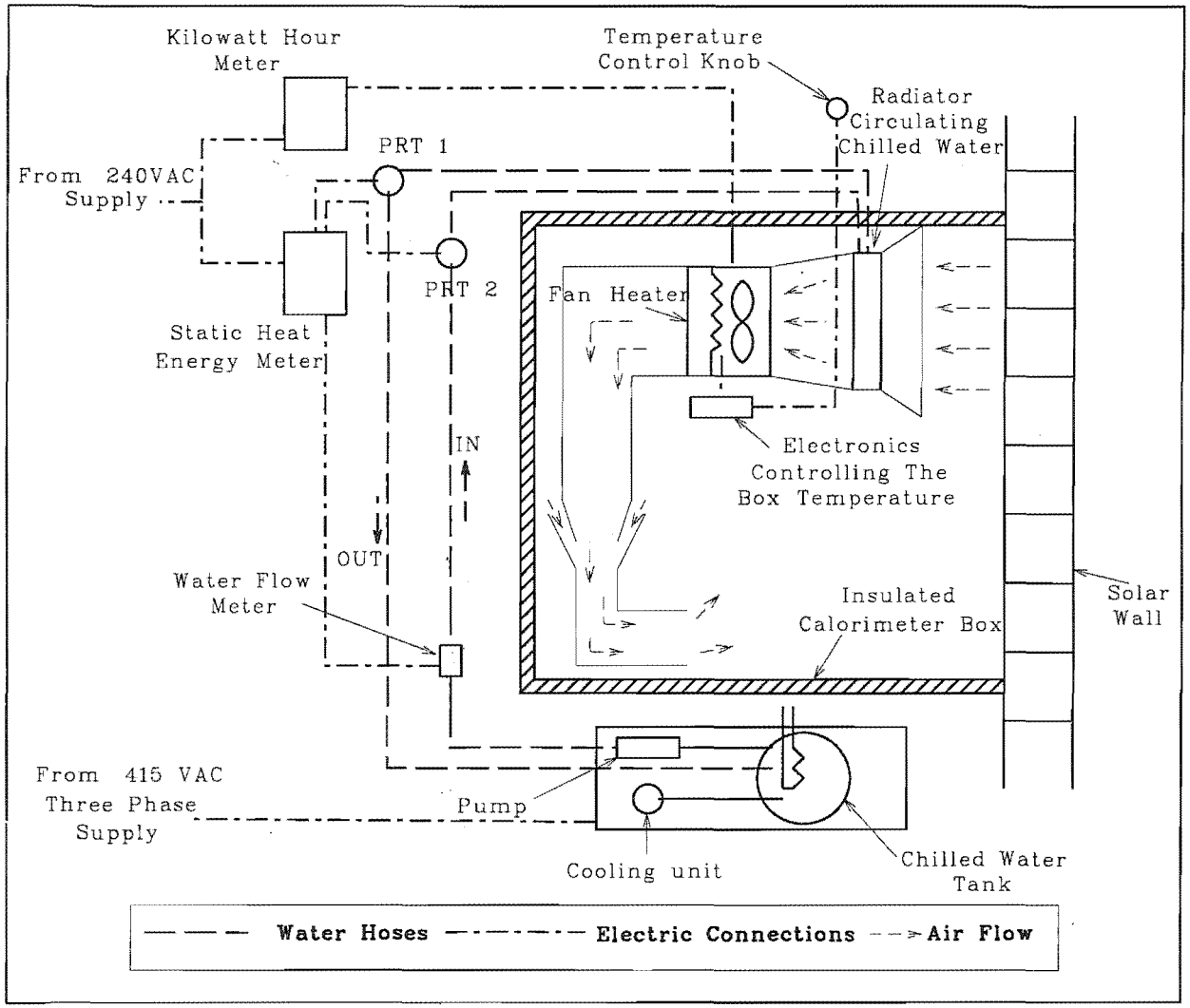

Figure 7.15 Schematic of Solar wall Performance Test

strip of Hardisheet was placed around the periphery of the open side of the calorimeter box (see Fig 7.16). The front area of the EPS panel also covered with aluminium foil to avoid any radiation heat gain from the solar wall. Although, the added strips of Hardisheet represented poor insulation in comparison with the EPS panels, they represented in total only about 3 % of the box surface area. The complete calorimeter box, now assembled as one unit, was placed tightly against the solar wall and all joining points were sealed with RTV.

A thermostated chilled water circulator, custom-built to the Mechanical Engineering Department's specifications was placed next to the calorimeter box, and drew its power from a 415 VAC three phase power supply. The outlet line of this chilled water circulator was connected by hoses to the magnetic flow meter of a 'ENERMET' static heat energy meter model (P)8EVL-MP 115, and then on to the calorimeter box chilled water inlet line. The outlet line from the calorimeter box was connected back to the return line of the water circulator unit to re-chill and recirculate the water. The two PRT probes from the static heat energy meter were connected, one in the inlet line and the other in the outlet line of the

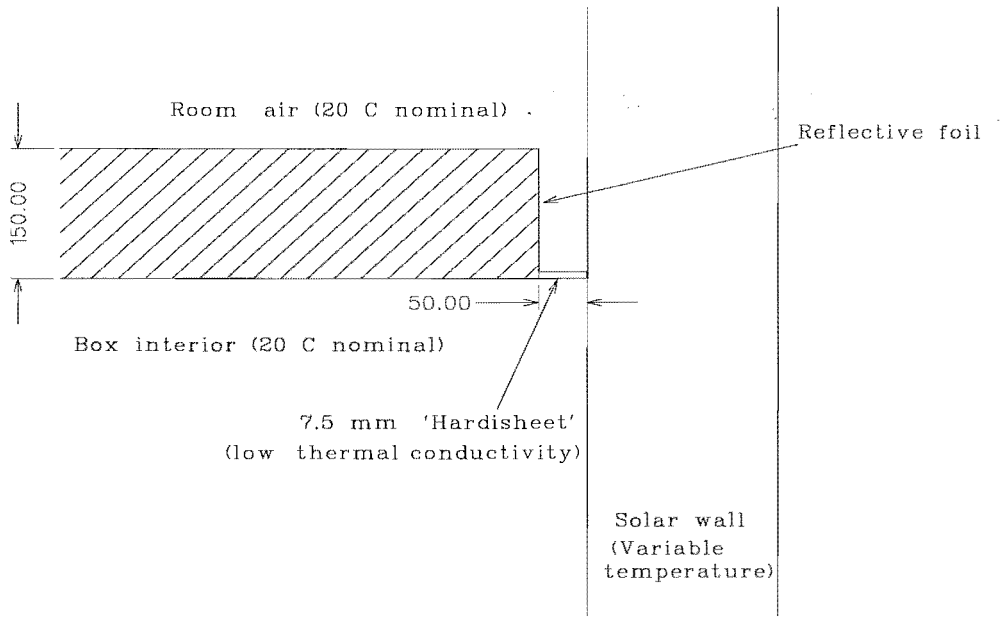

Figure 7.16 Open side of the calorimeter box with added Hardisheet and aluminium foil

calorimeter box chilled water circuit. As per the instructions with the heat meter, the same length of 0.5 mm^2 electric wires were used to connect the PRT probes to the static heat energy meter. The flow meter cable also connected to this unit. The operation of the calorimeter box unit was such that the air would be circulated in the box by the fan continuously and that cooling would also take place continuously at a fixed rate. The heating unit would come on and off as required to control the temperature at a set level. For this particular experiment the box temperature was fixed at 20°C.

The testing room temperature was controlled by its air-conditioning unit within a tolerance of ± 1.5°. Another PRT probe was placed inside a radiation shield and kept next to the box to measure the room temperature.

Each thermocouple was connected through a multiple switch unit to the Yokogawa Model 2455 K-type digital readout instrument used in previous tests.

7.4 READINGS AND CALCULATIONS

The thermostat of the fan heater unit was adjusted to maintain the box temperature at the required 20°C.

The controls of the thermostated chilled water circulator water tank were adjusted to provide a source of chilled water at 10°C. The control valve for the water flow was set to meet the condition suitable for the capabilities of the required static heat energy meter. This meter required a water flow rate of between 0.015 m^3/h and 3 m^3/h for acceptable flow meter accuracy, and could resolve water temperatures to 0.1°. The selected compromise was to have a flow such that a temperature difference of 2 to 2.5° was obtained, corresponding to a flow of about 0.10 m^3/h.

When the cooling system started to operate, it was necessary to make fine adjustments to the thermostat of the heating unit to maintain 20°C box temperature. The air-conditioning unit in the testing room was also controlled to maintain a 20°C nominal room temperature. After reaching a steady state, the readings of kilowatt-hour meter and static heat energy meter (energy gained in MWh, flow rate in m^3/h and the

temperature difference between inlet and outlet in degrees) were noted down against time of the day. As explained in Section 7.2.1, under these conditions all boundaries of the box (except for the front face) were in essentially adiabatic, and the total heat energy gain/loss from or to the wall should be equal to the difference between the readings of total heat gain by the chilled water and the total heat supplied to the system by the fan heater unit i.e. :

Energy gained from the wall = Water energy meter reading-Electrical energy meter reading

The experimental data was collected under two different categories :

1. A first set of data was collected to analyse the temperature patterns of the wall and to allow comparison with the model predictions (called hereafter the 24-hour test). This experiment was conducted during the mid-summer period, starting on 19th December 1994 (three days earlier than the longest day of the year) and the 24-hour test was conducted on a clear sunny day of 23rd and 24th December 1994. The data were collected every hour of the day for a continuous 24 hour time period and are tabulated in Table F.1 in Appendix F. The emphasis in this test was on the *temperatures* occurring through the wall and not on energy flow (since the test was too short to be able to assume that the initial and final stored energies were equal).

2. A second set of data was collected to analyse the long-term performance of the wall. The long-term test was necessary for a number of reasons :
   (a) The water energy meter would only resolve to 1 kWh as its smallest unit and long-term data gathering was necessary to minimise errors.
   (b) Because solar and outdoor temperatures can be very variable from day to day, a test which included a range of daily weather patterns was necessary in order to gauge the average performance of the wall.
   (c) Unless the stored energy in the wall at the end of a test period was the same as it was initially, the net measured energy flow could not be interpreted to be the net energy gained by the box from the wall. For a long-term test, any difference between the initial and final stored energy would be much less than the net

measured energy flow and this potential inaccuracy would become acceptably small.

This experiment was begun on 1st February 1995 and continued for a period of four weeks. The data were collected every day at 0900 hours and are tabulated in Table F.2 in Appendix F.

7.5 ANALYSIS OF THE 24-HOUR TEST

The important data for this analysis were selected from Table F.1 (from Appendix F) and tabulated in Table 7.1 with the corresponding temperature curves plotted in Fig 7.17.

From the results it was observed that both the n-hexane and the 'Pegasol 1516' panels were working in a very similar manner. It was also clear that the wall was performing generally as expected from the model. The wall was retaining stored energy throughout the night and the interior wall temperature never dropped below 20°C at any time of the day even though the outdoor air temperature dropped to 8.3°C. The interior wall surface temperature dropped to a low of 22.5°C at 0900 hours and climbed up as the sun shone to its maximum of 30.1°C at 1700 hours. The surface temperature was always above 27°C for the period when occupants need more evening comfort (between 1700 and 2200 hours). The evaporator reached its highest temperature value of 43.1°C at 1400 hours, showing that a time lag of about three hours existed between the maxima of the interior and exterior of the solar wall. Overall, the interior surface temperature of the wall fluctuated between 22.5°C and 30.1°C while the evaporator surface temperature fluctuated between 12.3°C and 43.1°C and ambient air temperature fluctuated between 8.3°C and 23.1°C.

Table 7.1 Different nodal temperatures (°C) of the wall for 24-hour test

HR	t_1	t_2	t_3	t_4	t_5	t_6	t_7	t_8*	t_9	t_{air}
0	26.0	27.6	28.6	29.2	29.6	29.8	29.7	16.0	13.3	11.6
100	25.4	26.8	27.8	28.4	28.7	29.0	28.8	15.9	13.4	11.7
200	25.1	26.3	27.2	27.6	28.0	28.2	28.0	14.6	11.7	10.8
300	24.5	25.7	26.5	27.0	27.2	27.4	27.3	13.7	11.2	10.7
400	24.2	25.2	26.0	26.3	26.6	26.7	26.6	14.8	13.0	11.5
500	23.6	24.7	25.4	25.7	25.9	26.0	26.0	14.2	11.3	10.3
600	23.3	24.3	24.9	25.2	25.4	25.5	25.4	12.4	9.2	8.3
700	22.8	23.6	24.2	24.4	24.6	24.6	24.6	19.2	12.5	9.5
800	22.7	23.4	24.0	24.2	24.4	24.5	24.6	25.2	15.8	11.3
900	22.5	23.2	23.8	24.1	24.4	24.5	24.6	28.4	19.4	14.0
1000	22.8	23.7	24.5	24.7	24.9	24.8	24.8	29.2	21.8	15.2
1100	23.5	24.3	25.2	25.6	25.7	25.5	25.6	32.7	24.3	16.1
1200	24.5	25.7	26.9	27.6	27.5	27.2	27.1	36.1	29.9	18.7
1300	25.5	27.1	28.7	29.4	29.3	28.9	28.9	38.8	36.4	23.1
1400	28.6	30.5	31.7	32.5	32.4	31.9	32.0	42.0	37.1	19.5
1500	28.8	30.7	32.5	33.5	33.6	33.4	33.4	41.1	32.8	19.4
1600	29.9	32.3	34.1	34.9	35.2	35.1	35.1	40.2	29.6	17.3
1700	30.1	32.4	34.1	35.0	35.4	35.5	35.5	38.8	26.3	16.7
1800	29.5	31.7	33.6	34.4	34.9	35.3	35.3	36.8	23.7	15.3
1900	28.8	31.0	32.6	33.4	34.1	34.5	34.5	32.3	20.4	14.5
2000	28.3	30.2	31.7	32.5	33.1	33.6	33.5	26.0	17.2	13.0
2100	27.7	29.5	30.9	31.8	32.3	32.7	32.6	19.7	14.7	12.1
2200	27.0	28.8	30.0	30.6	31.0	31.4	31.4	16.7	13.4	11.7
2300	26.5	28.1	29.2	29.9	30.2	30.5	30.4	16.2	13.4	11.8
2400	26.0	27.6	28.6	29.2	29.6	29.8	29.7	16.0	13.3	11.6

* The mean value of n-hexane and Pegasol 1516 evaporator temperatures.

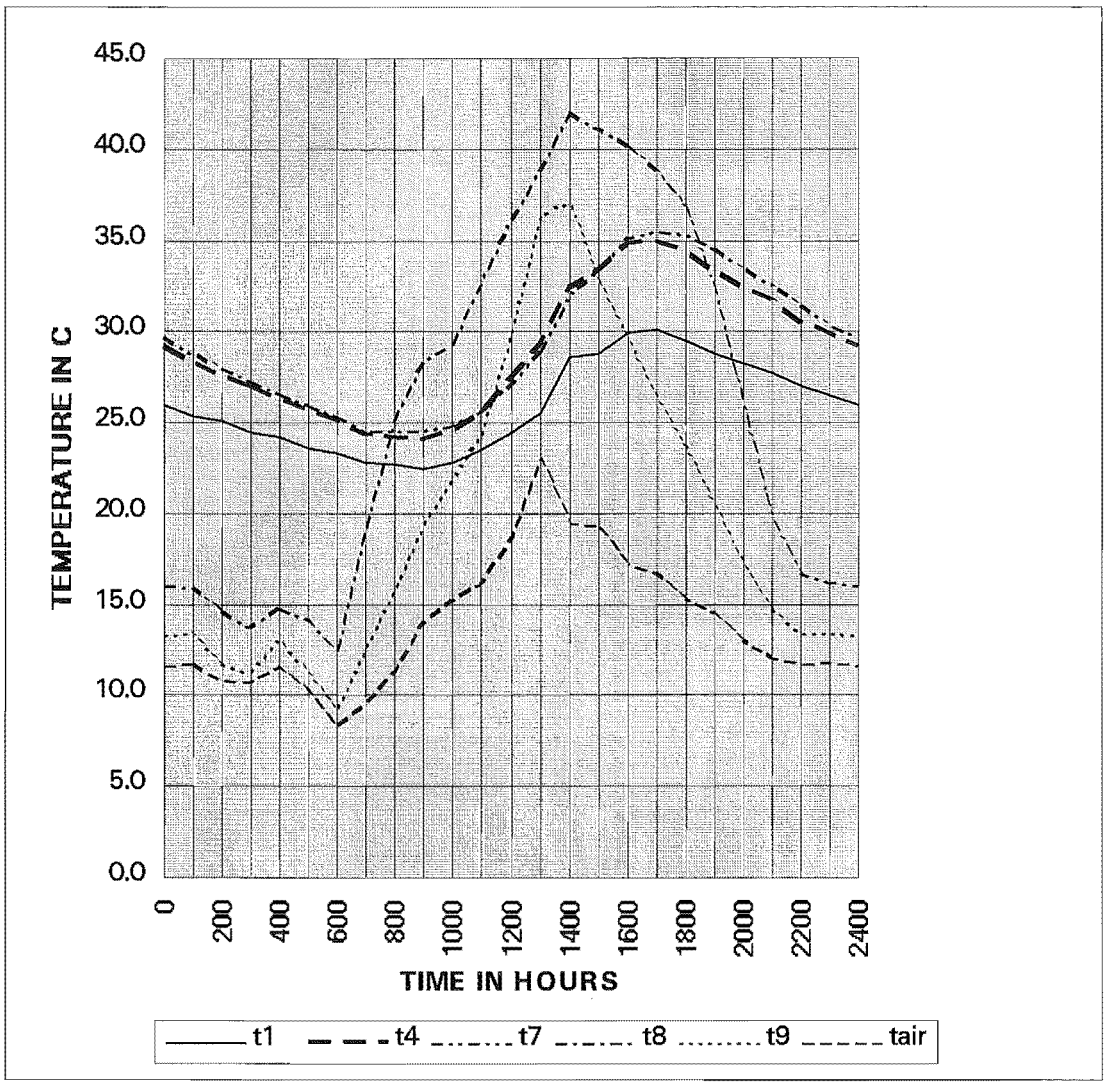

Figure 7.17 Record of selected nodal temperatures of the solar wall for 24-hour test

7.6 ANALYSIS OF THE LONG-PERIOD TEST

The important data from Table F.2 of Appendix F. have been selected and tabulated in Table 7.2.

Table 7.2 Measured energy values and approximate net energy gain from the wall.

Date	Area* (cm^2)	Energy available on a vertical surface measured value (MJ/m^2)*	Cooling in MWh Reading	Heating in kWh Reading	Net gain from wall (kWh/m^2) (Approx)
1/02/95	33.3	5.3	0.167	363.5	
2/02/95	92.6	14.8	0.174	369.0	1.5
3/02/95	25.0	4.0	0.181	373.7	2.3
4/02/95	40.2	6.4	0.188	379.5	1.2
5/02/95	30.1	4.8	0.195	385.3	1.2
6/02/95	61.8	9.8	0.201	391.4	-0.1
7/02/95	68.1	10.8	0.208	396.8	1.6
8/02/95	104.6	16.7	0.215	402.0	1.8
9/02/95	54.3	8.6	0.222	406.5	2.5
10/02/95	75.0	11.9	0.229	411.8	1.7
11/02/95	75.4	12.0	0.236	417.0	1.8
12/02/95	79.0	12.6	0.243	422.0	2.0
13/02/95	102.3	16.3	0.250	427.0	2.0
14/02/95	102.3	16.3	0.257	431.5	2.5
15/02/95	106.5	17.0	0.264	435.8	2.7
16/02/95	94.0	15.0	0.271	440.0	2.8
17/02/95	101.9	16.2	0.278	444.7	2.3
18/02/95	90.0	14.3	0.285	449.0	2.7
19/02/95	54.2	8.6	0.292	453.5	2.5
20/02/95	18.0	2.9	0.298	458.7	0.8
21/02/95	84.5	13.5	0.305	465.0	0.7
22/02/95	41.7	6.6	0.312	470.2	1.8
23/02/95	23.7	3.8	0.319	475.7	1.5
24/02/95	74.2	11.8	0.326	481.6	1.1
25/02/95	106.6	17.0	0.333	486.9	1.7
26/02/95	113.0	18.0	0.340	491.2	2.7
27/02/95	55.6	8.9	0.347	494.8	3.4
28/02/95	29.9	4.8	0.354	499.0	2.8
1/03/95			0.361	505.8	0.2

* Solar radiation was plotted in a chart, and the area under that curve was measured by planimeter.
* = (Area * 44.25 * 3.6 / 1000)

Net energy gain from wall is tabulated under the last column of the previous table is an approximate value because of the following reason :

The static energy meter reading could be resolvable only up to 1 kWh. So, the error band of this column calculation is very high, but these values were calculated and tabulated to do a rough comparison with the previous day solar radiation.

7.6.1 Energy calculations

Total externally available solar energy for the period from 1-2-95 to 1-3-95

$= 308.69\ MJ/m^2$

$= (85.747\ kWh/m^2)$

Total cooling in the calorimeter box from 1-2-95 to 1-3-95 = 361-167

$= (194\ kWh/m^2)$

$= 698.4\ MJ/m^2$

Heat supplied by the fan heater in the calorimeter box from 1-2-95 to 1-3-95

$= 505.8\text{-}363.5$

$= (142.3\ kWh/m^2)$

$= 512.3\ MJ/m^2$

$\therefore Q_{loss}$ to the calorimeter box from wall

$= 194\text{-}142.3$

$= (51.7\ kWh/m^2)$

$= 186.1\ MJ/m^2$

Efficiency of the wall $= 51.7/85.75$

$= 60.3\ \%$

Averaged over the full 24 hours of each day

$= (1.85\ kWh/m^2)$

$= 6.65\ MJ/m^2$

Power intensity from wall to the calorimeter box $= 77.1\ W/m^2$

The period covered for this long-term test contained a variety of Christchurch summer weather patterns. The day on 26 February 1995 was the hottest day during the period and produced 18 MJ/m^2 (5000 Wh/m^2) on a vertical surface. At the other extreme, 20 February 1995 was a cold and rainy day which produced only 2.9 MJ/m^2 (796 Wh/m^2) on the vertical surface. From 3/2/95 to 5/2/95 was the consecutive coldest period and the three days from 13/2/95 to 15/2/95 represented the consecutive hottest days in the test period.

The single most significant result from this long-term test was that the wall transferred around 60% of the solar energy available at its external surface into the interior of the room.

CHAPTER 8

8. COMPARISON, MODIFICATION AND PREDICTION

8.1 MODEL COMPARISON WITH 24-HOUR TEST

After obtaining the results from the prototype wall, a comparison was made with the results from the initial model. To achieve this the model was simulated again for summer solar data. All the simulated results containing nodal temperatures are tabulated in Appendix H. Three important nodal temperatures i.e. interior wall temperature (node 1), condenser node temperature (node 4) and evaporator temperature (node 8) were selected from Table H.1 and H.2 of Appendix H and are tabulated in Table 8.1 and plotted in Fig 8.1.

8.1.1 Analysis

As explained earlier in Chapter 3, the ground-reflected portion of the solar radiation was not considered in the initial modelling. Due to this, the nodal temperatures in the simulation were lower than the actual results and this is clearly seen in Fig 8.1.

In the model the condenser temperature was replaced with the evaporator temperature, whenever the evaporator temperature exceeded the condenser temperature (i.e. the panel in heat transferring mode). Thus the assumption in the model was that the panel would act as a 100 % efficient heat pipe. This is apparent in Fig 8.1 as both 't_4 model' and 't_8 model' curves are coincident during this period. But in the real situation, the panels did not behave in this ideal manner with the result that some temperature difference existed between the evaporator and the condenser during heat transferring mode. This temperature difference appeared to depend on both the temperature of the evaporator and time of day. The initial assumption of equating these two temperatures while in heat transferring mode was therefore invalid for the real situation.

In the prototype wall, the dummy aluminium sheets covering the top two courses of concrete blocks had a significant effect on its performance. The dummy plates

stagnated while the sun shone and increased the air-gap temperature between the front glass and the evaporator. This air gap temperature was also high on the top part of the wall and not uniform over the whole wall area. The elevated air-gap temperature helped to reduce any convective heat loss from the evaporator to the neighbouring glass node. Thus indirectly (and unintentionally) the stagnating top panels had an overall favourite effect on the wall's performance and this had not been allowed for in the model either.

For these two reasons (i.e. ground-reflected radiation and "artificially-elevated" air gap temperature) it was considered necessary to refine the model to enable it to be used the model more accurately the real performance of the wall.

Table 8.1 Selected temperature values from model and 24-hour test

HR	t_1 model	t_1 test	t_4 model	t_4 test	t_8 model	t_8 test
0	22.9	26.0	24.0	29.2	17.8	16.0
100	22.6	25.4	23.6	28.4	17.3	15.9
200	22.4	25.1	23.2	27.6	16.9	14.6
300	22.1	24.5	22.9	27.0	16.6	13.7
400	21.9	24.2	22.6	26.3	16.5	14.8
500	21.7	23.6	22.3	25.7	17.3	14.2
600	21.5	23.3	22.1	25.2	20.2	12.4
700	21.4	22.8	21.9	24.4	21.9	19.2
800	21.3	22.7	21.9	24.2	21.9	25.2
900	21.3	22.5	22.4	24.1	22.4	28.4
1000	21.6	22.8	23.6	24.7	23.6	29.2
1100	22.3	23.5	25.2	25.6	25.2	32.7
1200	23.3	24.5	26.8	27.6	26.8	36.1
1300	24.3	25.5	28.0	29.4	28.0	38.8
1400	25.0	28.6	28.5	32.5	28.5	42.0
1500	25.3	28.8	28.3	33.5	28.3	41.1
1600	25.3	29.9	27.6	34.9	27.6	40.2
1700	25.0	30.1	27.1	35.0	27.1	38.8
1800	24.6	29.5	26.6	34.4	26.6	36.8
1900	24.3	28.8	26.1	33.4	23.5	32.3
2000	24.0	28.3	25.7	32.5	20.9	26.0
2100	23.7	27.7	25.2	31.8	20.0	19.7
2200	23.4	27.0	24.8	30.6	19.2	16.7
2300	23.1	26.5	24.4	29.9	18.5	16.2
2400	22.9	26.0	24.0	29.2	17.9	16.0

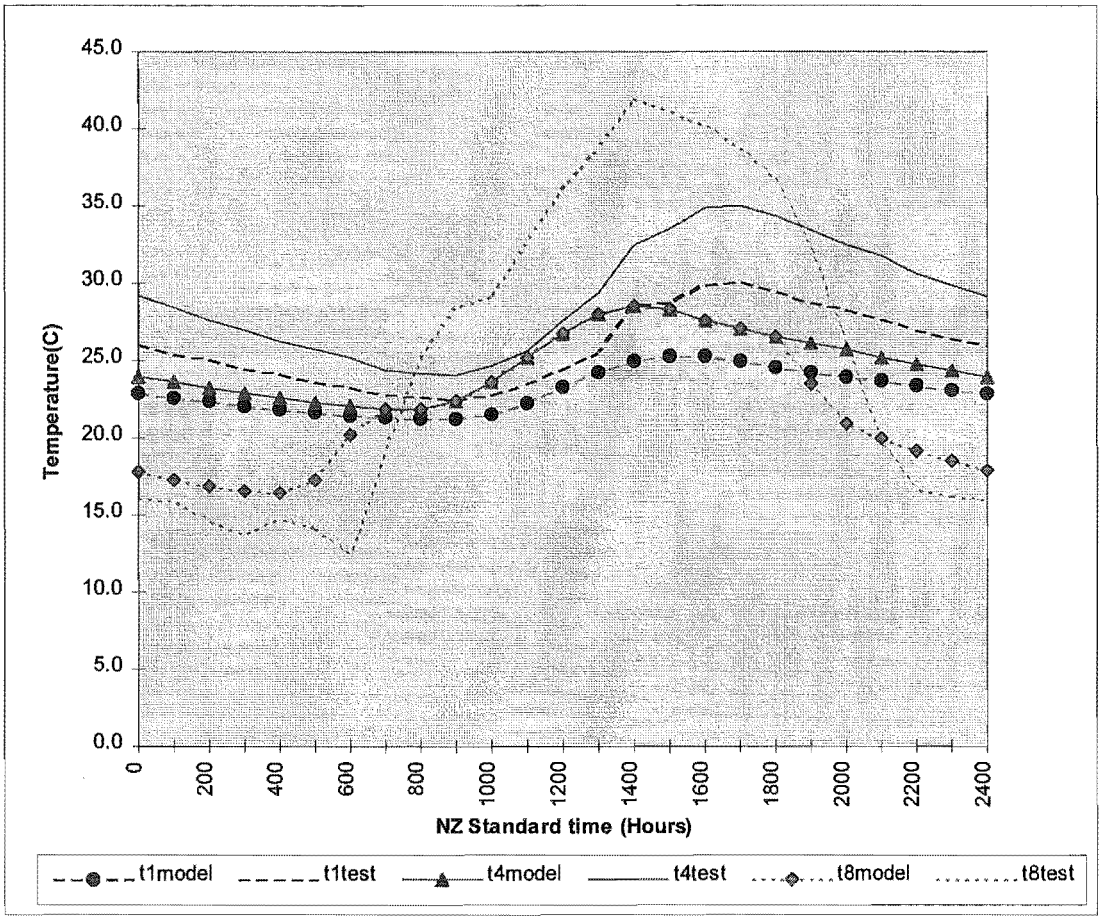

Figure 8.1 Comparison of temperatures t1, t4 and t8 of model and 24-hour test

8.2 MODEL MODIFICATION

The model was modified at three points.

1. When the panel is in heat transferring mode, the condenser temperature was changed to the evaporator temperature less a subtracted value. This subtracted value was noted from the 24-hour test. A few adjustments were made to those values to ensure a balance of the energy of the system. The value was also varied for different evaporator temperatures and different times of day.

   After the panel started to transfer heat and before 1300 hours, if the evaporator temperature was less than 28°C and was greater or equal to 27°C then the subtracted value was 1.1°C. If the evaporator temperature was less than 30°C and was greater or equal to 28°C then the subtracted value was 2°C. If the evaporator temperature

was less than 33°C and was greater or equal to 30°C then the subtracted value was 4°C. If the evaporator temperature was greater than or equal to 33°C then the subtracted value was 7.5°C. Otherwise if the evaporator temperature was less than 27°C then the subtracted value was 0.5°C.

After 1300 hours and before the panel stopped transferring heat, if the evaporator temperature was less than 37°C and greater or equal to 35°C then the subtracted value was 1°C. If the evaporator temperature was less than 40°C and greater or equal to 37°C then the subtracted value was 2.5°C. If the evaporator temperature was less than 42°C and greater or equal to 40°C then the subtracted value was 4.5°C. If the evaporator temperature was greater than or equal to 37°C then the subtracted value was 5.5°C. Otherwise if the evaporator temperature was less than 35°C then the subtracted value was 0.5°C.

This was achieved by adding these conditions by IF...THEN statements in the program.

2. Another node was added at the air-gap between the glass and the evaporator, (which brought the total number of nodes to 10) and the measured air-gap temperature from the 24-hour test applied to the new node. Unfortunately the thermocouple placed to measure this temperature in the 24-hour test was not at the mid-height of the wall to measure the average temperature, but instead had been placed near the top of the wall. Due to this, the measured temperatures are always higher than the average temperature would have been. Four different straight line functions based on the measured temperature profile were created and placed to calculate the average air-gap temperature.

   Between 0600 hours (inclusive) and 1400 hours (inclusive) this value was calculated by the following equation :

$$T_{air\ gap} = 3.84 * TIME - 13.03$$

   If the time of day was greater than 1400 hours and less than or equal to 1800 hours then the value was calculated by the following equation :

$$T_{air\ gap} = -3.625 * TIME + 91.45$$

If the time of day was greater than 1800 hours and less than or equal to 2400 hours then the value was calculated by the following equation :

$$T_{air\ gap} = -2.3 * TIME + 67.6$$

If the time of day was greater than 0000 hours and less than 0600 hours then the value was calculated by the following equation :

$$T_{air\ gap} = -0.4 * TIME + 12.4$$

The equations for the evaporator and the glass temperatures were coupled to the additional node in the model.

3. The 'Solar 1' subroutine which had been accessed in the original model was by-passed and replaced with measured real solar input and the ambient air temperatures of the 24-hour test. IF...THEN statements were used to give these inputs when the 'DAY = 183' (22 December).

Based on the above three points the model was modified and the program listing is presented in Appendix H Section H.2. In this way the modified model and the prototype wall were driven by essentially the same outside conditions. In the room, the calorimeter box was maintaining a 20°C temperature with a tolerance of ±0.2° and could be considered as the same inside conditions as those of the model. The modified model was run and its nodal temperatures and energy calculations had been tabulated in Table H.3 of Appendix H. The most relevant temperatures have been selected from both the modified model and the 24-hour test and tabulated in Table 8.2 and plotted in Fig 8.2.

Table 8.2 Selected temperatures from modified model and 24-hour test

HR	t_1 model	t_1 test	t_4 model	t_4 test	t_8 model	t_8 test
0	25.7	26.0	28.1	29.2	17.6	16.0
100	25.1	25.4	27.1	28.4	17.0	15.9
200	24.5	25.1	26.2	27.6	16.2	14.6
300	23.9	24.5	25.4	27.0	15.6	13.7
400	23.4	24.2	24.7	26.3	15.1	14.8
500	23.0	23.6	24.1	25.7	14.6	14.2
600	22.6	23.3	23.5	25.2	16.5	12.4
700	22.2	22.8	23.1	24.4	21.8	19.2
800	22.1	22.7	23.4	24.2	23.9	25.2
900	22.5	22.5	24.5	24.1	25.0	28.4
1000	23.3	22.8	26.0	24.7	27.1	29.2
1100	24.3	23.5	28.4	25.6	32.4	32.7
1200	25.4	24.5	30.6	27.6	38.1	36.1
1300	27.1	25.5	33.3	29.4	40.8	38.8
1400	28.7	28.6	35.5	32.5	43.0	42.0
1500	30.4	28.8	37.3	33.5	42.8	41.1
1600	30.8	29.9	37.2	34.9	42.7	40.2
1700	30.8	30.1	36.3	35.0	40.8	38.8
1800	30.3	29.5	35.1	34.4	37.6	36.8
1900	29.6	28.8	34.0	33.4	34.3	32.3
2000	28.8	28.3	32.7	32.5	27.7	26.0
2100	28.0	27.7	31.4	31.8	23.6	19.7
2200	27.2	27.0	30.2	30.6	21.5	16.7
2300	26.4	26.5	29.1	29.9	19.5	16.2
2400	25.7	26.0	28.1	29.2	17.6	16.0

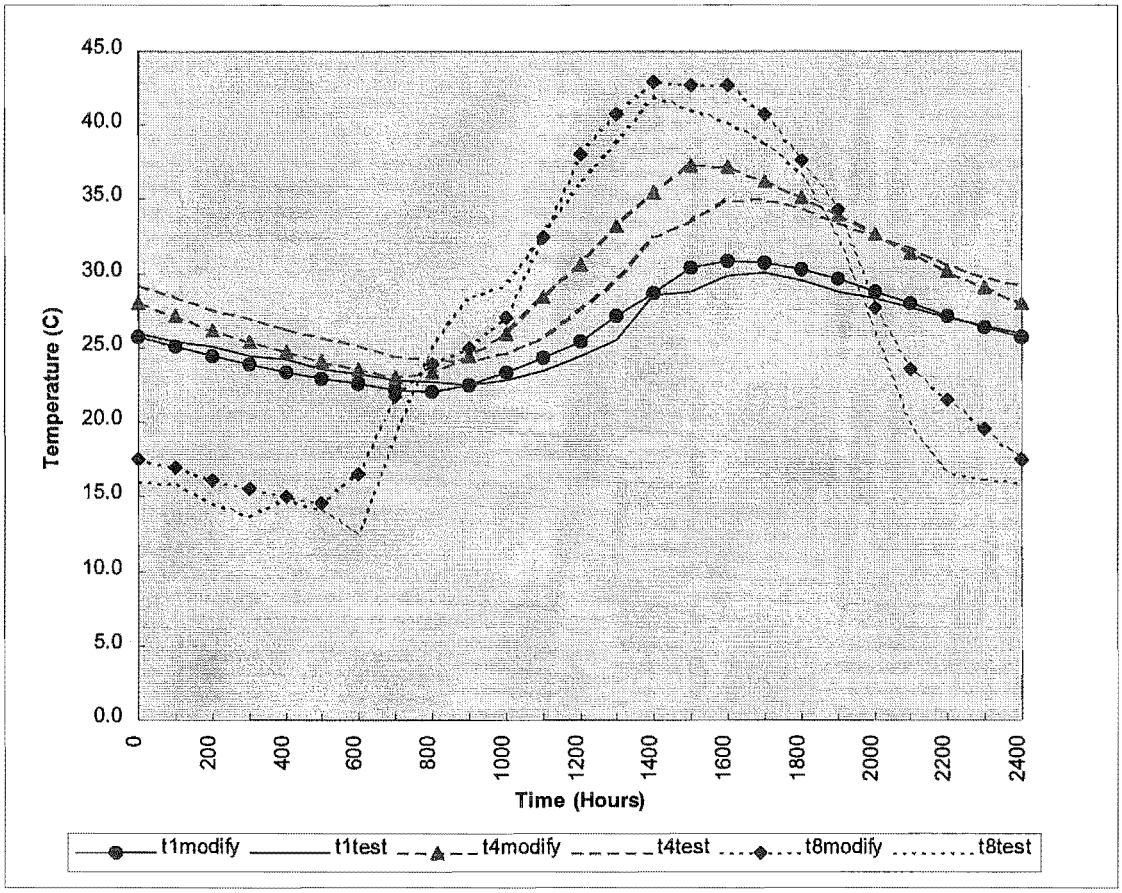

Figure 8.2 Comparison of temperature values t1, t4 and t8 of modified model and 24-hour test.

8.2.1 Analysis

From this comparison of the modified model results and the 24-hour test the interior wall temperature t_1 and exterior concrete wall temperature t_8 are closely matched. However, the middle of the concrete wall temperature, t_4 , did not match as well but this pattern was expected and explainable for the following reason : The prototype wall was not homogeneous in the node 4 plane whereas in the model the wall was considered as homogeneous on this plane. The Fig 8.3 clearly shows the non-homogenous characteristics of the node 4 plane and the thermocouple position in that plane. The pattern of the node 4 temperature discrepancies could be explained under two categories:

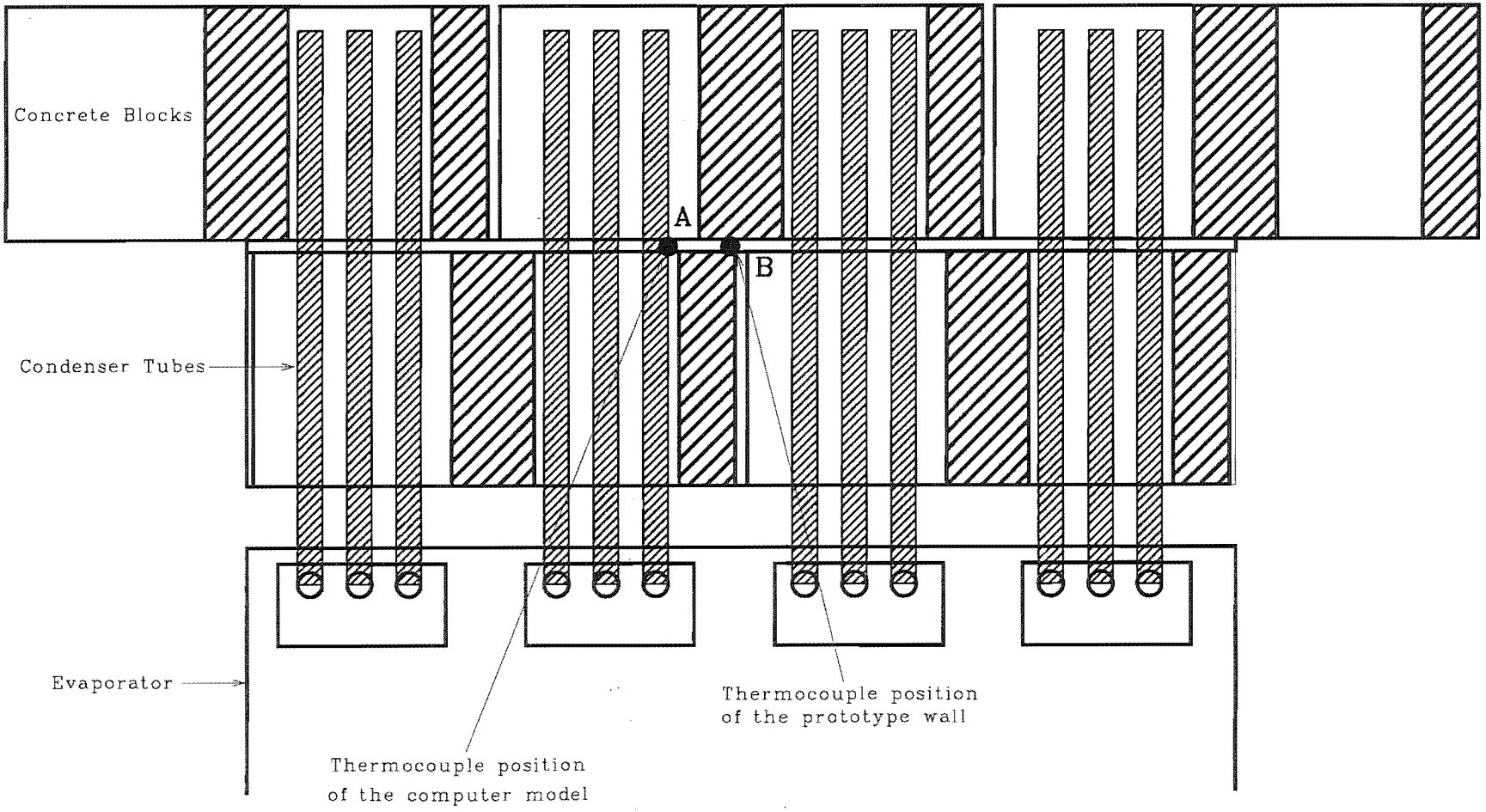

Figure 8.3 Non-homogeneous characteristics of the node 4 plane and thermocouple positions

1. *Panel in heat transferring mode* : When the panel was in heat transferring mode the steel condenser tube was the highest temperature point in that plane, while the thermocouple position (for the prototype wall) was the lowest temperature point because it was placed centrally between two sets of condenser tubes. The modified model calculated the condenser tube temperature (which is higher) and printed that as the node 4 temperature. However, the 24-hour test data for the node 4 plane temperature would have been the lowest value on that plane. In the real situation, the average temperature in the plane would be in between these two values.
2. *Panel not in a heat transferring mode* : The condenser tube will be the lowest temperature in the node 4 plane because the steel tube has a higher thermal conductivity than concrete and the tube has direct access to the low temperature evaporator. Due to this the tube temperature would cool down to be the lowest temperature of that plane and this value would be interpreted as node 4 temperature of the modified model. Meanwhile the temperature measured by the thermocouple would not have good conductive access to the cold evaporator and would therefore be maintained at a higher level. Because of the reversal of the direction of heat transfer, it is possible that the temperatures of other points on the node 4 plane might not always lie between the model's temperature prediction (A in Fig 8.3) and the measured temperature (B in Fig 8.3).

With these changes the modified model represents reasonably well the real wall behaviour. According to the simulation results from the modified model the wall would transfer 7.01 MJ/m^2 of energy into the room (52.2%) out of externally available solar energy of 13.43 MJ/m^2. This is in remarkably close agreement to the measured net energy gain of 1.92 kWh/m^2 (6.91 MJ/m^2) into the calorimeter box during the 24-hour test. "Remarkable" for two reasons :

1. The energy meter was only resolvable to 1 kWh so there is inevitable uncertainty in the net figure of 1.92 kWh.
2. The energy stored in the actual wall at the end of the 24-hour test could be significantly different from that in the wall initially.

8.2.2 Solar intensity modification

Experimental measurements had been made of real solar radiation on a vertical surface exposed to ground-reflected radiation as well as direct and sky-diffuse components of solar radiation. This data enabled a comparison to be made with the model's predictions of solar radiation, and the model adjusted to give a good match. In this way it was possible to deduce the value for the ground reflectivity to 'hand-written" into the solar subroutine of the model. This modified sub-routine would provide improvement in predicting the wall's behaviour under winter solar conditions.

Details of the basis for these modifications are :

1. Ground-reflected radiation was calculated according to the equation.

$$IR = 0.5 \times \rho_f \times (IDIR \times SIN(ALTR) + IDH)$$

where ρ_f = Reflectivity of the floor

IDIR = Direct solar radiation (calculated by interpolation of values obtained from smoothed meteorological data composed for Christchurch for clear sunny days). (W/m^2) (CIBSE Guide - 1986)

ALTR = Altitude angle (radians)

IDH = Diffuse radiation intensity (W/m^2) (Building Research Bureau - 1966)

2. For an assumed value of ground reflectivity (within the anticipated likely range of 0.2 to 0.4), this ground-reflected radiation was added to the direct and sky-diffuse components already computed by the solar subroutine in its original form.

3. The total radiation calculated in this way was compared with the measured radiation (allowing for shift between NZ standard time, and the daylight saving time that was in effect during the experiment).

4. By trial and error, the best match was obtained for a ground reflectivity of 0.3. This very good agreement can be seen in Fig 8.4.

Thus for the winter modelling which was to be done using the fully-modified version of program (section 8.3.), this ground reflectivity value of 0.3 would be used to best represent the solar radiation which the wall would receive under clear sky winter conditions.

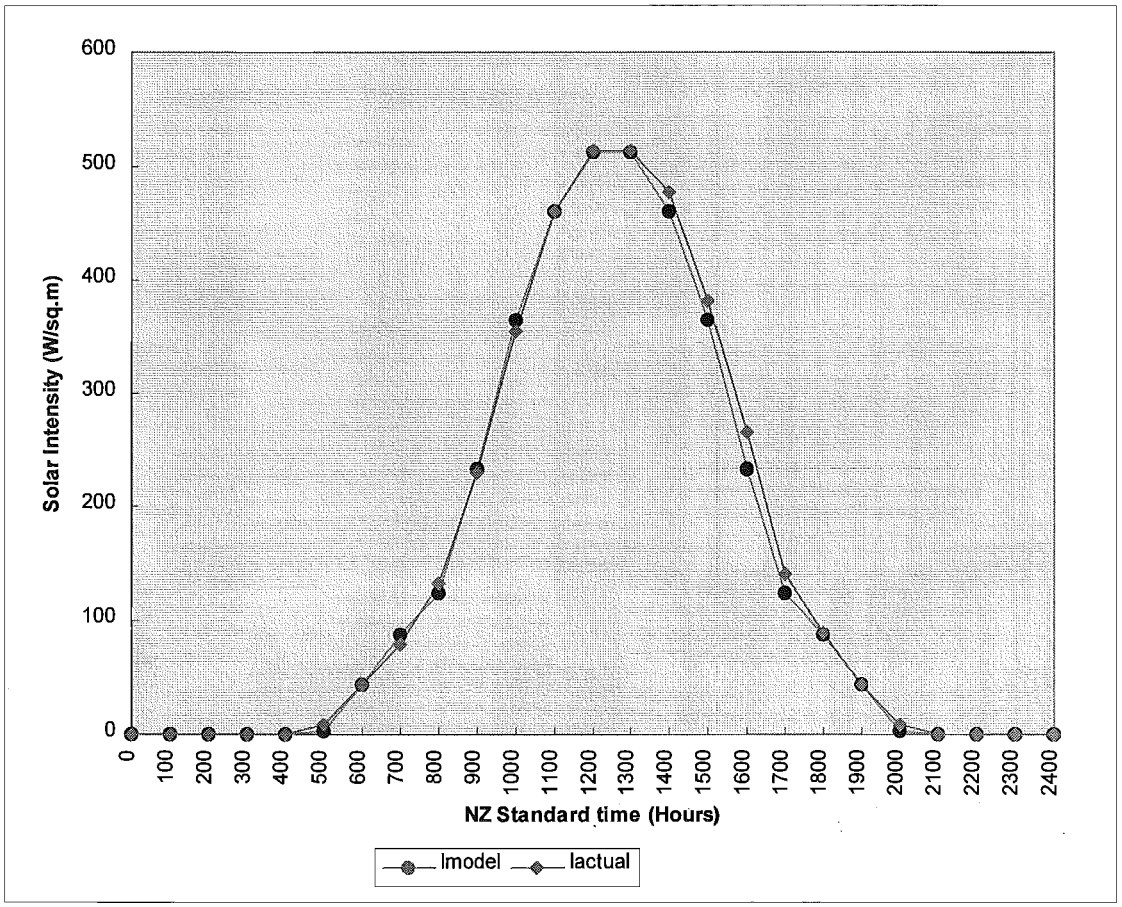

Figure 8.4 Comparison of solar intensity of actual and model.

8.3 WINTER PREDICTIONS USING THE MODIFIED MODEL

After having demonstrated that the modified model was representing the summer situation realistically, it was desirable to use it to predict the wall performance for winter conditions. However, predicting the air gap temperature during the winter remained outside the scope of the model, even its modified form.[♠] Thus the modifications were restricted to the experimentally-based corrections to the evaporator-condenser temperature differential, and the inclusion of ground-reflected solar radiation.

[♠] Recall that during modification and verification of the model, the measured air gap temperature was one of the "external drivers" supplied to the model, i.e. the model did not predict the air gap temperature itself.

One external drive for the winter modelling was the ambient air temperature which was again assumed to be a sinusoidal variation between 9.6°C at 1500 hours and 3.15°C at 0300 hours (these values corresponding well to averaging the hourly meteorological values for Christchurch in June). The other driver was the solar radiation data comprising: the clear sky direct component resolved on to a north-facing vertical surface in Christchurch in June; the corresponding sky-diffuse component; and the ground-reflected component, assuming the ground reflectivity value of 0.3 which had been deduced from the summer experimental observations. The interior room temperature was assumed to be constant at 20°C as before. With all these conditions the modified model was refined to predict winter conditions. The listing of such a program is presented in Appendix H, Section H.3. The results of running this refined model are tabulated in Table 8.4 and some selected temperatures are plotted in Fig 8.5.

Table 8.4 Nodal temperatures for winter predictions.

HR	t_1	t_2	t_3	t_4	t_5	t_6	t_7	t_8	t_9	t_{air}
0	24.8	25.8	26.6	27.0	27.2	27.2	26.8	12.9	6.7	4.5
100	24.3	25.2	25.8	26.2	26.4	26.3	25.9	12.2	6.1	4.0
200	23.8	24.6	25.2	25.5	25.6	25.5	25.1	11.6	5.6	3.5
300	23.4	24.0	24.5	24.8	24.9	24.7	24.3	11.2	5.3	3.3
400	23.0	23.5	24.0	24.2	24.2	24.0	23.6	10.9	5.2	3.3
500	22.6	23.1	23.4	23.6	23.6	23.4	23.0	10.7	5.3	3.5
600	22.2	22.7	23.0	23.1	23.1	22.9	22.5	10.7	5.6	4.0
700	21.9	22.3	22.5	22.6	22.6	22.4	22.0	10.9	6.1	4.5
800	21.6	21.9	22.1	22.2	22.1	21.9	21.6	11.2	6.7	5.2
900	21.4	21.7	22.1	22.7	22.2	21.9	21.8	23.2	10.8	6.0
1000	21.9	22.5	23.6	25.4	23.9	23.1	22.9	25.9	12.6	6.9
1100	23.2	24.2	25.5	27.1	26.0	25.2	25.0	31.1	14.7	7.7
1200	24.4	25.6	27.6	30.5	28.4	27.4	27.3	38.0	17.3	8.4
1300	26.2	27.9	30.3	33.5	31.5	30.4	30.3	41.0	18.5	9.0
1400	27.9	29.9	32.4	35.4	34.0	33.1	33.1	42.9	19.2	9.4
1500	29.4	31.6	34.2	36.8	36.0	35.5	35.4	41.3	18.7	9.6
1600	29.8	32.0	34.0	35.6	36.1	36.2	36.3	40.1	17.9	9.6
1700	29.6	31.6	33.4	34.7	35.5	35.9	36.0	28.5	15.4	9.4
1800	28.9	30.7	32.3	33.4	34.1	34.3	34.0	18.5	11.4	9.0
1900	28.1	29.8	31.2	32.1	32.7	32.8	32.4	17.5	10.7	8.4
2000	27.4	28.9	30.1	30.9	31.4	31.5	31.1	16.6	10.0	7.7
2100	26.7	28.0	29.1	29.8	30.2	30.3	29.9	15.6	9.1	6.9
2200	26.0	27.2	28.2	28.8	29.2	29.1	28.8	14.7	8.3	6.0
2300	25.4	26.5	27.4	27.9	28.2	28.1	27.7	13.8	7.4	5.2
2400	24.8	25.8	26.6	27.0	27.2	27.2	26.8	12.9	6.7	4.5

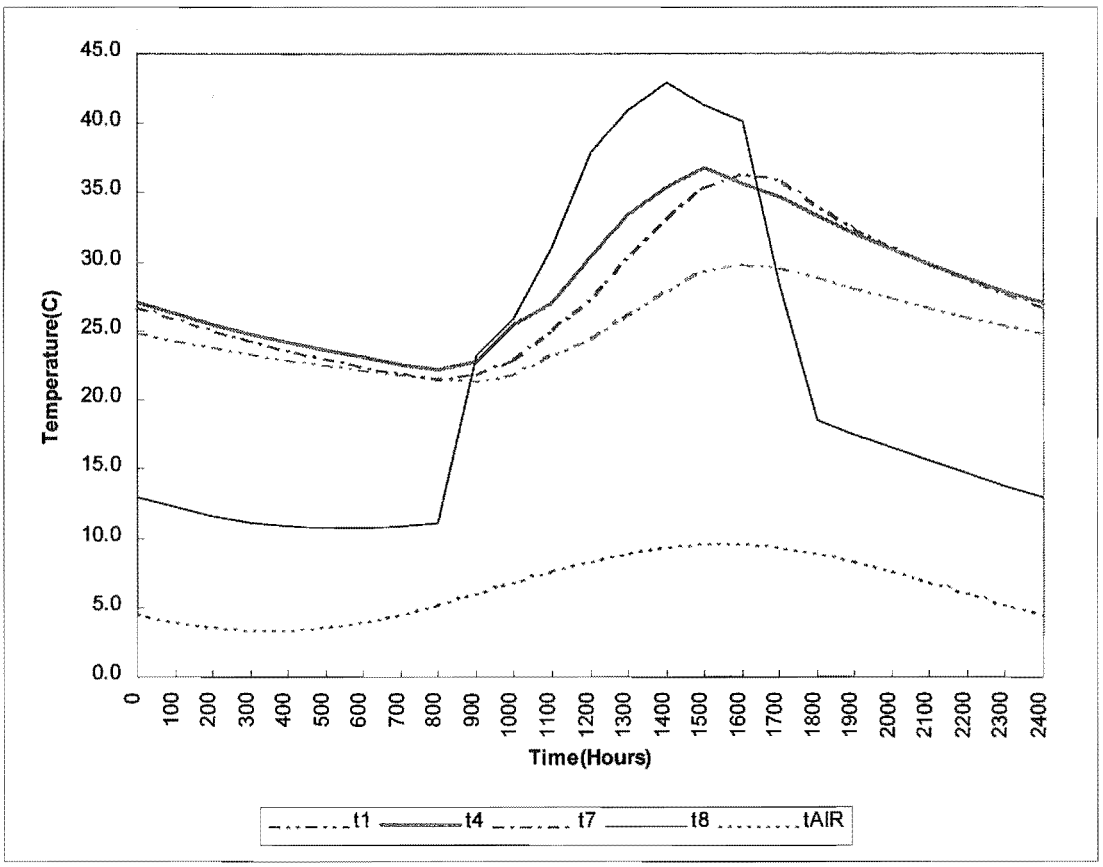

Figure 8.5 Temperature distribution of the wall for winter predictions.

8.3.1 Analysis

From the Fig 8.5 it is clear that the panel is still exhibiting the desired characteristics, even in winter. The interior wall temperature t_1 stays well above the ambient temperature and ranges between 21.4°C and 29.8°C. For these conditions the panel would transfer 5.94 MJ/m^2 (42%) energy into the room from the available 14.14 MJ/m^2. Energy loss to out side would be high of 8.31 MJ/m^2 because of the low ambient temperature.

Seasonal variation in solar geometry is such that the total daily solar radiation falling on a north-facing vertical surface in winter (14.14 MJ/m^2) is very similar to that available in summer (13.42 MJ/m^2). However, the low ambient temperature in winter leads to an inevitable increase in the heat losses to outside of 8.31 MJ/m^2 compared with the summer loss of 6.49 MJ/m^2 and a consequent significant drop in overall efficiency to 42%.

In view of the favourable effect of the elevated air gap temperature that was observed in the summer testing, it is probable that this efficiency value of 42% is conservative.

It is worth to compare the performance of this solar wall with the standard domestic wall. The following steps calculating the heat loss/gain of a domestic house wall, insulated to NZS 4218P: 1977 standard.

Thermal resistance of the wall = 1.5 m^2 °C/W (NZS 4218P - 1977)

Mean June-July ambient temperature in Christchurch = 5.5°C (Blackwell - 1981)

Temperature of the room = 20°C

$\therefore$ Heat gain in to the room = (5.5 - 20)/1.5

= -9.67 W/m^2

= -0.84 MJ/m^2/day

$\therefore$ Heat loss from the room = 0.84 MJ/m^2/day (0.232 kWh/m^2/day)

The standard domestic house wall *loose* around 0.84 MJ/m^2 in June in Christchurch while the solar wall *gain* around 5.94 MJ/m^2 for the same ambient conditions.

CHAPTER 9

9. CONCLUSIONS AND RECOMMENDATIONS

9.1 CONCLUSIONS

The solar wall was built into the north-facing side of a test room as planned, and experiments were conducted to check its performance. A mathematical model of the wall was validated for summer conditions and used to predict the winter performance. The following conclusions were derived from the work.

1. The concept of using a gravitational heat pipe to achieve a thermal diode effect was shown to be technically viable for the application of using solar energy for space heating purposes.

2. Combining this thermal diode effect with appropriate thermal storage in the form of concrete blocks with filled cavities, solar energy can be effectively utilised to heat a domestic space outside times of bright sunshine. The wall stores solar energy, distributing it over a full day with a time lag of four to five hours.

3. Even though the glass reflects back most of the available solar radiation in summer, on an average summer day the wall is transferring about 1.85 $kWh/m^2/day$ ($MJ/m^2/day$) into the room. This energy might overheat the house if the ambient air temperature is high but a suitable fixed external shading device (such as an eave) could be used to effectively guard against the possibility of summer overheating but retain winter heating performance.

4. A suitably large area of the solar wall may be sufficient to meet domestic space heating requirements during late autumn and early spring in Christchurch except during periods of sustained cloudy, cold weather. The vertical solar wall would intercept more solar energy during that time than any time of the year, as shown in the data of Table 9.1. Further long term testing would show whether or not this would be possible.

5. According to the winter predictions, the solar wall would provide significant space heating on a clear sunny day, approximately 5.94 MJ/m^2/day (1.65 kWh/m^2/day) for Christchurch, representing about 42% of the solar radiation incident on the wall.

6. To utilise the wall concept effectively, houses would have to be designed with significant area of north-facing living and bedroom walls.

Table 9.1

Solar radiation on a vertical plane on a clear sunny day for North facing Christchurch (43.5°) Wall. Data collected from Building Research Bureau of NZ. Inc (1966)

Month	Direct Solar radiation		Diffused solar radiation		Total solar radiation	
	Btu/ft^2	kWh/m^2	Btu/ft^2	kWh/m^2	Btu/ft^2	kWh/m^2
Jan-22	707	2.228	562	1.771	1269	4.000
Feb-22	1017	3.206	519	1.636	1536	4.841
Mar-22	1286	4.053	460	1.450	1746	5.503
Apr-22	1402	4.419	382	1.204	1784	5.623
May-22	1321	4.164	308	0.971	1629	5.135
Jun-22	1256	3.959	278	0.876	1534	4.835
Jul-22	1364	4.299	312	0.983	1676	5.283
Aug-22	1480	4.665	393	1.239	1873	5.904
Sep-22	1381	4.353	477	1.504	1858	5.856
Oct-22	1037	3.269	533	1.680	1570	4.949
Nov-22	702	2.213	574	1.809	1276	4.022
Dec-22	561	1.768	581	1.831	1142	3.600

9.2 RECOMMENDATIONS FOR FUTURE WORK

1. The panel's summer performance was tested and its winter performance was only predicted in this project. More experiments should be conducted to confirm the performance of the wall in winter.

2. In the current experimental set up the calorimeter was being cooled throughout, irrespective of the need. Some electronic control should be incorporated to provide demand-based cooling and thereby overcome the potential problem of trying to attach significance to the small difference between the heat input to, and heat extracted from the calorimeter box under test conditions where the wall is almost "neutral".

3. A standard domestic house wall could be built next to the solar wall with a separate calorimeter box, and these two walls could be tested at same time to compare actual performances. This data would be important for quantifying the true energy gain of the solar wall in comparison with a conventional wall which would be acting as an energy loser under winter conditions.

4. It was found that the wall was utilising about 60% of the available solar energy under the summer test conditions. The loss of 40% could be reduced to improve the wall's performance. The evaporator surface temperature rises up to 60°C during peak solar gain, mainly due to the condenser which can not transfer heat fast enough to the poorly conductive concrete. If the evaporator surface temperature could be reduced, then the convective and radiative losses to the outside would also reduce. One approach worth trying would be, to use a concrete block, the cavities of which are filled with material of higher thermal conductivity. The surface temperature of the condenser would not rise as much as at present since the heat will be conducted away from it more effectively. This, in turn, would reduce the evaporator temperature. Different combination of materials may be tested to optimise the results.

5. The geometry of suitable external shading or glazing arrangements to guard against summer overheating while maintaining good performance during the heating season should be considered.

6. Longer term testing would enable the economics of this wall and its pay back period to be compared with a standard wall.

7. Different ways of manufacturing the panel as one unit (rather than fabricating the condenser and evaporator separately) should be investigated as a possible way of reducing the cost of the panels.

8. The computer model could be modified with one more additional node in the air gap between glass and the evaporator for a better match with the actual wall.

9. A special concrete block could be designed specifically for use in this application to ease the laying of the panels in to the wall.

10. In order to enhance the wall's performance, a simple horizontal reflective surface could be designed to be used only in winter.

REFERENCES

- **Anderson, B with Riorder, M (1976)**

  The Solar Home Book. Heating Cooling and Designing with the Sun, Cheshire Books, USA: p31.

- **A.S.H.R.A.E Handbook (1989)**

  Handbook of ASHRAE Fundamentals, American Society of Heating Refrigerating and Air-Conditioning Engineers, Atlanta, USA: Fig 15, P27.21

- **Baines, J T (1993)**

  New Zealand Energy Information Handbook, Taylor Baines and Associates Christchurch New Zealand: p54.

- **Bakker, L G and Van Dijk, H A L (1994)**

  Transparent Insulation Technology in the Building Envelope
  Caddet Energy Efficiency News Letter, No 2/1994, pp 4-7.

- **Beckman, W A , Klein, S and Duffie, J A (1977)**

  Solar Heating Design, John Wiley and Sons New York, USA: pp 10-20

- **Blackwell, F N , Brickell, Moss and Partner (May 1981)**

  Standard Weather Data for New Zealand, New Zealand Research and Development Committee, Report No 62, NZ: p17, Table 8.

- **Breuer (August 1988)**

  Technical-Economic Assessment and Market Potential for Reducing Energy in Residential Buildings, New Zealand Research and Development Committee, Report No 172, NZ: p2.

- **Building Research Bureau - 1966**

  Solar Position and Radiation Tables for Christchurch New Zealand (43.5°), p3, Table 2.

- **Carless, J (1993)**

  Renewable Energy: A Concise Guide to Green Alternatives, Walker and Company, New York, USA: p12.

- **Christchurch Press (14 March 1995)**

  New Zealand Lags in Cutting Greenhouse Gases: UN.

- **CIBSE Guide (1986)**

  Design Data, Volume A, London UK: pp A2-59, Table A2.24

- **Cromarty (1993)**

  Experimental Design for Wall Heat Loss/Gain Measurement: Final Year Project Report No 54/93, Department of Mechanical Engineering, University of Canterbury.

- **Department of Statistics (1993)**

  New Zealand Official Year Book, 96th Edition, NZ: pp 365-385.

- **Dunn, P D and Reay, D A (1994)**

  Heat Pipes, Pegamon, Oxford, England: pp 1-23.

- **ECNZ (1993)**

  Electricity Generation in New Zealand, ECNZ, NZ.

- **Golob, R and Brus, E (1993)**

  The Almanac of Renewable Energy, Henry Holt, USA: pp 1-8 and pp 80-92.

- **Kaneff, S (1990)**

  Living in the Greenhouse: Proceedings of the Australian and New Zealand Solar Energy Society Conference, Auckland, NZ: pp 13-23.

- **Kreith, F and Black, W Z (1980)**

  Basic Heat Transfer, Harper and Row Publishers, New York, USA: p358.

- **Leslie, S F (November 1976)**

  Annual Heating Energy Demand of Heavy Domestic Buildings, New Zealand Energy Research and Development Committee, Report No 16, NZ: p4.

- **Liley, P E, Makita, T and Tanaka, Y (1988)**

  Properties of Inorganic and Organic fluids, Hemisphere Public Corp., USA.

- **Major, R (1978)**

  Solar Wall Feasibility Study: Final Year Project Report No 29/78, Department of Mechanical Engineering, University of Canterbury.

- **NZS 4214 (1977)**

  Methods of Determining the Total Thermal Resistance of Parts of Buildings, Standards Association of New Zealand, NZ.

- **NZS 4218P (1977)**

  Minimum Thermal Insulation Requirements for residential Buildings, Standards Association of New Zealand, NZ: p6, Table 1.

- **Prudhoe, K R (April 1991)**

  Thermal Stability - Phase Change Materials in Focus
  Australian Refrigeration, Air Conditioning and Heating, pp 33-38.

- **Ward, G T (1974)**

  Energy in New Zealand, Proceedings of the First New Zealand Energy Conference. "Solar and other renewable energy renewable energy resources - Global and New Zealand prospects", Auckland, NZ: pp 13-34.

- **Watson, L and Noble (March 1986)**

  Domestic Heat Energy Economics, New Zealand Research and Development Committee, Publication p107, NZ: pp 1-10.

- **Wood, J H and Adams, J R (1978)**

  Temperature Gradients in a Cylindrical Concrete Reservoir. Proc. of 6th ACMSM, Christchurch, pp 115-122.

- **Wright, J C and Baines, J (1986)**

  Supply Curves of Conserved Energy the Potential for Conservation in New Zealand's Houses, Table 3.13.3.

APPENDIX A

A. DERIVATION OF THE NODAL EQUATIONS

The detailed energy balance equations were determined for each individual node are presented below. The nodal positions in the wall are marked in Fig A.1.

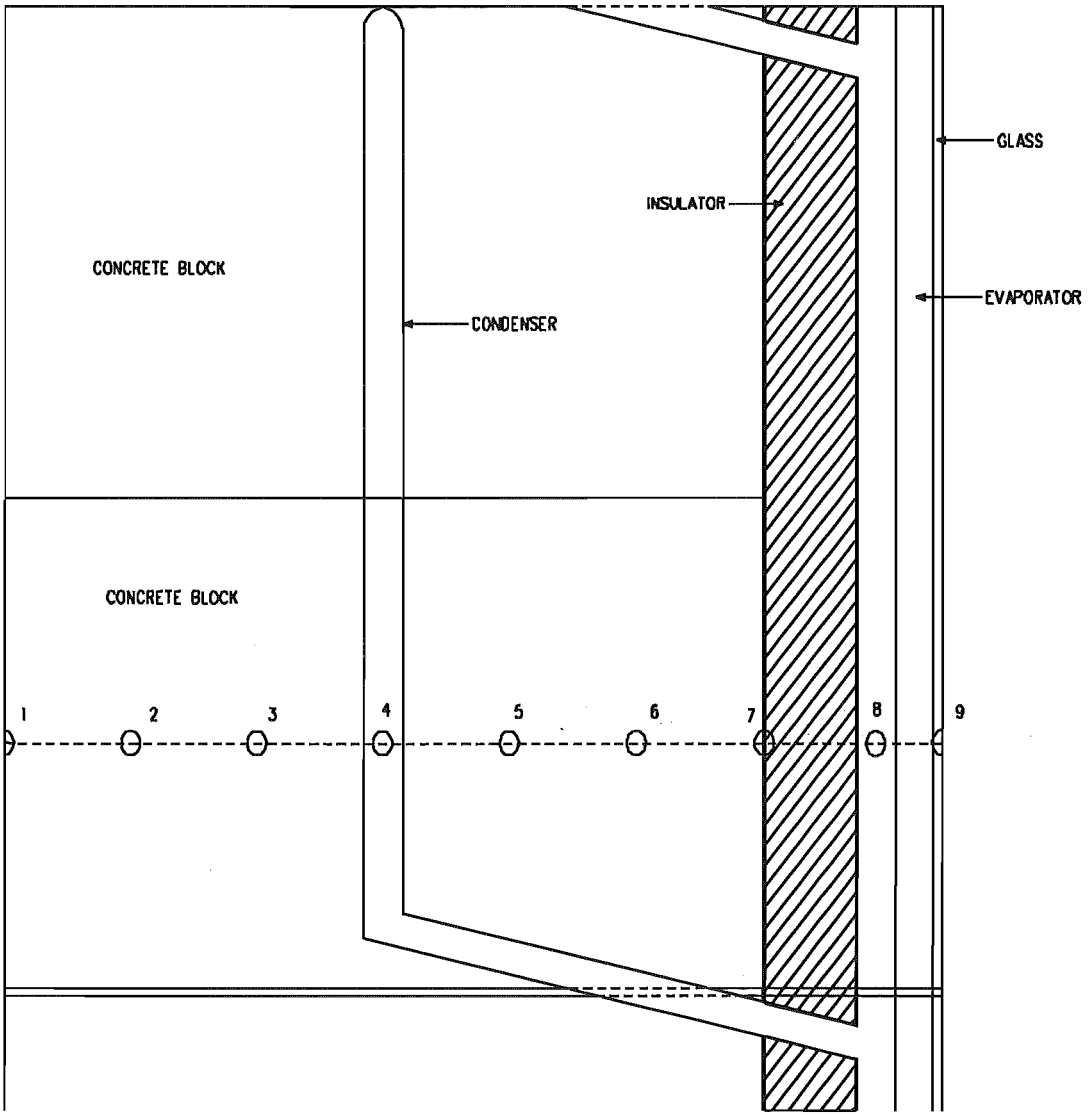

Figure A.1 Nodal positions on the solar wall

A.1 ENERGY BALANCE EQUATION FOR NODE 1

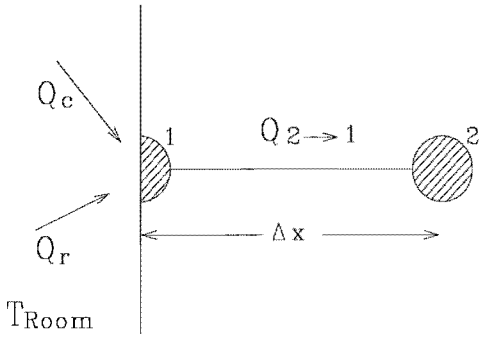

$$Q_{2\to1} + Q_{Convection} + Q_{Radiation} = \frac{\partial U_o}{\partial \tau}$$

$$\frac{kA}{\Delta x}(t_2^{old} - t_1^{old}) + \frac{(t_R - t_1^{old})A}{R_{Room}} = mc\frac{(t_1^{new} - t_1^{old})}{\Delta \tau}$$

where

R_{Room} is total thermal convective and radiative resistance of the interior surface of the wall

$$\frac{kA}{\Delta x}(t_2^{old} - t_1^{old}) + \frac{(t_R - t_1^{old})A}{R_{Room}} = \rho A\frac{\Delta x}{2}c\frac{(t_1^{new} - t_1^{old})}{\Delta \tau}$$

$$t_1^{new} = t_1^{old} + \frac{2\Delta \tau}{\rho\, \Delta x\, c}\left(\frac{k}{\Delta x}(t_2^{old} - t_1^{old}) + \frac{(t_R - t_1^{old})}{R_{Room}}\right) \text{---------- A.1}$$

A.2 ENERGY BALANCE EQUATION FOR NODE 2

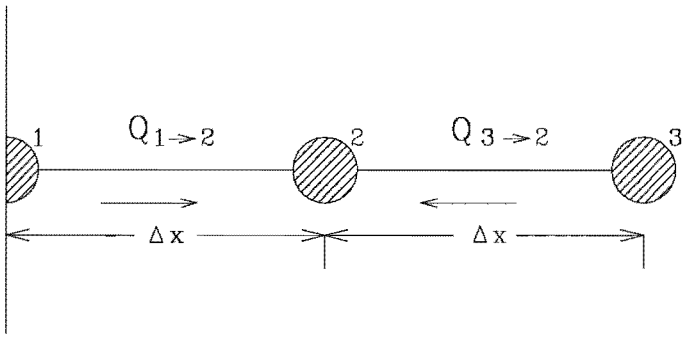

$$Q_{1\to2} + Q_{3\to2} = \frac{\partial U_o}{\partial \tau}$$

$$\frac{kA}{\Delta x}(t_1^{old} - t_2^{old}) + \frac{kA}{\Delta x}(t_3^{old} - t_2^{old}) = mc\frac{(t_2^{new} - t_2^{old})}{\Delta\tau}$$

$$\frac{kA}{\Delta x}(t_1^{old} - t_2^{old}) + \frac{kA}{\Delta x}(t_3^{old} - t_2^{old}) = \rho\, A\, \Delta x\, c\frac{(t_2^{new} - t_2^{old})}{\Delta\tau}$$

$$t_2^{new} = F_o(t_1^{old} + t_3^{old}) + t_2^{old}(1 - 2F_o) \text{ ---------- } \mathbf{A.2}$$

where

$F_o = (k\ \Delta\tau)/(\rho c \Delta x^2)$ is the Fourier number

A.3 ENERGY BALANCE EQUATION FOR NODE 3

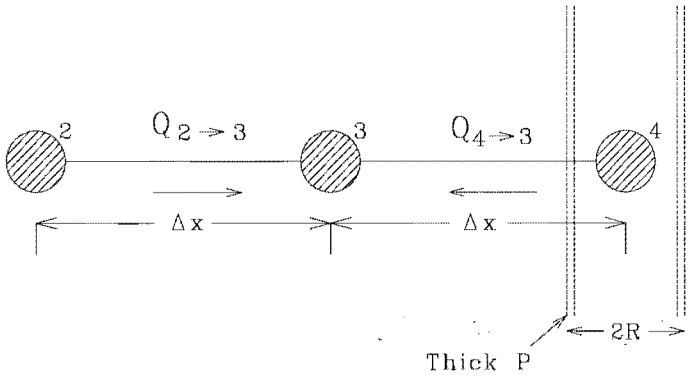

where

ThickP = is the equivalent thickness of condenser tube distributed over the one square meter area.

R = is the outer radius of the distributed pipe.

$$Q_{2\to3} + Q_{4\to3} = \frac{\partial U_o}{\partial\tau}$$

$$\frac{kA}{\Delta x}(t_2^{old} - t_3^{old}) + \frac{kA}{(\Delta x - R)}(t_4^{old} - t_3^{old}) = mc\frac{(t_3^{new} - t_3^{old})}{\Delta\tau}$$

$$\frac{kA}{\Delta x}(t_2^{old} - t_3^{old}) + \frac{kA}{(\Delta x - R)}(t_4^{old} - t_3^{old}) = \rho A \Delta x c \frac{(t_3^{new} - t_3^{old})}{\Delta \tau}$$

$$t_3^{new} = F_o (t_2^{old} + C_o t_4^{old}) + t_3^{old}(1 - F_o - F_o C_o) \text{ ---------- } \mathbf{A.3}$$

where

$C_o = (\Delta x)/(\Delta x - R)$

A.4 ENERGY BALANCE EQUATION FOR NODE 4

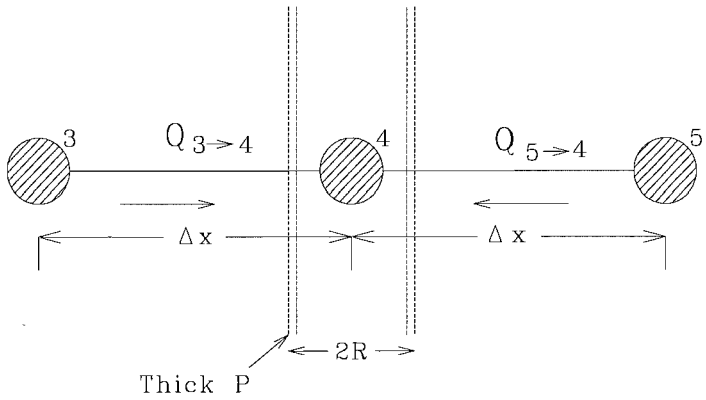

$$Q_{3\to4} + Q_{5\to4} = \frac{\partial U_o}{\partial \tau}$$

$$\frac{kA}{(\Delta x - R)}(t_3^{old} - t_4^{old}) + \frac{kA}{(\Delta x - R)}(t_5^{old} - t_4^{old}) = mc \frac{(t_4^{new} - t_4^{old})}{\Delta \tau}$$

$$\frac{kA}{(\Delta x - R)}(t_3^{old} - t_4^{old}) + \frac{kA}{(\Delta x - R)}(t_5^{old} - t_4^{old}) = A(2\rho_s ThickP\, C_s + \rho_c(\Delta x - 2R)C_c)\frac{(t_4^{new} - t_4^{old})}{\Delta \tau}$$

$$t_4^{new} = t_4^{old} + P_o(t_3^{old} + t_5^{old} - 2t_4^{old}) \text{ ---------- } \mathbf{A.4}$$

where

$$P_o = \frac{k\Delta\tau}{(2\rho_s ThcikP\, C_s + \rho_c(\Delta x - 2R)C_c)(\Delta x - R)}$$

A.5 ENERGY BALANCE EQUATION FOR NODE 5

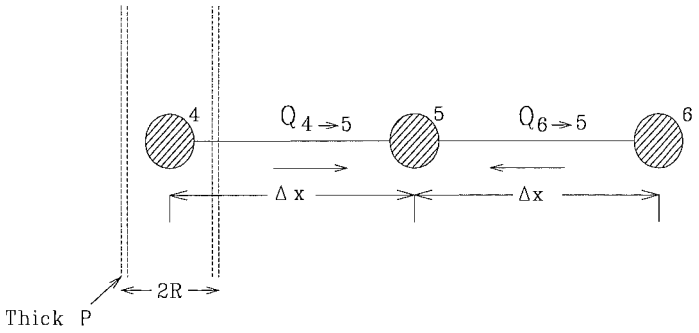

This node is in a similar situation to node 3. Therefore the same type of equation could be used.

$$t_5^{new} = F_o(t_6^{old} + C_o t_4^{old}) + t_5^{old}(1 - F_o - F_o C_o) \text{---------- A.5}$$

A.6 ENERGY BALANCE EQUATION FOR NODE 6

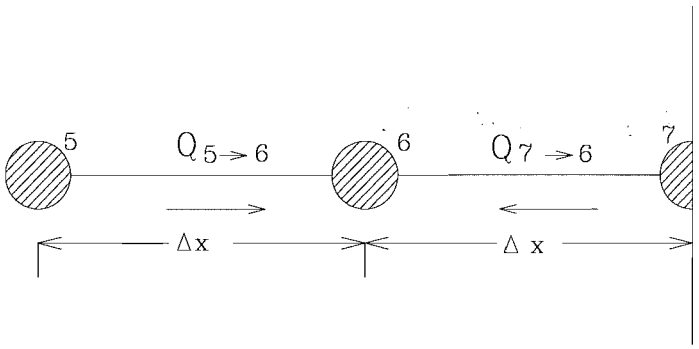

This node is similar to node 2. Therefore the same type of equation could be used.

$$t_6^{new} = F_o(t_5^{old} + t_7^{old}) + t_6^{old}(1 - 2F_o) \text{---------- A.6}$$

A.7 ENERGY BALANCE EQUATION FOR NODE 7

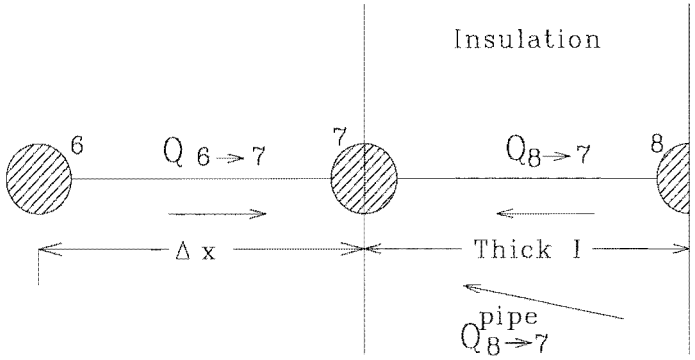

The assumptions explained in Section 2.4 in Chapter 2 were used in writing this equation.

$$Q_{6\to7} + Q_{8\to7} + Q_{8\to7}^{pipe} = \frac{\partial U_o}{\partial \tau}$$

$$\frac{kA}{\Delta x}(t_6^{old} - t_7^{old}) + \frac{k_I A}{ThickI}(t_8^{old} - t_7^{old}) + \frac{k_s A A_1}{ThickI}(t_8^{old} - t_7^{old}) = mc\frac{(t_7^{new} - t_7^{old})}{\Delta \tau}$$

$$\frac{kA}{\Delta x}(t_6^{old} - t_7^{old}) + \frac{k_I A}{ThickI}(t_8^{old} - t_7^{old}) + \frac{k_s A A_1}{ThickI}(t_8^{old} - t_7^{old}) = \left(\frac{\rho\,\Delta x\, C_c}{2} + \frac{\rho_I\, ThickI\, C_I}{2}\right)\frac{A(t_7^{new} - t_7^{old}}{\Delta \tau}$$

$$t_7^{new} = t_7^{old} + \frac{k}{\Delta x\,(Cons)}(t_6^{old} - t_7^{old}) + \frac{k_I}{ThickI(Cons)}(t_8^{old} - t_7^{old}) + \frac{k_s A_1}{ThickI(Cons)}(t_8^{old} - t_7^{old})$$

----------**A.7**

where

$$Cons = \left(\frac{\rho\,\Delta x\, C + \rho_I\, ThickI\, C_I}{2\,\Delta \tau}\right)$$

A.8 ENERGY BALANCE EQUATION FOR NODE 8

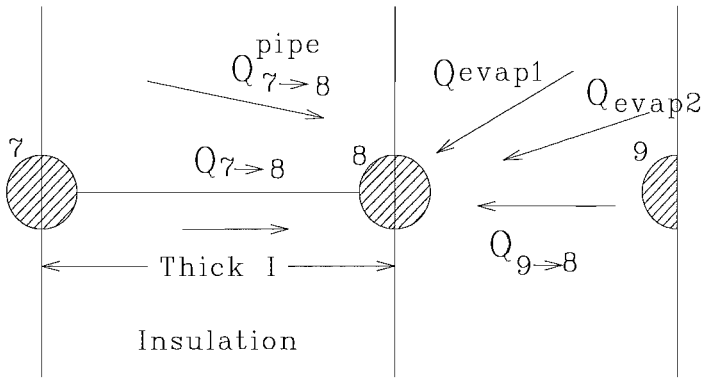

Again, the assumptions explained in Section 2.4 in Chapter 2 were used here.

A.8.1 When the panel is not transferring heat to the node 4

$$Q_{7\to 8} + Q_{7\to 8}^{pipe} + Q_{radiateglass} + Q_{evap1} + Q_{evap2} = \frac{\partial U_o}{\partial \tau}$$

$$\frac{k_I A}{ThickI}(t_7^{old} - t_8^{old}) + \frac{k_s A A_1}{ThickI}(t_7^{old} - t_8^{old}) + \frac{A(t_9^{old} - t_8^{old})}{R_{evap}} + AQ_{evap1} + AQ_{evap2} = mc\frac{(t_7^{new} - t_7^{old})}{\Delta\tau}$$

$$\frac{k_I A}{ThickI}(t_7^{old} - t_8^{old}) + \frac{k_s A A_1}{ThickI}(t_7^{old} - t_8^{old}) + \frac{A(t_9^{old} - t_8^{old})}{R_{evap}} + AQ_{evap1} + AQ_{evap2} =$$

$$\left(\frac{4\rho_s\, ThickS\, C_s}{2} + \frac{\rho_I\, ThickI\, C_I}{2}\right)\frac{A(t_8^{new} - t_8^{old})}{\Delta\tau}$$

where

R_{evap} is the total thermal radiation resistance of the evaporator surface

$$t_8^{new} = t_8^{old} + \frac{k_I}{ThickI(Cons1)}(t_7^{old} - t_8^{old}) + \frac{k_s A_1}{ThickI(Cons1)}(t_7^{old} - t_8^{old}) + \frac{(t_9^{old} - t_8^{old})}{R_{evap}(Cons1)} + \frac{(Q_{evap1} + Q_{eva}}{(Cons1)}$$

----------**A.8.1**

where

$$Cons1 = \left(\frac{4\rho_s \, ThickS \, C_s}{2} + \frac{\rho_I \, ThickI \, C_I}{2} \right) \frac{1}{\Delta\tau}$$

A.8.2 When the panel is transferring heat to the node 4

$$Q_{7\to8} + Q_{7\to8}^{pipe} + Q_{radiateglass} + Q_{evap1} + Q_{evap2} + Q_{3\to4} + Q_{5\to4} = \frac{\partial U_o}{\partial\tau}$$

$$\frac{k_I A}{ThickI}(t_7^{old} - t_8^{old}) + \frac{k_s A A_1}{ThickI}(t_7^{old} - t_8^{old}) + \frac{A(t_9^{old} - t_8^{old})}{R_{evap}} + A(Q_{evap1} + Q_{evap2})$$
$$+ \frac{kA}{(\Delta x - R)}(t_3^{old} - t_8^{old}) + \frac{kA}{(\Delta x - R)}(t_5^{old} - t_8^{old}) = mc\frac{(t_8^{new} - t_8^{old})}{\Delta\tau}$$

$$\frac{k_I A}{ThickI}(t_7^{old} - t_8^{old}) + \frac{k_s A A_1}{ThickI}(t_7^{old} - t_8^{old}) + \frac{A(t_9^{old} - t_8^{old})}{R_{evap}}$$
$$+ A(Q_{evap1} + Q_{evap2}) + \frac{kA}{(\Delta x - R)}(t_3^{old} + t_5^{old} - 2t_8^{old})$$
$$= \left((2\rho_s C_s (ThickS + ThickP)) + (\rho C(\Delta x - 2R)) + (\frac{\rho_I \, ThickI \, C_I}{2}) \right) \frac{A(t_8^{new} - t_8^{old})}{\Delta\tau}$$

$$t_8^{new} = t_8^{old} + Cons2\left(\frac{k_I}{ThickI}(t_7^{old} - t_8^{old}) + \frac{k_s A_1}{ThickI}(t_7^{old} - t_8^{old}) + \frac{(t_9^{old} - t_8^{old})}{R_{evap}} + Q_{evap1} + Q_{evap2}) \right)$$
$$+ Cons2\left(\frac{k}{(\Delta x - R)}(t_3^{old} + t_5^{old} - 2t_8^{old}) \right) \quad \text{----------A.8.2}$$

where

$$Cons2 = \frac{\Delta\tau}{\left((2\rho_s C_s (ThickS + ThickP)) + (\rho C(\Delta x - 2R)) + (\frac{\rho_I \, ThickI \, C_I}{2}) \right)}$$

$$Q_{evap1} = \frac{(\alpha_s \tau_g I_{VERT})}{\left(1 - (1 - \alpha_s)(1 - \tau_g - \alpha_g)\right)}$$

$$Q_{evap2} = \frac{(\alpha_s \tau_{g1} I_S)}{\left(1 - (1 - \alpha_s)(1 - \tau_{g1} - \alpha_g)\right)}$$

A.9 ENERGY BALANCE EQUATION FOR NODE 9

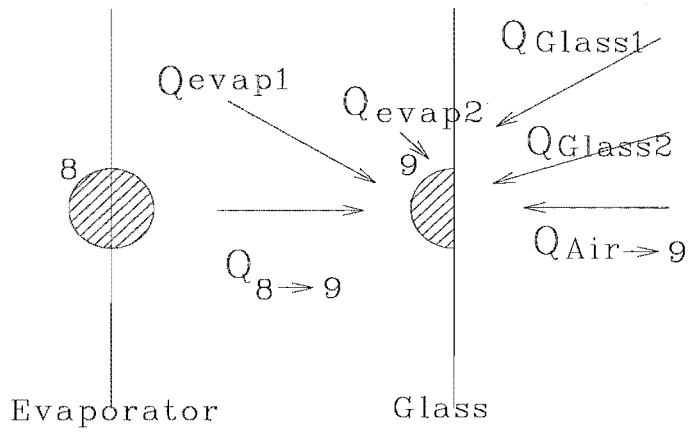

$$Q_{convectout} + Q_{glass1} + Q_{glass2} + Q_{radiateevap} = \frac{\partial U_o}{\partial \tau}$$

$$\frac{A(t_{Air}^{old} - t_9^{old})}{R_{Glass}} + \frac{A(t_8^{old} - t_9^{old})}{R_{evap}} + A(Q_{glass1} + Q_{glass2}) = mc\frac{(t_9^{new} - t_9^{old})}{\Delta\tau}$$

$$\frac{A(t_{Air}^{old} - t_9^{old})}{R_{Glass}} + \frac{A(t_8^{old} - t_9^{old})}{R_{evap}} + A(Q_{glass1} + Q_{glass2}) = \rho_g ThickG\, C_g A\frac{(t_9^{new} - t_9^{old})}{\Delta\tau}$$

$$t_9^{new} = t_9^{old} + \left(\frac{\Delta\tau}{\rho_g ThickG\, C_g}\right)\left((Q_{glass1} + Q_{glass2}) + \frac{(t_8^{old} - t_9^{old})}{R_{evap}} + \frac{(t_{Air}^{old} - t_9^{old})}{R_{Glass}}\right) \text{----------A.9}$$

where

$$Q_{glass1} = \frac{(\alpha_g I_{VERT})(1 + \tau_g(1 - \alpha_s))}{\left(1 - (1 - \alpha_s)(1 - \tau_g - \alpha_g)\right.}$$

$$Q_{glass2} = \frac{(\alpha_g I_S)(1 + \tau_{g1}(1 - \alpha_s))}{\left(1 - (1 - \alpha_s)(1 - \tau_{g1} - \alpha_g)\right)}$$

A.10 THERMAL BRIDGING CALCULATIONS

The thermal resistance in the bridging situation can be calculated by the following equation (NZS 4214 - 1977)

$$\frac{1}{R_L} = \frac{f}{R_1} + \frac{1-f}{R_2}$$

Thermal bridging value in between node 4 and node 7

$$f = 36 \times 0.019\,\pi \times 0.001 = 2.15 \times 10^{-3}$$

$$R_1 = \Delta x / K_S = 0.033 / 45 = 7.33 \times 10^{-4}$$

$$R_2 = \Delta x / K = 0.033 / 2 = 0.01665$$

$$\frac{1}{R_L} = 2.93 + 60.48$$

Thermal bridging value in between node 7 and node 8

$$f = 36 \times 0.019\,\pi \times 0.001 = 2.15 \times 10^{-3}$$

$$R_1 = \text{Thickl} / K_S = 0.05 / 45 = 1.11 \times 10^{-3}$$

$$R_2 = \text{Thickl} / K_I = 0.05 / 0.025 = 2$$

$$\frac{1}{R_L} = 1.94 + 0.499$$

A.11 EQUIVALENT DIMENSION CALCULATIONS

Calculating THICKP :

Number of 1 m long pipes in 1 m^2 cross-sectional area = 15

Condenser tube outer diameter = OD

Condenser tube inner diameter = OD1

Cross-sectional area of the tube = $\pi(OD^2 - OD1^2)/4$

Total mass of the condenser tube AR = $\rho \times \pi(OD^2 - OD1^2)/4 \times 1 \times 15$

If this mass of tube is divided into two sheet of THICKP thickness for the area of 1 m^2 then;

$$2 \times THICKP \times 1 \times \rho = AR$$

$$THICKP = AR/2$$

Calculating R :

If the tube will be squeezed to form an ellipse of SQ mm minor axis, then the major axis B would be :

$$2 \times \pi \times (SQ^2 + B^2)^{1/2} = 2 \times \pi \times OD \text{ (Equating the circumferences)}$$

$$B = (2 \times OD^2 - SQ^2)^{1/2}$$

$$\text{Area of the ellipse tube} = \pi \times SQ \times B /4$$

$$\text{Total volume of the tube} = 15 \times \pi \times SQ \times B /4$$

If this volume is distributed over 1 m^2 area of 2R thickness

$$2 \times R \times 1 = 15 \times \pi \times SQ \times B /4$$

$$R = 15 \times \pi \times SQ \times B /8$$

Calculating A :

Total of 38 tubes cross in between node 7 and 8 in 1 m^2 cross-sectional area.

$$\text{Total area of these tubes } A = 38 \times \pi \times (OD^2 - OD1^2)/4$$

APPENDIX B

B. PROGRAM LISTING

This appendix comprises of :

Computer source listing

Main program listing

Subroutine Solar 1 listing

Subroutine Solar 2 listing and

Subroutine Pipe listing.

B.1 COMPUTER SOURCE LISTING

VARIABLE	DEFINITION	UNITS
A	Area of pipe passing through insulation for $1m^2$ area	m^2
AIM	Minimum angle of incidence at time	degrees
AINCID	Angle of incident of solar radiation	degrees
ALPHAG	Solar absorptivity of glass	
ALPHAS	Solar absorptivity of black solar panel	
ALT	Altitude angle	degrees
ALTR	Altitude angle	radians
BI	Biot number	
C	Specific heat for concrete	J/kg K
CG	Specific heat for glass	J/kg K
CI	Specific heat for insulation	J/kg K
CO	Calculated constant for a particular values	
COND	Condition for steady state	
CONS	Calculated value for a particular time	
CONS1	Calculated value for a particular time	
CONS2	Calculated value for a particular time	
CS	Specific heat for steel	J/kg K

VARIABLE	DEFINITION	UNITS
DECR	Declination angles	radians
DELA	Difference in angle of incidence	degrees
DELT	Time between two readings	hours
DELX	Nodal separation in concrete wall	m
DIFFUS	Diffusivity of concrete	m^2/s
FO	Fourier number	
IS	Intensity of scattered radiation on a vertical surface	W/m^2
IVERT	Direct component of the total solar intensity	W/m^2
J	Node variable	
K	Thermal conductivity of concrete	W/m K
KI	Thermal conductivity of insulation	W/m K
KS	Thermal conductivity of steel	W/m K
LAT	Latitudinal position	degrees
LATR	Latitudinal position	radians
N	Number of nodes	
NHOURS	Time in full hours	hours
NPIPE	Condenser position in the wall	
OD	Outer diameter of condenser tube	m
OD1	Inner diameter of condenser tube	m
PI	pi	
PO	Calculated constant for a particular values	
QLG	Energy lost through glass for a 24 hour day	mJ
QLG1	Energy loss through the glass for a time interval	mJ
QLR	Energy released inside the room for a 24 hour day	mJ
QLR1	Energy released in to the room for a time interval	mJ
QSA	Total Solar energy available at outside wall for a 24 hour day	mJ
QSA1	Solar energy available outside for a time interval	mJ
QSE	Total Solar energy available at evaporator for a 24 hour day	mJ
QSE1	Solar energy available at evaporator for a time interval	mJ
R	Radius of the distributed pipe for $1m^2$ area	m
REVAP	Thermal resistance of a evaporator for a radiative heat transfer	m^2K/W

VARIABLE	DEFINITION	UNITS
RHO	Mass density of concrete	kg/m^3
RHOG	Mass density of glass	kg/m^3
RHOI	Mass density of insulation	kg/m^3
RHOS	Mass density of steel	kg/m^3
RPC	Number of readings per hour	
RROOM	Thermal resistance of a interior wall surface for convective and radiative heat transfer	m^2K/W
T2	Maximum interior wall temperature	°C
TAIR	Ambient air temperature	°C
THICK	Thickness of the concrete block	m
THICKG	Thickness of the glass	m
THICKI	Thickness of the insulation	m
THICKP	Thickness of the distributed pipe for $1m^2$ area	m
THICKS	Thickness of the steel sheet in evaporator	m
TIME	Time of day	hours
TIME1	Time for maximum interior wall temperature	hours
TNEW	Temperature variable	°C
TNEW2	Temperature variable	°C
TNEW3	Temperature variable	°C
TOLD	Temperature variable	°C
TOWG	Transmissivity of glass for direct solar radiation	
TOWG1	Transmissivity of glass for scattered solar radiation	
TOWMAX	Maximum transmissivity of glass for a given angle of incidence	
TOWMIN	Minimum transmissivity of glass for a given angle of incidence	
TR	Temperature of the room	°C
WALL	Position of the wall (degrees east of north)	degrees
WALLR	Position of the wall (degrees east of north)	radians
WAZ	Solar wall azimuth angle	degrees
WAZR	Solar wall azimuth angle	radians
X	Positive real number	

B.2 MAIN PROGRAM LISTING

```
*   SUMMER AND WINTER
*   STEEL PIPE AS A CONDENSER. (3 PIPES PER CAVITY)
*   CONDENSER AT NODES 3,4 & 5
*   STEADY DAY PATTERN.
*   STEEL PIPE IS CONDUCTING HEAT BETWEEN 7 & 8.

*   THIS PROGRAM CALCULATES THE INTERIOR AND EXTERIOR NODAL
*   TEMPERATURES OF A CONCRETE WALL FROM PREVIOUS TEMPERATURE
*   READINGS.

      REAL TNEW(1000),TOLD(1000),K,RHO,C,H,TR,THICK,RPC
      REAL TIME,X
      REAL RHOS,THICKS,CS,ALPHAS
      REAL LAT,WALL,LATR,IVERT,IS,TOWG,TOWG1
      REAL TNEW2(1000),TNEW3(1000)
      REAL QSA,QSE,QLR,QLG,QSA1,QSE1,QLR1,QLG1,QLG2,KI,KS
      DOUBLE PRECISION CONS,CONS1,CONS2

      INTEGER  N,NPIPE,NHOURS,DAY


*     PROPERTIES OF CONCRETE
      DATA K/2.0/
      DATA RHO/2350/
      DATA C/950/

*     PROPERTIES OF INSULATION
      DATA KI/0.025/
      DATA RHOI/30/
      DATA CI/1000/
      DATA THICKI/0.05/

*     PROPERTIES OF EVAPORATOR/CONDESER MATERIAL
      DATA RHOS/7800/
      DATA THICKS/0.0006/
      DATA CS/460/
      DATA ALPHAS/0.9/
      DATA KS/45.0/
      DATA REVAP/0.18/

*     PROPERTIES OF GLASS
      DATA TOWG1/0.79/
      DATA RHOG/2800/
      DATA THICKG/0.004/
      DATA CG/840/
      DATA ALPHAG/0.05/
      DATA RGLASS/0.06/

*     OTHER CONSTANTS
      DATA H/10/
      DATA TR/20/
      DATA PI/3.1415927/
      DATA RROOM/0.09/

*     OUTER DIA OF THE PIPE
      DATA OD/0.019/
*     INNER DIA OF THE PIPE
```

```
      DATA OD1/0.017/
*     SQUEEZED PIPE SIZE FOR CONDENSOR
      DATA SQ/0.01/

5     PRINT*,'ENTER NUMBER OF NODES=9'
      DATA N/9/
      PRINT*,'THICKNESS OF CONCRETE WALL=.2'
      DATA THICK/0.2/

      DIFFUS=K/(RHO*C)
      DELX=THICK/(N-3)

      PRINT*,'NUMBER OF READINGS PER HOUR=24'
      DATA RPC/24/

      DELT=1/RPC

*     CALCULATING THE STABILITY CONDITIONS

      FO=(DIFFUS*DELT*3600)/(DELX*DELX)
      PRINT*,'FO=',FO
      BI=(H*DELX)/K
      PRINT*,'BI=',BI
      COND=FO*(1+BI)

*     TESTING THE STABILITY CONDITIONS

      IF(FO.GT.0.5.OR.COND.GT.0.5) THEN
      PRINT*,'DELT AND DELX ARE NOT UNDER THE CONDITION'
      PRINT*,'PLEASE CHANGE THOSE VALUES AND TRY AGAIN'
      GOTO 5
      END IF

      CALL PIPE (THICKP,R,OD,OD1,PI,SQ,A)
      PRINT *,THICKP,R,A

      PRINT*,'CONDENSOR POSITION-NPIPE-'
      DATA NPIPE/3/

      IF (DELX.GT.2*R) THEN
      CO=DELX/(DELX-R)
      ELSE
      PRINT *,'PLEASE CHANGE THE VALUES OF SQ & OD'
      END IF

      PO=(K*DELT*3600)/((2*THICKP*RHOS*CS+RHO*C*(DELX-2*R))*(DELX-R))

      PRINT*,'LATITUDE OF THE PLACE -LAT-'
      DATA  LAT/-43.5/
      PRINT*,'NUMBER OF DAYS SINCE JUNE 22nd.(0 OR 183) -DAY-'
      DATA DAY/0/
      PRINT*,'POSITION OF THE WALL (DEGREES EAST OF NORTH)-WALL-'
      DATA  WALL/0/
      LATR=LAT*PI/180
      DECR=23.5*PI*COS(DAY*2*PI/365.25)/180
      WALLR=WALL*PI/180

76    TIME=0.0

      IF (TIME.EQ.0.0) THEN
```

```
      DO 20 J=1,N
      TOLD(J)=20.0
      TNEW2(J)=10.0
      TNEW3(J)=20.0
20    CONTINUE
     ENDIF

      QSA=0
      QSE=0
      QLR=0
      QLG=0
      T2=20

85     DO 50 J=1,N

      IF (DAY.EQ.183) THEN
      CALL SOLAR1 (TAIR,TIME,DECR,WALLR,LATR,PI,ALT,WAZ,IVERT,IS)
      ELSE IF (DAY.EQ.0) THEN
      CALL SOLAR2 (TAIR,TIME,DECR,WALLR,LATR,PI,ALT,WAZ,IVERT,IS)
      END IF

      ALTR=ALT*PI/180
      WAZR=WAZ*PI/180
      AINCID=ACOS(COS(ALTR)*COS(WAZR))*180/PI

*     CALCULATING THE TRANSMISSIVITIES

      IF (AINCID.GE.0.AND.AINCID.LT.20) THEN
      AIM=0
      DELA=20
      TOWMAX=0.87
      TOWMIN=0.87

      ELSE IF (AINCID.GE.20.AND.AINCID.LT.40) THEN
      AIM=20
      DELA=20
      TOWMAX=0.87
      TOWMIN=0.86

      ELSE IF (AINCID.GE.40.AND.AINCID.LT.50) THEN
      AIM=40
      DELA=10
      TOWMAX=0.86
      TOWMIN=0.84

      ELSE IF (AINCID.GE.50.AND.AINCID.LT.60) THEN
      AIM=50
      DELA=10
      TOWMAX=0.84
      TOWMIN=0.79

      ELSE IF (AINCID.GE.60.AND.AINCID.LT.70) THEN
      AIM=60
      DELA=10
      TOWMAX=0.79
      TOWMIN=0.67

      ELSE IF (AINCID.GE.70.AND.AINCID.LT.80) THEN
      AIM=70
      DELA=10
```

```
      TOWMAX=0.67
      TOWMIN=0.42

      ELSE IF (AINCID.GE.80.AND.AINCID.LT.90) THEN
      AIM=80
      DELA=10
      TOWMAX=0.42
      TOWMIN=0.00

      ELSE
      TOWMAX=0.00
      TOWMIN=0.00

      END IF

     TOWG=TOWMAX-(AINCID-AIM)/DELA*(TOWMAX-TOWMIN)

*     ROOM SIDE WALL TEMPERATURE

      IF (J.EQ.1) THEN
      TNEW(J)=TOLD(J)+((2*DELT*3600)/(RHO*DELX*C))*(K*(TOLD(J+1)
     .      -TOLD(J))/DELX+(TR-TOLD(J))/RROOM)

*     INTERNAL NODE TEMPERATURE

      ELSE IF (J.GT.1.AND.J.LT.NPIPE-1) THEN
      TNEW(J)=FO*(TOLD(J-1)+TOLD(J+1))+(1-2*FO)*TOLD(J)

      ELSE IF (J.EQ.NPIPE-1) THEN
      TNEW(J)=FO*(TOLD(J-1)+CO*TOLD(J+1))+TOLD(J)*(1-FO-FO*CO)

*     CONDENSOR TEMPERATURE

      ELSE IF (J.EQ.NPIPE) THEN
      TNEW(J)=TOLD(J)+PO*(TOLD(J-1)+TOLD(J+1)-2*TOLD(J))

*     INTERNAL NODE TEMPERATURE

      ELSE IF (J.EQ.NPIPE+1) THEN
      TNEW(J)=FO*(TOLD(J+1)+CO*TOLD(J-1))+TOLD(J)*(1-FO-FO*CO)

      ELSE IF (J.GT.NPIPE+1.AND.J.LT.N-2) THEN
      TNEW(J)=FO*(TOLD(J-1)+TOLD(J+1))+(1-2*FO)*TOLD(J)

*     INSULATION SIDE WALL TEMPERARTURE

      ELSE IF (J.EQ.N-2) THEN
      CONS=(2*DELT*3600)/(RHO*DELX*C+RHOI*THICKI*CI)

      TNEW(J)=TOLD(J)+CONS*(K*(TOLD(J-1)-TOLD(J))/DELX
     .      +KI*(TOLD(J+1)-TOLD(J))/THICKI
     .      +KS*A*(TOLD(J+1)-TOLD(J))/THICKI)

*     EVAPORATOR TEMPERATURE

      ELSE IF (J.EQ.N-1) THEN
      QEVAP1=(ALPHAS*TOWG*IVERT)/(1-(1-ALPHAS)*(1-TOWG-ALPHAG))
      QEVAP2=(ALPHAS*TOWG1*IS)/(1-(1-ALPHAS)*(1-TOWG1-ALPHAG))
      CONS1=2*DELT*3600/(RHOS*THICKS*CS*4+RHOI*THICKI*CI)
```

```
      TNEW(J)=TOLD(J)+CONS1*(QEVAP1+QEVAP2
     . +(TOLD(J+1)-TOLD(J))/REVAP
     . +(KI/THICKI)*(TOLD(J-1)-TOLD(J))
     . + (KS*A/THICKI)*(TOLD(J-1)-TOLD(J)))


      IF (TOLD(J).GT.TNEW(NPIPE)) THEN

      CONS2=(DELT*3600)/((RHOS*THICKS*CS*2)+(RHO*C*(DELX-2*R))+
     .  (RHOS*2*THICKP*CS)+(RHOI*THICKI*CI/2))


      TNEW(J)=TOLD(J)+CONS2*(QEVAP1+QEVAP2+
     .  (TOLD(J+1)-TOLD(J))/REVAP
     .  +(KI/THICKI)*(TOLD(J-1)-TOLD(J))
     .  +(KS*A/THICKI)*(TOLD(J-1)-TOLD(J))
     .  + (K/(DELX-R))*(TOLD(NPIPE+1)+TOLD(NPIPE-1)
     .  -2*TOLD(J)))


      TNEW(NPIPE)=TNEW(J)
      ENDIF

*     GLASS TEMPERATURE

      ELSE
      QGLAS1=ALPHAG*IVERT*(1+(TOWG*(1-ALPHAS))/(1-(1-ALPHAS)
     .  *(1-TOWG-ALPHAG)))
      QGLAS2=ALPHAG*IS*(1+(TOWG1*(1-ALPHAS))/(1-(1-ALPHAS)
     .  *(1-TOWG1-ALPHAG)))

      TNEW(J)=TOLD(J)+(DELT*3600/(RHOG*THICKG*CG))*(
     .  QGLAS1+QGLAS2+(TOLD(J-1)-TOLD(J))/REVAP
     .  +(TAIR-TOLD(J))/RGLASS)

      END IF


50    CONTINUE

      IF (TNEW(1).GT.T2) THEN
      T2=TNEW(1)
      TIME1=TIME
      END IF

     P1=24.0-DELT

     IF (TIME.LE.P1) THEN
     QSA1=(IVERT+IS)*DELT*0.0036
     QSE1=(QEVAP1+QEVAP2)*DELT*0.0036
     QLR1=((TNEW(1)-TR)/RROOM)*DELT*0.0036
     QLG1=((TNEW(9)-TAIR)/RGLASS)*DELT*0.0036
     QLG2=((IVERT-QEVAP1-QGLAS1)+(IS-QEVAP2-QGLAS2))*DELT*0.0036

     QSA=QSA+QSA1
     QSE=QSE+QSE1
     QLR=QLR+QLR1
     QLG=QLG+QLG1+QLG2
     END IF
```

```
      IF (TIME.EQ.0.0) THEN
       DO 55 J=1,N
       TNEW(J)=TNEW3(J)
55     CONTINUE
       END IF

     X=ABS(TIME-FLOAT(IFIX(TIME)))

     IF (X.LE.0.0001.OR.X.EQ.0.0.OR.X.GE.0.9999) THEN
     NHOURS = IFIX(TIME+0.01)

      IF(NHOURS.EQ.0) THEN
      PRINT 70
      WRITE (50,70)
 70    FORMAT(1X,'HR',3X,'T1',4X,'T2',4X,'T3',4X,'T4',4X,'T5',5X,'T6'
     .  ,5X,'T7',5X,'T8',5X,'T9',5X,'TAIR')
      PRINT*
      WRITE (50,*)
      ENDIF

      PRINT 71,NHOURS,TNEW(1),TNEW(2),TNEW(3),TNEW(4),TNEW(5)
     . ,TNEW(6),TNEW(7),TNEW(8),TNEW(9),TAIR
      WRITE(50,71)NHOURS,TNEW(1),TNEW(2),TNEW(3),TNEW(4),TNEW(5)
     . ,TNEW(6),TNEW(7),TNEW(8),TNEW(9),TAIR
 71   FORMAT (I2,2X,F5.2,1X,F5.2,1X,F5.2,1X,F5.2,1X,F6.2,1X,F6.2,
     . 1X,F6.2,1X,F6.2,1X,F6.2,1X,F6.2)

       DO 90 J=1,N
        IF(NHOURS.EQ.0) THEN
        TNEW2(J)=TNEW(J)
        END IF

        IF (NHOURS.EQ.24) THEN
        TNEW3(J)=TNEW(J)
        ENDIF
90     CONTINUE

     ENDIF

     DO 60 J=1,N
     TOLD(J)=TNEW(J)
 60  CONTINUE

     TIME=TIME+DELT

      IF(TIME.LE.24.0) THEN
      GOTO 85
      END IF



     WRITE (50,*)
     PRINT*
     WRITE(50,*)'QSOLAR AVAILABLE =    ',QSA
     PRINT *,'QSOLAR AVAILABLE=    ',QSA
     WRITE(50,*)
     PRINT*
     WRITE(50,*)'QSOLAR AT EVAPORAYOR = ',QSE
     PRINT *,'QSOLAR AT EVAPORATOR= ',QSE
     WRITE(50,*)
```

```
      PRINT*
      WRITE(50,*)'QLOSS TO ROOM=        ',QLR
      PRINT*,'QLOSS TO ROOM=        ',QLR
      WRITE(50,*)
      PRINT*
      WRITE(50,*)'QLOSS TO GLASS=       ',QLG
      PRINT *,'QLOSS TO GLASS=      ',QLG

      EFFI=QLR*100/QSA

      DO 230 J=1,N

       IF ((ABS(TNEW2(J)-TNEW3(J))).GT.0.01)THEN
       PRINT*,'NEXT DAY READING'
       TOLD(J)=TNEW3(J)
       QSA=0
       QSE=0
       QLR=0
       QLG=0
       TIME=0.0
       GOTO 85
       END IF

230CONTINUE

      IF (NPIPE.EQ.3) THEN
      PRINT 240
      WRITE (60,240)
240    FORMAT(1X,'CONDENSOR POSITION',3X,'WALL TEMP(MAX)',3X,'TIME',3X,
     .    'QSA',3X,'QSE',9X,'QLR',7X,'QLG',3X,'EFFICIENCY')
      END IF

      PRINT *
      WRITE (60,*)
      PRINT 250,NPIPE,T2,TIME1,QSA,QSE,QLR,QLG,EFFI
      WRITE(60,250)NPIPE,T2,TIME1,QSA,QSE,QLR,QLG,EFFI
250    FORMAT(10X,I1,14X,F6.1,7X,F6.1,4X,F8.2,3X,F8.2,3X,F8.2,3X,F7.2
     .    ,3X,F6.1)

      NPIPE=NPIPE+1
      T2=0
      TIME1=0
       IF (NPIPE.LE.5) THEN
       GOTO 76
       END IF

300   END
```

B.3 SUBROUTINE 'PIPE' LISTING

```
SUBROUTINE PIPE (THICKP,R,OD,OD1,PI,SQ,A)
REAL OD,OD1,SQ

A=PI*38*(OD**2-OD1**2)/4
AR=PI*15*(OD**2-OD1**2)/4
THICKP=AR/2

B=(2*OD**2-SQ**2)
B=B**0.5
R=PI*B*SQ*15/8
RETURN
END
```

B.4 SUBROUTINE 'SOLAR1' LISTING

```
SUBROUTINE SOLAR1 (TAIR,TIME,DECR,WALLR,LATR,PI,ALT,WAZ,IVERT,IS)

REAL TIME,DECR,LATR,T,HR,ISMAX,WAZR,AZR,ALT,ALTR,WALLR
REAL AMIN,DALT,IMIN,IMAX,IVERT,IDIR,PI,IS,ISMIN

T=TIME-12.5
HR=T*PI/12
ALTR=ASIN(SIN(DECR)*SIN(LATR)+COS(DECR)*COS(LATR)*COS(HR))
AZR=ATAN(SIN(HR)/(SIN(LATR)*COS(HR)-COS(LATR)*TAN(DECR)))
WAZR=AZR-WALLR
WAZ=WAZR*180/PI
ALT=ALTR*180/PI

IF (ALT.GE.0.AND.ALT.LT.5)THEN
AMIN = 0
DALT = 5
IMIN = 0
IMAX = 210
ISMIN = 0
ISMAX = 7

ELSEIF (ALT.GE.5.AND.ALT.LT.10)THEN
AMIN = 5
DALT = 5
IMIN = 210
IMAX = 388
ISMIN = 7
ISMAX = 22

ELSEIF (ALT.GE.10.AND.ALT.LT.15)THEN
AMIN = 10
DALT = 5
IMIN = 388
IMAX = 524
ISMIN = 22
ISMAX = 33

ELSEIF (ALT.GE.15.AND.ALT.LT.20)THEN
AMIN = 15
DALT = 5
IMIN = 524
IMAX = 620
```

```
ISMIN = 33
ISMAX = 40

ELSEIF (ALT.GE.20.AND.ALT.LT.25)THEN
AMIN = 20
DALT = 5
IMIN = 620
IMAX = 688
ISMIN = 40
ISMAX = 45

ELSEIF (ALT.GE.25.AND.ALT.LT.30)THEN
AMIN = 25
DALT = 5
IMIN = 688
IMAX = 740
ISMIN = 45
ISMAX = 48

ELSEIF (ALT.GE.30.AND.ALT.LT.35)THEN
AMIN = 30
DALT = 5
IMIN = 740
IMAX = 782
ISMIN = 48
ISMAX = 51

ELSEIF (ALT.GE.35.AND.ALT.LT.40)THEN
AMIN = 35
DALT = 5
IMIN = 782
IMAX = 814
ISMIN = 51
ISMAX = 53

ELSEIF (ALT.GE.40.AND.ALT.LT.50)THEN
AMIN = 40
DALT = 10
IMIN = 814
IMAX = 860
ISMIN = 53
ISMAX = 56

ELSEIF (ALT.GE.50.AND.ALT.LT.60)THEN
AMIN = 50
DALT = 10
IMIN = 860
IMAX = 893
ISMIN = 56
ISMAX = 57

ELSEIF (ALT.GE.60.AND.ALT.LT.70)THEN
AMIN = 60
DALT = 10
IMIN = 893
IMAX = 912
ISMIN = 57
ISMAX = 59

ELSEIF (ALT.GE.70.AND.ALT.LT.80)THEN
```

```
AMIN = 70
DALT = 10
IMIN = 912
IMAX = 920
ISMIN = 59
ISMAX = 59

ELSEIF (ALT.GE.80.AND.ALT.LT.90)THEN
AMIN = 80
DALT = 10
IMIN = 920
IMAX = 925
ISMIN = 59
ISMAX = 59

ELSE
AMIN = ALT
DALT = 1
IMIN = 0
IMAX = 0
ISMIN = 0
ISMAX = 0

ENDIF

IF (TIME.GE.12.0.AND.WAZR.GT.0.53)THEN
WAZR=WAZR-PI
ELSEIF(TIME.LT.12.0.AND.WAZR.LT.-0.5)THEN
WAZR=PI+WAZR
ENDIF

WAZ=WAZR*180/PI
IDIR = IMIN+(ALT-AMIN)/DALT*(IMAX-IMIN)

IF (WAZR.GT.-PI/2.AND.WAZR.LT.PI/2)THEN
IVERT = IDIR*COS(ALTR)*COS(WAZR)
ELSE
IVERT = 0
END IF

IS = ISMIN+(ALT-AMIN)/DALT*(ISMAX-ISMIN)

TAIR = (16.5+3.5*COS(HR-PI/4))

RETURN

END
```

B.5 SUBROUTINE 'SOLAR2' LISTING

```
SUBROUTINE SOLAR2 (TAIR,TIME,DECR,WALLR,LATR,PI,ALT,WAZ,IVERT,IS)

REAL TIME,DECR,LATR,T,HR,ISMAX,WAZR,AZR,ALT,ALTR,WALLR
REAL AMIN,DALT,IMIN,IMAX,IVERT,IDIR,PI,IS,ISMIN

T=TIME-12
HR=T*PI/12
ALTR=ASIN(SIN(DECR)*SIN(LATR)+COS(DECR)*COS(LATR)*COS(HR))
AZR=ATAN(SIN(HR)/(SIN(LATR)*COS(HR)-COS(LATR)*TAN(DECR)))
```

```
WAZR=AZR-WALLR
WAZ=WAZR*180/PI
ALT=ALTR*180/PI

IF (ALT.GE.0.AND.ALT.LT.5)THEN
AMIN = 0
DALT = 5
IMIN = 0
IMAX = 210
ISMIN = 0
ISMAX = 7

ELSEIF (ALT.GE.5.AND.ALT.LT.10)THEN
AMIN = 5
DALT = 5
IMIN = 210
IMAX = 388
ISMIN = 7
ISMAX = 16

ELSEIF (ALT.GE.10.AND.ALT.LT.15)THEN
AMIN = 10
DALT = 5
IMIN = 388
IMAX = 524
ISMIN = 16
ISMAX = 20

ELSEIF (ALT.GE.15.AND.ALT.LT.20)THEN
AMIN = 15
DALT = 5
IMIN = 524
IMAX = 620
ISMIN = 20
ISMAX = 23

ELSEIF (ALT.GE.20.AND.ALT.LT.25)THEN
AMIN = 20
DALT = 5
IMIN = 620
IMAX = 688
ISMIN = 23
ISMAX = 25

ELSEIF (ALT.GE.25.AND.ALT.LT.30)THEN
AMIN = 25
DALT = 5
IMIN = 688
IMAX = 740
ISMIN = 25
ISMAX = 26

ELSEIF (ALT.GE.30.AND.ALT.LT.35)THEN
AMIN = 30
DALT = 5
IMIN = 740
IMAX = 782
ISMIN = 26
ISMAX = 27
```

```
ELSEIF (ALT.GE.35.AND.ALT.LT.40)THEN
AMIN = 35
DALT = 5
IMIN = 782
IMAX = 814
ISMIN = 27
ISMAX = 28

ELSEIF (ALT.GE.40.AND.ALT.LT.50)THEN
AMIN = 40
DALT = 10
IMIN = 814
IMAX = 860
ISMIN = 28
ISMAX = 29

ELSEIF (ALT.GE.50.AND.ALT.LT.60)THEN
AMIN = 50
DALT = 10
IMIN = 860
IMAX = 893
ISMIN = 29
ISMAX = 30

ELSEIF (ALT.GE.60.AND.ALT.LT.70)THEN
AMIN = 60
DALT = 10
IMIN = 893
IMAX = 912
ISMIN = 30
ISMAX = 30

ELSEIF (ALT.GE.70.AND.ALT.LT.80)THEN
AMIN = 70
DALT = 10
IMIN = 912
IMAX = 920
ISMIN = 30
ISMAX = 30

ELSEIF (ALT.GE.80.AND.ALT.LT.90)THEN
AMIN = 80
DALT = 10
IMIN = 920
IMAX = 925
ISMIN = 30
ISMAX = 30

ELSE
AMIN = ALT
DALT = 1
IMIN = 0
IMAX = 0
ISMIN = 0
ISMAX = 0

ENDIF

IF (TIME.GE.12.0.AND.WAZR.GT.0.53)THEN
WAZR=WAZR-PI
```

```
ELSEIF(TIME.LT.12.0.AND.WAZR.LT.-0.5)THEN
WAZR=PI+WAZR
ENDIF

WAZ=WAZR*180/PI
IDIR = IMIN+(ALT-AMIN)/DALT*(IMAX-IMIN)

IF (WAZR.GT.-PI/2.AND.WAZR.LT.PI/2)THEN
IVERT = IDIR*COS(ALTR)*COS(WAZR)
ELSE
IVERT = 0
END IF

IS = ISMIN+(ALT-AMIN)/DALT*(ISMAX-ISMIN)
TAIR = (6.45+3.15*COS(HR-PI/4))

RETURN

END
```

APPENDIX C

C. PANEL DESIGN DETAILS

The die used for manufacturing the evaporator has two parts as shown in Figs. C.1 and C.2. All the dimensions are clearly given in the figures. In Fig. C.1, the shaded portions were retained and the rest of the area was milled from 20 mm Customwood to a depth of 4 mm.

In Fig C.2 the bulges were placed according to the concrete cavity hole positions. Only the bulge areas were milled out in this part to the shape shown in the side view of the Fig C.3.

Figure C.4 shows the final shape and dimensions of the condenser tubes.

Figure C.5 shows a cross section view of the wall and the position of the holes in the evaporator with connected condenser tubes.

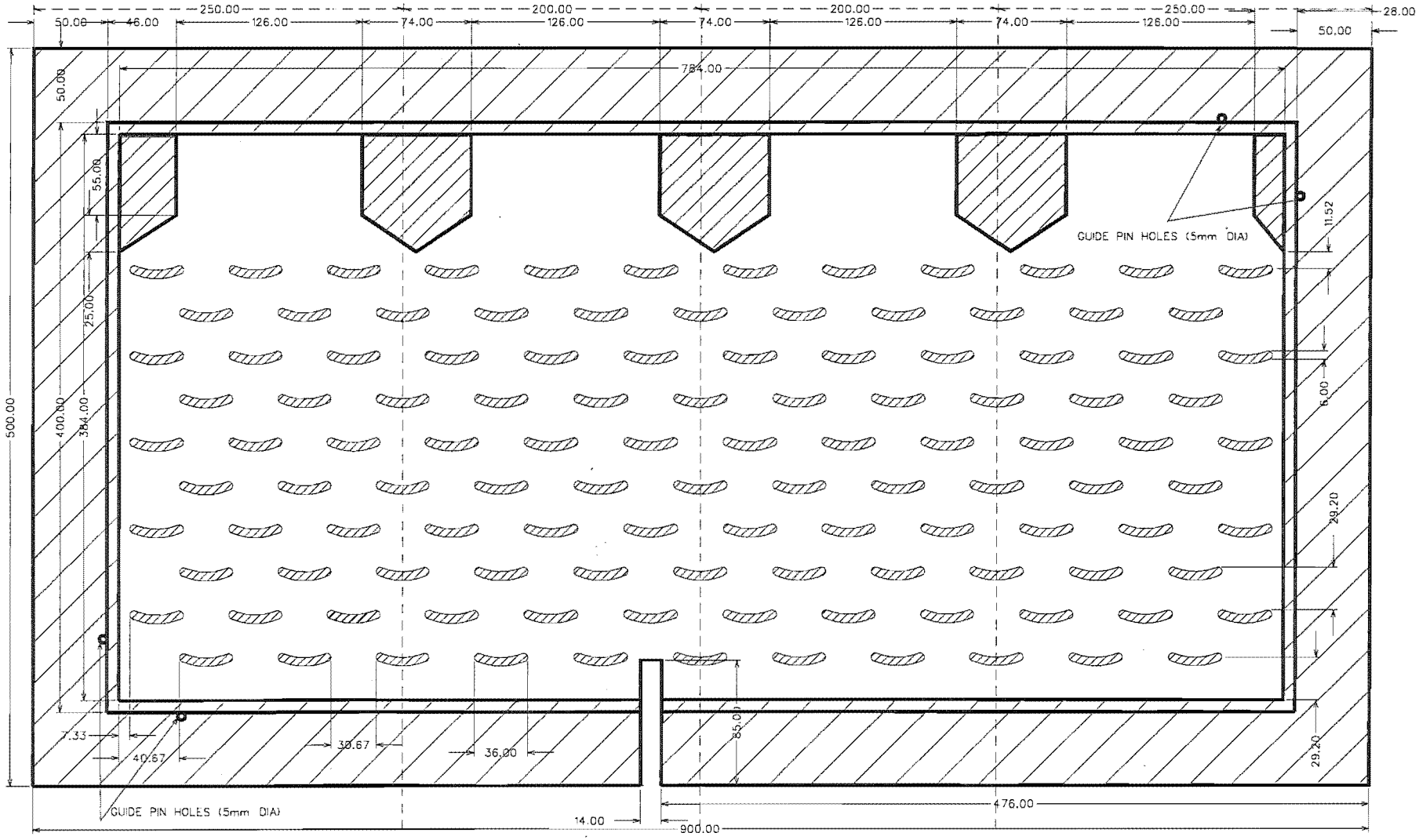

Figure C.1 Evaporator die part 1

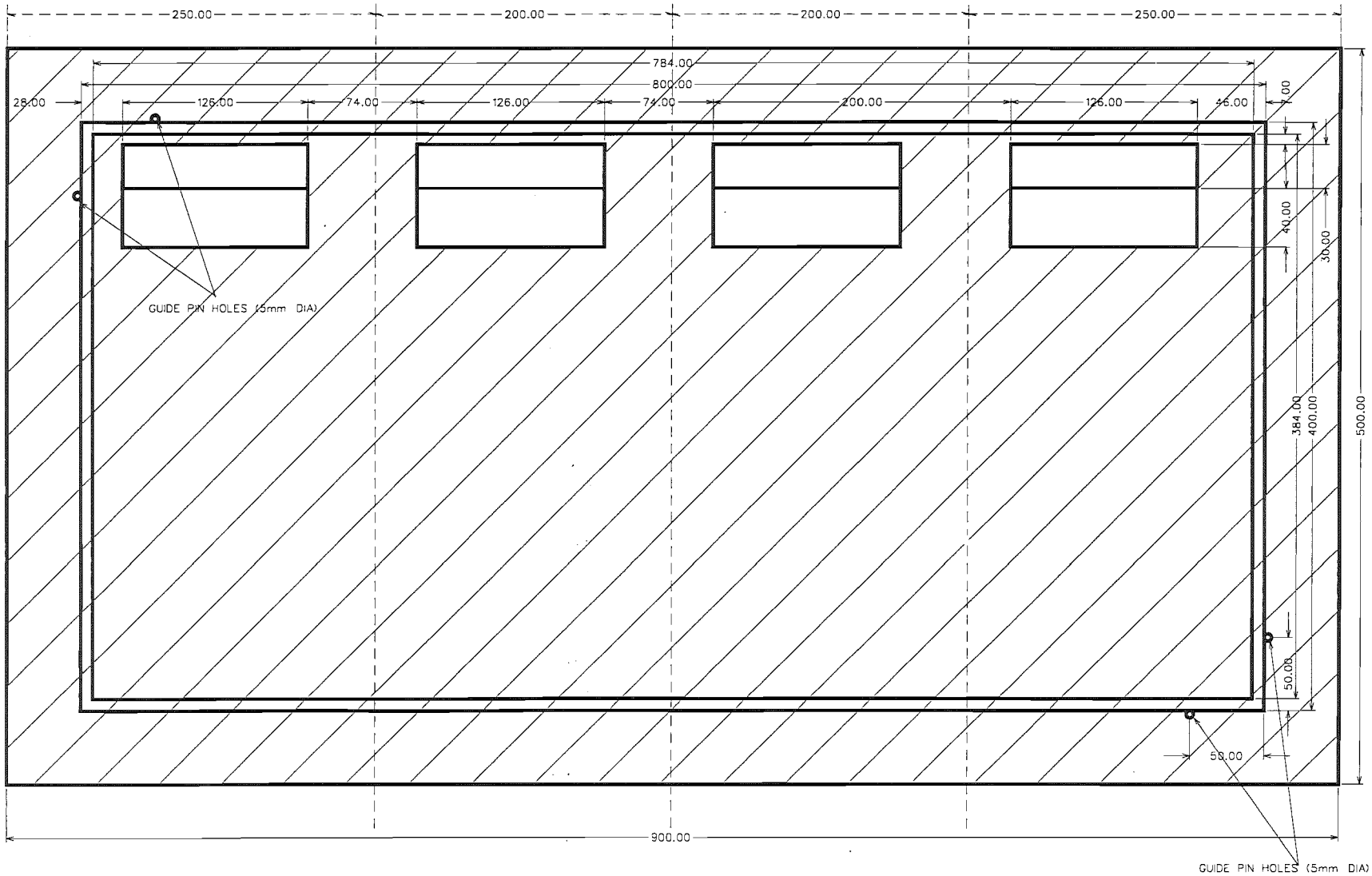

Figure C.2 Evaporator die part 2

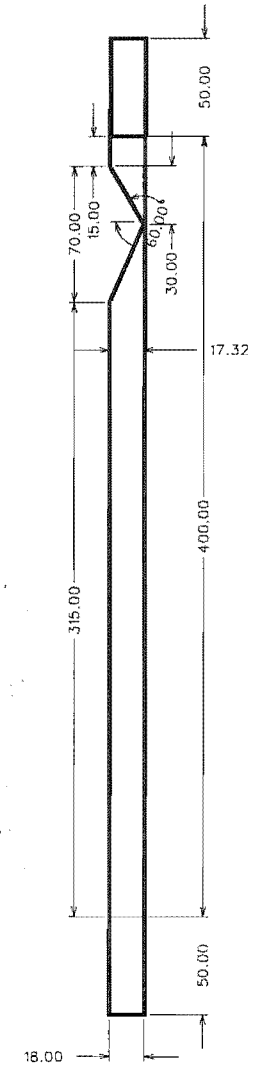

Figure C.3 Side view of the evaporator die part 2

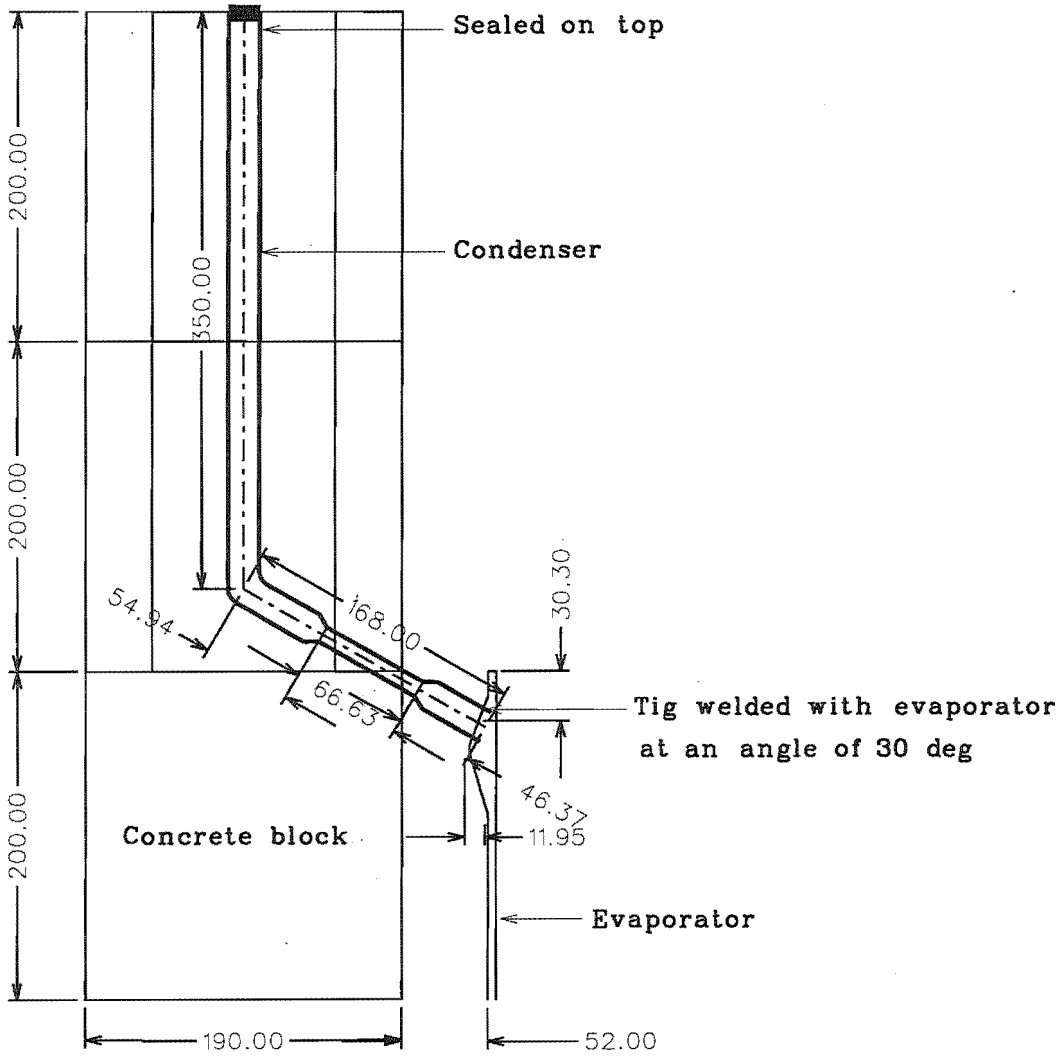

Figure C.4 Condenser pipe shape and dimensions

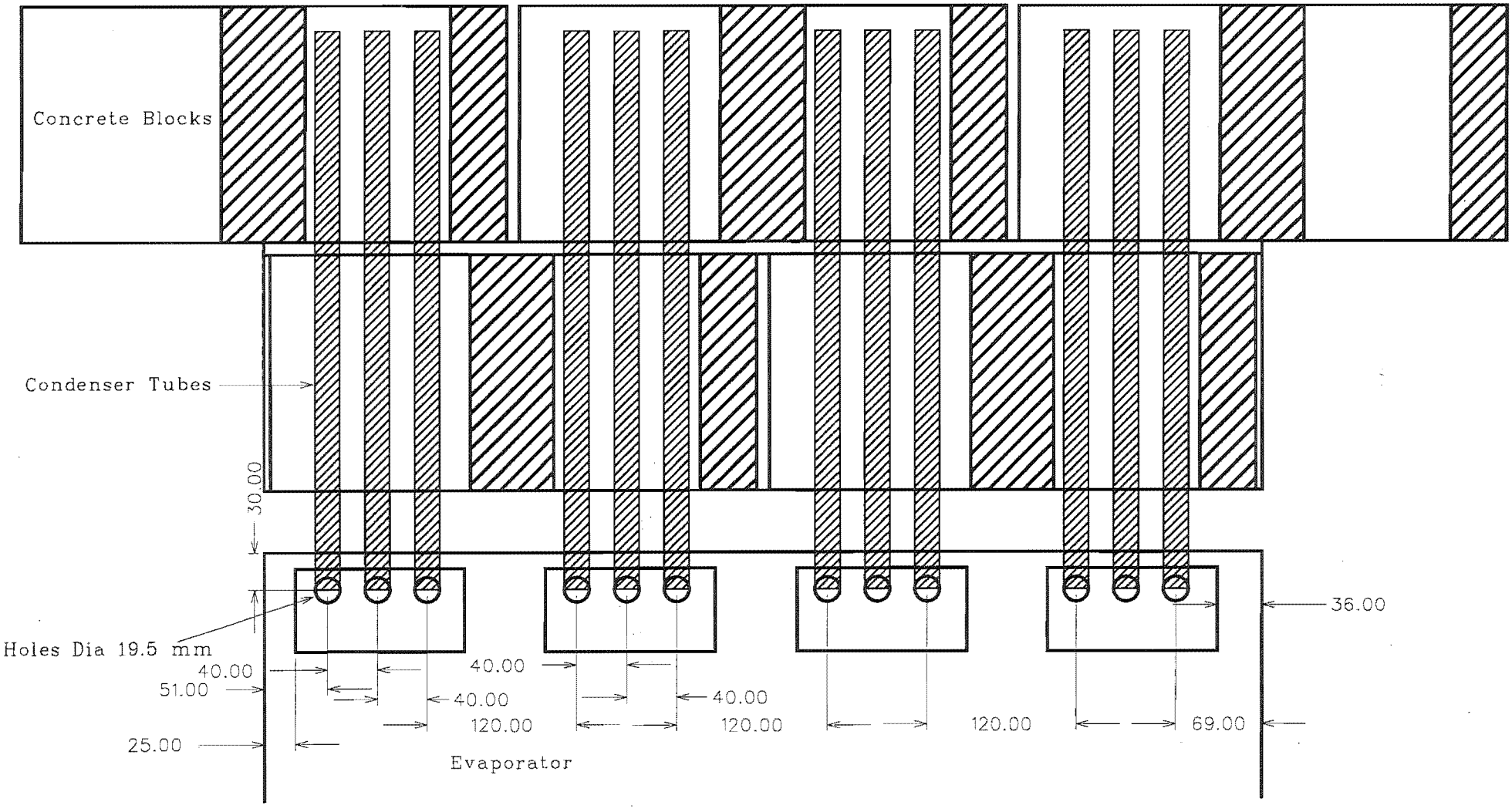

Figure C.5 Cross section of panel position in the wall and hole position on back of the evaporator

APPENDIX D

D. EXPERIMENTAL READINGS FROM GENERAL PERFORMANCE TEST

Experiment Number : 1

Working fluid Toluene.

Condenser at 20 °C.

Table D.1 General performance test results (evaporator tank).

Room Temperature (°C)	Mass flow rate of the Evaporator tank $\dot{m}_e$ (Kg/Sec)	Evaporator tank inlet temperature te_i (°C)	Evaporator tank outlet temperature te_o (°C)	($\Delta t_e = te_i - te_o$) (°C)	Total heat gain in the Evaporator $\dot{Q}_{evap}$ (W)
20.0	5.68×10^{-3}	26.0	24.2	1.80	42
20.0	17.12×10^{-3}	31.0	29.1	1.9	136
20.0	32.77×10^{-3}	36.0	34.0	2.0	273
20.5	38.15×10^{-3}	41.1	38.9	2.2	350
20.0	85.35×10^{-3}	43.0	40.4	2.6	926
20.5	90.43×10^{-3}	46.2	43.7	2.5	944
20.0	116.83×10^{-3}	51.0	48.5	2.5	1220
20.5	146.20×10^{-3}	61	58.3	2.7	1650

Repeated Readings

20.0	37.34×10^{-3}	41.1	38.9	2.2	343
20.0	27.40×10^{-3}	36.1	34.0	2.1	240
20.0	183.30×10^{-3}	50.0	48.1	1.9	1456

Table D.2 General performance test results (condenser tank).

Evaporator Temperature (°C)	Mass flow rate of the Condenser tank $\dot{m}_c$ (Kg/sec)	Condenser tank inlet temperature tc_i (°C)	Condenser tank outlet temperature tc_o (°C)	$(\Delta t_c = tc_o - tc_i)$ (°C)	Total heat gain in the Condenser $\dot{Q}_{cond}$ (W)
25.0	8.66×10^{-3}	19.6	20.7	1.1	40
30.0	19.48×10^{-3}	19.3	20.9	1.6	130
35.0	35.50×10^{-3}	19.3	20.8	1.5	223
40.0	47.25×10^{-3}	19.3	20.9	1.6	316
41.7	79.46×10^{-3}	19.0	21.7	2.7	897
45.0	79.98×10^{-3}	18.9	21.7	2.8	937
49.8	103.15×10^{-3}	18.6	21.4	2.8	1208
59.7	136.55×10^{-3}	18.7	21.5	2.8	1599

Repeated Readings

40.0	46.30×10^{-3}	19.3	20.9	1.6	310
35.0	27.63×10^{-3}	19.1	21.0	1.9	220
49.0	110.36×10^{-3}	18.7	21.4	2.7	1246

Table D.3 General performance test results (other temperature readings).

Condenser Pipe Bottom Temperature t_{CB} (°C)	Condenser Pipe Top Temperature t_{CT} (°C)	Evaporator Top Temperature t_{ET} (°C)
19.8	21.1	22.8
19.9	21.8	27.1
19.8	22.2	32.5
19.9	23.4	37.7
20.9	27.5	31.7
21.2	28.4	33.6
21.2	29.5	35.9
21.6	30.9	40.4

Repeated Reading

20.4	23.1	36.9
20.5	22.2	30.9
21.7	29.9	33.5

Experiment Number : 2

Working fluid Toluene.

Condenser at 25 °C.

Table D.4 General performance test results (evaporator tank).

Room Temperature (°C)	Mass flow rate of the Evaporator tank $\dot{m}_e$ (Kg/Sec)	Evaporator tank inlet temperature te_i (°C)	Evaporator tank outlet temperature te_o (°C)	($\Delta t_e = te_i - te_o$) (°C)	Total heat gain in the Evaporator $\dot{Q}_{evap}$ (W)
20.0	9.58×10^{-3}	31.0	29.0	2.0	80
20.0	18.48×10^{-3}	36.0	34.0	2.0	154
19.5	42.78×10^{-3}	40.8	39.0	1.8	321
21.0	56.30×10^{-3}	46.0	43.9	2.1	494
20.5	68.56×10^{-3}	51.0	48.8	2.2	630

Table D.5 General performance test results (condenser tank).

Evaporator Temperature (°C)	Mass flow rate of the Condenser tank $\dot{m}_c$ (Kg/sec)	Condenser tank inlet temperature tc_i (°C)	Condenser tank outlet temperature tc_o (°C)	($\Delta t_c = tc_o - tc_i$) (°C)	Total heat gain in the Condenser $\dot{Q}_{cond}$ (W)
30.0	13.78×10^{-3}	24.6	25.2	0.6	35
35.0	21.83×10^{-3}	24.1	25.6	1.5	137
39.9	27.76×10^{-3}	24.1	26.1	2.0	232
45.0	45.27×10^{-3}	24.0	26.1	2.1	398
49.9	61.47×10^{-3}	23.9	26.1	2.2	566

Table D.6 General performance test results (other temperature readings).

Condenser Pipe Bottom Temperature t_{CB} (°C)	Condenser Pipe Top Temperature t_{CT} (°C)	Evaporator Top Temperature t_{ET} (°C)
25.0	25.3	27.4
25.0	26.0	32.2
25.0	27.1	36.9
25.3	28.0	41.7
25.4	29.2	42.1

Experiment :3

Working Fluid : N - Hexane.

Condenser at 20 °c.

Table D.7 General performance test results (evaporator tank).

Room Temperature (°C)	Mass flow rate of the Evaporator tank $\dot{m}_e$ (Kg/Sec)	Evaporator tank inlet temperature te_i (°C)	Evaporator tank outlet temperature te_o (°C)	($\Delta t_e = te_i - te_o$) (°C)	Total heat gain in the Evaporator $\dot{Q}_{evap}$ (W)
19.5	11.86×10^{-3}	25.6	24.6	1.0	50
20.0	21.81×10^{-3}	30.7	29.3	1.4	128
20.0	39.26×10^{-3}	36.0	34.0	2.0	328
20.0	88.52×10^{-3}	39.8	38.7	2.1	776
20.0	116.02×10^{-3}	46	43.8	2.2	1115

Repeated Readings

20.0	16.86×10^{-3}	30.9	29.1	1.8	127
20.0	87.50×10^{-3}	41.0	38.9	2.1	767

Table D.8 General performance test results (condenser tank).

Evaporator Temperature (°C)	Mass flow rate of the Condenser tank $\dot{m}_c$ (Kg/sec)	Condenser tank inlet temperature tc_i (°C)	Condenser tank outlet temperature tc_o (°C)	$(\Delta t_c = tc_o - tc_i)$ (°C)	Total heat gain in the Condenser $\dot{Q}_{cond}$ (W)
25.1	14.35×10^{-3}	19.7	20.3	0.6	36
30.0	19.99×10^{-3}	19.4	20.8	1.4	117
35.0	35.69×10^{-3}	19.0	21.0	2.0	298
39.3	69.90×10^{-3}	18.9	21.1	2.2	643
44.9	84.73×10^{-3}	18.8	21.2	2.4	850
Repeated Readings					
30.0	19.26×10^{-3}	19.3	20.7	1.4	113
40.0	63.33×10^{-3}	19.0	21.4	2.4	636

Table D.9 General performance test results (other temperature readings).

Condenser Pipe Bottom Temperature t_{CB} (°C)	Condenser Pipe Top Temperature t_{CT} (°C)	Evaporator Top Temperature t_{ET} (°C)
21.3	20.2	22.9
21.9	20.9	26.6
22.8	21.7	30.6
22.9	24.7	32.9
23.1	30.8	35.9
Repeated Reading		
22.2	20.9	26.6
25.2	23.9	34.7

Experiment : 4

Working Fluid : N - Hexane.

Condenser at 25 °c.

Table D.10 General performance test results (evaporator tank).

Room Temperature (°C)	Mass flow rate of the Evaporator tank $\dot{m}_e$ (Kg/Sec)	Evaporator tank inlet temperature te_i (°C)	Evaporator tank outlet temperature te_o (°C)	($\Delta t_e = te_i - te_o$) (°C)	Total heat gain in the Evaporator $\dot{Q}_{evap}$ (W)
19.0	13.33×10^{-3}	30.5	29.6	0.9	50
19.5	22.02×10^{-3}	35.8	34.3	1.5	138
19.5	30.63×10^{-3}	40.8	39.0	1.8	230
19.5	94.33×10^{-3}	45.9	43.8	2.1	827
Repeated Readings					
20.0	57.50×10^{-3}	41.0	39.0	2.0	480
20.0	52.93×10^{-3}	41.2	38.9	2.3	508

Table D.11 General performance test results (condenser tank).

Evaporator Temperature (°C)	Mass flow rate of the Condenser tank $\dot{m}_c$ (Kg/sec)	Condenser tank inlet temperature tc_i (°C)	Condenser tank outlet temperature tc_o (°C)	($\Delta t_c = tc_o - tc_i$) (°C)	Total heat gain in the Condenser $\dot{Q}_{cond}$ (W)
30.0	8.10×10^{-3}	24.5	25.6	1.1	37
35.0	15.15×10^{-3}	24.1	25.9	1.8	114
39.9	24.03×10^{-3}	24.0	26.0	2.0	201
44.9	63.05×10^{-3}	23.9	26.6	2.7	712
Repeated Readings					
40.0	40.91×10^{-3}	23.9	26.4	2.5	428
40.0	46.40×10^{-3}	24.0	26.3	2.3	446

Table D.12 General performance test results (other temperature readings).

Condenser Pipe Bottom Temperature t_{CB} (°C)	Condenser Pipe Top Temperature t_{CT} (°C)	Evaporator Top Temperature t_{ET} (°C)
27.0	25.5	28.1
27.8	26.0	31.7
28.2	26.2	35.9
29.7	31.0	39.5
Repeated Reading		
28.9	27.4	35.9
29.4	27.0	36.6

REVERSE HEATING TEST.

Experiment : 5

Working Fluid : N - Hexane.

Condenser at 40 °c And the Evaporator at 20 °c.

Table D.13 Reverse heating test results (evaporator tank).

Room Temperature (°C)	Mass flow rate of the Evaporator tank $\dot{m}_e$ (Kg/Sec)	Evaporator tank inlet temperature te_i (°C)	Evaporator tank outlet temperature te_o (°C)	($\Delta t_e = te_i - te_o$) (°C)	Total heat gain in the Evaporator $\dot{Q}_{evap}$ (W)
20.0	43.73×10^{-3}	20.0	20.05	0.05	9.14
Repeated Readings					
20.0	11.82×10^{-3}	19.9	20.1	0.2	9.88

Table D.14 Reverse heating test results (condenser tank).

Evaporator Temperature (°C)	Mass flow rate of the Condenser tank $\dot{m}_c$ (Kg/sec)	Condenser tank inlet temperature tc_i (°C)	Condenser tank outlet temperature tc_o (°C)	$(\Delta t_c = tc_o - tc_i)$ (°C)	Total heat gain in the Condenser $\dot{Q}_{cond}$ (W)
20.0	56.27×10^{-3}	40.3	40.1	0.2	46.98

Repeated Readings

20.0	55.22×10^{-3}	40.1	39.9	0.2	46.10

Table D.15 Reverse heating test results (other temperature readings).

Condenser Pipe Bottom Temperature t_{CB} (°C)	Condenser Pipe Top Temperature t_{CT} (°C)	Evaporator Top Temperature t_{ET} (°C)
39.6	40.0	21.8

Repeated Reading

39.4	39.8	22.5

APPENDIX E

E. EXPERIMENTAL RESULTS OF A PANEL SUN TEST AND MODIFIED EQUATION

E.1 EXPERIMENTAL RESULTS OF A PANEL SUN TEST.

Table E.1 Experimental and calculated values of panel test

Intensity / Panel (W)	Evap.bottom Temp (°C)	Evap.top Temp (°C)	Avg Temp t_c (°C)	Air Temp t_a (°C)	$(t_c+t_{avg}-2t_a)/I$ (°C)	Efficie-ncy	tavg (°C)
210	31.0	38.2	34.6	12.0	0.047	47.7	20.0
229	31.4	39.2	35.3	12.9	0.041	54.9	20.0
249	31.2	40.8	36.0	13.2	0.038	61.8	20.0
260	30.4	39.7	35.1	13.1	0.036	72.4	20.0
265	31.2	41.1	36.2	13.9	0.034	74.6	20.0
263	31.1	40.5	35.8	13.4	0.035	74.4	20.0
259	31.0	39.8	35.4	13.9	0.034	72.4	20.0
249	30.6	38.9	34.8	13.7	0.035	72.1	20.0
232	30.1	38.1	34.1	13.2	0.038	71.8	20.0
211	29.4	35.6	32.5	13.1	0.040	66.8	20.0
187	28.1	34.3	31.2	12.7	0.044	55.2	20.0
159	27.0	31.7	29.4	12.6	0.049	55.1	20.0
215	33.5	43.3	38.4	16.4	0.046	45.2	25.0
232	33.5	45.9	39.7	16.3	0.044	47.5	25.0
244	32.6	45.5	39.1	17.8	0.037	62.8	25.0
251	32.4	46.5	39.5	15.2	0.043	68.3	25.0
253	32.9	45.1	39.0	17.0	0.038	68.2	25.0
252	33.3	46.2	39.8	18.0	0.037	68.4	25.0
244	33.5	48.0	40.8	19.0	0.036	68.3	25.0
232	33.0	46.1	39.6	17.5	0.041	67.1	25.0
224	32.2	45.2	38.7	17.6	0.041	67.4	25.0
204	32.0	42.1	37.1	17.7	0.042	64.4	25.0
173	31.8	41.3	36.6	15.0	0.058	49.9	25.0
150	31.6	36.0	33.8	14.2	0.065	45.9	25.0

Contd..... Table E.1

Intensity / Panel (W)	Evap.bottom Temp (°C)	Evap.top Temp (°C)	Avg Temp t_c (°C)	AirTemp t_a (°C)	$(t_c+t_{avg}-2t_a)/I$ (°C)	Efficie -ncy	tavg (°C
212	37.5	47.5	42.5	12.5	0.072	18.4	30.0
232	38.6	48.9	43.8	14.4	0.062	39.9	30.0
248	39.1	49.8	44.5	14.0	0.060	55.4	30.0
258	40.7	50.0	45.4	13.0	0.061	63.0	30.0
261	40.2	49.9	45.1	13.9	0.058	62.6	30.0
258	40.4	49.6	45.0	13.0	0.061	57.3	30.0
252	40.6	49.2	44.9	12.0	0.065	55.5	30.0
241	39.7	47.1	43.4	12.4	0.065	52.6	30.0
224	38.3	45.9	42.1	12.4	0.068	49.8	30.0
202	38.9	43.4	41.2	12.1	0.074	36.5	30.0
173	37.9	41.0	39.5	11.2	0.087	26.0	30.0
143	35.5	38.2	36.9	11.0	0.100	22.7	30.0
204	44.0	49.2	46.6	11.0	0.093	4.8	35.0
221	43.7	51.4	47.6	11.1	0.087	16.7	35.0
234	44.7	52.7	48.7	13.2	0.078	26.9	35.0
242	44.4	52.1	48.3	14.0	0.073	34.5	35.0
246	46.2	53.1	49.7	12.3	0.078	47.5	35.0
246	45.7	52.5	49.1	12.2	0.078	39.2	35.0
239	45.1	51.1	48.1	12.3	0.078	30.2	35.0
228	44.6	49.9	47.3	11.4	0.083	26.4	35.0
212	43.9	48.3	46.1	11.3	0.088	24.7	35.0
194	42.2	46.0	44.1	10.1	0.097	20.3	35.0
174	40.3	42.8	41.6	10.1	0.104	3.7	35.0
143	40.0	41.0	40.5	10.0	0.124	0.1	35.0

E.2 MODIFIED EQUATION TO COMPARE THE SOLAR PANEL WITH CONVENTIONAL FLAT PLATE COLLECTORS

Heat gain by solar radiation $\dot{Q}_1 = (I \times \tau \times \alpha) A$

Heat loss from evaporator $\dot{Q}_2 = U_e \times A(t_e - t_a)$

$\therefore$ Energy collected $= \dot{Q}_1 - \dot{Q}_2$

Useful energy $\dot{Q}_3 = \dot{m} C_p (t_o - t_i)$

Heat loss from condenser tank $= \dot{Q}_4 = U_c \times A_p (t_{avg} - t_a)$

Apply the energy balance :

$$\dot{Q}_1 - Q_2 = \dot{Q}_3 + \dot{Q}_4$$

$$(I \times \tau \times \alpha) A - U_e \times A(t_e - t_a) = \dot{m} C_p (t_o - t_i) + U_c \times A(t_{avg} - t_a)$$

By re-arranging this equation :

$$\frac{\dot{m} C_p (t_o - t_i)}{I \times A} = \tau \alpha - U \left(\frac{t_e + t_{avg} - 2t_a}{I} \right)$$

$$\eta = \tau \alpha - U \left(\frac{t_e + t_{avg} - 2t_a}{I} \right)$$

$$\downarrow \quad \downarrow \quad \downarrow \quad \downarrow$$

$$y = c - m \quad x$$

APPENDIX F

F. EXPERIMENTAL DATA FROM 24-HOUR TEST AND LONG PERIOD TEST

The temperature readings, static heat energy meter readings and kWh meter readings were recorded for every hour for the 24-hour test and tabulated in Table F1.

The temperature readings, static heat energy meter reading and kWh meter readings were recorded every day at 0900 hours in February 1995 for the 'long period test' and tabulated in Table F2.

Table F.1 Experimental data of 24-hour test (Continues on next page)

Time of Day Hours	1300	1400	1500	1600	1700	1800	1900	2000	2100	2200	2300	2400
Node 1	25.5	28.6	28.8	29.9	30.1	29.5	28.8	28.3	27.7	27.0	26.5	26.0
Node 2	27.1	30.5	30.7	32.3	32.4	31.7	31.0	30.2	29.5	28.8	28.1	27.6
Node 3	28.7	31.7	32.5	34.1	34.1	33.6	32.6	31.7	30.9	30.0	29.2	28.6
Node 4	29.4	32.5	33.5	34.9	35.0	34.4	33.4	32.5	31.8	30.6	29.9	29.2
Node 5	29.3	32.4	33.6	35.2	35.4	34.9	34.1	33.1	32.3	31.0	30.2	29.6
Node 6	28.9	31.9	33.4	35.1	35.5	35.3	34.5	33.6	32.7	31.4	30.5	29.8
Node 7	28.9	32.0	33.4	35.1	35.5	35.3	34.5	33.5	32.6	31.4	30.4	29.7
Cond. N-Hexane (Top Panel)	33.6	36.7	37.0	37.4	36.5	35.5	34.4	33.5	32.8	31.8	31.0	30.4
Cond. Pegasol 1516 (Top Panel)	33.1	36.1	36.6	37.3	35.7	34.9	34.2	33.5	32.9	32.1	31.5	30.9
Evap.N-Hex (Middle Panel) Node 8	40.0	43.1	41.7	39.9	37.4	35.8	32.3	26.2	19.7	16.7	16.2	15.9
Evap.Pegasol 1516(Middle Panel) Node 8	37.6	41.0	40.5	40.5	40.2	37.9	32.3	25.9	19.7	16.7	16.3	16.1
Cond. N-Hexane (Middle Panel)	33.1	36.0	36.4	36.6	35.8	34.7	33.2	32.2	31.4	30.2	29.6	28.9
Cond. Pegasol 1516 (Middle Panel)	33.0	35.8	36.4	36.9	36.2	34.6	33.6	32.6	31.9	30.8	30.2	29.5
Top Plate Temperature	75.9	76.7	66.6	54.8	44.2	37.5	29.8	23.5	16.9	14.5	14.3	14.2
Glass Temperature -Node 9	36.4	37.1	32.8	29.6	26.3	23.7	20.4	17.2	14.7	13.4	13.4	13.3
Air Temperature Behind Glass	49.6	51.7	47.5	45.1	38.9	33.2	28.6	23.5	18.3	15.8	15.6	15.4
Ambient Temperature	23.1	19.5	19.4	17.3	16.7	15.3	14.5	13.0	12.1	11.7	11.8	11.6
Calorimeter Box Temperature	20.1	20.1	20.3	20.1	20.2	20.2	20.2	20.1	20.2	20.0	20.2	20.1
Chilled Water Temperature	10.2	10.1	10.2	10.0	10.2	10.1	10.1	10.1	10.1	10.0	10.2	10.1
Room Temperature	21.2	20.7	21.0	21.6	21.2	20.7	21.0	20.0	21.4	19.7	20.0	21.2
Accumulated Water Flow (m^3)	29.26	29.37	29.47	29.59	29.69	29.79	29.90	30.01	30.11	30.20	30.32	30.43
Temperature Difference	2.2	2.3	2.4	2.3	2.3	2.3	2.3	2.4	2.3	2.3	2.3	2.3
Accumulated MWh Reading	0.080	0.081	0.081	0.081	0.082	0.082	0.082	0.082	0.083	0.083	0.083	0.084
Accumulated kWh Reading	1.03	1.25	1.40	1.60	1.75	1.93	2.12	2.30	2.49	2.70	2.89	3.10

Table F.1.... Continued from previous page

Time of Day Hours	0100	0200	0300	0400	0500	0600	0700	0800	0900	1000	1100	1200	1300
Node 1	25.4	25.1	24.5	24.2	23.6	23.3	22.8	22.7	22.5	22.8	23.5	24.5	25.8
Node 2	26.8	26.3	25.7	25.2	24.7	24.3	23.6	23.4	23.2	23.7	24.3	25.7	27.5
Node 3	27.8	27.2	26.5	26.0	25.4	24.9	24.2	24.0	23.8	24.5	25.2	26.9	29.0
Node 4	28.4	27.6	27.0	26.3	25.7	25.2	24.4	24.2	24.1	24.7	25.6	27.6	29.8
Node 5	28.7	28.0	27.2	26.6	25.9	25.4	24.6	24.4	24.4	24.9	25.7	27.5	29.8
Node 6	29.0	28.2	27.4	26.7	26.0	25.5	24.6	24.5	24.5	24.8	25.5	27.2	29.3
Node 7	28.8	28.0	27.3	26.6	26.0	25.4	24.6	24.6	24.6	24.8	25.6	27.1	29.2
Cond. N-Hexane (Top Panel)	29.6	28.9	28.2	27.5	27.0	26.5	25.7	25.4	25.9	26.8	28.2	31.2	33.9
Cond. Pegasol 1516 (Top Panel)	30.2	29.6	29.0	28.4	27.8	27.3	26.4	26.2	25.9	26.6	26.6	30.5	33.1
Evap.N-Hex (Middle) Node 8	15.8	14.5	13.6	14.7	14.1	12.3	19.0	25.1	27.0	28.7	31.8	37.1	39.5
Evap.Pegasol 1516(Middle) Node 8	16.0	14.8	13.9	14.9	14.3	12.6	19.4	25.3	29.9	29.8	33.7	35.1	37.6
Cond. N-Hexane (Middle Panel)	28.0	27.4	26.7	26.1	25.5	25.0	24.3	24.0	24.9	25.9	27.6	30.7	33.4
Cond. Pegasol 1516 (Middle Panel)	28.7	28.0	27.4	26.7	26.1	25.6	25.0	24.5	24.7	25.3	27.9	30.5	33.2
Top Plate Temperature	14.3	13.0	12.5	13.6	12.7	11.2	20.0	25.6	34.3	37.4	48.0	67.3	68.4
Glass Temperature -Node 9	13.4	11.7	11.2	13.0	11.3	9.2	12.5	15.8	19.4	21.8	24.3	29.9	31.3
Air Temperature Behind Glass	15.4	13.9	13.2	14.5	13.6	11.6	17.0	21.7	26.8	31.2	35.4	42.8	45.7
Ambient Temperature	11.7	10.8	10.7	11.5	10.3	8.3	9.5	11.3	14.0	15.2	16.1	18.7	17.8
Calorimeter Box Temperature	20.1	20.0	20.0	19.9	20.0	19.9	19.9	19.8	20.0	19.9	19.9	20.0	20.1
Chilled Water Temperature	10.2	10.1	10.2	10.1	10.0	10.1	10.1	10.1	10.3	10.1	10.2	10.1	10.3
Room Temperature	20.8	20.9	21.0	21.0	20.9	20.7	20.6	20.8	21.4	20.9	20.6	21.3	20.1
Accumulated Water Flow (m^3)	30.53	30.64	30.75	30.86	30.96	31.07	31.20	31.28	31.38	31.50	31.60	31.71	31.80
Temperature Difference	2.3	2.3	2.3	2.3	2.3	2.3	2.3	2.3	2.3	2.3	2.4	2.3	2.3
Accumulated MWh Reading	0.084	0.084	0.085	0.085	0.085	0.085	0.086	0.086	0.086	0.087	0.087	0.087	0.087
Accumulated kWh Reading	3.30	3.51	3.74	3.98	4.20	4.42	4.66	4.92	5.18	5.42	5.66	5.90	6.10

Table F.2 The experimental data from long period test (Continuing in next page)

Calender day and time	1-2-95 0900	2-2-95 0900	3-2-95 0900	4-2-95 0900	5-2-95 0900	6-2-95 0900	7-2-95 0900	8-2-95 0900	9-2-95 0900	10-2-95 0900
Node 1	24.2	21.3	23.4	20.7	20.5	20.3	21.9	22.6	23.7	21.8
Node 2	25.4	21.8	24.4	21.1	20.9	20.6	22.5	23.4	24.7	22.3
Node 3	26.2	22.2	25.1	21.6	21.2	20.9	22.9	23.9	25.3	22.7
Node 4	26.7	22.4	25.5	21.8	21.3	21.0	23.1	24.1	25.7	23.0
Node 5	27.0	22.5	25.8	21.8	21.3	21.1	23.3	24.3	26.0	23.1
Node 6	27.3	22.6	25.9	21.8	21.4	21.1	23.5	24.4	26.2	23.2
Node 7	27.3	22.6	25.9	21.8	21.3	21.2	23.4	24.5	26.3	23.3
Cond. N-Hexane (Top Panel)	27.9	23.5	26.5	23.1	22.5	22.3	24.2	25.6	27.0	24.1
Cond. Pegasol 1516 (Top Panel)	29.2	23.7	27.7	22.6	22.9	22.3	24.8	26.0	28.2	24.7
Evap.N-Hex (Middle) Node 8	28.4	24.0	19.3	24.0	19.8	22.7	25.1	26.3	28.5	22.4
Evap.Pegasol 1516(Middle) Node 8	29.5	25.6	19.6	27.1	19.8	23.9	25.4	28.1	29.2	22.3
Cond. N-Hexane (Middle Panel)	26.7	22.8	25.1	22.5	21.3	21.5	23.4	24.6	25.9	23.0
Cond. Pegasol 1516 (Middle Panel)	27.2	22.6	26.0	22.8	21.5	21.2	23.5	24.7	26.2	23.3
Top Plate Temperature	26.6	24.8	17.7	26.2	18.4	22.0	23.6	26.6	26.2	20.4
Glass Temperature -Node 9	23.3	20.7	17.0	20.1	16.6	17.8	19.1	20.5	20.4	18.7
Air Temperature Behind Glass	27.5	24.3	19.0	25.2	18.8	22.2	23.0	25.9	26.2	21.2
Ambient Temperature	19.4	18.5	15.3	16.2	14.2	13.8	15.7	18.2	16.6	16.3
Calorimeter Box Temperature	20.0	19.9	20.0	19.8	19.8	20.0	19.8	19.9	20.0	20.0
Chilled Water Temperature	10.2	10.1	10.0	10.0	10.1	10.2	10.0	10.2	10.1	10.2
Room Temperature	20.4	20.7	21.1	21.1	20.1	21.5	20.8	19.7	21.5	20.7
Accumulated Water Flow (m^3)	59.99	62.46	64.86	67.27	69.66	72.06	74.40	76.79	79.14	81.44
Temperature Difference	1.6	2.4	2.4	2.5	2.5	2.5	2.4	2.4	2.5	2.5
Accumulated MWh Reading	0.167	0.174	0.181	0.188	0.195	0.201	0.208	0.215	0.222	0.229
Accumulated kWh Reading	363.5	369.0	373.7	379.5	385.3	391.4	396.8	402.0	406.5	411.8

Table F2.... Continued from previous page

Calender day and time	11-2-95 0900	12-2-95 0900	13-2-95 0900	14-2-95 0900	15-2-95 0900	16-2-95 0900	17-2-95 0900	18-2-95 0900	19-2-95 0900	20-2-95 0900
Node 1	22.8	22.7	22.9	23.6	24.0	24.3	23.5	24.0	23.8	22.0
Node 2	23.7	23.5	23.8	24.7	25.0	25.7	24.5	25.0	24.9	22.5
Node 3	24.3	24.1	24.4	25.5	25.8	26.4	25.3	25.8	25.6	23.0
Node 4	24.6	24.3	24.6	25.8	26.2	26.9	25.6	26.3	26.0	23.2
Node 5	24.8	24.6	24.9	26.1	26.5	27.1	26.0	26.6	26.2	23.4
Node 6	24.9	24.9	25.0	26.4	26.7	27.4	26.1	26.8	26.4	23.5
Node 7	25.0	24.8	25.1	26.4	26.8	27.5	26.1	26.9	26.5	23.8
Cond. N-Hexane (Top Panel)	26.4	25.5	26.0	27.4	27.5	28.6	27.0	28.3	27.6	24.3
Cond. Pegasol 1516 (Top Panel)	26.2	26.5	26.8	28.3	28.9	29.6	27.9	28.8	28.3	25.0
Evap.N-Hex (Middle) Node 8	27.8	23.4	27.0	28.5	28.7	29.6	28.1	29.7	28.4	24.5
Evap.Pegasol 1516(Middle) Node 8	31.3	23.6	28.5	30.3	29.5	31.7	29.8	31.6	30.6	24.6
Cond. N-Hexane (Middle Panel)	25.5	24.2	25.0	26.4	26.3	27.4	25.8	27.2	26.6	23.2
Cond. Pegasol 1516 (Middle Panel)	25.0	24.8	25.1	26.5	26.8	27.6	26.1	27.3	26.5	23.6
Top Plate Temperature	30.4	21.9	25.7	28.2	26.6	30.0	26.7	31.5	29.7	22.7
Glass Temperature -Node 9	23.7	19.6	20.0	21.9	20.6	23.4	21.8	25.0	23.9	20.2
Air Temperature Behind Glass	29.0	22.2	25.3	28.0	26.3	29.7	26.9	30.1	29.3	23.0
Ambient Temperature	18.1	16.6	17.8	19.5	18.2	17.3	17.1	25.6	21.0	17.7
Calorimeter Box Temperature	19.9	20.0	19.9	20.1	20.2	20.2	20.1	20.2	20.1	20.0
Chilled Water Temperature	10.1	10.1	10.0	10.1	10.2	10.1	10.0	20.2	10.0	10.1
Room Temperature	20.6	21.3	20.1	21.4	21.3	21.2	21.2	21.3	21.1	19.9
Accumulated Water Flow (m^3)	83.78	86.05	88.33	90.63	92.87	95.12	97.54	99.97	102.34	104.76
Temperature Difference	2.5	2.5	2.6	2.5	2.6	2.6	2.5	2.4	2.4	2.4
Accumulated MWh Reading	0.236	0.243	0.250	0.257	0.264	0.271	0.278	0.285	0.292	298
Accumulated kWh Reading	417.0	422.0	427.0	431.5	435.75	440.0	444.7	449.0	453.5	458.7

Table F2.... Continued from previous page

Calender day and time	21-2-95 0900	22-2-95 0900	23-2-95 0900	24-2-95 0900	25-2-95 0900	26-2-95 0900	27-2-95 0900	28-2-95 0900	1-3-95 0900
Node 1	19.8	22.5	21.3	20.4	22.3	24.2	25.3	22.1	20.0
Node 2	20.0	23.4	21.9	20.7	23.0	25.3	26.6	22.7	20.3
Node 3	20.2	23.8	22.3	21.1	23.4	26.3	27.5	23.2	20.6
Node 4	20.3	24.0	22.4	21.2	23.7	26.7	28.0	23.4	20.7
Node 5	20.3	24.3	22.6	21.4	23.8	27.0	28.4	23.6	20.7
Node 6	20.3	24.5	22.7	21.5	24.1	27.2	28.7	23.8	20.7
Node 7	20.3	24.6	22.7	21.4	24.0	27.3	29.0	23.7	20.8
Cond. N-Hexane (Top Panel)	22.0	25.5	23.5	22.5	24.8	28.5	30.0	24.7	22.3
Cond. Pegasol 1516 (Top Panel)	21.4	26.1	24.2	22.7	25.7	29.6	31.2	25.6	22.1
Evap.N-Hex (Middle) Node 8	24.7	26.3	18.8	17.0	25.2	29.4	31.0	24.8	23.0
Evap.Pegasol 1516(Middle) Node 8	24.6	27.9	18.9	17.0	26.0	32.0	33.6	24.9	24.5
Cond. N-Hexane (Middle Panel)	21.6	24.5	22.4	21.3	23.7	27.3	28.5	23.3	21.5
Cond. Pegasol 1516 (Middle Panel)	20.9	24.5	22.8	21.6	24.1	27.4	28.8	23.7	21.1
Top Plate Temperature	26.7	25.5	17.3	15.3	22.5	28.8	29.5	21.2	22.7
Glass Temperature -Node 9	19.2	21.0	15.9	14.6	17.7	23.4	23.9	17.3	17.6
Air Temperature Behind Glass	24.3	25.7	18.1	16.4	22.6	28.4	29.9	22.1	22.0
Ambient Temperature	15.8	17.8	13.6	13.2	16.5	24.8	20.6	13.3	19.0
Calorimeter Box Temperature	20.0	19.9	19.9	20.1	19.8	20.1	20.3	20.1	20.0
Chilled Water Temperature	10.2	10.2	10.0	10.0	10.1	10.1	10.0	10.1	10.1
Room Temperature	21.3	19.4	21.1	21.5	20.7	22.1	21.7	21.3	21.2
Accumulated Water Flow (m^3)	107.24	109.68	112.14	114.57	116.98	119.41	121.81	124.19	126.58
Temperature Difference	2.4	2.4	2.4	2.4	2.4	2.4	2.4	2.5	2.4
Accumulated MWh Reading	0.305	0.312	0.319	0.326	0.333	0.340	0.347	0.354	0.361
Accumulated kWh Reading	465.0	470.2	475.7	481.6	486.9	491.2	494.8	499.0	505.8

APPENDIX G

G. COMPARISON OF SOLAR ENERGY MEASURED AND METEOROLOGICAL DATA

Table G.1 Comparison of measured and Meteorological solar energy data over the period of February 1995.

Date	Area (cm^2)	Energy available on a vertical surface measured value (MJ/m^2)	Energy available on a horizontal surface MET Data♦ (MJ/m^2)
1/02/95	33.3	5.3	11.3
2/02/95	92.6	14.8	24.0
3/02/95	25.0	4.0	9.0
4/02/95	40.2	6.4	16.4
5/02/95	30.1	4.8	11.4
6/02/95	61.8	9.8	25.0
7/02/95	68.1	10.8	24.0
8/02/95	104.6	16.7	27.8
9/02/95	54.3	8.6	9.4
10/02/95	75.0	11.9	17.4
11/02/95	75.4	12.0	22.8
12/02/95	79.0	12.6	19.9
13/02/95	102.3	16.3	28.4
14/02/95	102.3	16.3	28.3
15/02/95	106.5	17.0	27.2
16/02/95	94.0	15.0	24.3
17/02/95	101.9	16.2	26.1
18/02/95	90.0	14.3	22.8
19/02/95	54.2	8.6	11.3
20/02/95	18.0	2.9	5.1
21/02/95	84.5	13.5	22.6
22/02/95	41.7	6.6	15.0
23/02/95	23.7	3.8	10.0
24/02/95	74.2	11.8	14.9
25/02/95	106.6	17.0	24.7
26/02/95	113.0	18.0	25.5
27/02/95	55.6	8.9	10.4
28/02/95	29.9	4.8	10.0
1/03/95			

♦ The closest Meteorological department recording solar radiation on a horizontal surface is at Lincoln, about 15 km away from the experimental location.

During the experiment period the solar radiation available on a vertical plane was measured by solarimeter and recorded on a chart recorder. The area under the curve is measured by a Planimeter and presented in Column 2 of the Table 7.2. The area then converted into MJ/m^2 in the next column by using the following formula :

$$Energy\ in\ MJ\ /\ m^2 = \left(\frac{AREA \times 44.25 \times 3.6}{1000} \right)$$

As an approximate check on the integrated values of solar intensity on a vertical surface, the total daily solar radiation measured on a horizontal surface at Lincoln University* also included in Table G.1. It was hard to compare the measured vertical solar intensity with the horizontal solar intensity of Meteorological department records. Even though, these values were plotted against the calender day in Fig G.1. and the measured value was scattered against the Meteorological department values on Fig G.2. A comparison between these two sets of solar data would necessarily be approximate but may be potentially useful in predicting the likely solar wall performance at locations for which the standard meteorological solar data (i.e. total radiation on a horizontal surface) is available.

The comparison curves are not exact because of the different location of two points, but reasonably close patterns are noted in Fig 7.18(a). On partly cloudy days the difference was more obvious because of the experimental location was very closer to the coastal side and the coastal clouds had more influence on these values. The scattered pattern and the best fit line were plotted in Fig 7.18(b) could be useful to find the vertical energy available on a panel, with the information obtained from the MET department.

* Christchurch Meteorological office records hours of sunshine but not the solar radiation. The data from Lincoln represented the closest available to the experimental site. Lincoln is located approximately 15 km inland from University of Canterbury.

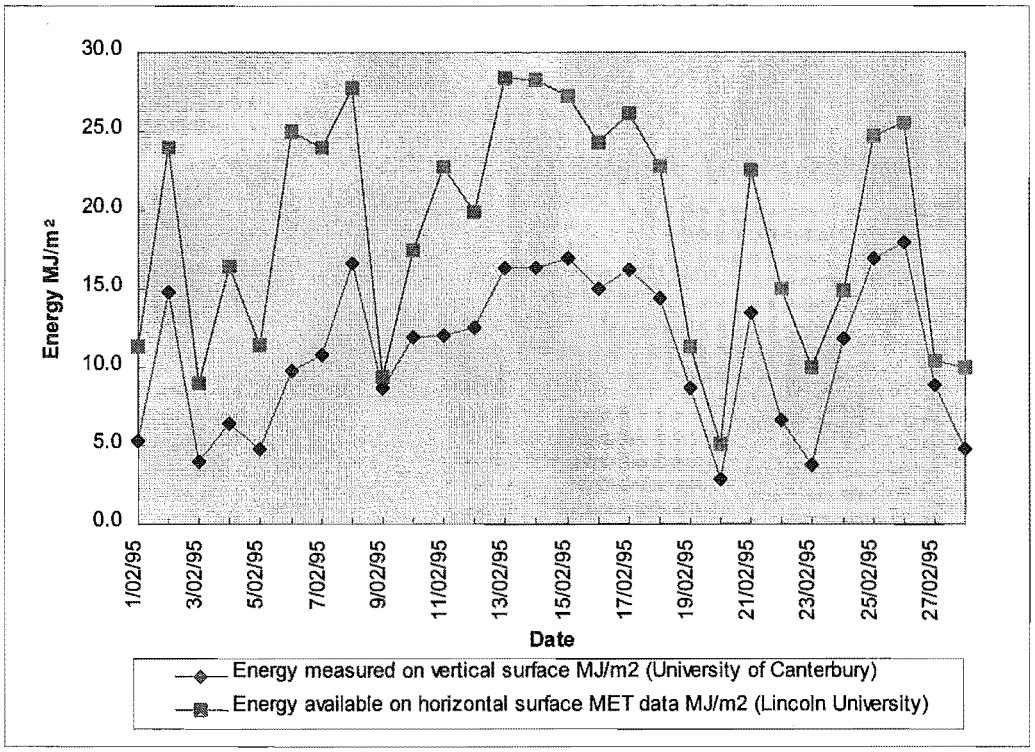

Figure G.1. Comparison of solar energy profiles during February 1995 on horizontal and vertical surfaces

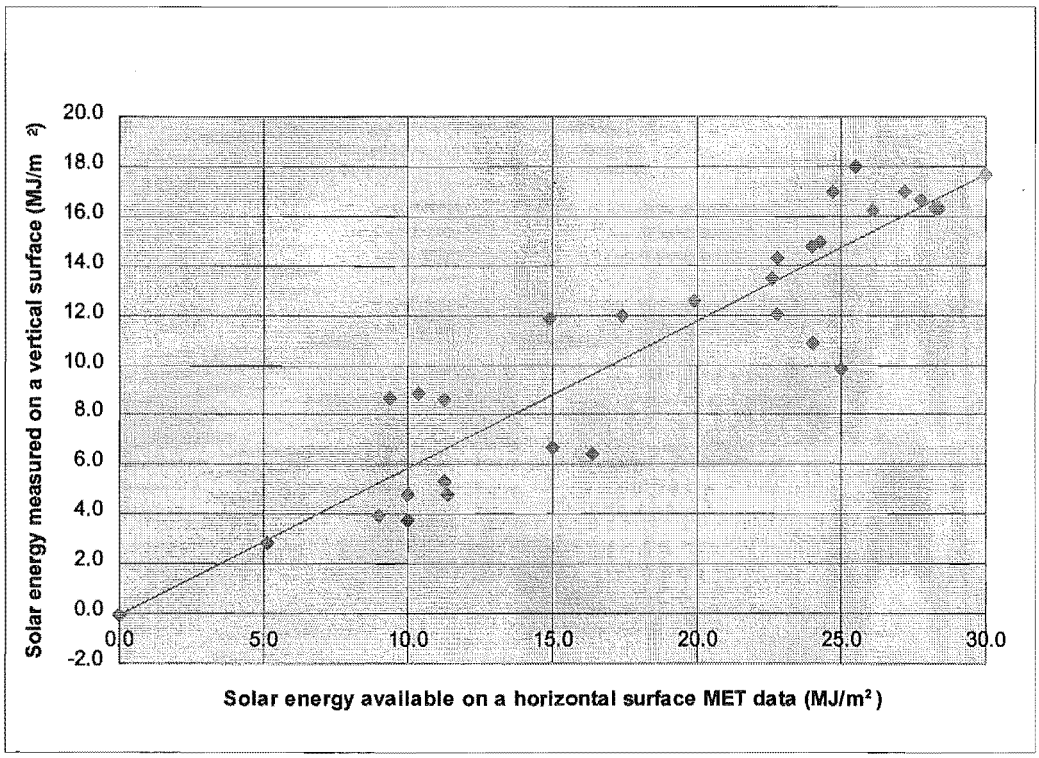

Figure G.2. Daily measured vertical solar energy plotted against the corresponding horizontal solar energy data. The best-fit line is also shown.

APPENDIX H

H.1 TEMPERATURE READINGS FOR MODEL SIMULATION AND 24-HOUR TEST.

Table H.1 Different nodal temperatures (°C) of the wall for model simulation for summer conditions

HR	t_1	t_2	t_3	t_4	t_5	t_6	t_7	t_8	t_9	t_{air}
0	22.9	23.4	23.7	24.0	24.1	24.1	23.9	17.8	15.0	14.0
100	22.6	23.0	23.4	23.6	23.7	23.7	23.5	17.3	14.5	13.5
200	22.4	22.8	23.1	23.2	23.3	23.3	23.1	16.9	14.1	13.1
300	22.1	22.5	22.7	22.9	23.0	22.9	22.7	16.6	13.9	13.0
400	21.9	22.2	22.5	22.6	22.6	22.6	22.4	16.5	14.0	13.1
500	21.7	22.0	22.2	22.3	22.3	22.3	22.1	17.3	14.4	13.5
600	21.5	21.8	22.0	22.1	22.1	22.1	22.0	20.2	15.5	14.0
700	21.4	21.6	21.8	21.9	22.0	22.0	22.0	21.9	16.6	14.8
800	21.3	21.5	21.7	21.9	21.9	21.9	21.9	21.9	17.3	15.6
900	21.3	21.6	21.9	22.4	22.1	22.0	22.0	22.4	18.3	16.5
1000	21.6	22.0	22.7	23.6	22.9	22.5	22.5	23.6	19.5	17.4
1100	22.3	22.9	23.9	25.2	24.2	23.6	23.4	25.2	20.7	18.3
1200	23.3	24.1	25.3	26.8	25.7	25.0	24.8	26.8	21.8	19.0
1300	24.3	25.2	26.5	28.0	27.1	26.4	26.3	28.0	22.5	19.5
1400	25.0	26.0	27.2	28.5	28.0	27.5	27.4	28.5	22.7	19.9
1500	25.3	26.3	27.4	28.3	28.2	28.1	28.1	28.3	22.6	20.0
1600	25.3	26.2	27.0	27.6	27.9	28.0	28.1	27.6	22.0	19.9
1700	25.0	25.8	26.6	27.1	27.5	27.7	27.7	27.1	21.6	19.5
1800	24.6	25.4	26.1	26.6	27.0	27.2	27.3	26.6	21.0	19.0
1900	24.3	25.0	25.7	26.1	26.5	26.7	26.7	23.5	19.8	18.3
2000	24.0	24.7	25.3	25.7	26.0	26.1	26.0	20.9	18.4	17.4
2100	23.7	24.4	24.9	25.2	25.5	25.5	25.4	20.0	17.5	16.5
2200	23.4	24.0	24.5	24.8	25.0	25.0	24.9	19.2	16.6	15.6
2300	23.1	23.7	24.1	24.4	24.5	24.5	24.4	18.5	15.8	14.8
2400	22.9	23.4	23.7	24.0	24.1	24.1	23.9	17.9	15.0	14.0

Table H.2 Different nodal temperatures (°C) of the wall for 24-hour test

HR	t_1	t_2	t_3	t_4	t_5	t_6	t_7	t_8	t_9	t_{air}
0	26.0	27.6	28.6	29.2	29.6	29.8	29.7	16.0	13.3	11.6
100	25.4	26.8	27.8	28.4	28.7	29.0	28.8	15.9	13.4	11.7
200	25.1	26.3	27.2	27.6	28.0	28.2	28.0	14.6	11.7	10.8
300	24.5	25.7	26.5	27.0	27.2	27.4	27.3	13.7	11.2	10.7
400	24.2	25.2	26.0	26.3	26.6	26.7	26.6	14.8	13.0	11.5
500	23.6	24.7	25.4	25.7	25.9	26.0	26.0	14.2	11.3	10.3
600	23.3	24.3	24.9	25.2	25.4	25.5	25.4	12.4	9.2	8.3
700	22.8	23.6	24.2	24.4	24.6	24.6	24.6	19.2	12.5	9.5
800	22.7	23.4	24.0	24.2	24.4	24.5	24.6	25.2	15.8	11.3
900	22.5	23.2	23.8	24.1	24.4	24.5	24.6	28.4	19.4	14.0
1000	22.8	23.7	24.5	24.7	24.9	24.8	24.8	29.2	21.8	15.2
1100	23.5	24.3	25.2	25.6	25.7	25.5	25.6	32.7	24.3	16.1
1200	24.5	25.7	26.9	27.6	27.5	27.2	27.1	36.1	29.9	18.7
1300	25.5	27.1	28.7	29.4	29.3	28.9	28.9	38.8	36.4	23.1
1400	28.6	30.5	31.7	32.5	32.4	31.9	32.0	42.0	37.1	19.5
1500	28.8	30.7	32.5	33.5	33.6	33.4	33.4	41.1	32.8	19.4
1600	29.9	32.3	34.1	34.9	35.2	35.1	35.1	40.2	29.6	17.3
1700	30.1	32.4	34.1	35.0	35.4	35.5	35.5	38.8	26.3	16.7
1800	29.5	31.7	33.6	34.4	34.9	35.3	35.3	36.8	23.7	15.3
1900	28.8	31.0	32.6	33.4	34.1	34.5	34.5	32.3	20.4	14.5
2000	28.3	30.2	31.7	32.5	33.1	33.6	33.5	26.0	17.2	13.0
2100	27.7	29.5	30.9	31.8	32.3	32.7	32.6	19.7	14.7	12.1
2200	27.0	28.8	30.0	30.6	31.0	31.4	31.4	16.7	13.4	11.7
2300	26.5	28.1	29.2	29.9	30.2	30.5	30.4	16.2	13.4	11.8
2400	26.0	27.6	28.6	29.2	29.6	29.8	29.7	16.0	13.3	11.6

* The mean value of n - hexane and Pegasol 1516 evaporator temperatures.

H.2 PROGRAM LISTING OF MODIFIED MODEL AND ITS SIMULATION RESULTS.

```
*   MODIFIED PROGRAM
*   ONLY FOR SUMMER MONTH OF DECEMBER
*   STEEL PIPE AS A CONDENSOR. (3 PIPES PER CAVITY)
*   CONDENSOR AT NODE 4
*   STEADY DAY PATTERN.
*   STEEL PIPE IS CONDUCTING HEAT BETWEEN 7 & 8.
*   SINGLE GLAZED GLASS

*   THIS PROGRAM CALCULATES THE INTERIOR AND EXTERIOR NODAL
*   TEMPERATURES OF A CONCRETE WALL FROM PREVIOUS TEMPERATURE
*   READINGS.

    REAL TNEW(1000),TOLD(1000),K,RHO,C,H,TR,THICK,RPC
    REAL TIME,X
    REAL RHOS,THICKS,CS,ALPHAS
    REAL LAT,WALL,LATR,TOWG1
    REAL TNEW2(1000),TNEW3(1000)
    REAL QSA,QSE,QLR,QLG,QSA1,QSE1,QLR1,QLG1,QLG2,KI,KS
    DOUBLE PRECISION CONS,CONS1,CONS2

    INTEGER  N,NPIPE,NHOURS,DAY


*   PROPERTIES OF CONCRETE
    DATA K/2.0/
    DATA RHO/2350/
    DATA C/950/

*   PROPERTIES OF INSULATION
    DATA KI/0.025/
    DATA RHOI/30/
    DATA CI/1000/
    DATA THICKI/0.05/

*   PROPERTIES OF EVAPORATOR/CONDESER MATERIAL
    DATA RHOS/7800/
    DATA THICKS/0.0006/
    DATA CS/460/
    DATA ALPHAS/0.9/
    DATA KS/45.0/
    DATA REVAP/0.18/

*   PROPERTIES OF GLASS
    DATA TOWG1/0.78/
    DATA RHOG/2800/
    DATA THICKG/0.004/
    DATA CG/840/
    DATA ALPHAG/0.05/
    DATA RGLASS/0.06/

*   OTHER CONSTANTS
    DATA H/10/
    DATA TR/20/
```

```
      DATA PI/3.1415927/
      DATA RROOM/0.075/

*     OUTER DIA OF THE PIPE
      DATA OD/0.019/
*     INNER DIA OF THE PIPE
      DATA OD1/0.017/
*     SQUEEZED PIPE SIZE FOR CONDENSOR
      DATA SQ/0.01/

5     PRINT*,'ENTER NUMBER OF NODES(10)'
      READ*, N
      PRINT*,'THICKNESS OF CONCRETE WALL(.2)'
      READ*,THICK

      DIFFUS=K/(RHO*C)
      DELX=THICK/(N-3)

      PRINT*,'NUMBER OF READINGS PER HOUR(20)'
      READ*, RPC

      DELT=1/RPC

*     CALCULATING THE STABILITY CONDITIONS

      FO=(DIFFUS*DELT*3600)/(DELX*DELX)
      PRINT*,'FO=',FO
      BI=(H*DELX)/K
      PRINT*,'BI=',BI
      COND=FO*(1+BI)

*     TESTING THE STABILITY CONDITIONS

      IF(FO.GT.0.5.OR.COND.GT.0.5) THEN
      PRINT*,'DELT AND DELX ARE NOT UNDER THE CONDITION'
      PRINT*,'PLEASE CHANGE THOSE VALUES AND TRY AGAIN'
      GOTO 5
      END IF

      CALL PIPE (THICKP,R,OD,OD1,PI,SQ,A)
      PRINT *,THICKP,R,A

      PRINT*,'CONDENSOR POSITION-NPIPE-(4)'
      READ*, NPIPE

      IF (DELX.GT.2*R) THEN
      CO=DELX/(DELX-R)
      ELSE
      PRINT *,'PLEASE CHANGE THE VALUES OF SQ & OD'
      END IF

      PO=(K*DELT*3600)/((2*THICKP*RHOS*CS+RHO*C*(DELX-2*R))*(DELX-R))

      PRINT*,'LATITUDE OF THE PLACE -LAT-(-43.5)'
      READ*,LAT
      PRINT*,'NUMBER OF DAYS SINCE JUNE 22nd.(183) -DAY-'
      READ*, DAY
      PRINT*,'POSITION OF THE WALL (DEGREES EAST OF NORTH)-WALL-(0)'
      READ*, WALL
      LATR=LAT*PI/180
```

```
      DECR=23.5*PI*COS(DAY*2*PI/365.25)/180
      WALLR=WALL*PI/180

76    TIME=0.0
      NHOURS=0
      IF (TIME.EQ.0.0) THEN
        DO 20 J=1,N
        TOLD(J)=20.0
        TNEW2(J)=10.0
        TNEW3(J)=20.0
20    CONTINUE
      ENDIF

       QSA=0
       QSE=0
       QLR=0
       QLG=0
       T2=20

85     DO 50 J=1,N

       IF (DAY.EQ.183) THEN
        IF (NHOURS.GE.0.AND.NHOURS.LT.1) THEN
        TAIR=11.6
        STOT=0
        ELSE IF (NHOURS.GE.1.AND.NHOURS.LT.2) THEN
        TAIR=11.7
        STOT=0
        ELSE IF (NHOURS.GE.2.AND.NHOURS.LT.3) THEN
        TAIR=10.8
        STOT=0
        ELSE IF (NHOURS.GE.3.AND.NHOURS.LT.4) THEN
        TAIR=10.7
        STOT=0
        ELSE IF (NHOURS.GE.4.AND.NHOURS.LT.5) THEN
        TAIR=11.5
        STOT=0
        ELSE IF (NHOURS.GE.5.AND.NHOURS.LT.6) THEN
        TAIR=10.3
        STOT=26.5
        ELSE IF (NHOURS.GE.6.AND.NHOURS.LT.7) THEN
        TAIR=8.3
        STOT=61.9
        ELSE IF (NHOURS.GE.7.AND.NHOURS.LT.8) THEN
        TAIR=9.5
        STOT=106.2
        ELSE IF (NHOURS.GE.8.AND.NHOURS.LT.9) THEN
        TAIR=11.3
        STOT=181.4
        ELSE IF (NHOURS.GE.9.AND.NHOURS.LT.10) THEN
        TAIR=14.0
        STOT=292
        ELSE IF (NHOURS.GE.10.AND.NHOURS.LT.11) THEN
        TAIR=15.2
        STOT=407
        ELSE IF (NHOURS.GE.11.AND.NHOURS.LT.12) THEN
        TAIR=16.1
        STOT=486.7
        ELSE IF (NHOURS.GE.12.AND.NHOURS.LT.13) THEN
        TAIR=18.7
```

```
      STOT=513.2
      ELSE IF (NHOURS.GE.13.AND.NHOURS.LT.14) THEN
      TAIR=23.1
      STOT=495.5
      ELSE IF (NHOURS.GE.14.AND.NHOURS.LT.15) THEN
      TAIR=19.5
      STOT=429.2
      ELSE IF (NHOURS.GE.15.AND.NHOURS.LT.16) THEN
      TAIR=19.4
      STOT=323
      ELSE IF (NHOURS.GE.16.AND.NHOURS.LT.17) THEN
      TAIR=17.3
      STOT=203.5
      ELSE IF (NHOURS.GE.17.AND.NHOURS.LT.18) THEN
      TAIR=16.7
      STOT=115
      ELSE IF (NHOURS.GE.18.AND.NHOURS.LT.19) THEN
      TAIR=15.3
      STOT=66.4
      ELSE IF (NHOURS.GE.19.AND.NHOURS.LT.20) THEN
      TAIR=14.5
      STOT=22.1
      ELSE IF (NHOURS.GE.20.AND.NHOURS.LT.21) THEN
      TAIR=13.0
      STOT=0
      ELSE IF (NHOURS.GE.21.AND.NHOURS.LT.22) THEN
      TAIR=12.1
      STOT=0
      ELSE IF (NHOURS.GE.22.AND.NHOURS.LT.23) THEN
      TAIR=11.7
      STOT=0
      ELSE IF (NHOURS.GE.23.AND.NHOURS.LT.24) THEN
      TAIR=11.8
      STOT=0
      ELSE
      TAIR=11.6
      STOT=0
      ENDIF
     ENDIF

*     ROOM SIDE WALL TEMPERATURE

      IF (J.EQ.1) THEN
      TNEW(J)=TOLD(J)+((2*DELT*3600)/(RHO*DELX*C))*(K*(TOLD(J+1)
     .      -TOLD(J))/DELX+(TR-TOLD(J))/RROOM)

*     INTERNAL NODE TEMPERATURE

      ELSE IF (J.GT.1.AND.J.LT.NPIPE-1) THEN
      TNEW(J)=FO*(TOLD(J-1)+TOLD(J+1))+(1-2*FO)*TOLD(J)

      ELSE IF (J.EQ.NPIPE-1) THEN
      TNEW(J)=FO*(TOLD(J-1)+CO*TOLD(J+1))+TOLD(J)*(1-FO-FO*CO)

*     CONDENSOR TEMPERATURE

      ELSE IF (J.EQ.NPIPE) THEN
      TNEW(J)=TOLD(J)+PO*(TOLD(J-1)+TOLD(J+1)-2*TOLD(J))

*     INTERNAL NODE TEMPERATURE
```

```
      ELSE IF (J.EQ.NPIPE+1) THEN
      TNEW(J)=FO*(TOLD(J+1)+CO*TOLD(J-1))+TOLD(J)*(1-FO-FO*CO)

      ELSE IF (J.GT.NPIPE+1.AND.J.LT.N-3) THEN
      TNEW(J)=FO*(TOLD(J-1)+TOLD(J+1))+(1-2*FO)*TOLD(J)

*     INSULATION SIDE WALL TEMPERARTURE

      ELSE IF (J.EQ.N-3) THEN
      CONS=(2*DELT*3600)/(RHO*DELX*C+RHOI*THICKI*CI)

      TNEW(J)=TOLD(J)+CONS*(K*(TOLD(J-1)-TOLD(J))/DELX
     .     +KI*(TOLD(J+1)-TOLD(J))/THICKI
     .     +KS*A*(TOLD(J+1)-TOLD(J))/THICKI)

*     EVAPORATOR TEMPERATURE

      ELSE IF (J.EQ.N-2) THEN
      QEVAP=(ALPHAS*TOWG1*STOT)/(1-(1-ALPHAS)*(1-TOWG1-ALPHAG))
      CONS1=2*DELT*3600/(RHOS*THICKS*CS*4+RHOI*THICKI*CI)

      TNEW(J)=TOLD(J)+CONS1*(QEVAP
     . +(TOLD(J+1)-TOLD(J))/REVAP
     . +(KI/THICKI)*(TOLD(J-1)-TOLD(J))
     . + (KS*A/THICKI)*(TOLD(J-1)-TOLD(J)))


       IF (TOLD(J).GT.TNEW(NPIPE)) THEN

       CONS2=(DELT*3600)/((RHOS*THICKS*CS*2)+(RHO*C*(DELX-2*R))+
     .   (RHOS*2*THICKP*CS)+(RHOI*THICKI*CI/2))


       TNEW(J)=TOLD(J)+CONS2*(QEVAP+
     .     (TOLD(J+1)-TOLD(J))/REVAP
     .     +(KI/THICKI)*(TOLD(J-1)-TOLD(J))
     .     +(KS*A/THICKI)*(TOLD(J-1)-TOLD(J))
     .     + (K/(DELX-R))*(TOLD(NPIPE+1)+TOLD(NPIPE-1)
     .     -2*TOLD(NPIPE)))
        IF (NHOURS.LE.13) THEN
        IF (TNEW(J).GE.27.AND.TNEW(J).LT.28) THEN
        T3=TNEW(J)-1.1
        ELSE IF (TNEW(J).GE.28.AND.TNEW(J).LT.30) THEN
        T3=TNEW(J)-2
        ELSE IF (TNEW(J).GE.30.AND.TNEW(J).LT.33) THEN
        T3=TNEW(J)-4
        ELSE IF (TNEW(J).GE.33.AND.NHOURS.LT.70) THEN
        T3=TNEW(J)-7.5
        ELSE
        T3=TNEW(J)-0.5
        END IF
       ELSE
        IF (TNEW(J).GE.35.AND.TNEW(J).LT.37) THEN
        T3=TNEW(J)-1
        ELSE IF (TNEW(J).GE.37.AND.TNEW(J).LT.40) THEN
        T3=TNEW(J)-2.5
        ELSE IF (TNEW(J).GE.40.AND.TNEW(J).LT.42) THEN
        T3=TNEW(J)-4.5
        ELSE IF (TNEW(J).GE.42.AND.TNEW(J).LT.70) THEN
```

```
          T3=TNEW(J)-5.5
          ELSE
          T3=TNEW(J)-0.5
          END IF
         END IF

          IF (T3.GT.TNEW(NPIPE)) THEN
          TNEW(NPIPE) = T3
          END IF
        END IF

*     AIR GAP TEMPERATURE

        ELSE IF(J.EQ.N-1)THEN

         IF (NHOURS.GE.6.AND.NHOURS.LE.14)THEN
         TNEW(J)=3.84*TIME-13.025
         ELSE IF (NHOURS.GT.14.AND.NHOURS.LE.18)THEN
         TNEW(J)=-3.625*TIME+91.45
         ELSE IF (NHOURS.GT.18.AND.NHOURS.LE.24)THEN
         TNEW(J)=-2.3*TIME+67.6
         ELSE IF (NHOURS.GT.0.AND.NHOURS.LT.6)THEN
         TNEW(J)=-0.4*TIME+12.4
         END IF
*     GLASS TEMPERATURE

        ELSE
        QGLAS=ALPHAG*STOT*(1+(TOWG1*(1-ALPHAS))/(1-(1-ALPHAS)
     .       *(1-TOWG1-ALPHAG)))

        TNEW(J)=TOLD(J)+(DELT*3600/(RHOG*THICKG*CG))*(
     . QGLAS+(TOLD(J-1)-TOLD(J))/REVAP
     . +(TAIR-TOLD(J))/RGLASS)

        END IF


50      CONTINUE

        IF (TNEW(1).GT.T2) THEN
        T2=TNEW(1)
        TIME1=TIME
        END IF

       P1=24.0-DELT

       IF (TIME.LE.P1) THEN
       QSA1=(STOT)*DELT*0.0036
       QSE1=(QEVAP)*DELT*0.0036
       QLR1=((TNEW(1)-TR)/RROOM)*DELT*0.0036
       QLG1=((TNEW(10)-TAIR)/RGLASS)*DELT*0.0036
       QLG2=((STOT-QEVAP-QGLAS))*DELT*0.0036

       QSA=QSA+QSA1
       QSE=QSE+QSE1
       QLR=QLR+QLR1
       QLG=QLG+QLG1+QLG2
       END IF

        IF (TIME.EQ.0.0) THEN
```

```
      DO 55 J=1,N
      TNEW(J)=TNEW3(J)
55     CONTINUE
      END IF

    X=ABS(TIME-FLOAT(IFIX(TIME)))

    IF (X.LE.0.0001.OR.X.EQ.0.0.OR.X.GE.0.9999) THEN
    NHOURS = IFIX(TIME+0.01)

     IF(NHOURS.EQ.0) THEN
     PRINT 70
     WRITE (50,70)
 70   FORMAT(1X,'HR',3X,'T1',4X,'T2',4X,'T3',4X,'T4',4X,'T5',5X,'T6'
    .      ,5X,'T7',5X,'T8',5X,'T9',5X,'T10')
     PRINT*
     WRITE (50,*)
     ENDIF

     PRINT 71,NHOURS,TNEW(1),TNEW(2),TNEW(3),TNEW(4),TNEW(5)
    .      ,TNEW(6),TNEW(7),TNEW(8),TNEW(9),TAIR
     WRITE(50,71)NHOURS,TNEW(1),TNEW(2),TNEW(3),TNEW(4),TNEW(5)
    .      ,TNEW(6),TNEW(7),TNEW(8),TNEW(9),TNEW(10)
 71   FORMAT (I2,2X,F5.2,1X,F5.2,1X,F5.2,1X,F5.2,1X,F6.2,1X,F6.2,
    .       1X,F6.2,1X,F6.2,1X,F6.2,1X,F6.2)

      DO 90 J=1,N
       IF(NHOURS.EQ.0) THEN
       TNEW2(J)=TNEW(J)
       END IF

       IF (NHOURS.EQ.24) THEN
       TNEW3(J)=TNEW(J)
       ENDIF
90     CONTINUE

    ENDIF

    DO 60 J=1,N
    TOLD(J)=TNEW(J)
 60  CONTINUE

    TIME=TIME+DELT

     IF(TIME.LE.24.0) THEN
     GOTO 85
     END IF


    WRITE (50,*)
    PRINT*
    WRITE(50,*)'QSOLAR AVAILABLE =    ',QSA
    PRINT *,'QSOLAR AVAILABLE=    ',QSA
    WRITE(50,*)
    PRINT*
    WRITE(50,*)'QSOLAR AT EVAPORAYOR = ',QSE
    PRINT *,'QSOLAR AT EVAPORATOR= ',QSE
    WRITE(50,*)
    PRINT*
    WRITE(50,*)'QLOSS TO ROOM=       ',QLR
```

```
      PRINT*,'QLOSS TO ROOM=        ',QLR
      WRITE(50,*)
      PRINT*
      WRITE(50,*)'QLOSS TO GLASS=       ',QLG
      PRINT *,'QLOSS TO GLASS=      ',QLG

      EFFI=QLR*100/QSA


      DO 230 J=1,N

       IF ((ABS(TNEW2(J)-TNEW3(J))).GT.0.01)THEN
       PRINT*,'NEXT DAY READING'
       TOLD(J)=TNEW3(J)
       QSA=0
       QSE=0
       QLR=0
       QLG=0
       TIME=0.0
       GOTO 85
       END IF

230   CONTINUE

       IF (NPIPE.EQ.4) THEN
       PRINT 240
       WRITE (60,240)
240     FORMAT(1X,'CONDENSOR POSITION',3X,'WALL TEMP(MAX)',3X,'TIME',3X,
     .      'QSA',3X,'QSE',9X,'QLR',7X,'QLG',3X,'EFFICIENCY')
       END IF

       PRINT *
       WRITE (60,*)
       PRINT 250,NPIPE,T2,TIME1,QSA,QSE,QLR,QLG,EFFI
       WRITE(60,250)NPIPE,T2,TIME1,QSA,QSE,QLR,QLG,EFFI
250     FORMAT(10X,I1,14X,F6.1,7X,F6.1,4X,F8.2,3X,F8.2,3X,F8.2,3X,F7.2
     .      ,3X,F6.1)

       NPIPE=NPIPE+1
       T2=0
       TIME1=0
        IF (NPIPE.LE.4) THEN
        GOTO 76
        END IF

300   END


      SUBROUTINE PIPE (THICKP,R,OD,OD1,PI,SQ,A)
      REAL OD,OD1,SQ

      A=PI*38*(OD**2-OD1**2)/4
      AR=PI*15*(OD**2-OD1**2)/4
      THICKP=AR/2

      B=(2*OD**2-SQ**2)
      B=B**0.5
      R=PI*B*SQ*15/8
      RETURN
      END
```

Table H.3 Different nodal temperatures (°C) of the of the modified model simulation for summer conditions

HR	t_1	t_2	t_3	t_4	t_5	t_6	t_7	t_8	t_9	t_{10}
0	25.7	26.7	27.5	28.1	28.4	28.4	28.2	17.6	12.4	12.0
100	25.1	26.0	26.6	27.1	27.4	27.4	27.2	17.0	12.4	11.8
200	24.5	25.2	25.8	26.2	26.4	26.4	26.2	16.2	11.6	11.7
300	23.9	24.6	25.1	25.4	25.6	25.6	25.3	15.6	11.2	10.9
400	23.4	24.0	24.5	24.7	24.9	24.8	24.6	15.1	10.8	10.7
500	23.0	23.5	23.9	24.1	24.2	24.1	23.9	14.6	10.4	11.2
600	22.6	23.0	23.3	23.5	23.6	23.6	23.4	16.5	10.0	10.3
700	22.2	22.6	22.9	23.1	23.2	23.2	23.2	21.8	13.9	9.7
800	22.1	22.5	22.9	23.4	23.3	23.3	23.3	23.9	17.7	11.7
900	22.5	23.0	23.7	24.5	24.1	23.8	23.8	25.0	21.5	14.2
1000	23.3	24.1	25.2	26.0	25.7	25.2	25.0	27.1	25.4	17.4
1100	24.3	25.3	26.6	28.4	27.3	26.8	26.7	32.4	29.2	19.6
1200	25.4	26.7	28.4	30.6	29.4	28.7	28.7	38.1	33.1	21.4
1300	27.1	28.7	30.8	33.3	32.0	31.3	31.3	40.8	36.9	24.4
1400	28.7	30.5	32.8	35.5	34.4	33.8	33.8	43.0	40.7	28.6
1500	30.4	32.5	34.8	37.3	36.6	36.2	36.2	42.8	44.6	26.7
1600	30.8	32.9	35.1	37.2	37.1	37.1	37.2	42.7	33.5	23.8
1700	30.8	32.8	34.7	36.3	36.7	37.0	37.2	40.8	29.8	21.0
1800	30.3	32.2	33.8	35.1	35.9	36.3	36.5	37.6	26.2	19.5
1900	29.6	31.4	32.9	34.0	34.7	35.2	35.3	34.3	22.6	17.4
2000	28.8	30.4	31.7	32.7	33.4	33.7	33.7	27.7	21.6	16.4
2100	28.0	29.4	30.6	31.4	32.0	32.2	32.1	23.6	19.3	14.6
2200	27.2	28.4	29.5	30.2	30.7	30.9	30.7	21.5	17.0	13.4
2300	26.4	27.6	28.5	29.1	29.5	29.6	29.4	19.5	14.7	12.5
2400	25.7	26.7	27.5	28.1	28.4	28.4	28.2	17.6	12.4	12.0

H.3 PROGRAM LISTING OF REFINED MODEL (FOR WINTER PREDICTIONS)

```
*   MODIFIED PROGRAM
*   FOR WINTER MONTHS OF JUNE-JULY IN CHRISTCHURCH
*   STEEL PIPE AS A CONDENSOR. (3 PIPES PER CAVITY)
*   CONDENSOR AT NODE 4
*   STEADY DAY PATTERN.
*   STEEL PIPE IS CONDUCTING HEAT BETWEEN 7 & 8.
*   SINGLE GLAZED GLASS

*   THIS PROGRAM CALCULATES THE INTERIOR AND EXTERIOR NODAL
*   TEMPERATURES OF A CONCRETE WALL FROM PREVIOUS TEMPERATURE
*   READINGS.

    REAL TNEW(1000),TOLD(1000),K,RHO,C,H,TR,THICK,RPC
    REAL TIME,X,IR
    REAL RHOS,THICKS,CS,ALPHAS
    REAL LAT,WALL,LATR,IVERT,IS,TOWG,TOWG1
    REAL TNEW2(1000),TNEW3(1000)
    REAL QSA,QSE,QLR,QLG,QSA1,QSE1,QLR1,QLG1,QLG2,KI,KS
    DOUBLE PRECISION CONS,CONS1,CONS2

    INTEGER  N,NPIPE,NHOURS,DAY



*   PROPERTIES OF CONCRETE
    DATA K/2.0/
    DATA RHO/2350/
    DATA C/950/

*   PROPERTIES OF INSULATION
    DATA KI/0.025/
    DATA RHOI/30/
    DATA CI/1000/
    DATA THICKI/0.05/

*   PROPERTIES OF EVAPORATOR/CONDESER MATERIAL
    DATA RHOS/7800/
    DATA THICKS/0.0006/
    DATA CS/460/
    DATA ALPHAS/0.9/
    DATA KS/45.0/
    DATA REVAP/0.18/

*   PROPERTIES OF GLASS
    DATA TOWG1/0.79/
    DATA RHOG/2800/
    DATA THICKG/0.004/
    DATA CG/840/
    DATA ALPHAG/0.05/
    DATA RGLASS/0.06/

*   OTHER CONSTANTS
    DATA H/10/
    DATA TR/20/
    DATA PI/3.1415927/
```

```
      DATA RROOM/0.075/

*     OUTER DIA OF THE PIPE
      DATA OD/0.019/
*     INNER DIA OF THE PIPE
      DATA OD1/0.017/
*     SQUEEZED PIPE SIZE FOR CONDENSOR
      DATA SQ/0.01/

5     PRINT*,'ENTER NUMBER OF NODES(9)'
      READ*, N
      PRINT*,'THICKNESS OF CONCRETE WALL(.2)'
      READ*, THICK

      DIFFUS=K/(RHO*C)
      DELX=THICK/(N-3)

      PRINT*,'NUMBER OF READINGS PER HOUR(20)'
      READ*,RPC

      DELT=1/RPC

*     CALCULATING THE STABILITY CONDITIONS

      FO=(DIFFUS*DELT*3600)/(DELX*DELX)
      PRINT*,'FO=',FO
      BI=(H*DELX)/K
      PRINT*,'BI=',BI
      COND=FO*(1+BI)

*     TESTING THE STABILITY CONDITIONS

       IF(FO.GT.0.5.OR.COND.GT.0.5) THEN
       PRINT*,'DELT AND DELX ARE NOT UNDER THE CONDITION'
       PRINT*,'PLEASE CHANGE THOSE VALUES AND TRY AGAIN'
       GOTO 5
       END IF

      CALL PIPE (THICKP,R,OD,OD1,PI,SQ,A)
      PRINT *,THICKP,R,A

      PRINT*,'CONDENSOR POSITION-NPIPE-(4)'
      READ*, NPIPE

       IF (DELX.GT.2*R) THEN
       CO=DELX/(DELX-R)
       ELSE
       PRINT *,'PLEASE CHANGE THE VALUES OF SQ & OD'
       END IF

      PO=(K*DELT*3600)/((2*THICKP*RHOS*CS+RHO*C*(DELX-2*R))*(DELX-R))

      PRINT*,'LATITUDE OF THE PLACE -LAT-(-43.5)'
      READ*, LAT
      PRINT*,'NUMBER OF DAYS SINCE JUNE 22nd.(0) -DAY-'
      READ*,DAY
      PRINT*,'POSITION OF THE WALL (DEGREES EAST OF NORTH)-WALL-(0)'
      READ*,WALL
      LATR=LAT*PI/180
      DECR=23.5*PI*COS(DAY*2*PI/365.25)/180
```

```
      WALLR=WALL*PI/180

76    TIME=0.0

      IF (TIME.EQ.0.0) THEN
       DO 20 J=1,N
       TOLD(J)=20.0
       TNEW2(J)=10.0
       TNEW3(J)=20.0
20     CONTINUE
       NHOURS=0
      ENDIF

      QSA=0
      QSE=0
      QLR=0
      QLG=0
      T2=20

85     DO 50 J=1,N

      IF (DAY.EQ.0) THEN
      CALL SOLAR2 (TAIR,TIME,DECR,WALLR,LATR,PI,ALT,WAZ,IVERT,IS,
     .          IR)
      END IF

      ALTR=ALT*PI/180
      WAZR=WAZ*PI/180
      AINCID=ACOS(COS(ALTR)*COS(WAZR))*180/PI

*     CALCULATING THE TRANSMISSIVITIES

      IF (AINCID.GE.0.AND.AINCID.LT.20) THEN
      AIM=0
      DELA=20
      TOWMAX=0.87
      TOWMIN=0.87

      ELSE IF (AINCID.GE.20.AND.AINCID.LT.40) THEN
      AIM=20
      DELA=20
      TOWMAX=0.87
      TOWMIN=0.86

      ELSE IF (AINCID.GE.40.AND.AINCID.LT.50) THEN
      AIM=40
      DELA=10
      TOWMAX=0.86
      TOWMIN=0.84

      ELSE IF (AINCID.GE.50.AND.AINCID.LT.60) THEN
      AIM=50
      DELA=10
      TOWMAX=0.84
      TOWMIN=0.79

      ELSE IF (AINCID.GE.60.AND.AINCID.LT.70) THEN
      AIM=60
      DELA=10
      TOWMAX=0.79
```

```
      TOWMIN=0.67

      ELSE IF (AINCID.GE.70.AND.AINCID.LT.80) THEN
      AIM=70
      DELA=10
      TOWMAX=0.67
      TOWMIN=0.42

      ELSE IF (AINCID.GE.80.AND.AINCID.LT.90) THEN
      AIM=80
      DELA=10
      TOWMAX=0.42
      TOWMIN=0.00

      ELSE
      TOWMAX=0.00
      TOWMIN=0.00

      END IF

      TOWG=TOWMAX-(AINCID-AIM)/DELA*(TOWMAX-TOWMIN)

*     ROOM SIDE WALL TEMPERATURE

      IF (J.EQ.1) THEN
      TNEW(J)=TOLD(J)+((2*DELT*3600)/(RHO*DELX*C))*(K*(TOLD(J+1)
     .      -TOLD(J))/DELX+(TR-TOLD(J))/RROOM)

*     INTERNAL NODE TEMPERATURE

      ELSE IF (J.GT.1.AND.J.LT.NPIPE-1) THEN
      TNEW(J)=FO*(TOLD(J-1)+TOLD(J+1))+(1-2*FO)*TOLD(J)

      ELSE IF (J.EQ.NPIPE-1) THEN
      TNEW(J)=FO*(TOLD(J-1)+CO*TOLD(J+1))+TOLD(J)*(1-FO-FO*CO)

*     CONDENSOR TEMPERATURE

      ELSE IF (J.EQ.NPIPE) THEN
      TNEW(J)=TOLD(J)+PO*(TOLD(J-1)+TOLD(J+1)-2*TOLD(J))

*     INTERNAL NODE TEMPERATURE

      ELSE IF (J.EQ.NPIPE+1) THEN
      TNEW(J)=FO*(TOLD(J+1)+CO*TOLD(J-1))+TOLD(J)*(1-FO-FO*CO)

      ELSE IF (J.GT.NPIPE+1.AND.J.LT.N-2) THEN
      TNEW(J)=FO*(TOLD(J-1)+TOLD(J+1))+(1-2*FO)*TOLD(J)

*     INSULATION SIDE WALL TEMPERARTURE

      ELSE IF (J.EQ.N-2) THEN
      CONS=(2*DELT*3600)/(RHO*DELX*C+RHOI*THICKI*CI)

      TNEW(J)=TOLD(J)+CONS*(K*(TOLD(J-1)-TOLD(J))/DELX
     .      +KI*(TOLD(J+1)-TOLD(J))/THICKI
     .      +KS*A*(TOLD(J+1)-TOLD(J))/THICKI)

*     EVAPORATOR TEMPERATURE
```

```
      ELSE IF (J.EQ.N-1) THEN
      QEVAP1=(ALPHAS*TOWG*IVERT)/(1-(1-ALPHAS)*(1-TOWG-ALPHAG))
      QEVAP2=(ALPHAS*TOWG1*IS)/(1-(1-ALPHAS)*(1-TOWG1-ALPHAG))
      QEVAP3=(ALPHAS*TOWG1*IR)/(1-(1-ALPHAS)*(1-TOWG1-ALPHAG))
      CONS1=2*DELT*3600/(RHOS*THICKS*CS*4+RHOI*THICKI*CI)

      TNEW(J)=TOLD(J)+CONS1*(QEVAP1+QEVAP2+QEVAP3
     . +(TOLD(J+1)-TOLD(J))/REVAP
     . +(KI/THICKI)*(TOLD(J-1)-TOLD(J))
     . + (KS*A/THICKI)*(TOLD(J-1)-TOLD(J)))


       IF (TOLD(J).GT.TNEW(NPIPE)) THEN

       CONS2=(DELT*3600)/((RHOS*THICKS*CS*2)+(RHO*C*(DELX-2*R))+
     .   (RHOS*2*THICKP*CS)+(RHOI*THICKI*CI/2))


       TNEW(J)=TOLD(J)+CONS2*(QEVAP1+QEVAP2+QEVAP3+
     .     (TOLD(J+1)-TOLD(J))/REVAP
     .     +(KI/THICKI)*(TOLD(J-1)-TOLD(J))
     .     +(KS*A/THICKI)*(TOLD(J-1)-TOLD(J))
     .     + (K/(DELX-R))*(TOLD(NPIPE+1)+TOLD(NPIPE-1)
     .     -2*TOLD(NPIPE)))

        IF (NHOURS.LE.13) THEN
        IF (TNEW(J).GE.27.AND.TNEW(J).LT.28) THEN
        T3=TNEW(J)-1.1
        ELSE IF (TNEW(J).GE.28.AND.TNEW(J).LT.30) THEN
        T3=TNEW(J)-2
        ELSE IF (TNEW(J).GE.30.AND.TNEW(J).LT.33) THEN
        T3=TNEW(J)-4
        ELSE IF (TNEW(J).GE.33.AND.NHOURS.LT.70) THEN
        T3=TNEW(J)-7.5
        ELSE
        T3=TNEW(J)-0.5
        END IF
       ELSE
        IF (TNEW(J).GE.35.AND.TNEW(J).LT.37) THEN
        T3=TNEW(J)-1
        ELSE IF (TNEW(J).GE.37.AND.TNEW(J).LT.40) THEN
        T3=TNEW(J)-2.5
        ELSE IF (TNEW(J).GE.40.AND.TNEW(J).LT.42) THEN
        T3=TNEW(J)-4.5
        ELSE IF (TNEW(J).GE.42.AND.TNEW(J).LT.70) THEN
        T3=TNEW(J)-5.5
        ELSE
        T3=TNEW(J)-0.5
        END IF
       END IF

        IF (T3.GT.TNEW(NPIPE)) THEN
        TNEW(NPIPE) = T3
        END IF
       END IF

*     GLASS TEMPERATURE

      ELSE
      QGLAS1=ALPHAG*IVERT*(1+(TOWG*(1-ALPHAS))/(1-(1-ALPHAS)
```

```
     .       *(1-TOWG-ALPHAG)))
            QGLAS2=ALPHAG*IS*(1+(TOWG1*(1-ALPHAS))/(1-(1-ALPHAS)
     .       *(1-TOWG1-ALPHAG)))
            QGLAS3=ALPHAG*IR*(1+(TOWG1*(1-ALPHAS))/(1-(1-ALPHAS)
     .       *(1-TOWG1-ALPHAG)))

            TNEW(J)=TOLD(J)+(DELT*3600/(RHOG*THICKG*CG))*(
     .      QGLAS1+QGLAS2+QGLAS3+(TOLD(J-1)-TOLD(J))/REVAP
     .      +(TAIR-TOLD(J))/RGLASS)

            END IF


   50       CONTINUE

            IF (TNEW(1).GT.T2) THEN
            T2=TNEW(1)
            TIME1=TIME
            END IF

           P1=24.0-DELT

           IF (TIME.LE.P1) THEN
           QSA1=(IVERT+IS+IR)*DELT*0.0036
           QSE1=(QEVAP1+QEVAP2+QEVAP3)*DELT*0.0036
           QLR1=((TNEW(1)-TR)/RROOM)*DELT*0.0036
           QLG1=((TNEW(9)-TAIR)/RGLASS)*DELT*0.0036
           QLG2=((IVERT-QEVAP1-QGLAS1)+(IS-QEVAP2-QGLAS2)+
     .       (IR-QEVAP3-QGLAS3))*DELT*0.0036

           QSA=QSA+QSA1
           QSE=QSE+QSE1
           QLR=QLR+QLR1
           QLG=QLG+QLG1+QLG2
           END IF
           STOT=IVERT+IS+IR
            IF (TIME.EQ.0.0) THEN
            DO 55 J=1,N
            TNEW(J)=TNEW3(J)
   55       CONTINUE
            END IF

          X=ABS(TIME-FLOAT(IFIX(TIME)))

          IF (X.LE.0.0001.OR.X.EQ.0.0.OR.X.GE.0.9999) THEN
          NHOURS = IFIX(TIME+0.01)

           IF(NHOURS.EQ.0) THEN
           PRINT 70
           WRITE (50,70)
    70     FORMAT(1X,'HR',3X,'T1',4X,'T2',4X,'T3',4X,'T4',4X,'T5',5X,'T6'
     .       ,5X,'T7',5X,'T8',5X,'T9',5X,'TAIR')
           PRINT*
           WRITE (50,*)
           ENDIF

           PRINT 71,NHOURS,TNEW(1),TNEW(2),TNEW(3),TNEW(4),TNEW(5)
     .       ,TNEW(6),TNEW(7),TNEW(8),TNEW(9),TAIR
           WRITE(50,71)NHOURS,TNEW(1),TNEW(2),TNEW(3),TNEW(4),TNEW(5)
     .       ,TNEW(6),TNEW(7),TNEW(8),TNEW(9),TAIR
```

```
 71   FORMAT (I2,2X,F5.2,1X,F5.2,1X,F5.2,1X,F5.2,1X,F6.2,1X,F6.2,
     .        1X,F6.2,1X,F6.2,1X,F6.2,1X,F6.2)

      DO 90 J=1,N
      IF(NHOURS.EQ.0) THEN
      TNEW2(J)=TNEW(J)
      END IF

      IF (NHOURS.EQ.24) THEN
      TNEW3(J)=TNEW(J)
      ENDIF
90    CONTINUE

   ENDIF

   DO 60 J=1,N
   TOLD(J)=TNEW(J)
60 CONTINUE

   TIME=TIME+DELT

   IF(TIME.LE.24.0) THEN
   GOTO 85
   END IF


   WRITE (50,*)
   PRINT*
   WRITE(50,*)'QSOLAR AVAILABLE =    ',QSA
   PRINT *,'QSOLAR AVAILABLE=    ',QSA
   WRITE(50,*)
   PRINT*
   WRITE(50,*)'QSOLAR AT EVAPORAYOR = ',QSE
   PRINT *,'QSOLAR AT EVAPORATOR= ',QSE
   WRITE(50,*)
   PRINT*
   WRITE(50,*)'QLOSS TO ROOM=       ',QLR
   PRINT*,'QLOSS TO ROOM=       ',QLR
   WRITE(50,*)
   PRINT*
   WRITE(50,*)'QLOSS TO GLASS=      ',QLG
   PRINT *,'QLOSS TO GLASS=      ',QLG

   EFFI=QLR*100/QSA


   DO 230 J=1,N

   IF ((ABS(TNEW2(J)-TNEW3(J))).GT.0.01)THEN
   PRINT*,'NEXT DAY READING'
   TOLD(J)=TNEW3(J)
   QSA=0
   QSE=0
   QLR=0
   QLG=0
   TIME=0.0
   GOTO 85
   END IF

230 CONTINUE
```

```
      IF (NPIPE.EQ.4) THEN
      PRINT 240
      WRITE (60,240)
240    FORMAT(1X,'CONDENSOR POSITION',3X,'WALL TEMP(MAX)',3X,'TIME',3X,
     .     'QSA',3X,'QSE',9X,'QLR',7X,'QLG',3X,'EFFICIENCY')
      END IF

      PRINT *
      WRITE (60,*)
      PRINT 250,NPIPE,T2,TIME1,QSA,QSE,QLR,QLG,EFFI
      WRITE(60,250)NPIPE,T2,TIME1,QSA,QSE,QLR,QLG,EFFI
250    FORMAT(10X,I1,14X,F6.1,7X,F6.1,4X,F8.2,3X,F8.2,3X,F8.2,3X,F7.2
     .     ,3X,F6.1)

      NPIPE=NPIPE+1
      T2=0
      TIME1=0
       IF (NPIPE.LE.4) THEN
       GOTO 76
       END IF

300   END

      SUBROUTINE PIPE (THICKP,R,OD,OD1,PI,SQ,A)
* THIS SUBROUTINE CALCULATES THE EQUIVALENT DIMENSIONS
* OF THE WALL WHERE EVER IT IS NON-HOMOGENEOUS.
      REAL OD,OD1,SQ

      A=PI*38*(OD**2-OD1**2)/4
      AR=PI*15*(OD**2-OD1**2)/4
      THICKP=AR/2

      B=(2*OD**2-SQ**2)
      B=B**0.5
      R=PI*B*SQ*15/8
      RETURN
      END


      SUBROUTINE SOLAR2 (TAIR,TIME,DECR,WALLR,LATR,PI,ALT,WAZ,IVERT,IS
     .              ,IR)

* THIS SUBROUTINE CALCULATES THE VERTICAL, SCATTERED AND REFLECTED
* COMPONENTS OF THE SOLAR RADIATION ON A VERTICAL WALL AND THE
* AMBIENT AIR TEMPERATURE FOR A CLEAR SKY WINTER DAY.

      REAL TIME,DECR,LATR,T,HR,ISMAX,WAZR,AZR,ALT,ALTR,WALLR
      REAL AMIN,DALT,IMIN,IMAX,IVERT,IDIR,PI,IS,ISMIN
      REAL IDH,IDHMIN,IDHMAX,IR


      T=TIME-12.5
      HR=T*PI/12
      ALTR=ASIN(SIN(DECR)*SIN(LATR)+COS(DECR)*COS(LATR)*COS(HR))
      AZR=ATAN(SIN(HR)/(SIN(LATR)*COS(HR)-COS(LATR)*TAN(DECR)))
      WAZR=AZR-WALLR
      WAZ=WAZR*180/PI
      ALT=ALTR*180/PI
```

```
IF (ALT.GE.0.AND.ALT.LT.5)THEN
AMIN = 0
DALT = 5
IMIN = 0
IMAX = 210
ISMIN = 0
ISMAX = 7
IDHMIN = 0
IDHMAX = 28

ELSEIF (ALT.GE.5.AND.ALT.LT.10)THEN
AMIN = 5
DALT = 5
IMIN = 210
IMAX = 388
ISMIN = 7
ISMAX = 16
IDHMIN = 28
IDHMAX = 50

ELSEIF (ALT.GE.10.AND.ALT.LT.15)THEN
AMIN = 10
DALT = 5
IMIN = 388
IMAX = 524
ISMIN = 16
ISMAX = 20
IDHMIN = 50
IDHMAX = 65

ELSEIF (ALT.GE.15.AND.ALT.LT.20)THEN
AMIN = 15
DALT = 5
IMIN = 524
IMAX = 620
ISMIN = 20
ISMAX = 23
IDHMIN = 65
IDHMAX = 77

ELSEIF (ALT.GE.20.AND.ALT.LT.25)THEN
AMIN = 20
DALT = 5
IMIN = 620
IMAX = 688
ISMIN = 23
ISMAX = 25
IDHMIN = 77
IDHMAX = 87

ELSEIF (ALT.GE.25.AND.ALT.LT.30)THEN
AMIN = 25
DALT = 5
IMIN = 688
IMAX = 740
ISMIN = 25
ISMAX = 26
IDHMIN = 87
IDHMAX = 95
```

```
ELSEIF (ALT.GE.30.AND.ALT.LT.35)THEN
AMIN = 30
DALT = 5
IMIN = 740
IMAX = 782
ISMIN = 26
ISMAX = 27
IDHMIN = 95
IDHMAX = 102

ELSEIF (ALT.GE.35.AND.ALT.LT.40)THEN
AMIN = 35
DALT = 5
IMIN = 782
IMAX = 814
ISMIN = 27
ISMAX = 28
IDHMIN = 102
IDHMAX = 108

ELSEIF (ALT.GE.40.AND.ALT.LT.50)THEN
AMIN = 40
DALT = 10
IMIN = 814
IMAX = 860
ISMIN = 28
ISMAX = 29
IDHMIN = 108
IDHMAX = 119

ELSEIF (ALT.GE.50.AND.ALT.LT.60)THEN
AMIN = 50
DALT = 10
IMIN = 860
IMAX = 893
ISMIN = 29
ISMAX = 30
IDHMIN = 119
IDHMAX = 126

ELSEIF (ALT.GE.60.AND.ALT.LT.70)THEN
AMIN = 60
DALT = 10
IMIN = 893
IMAX = 912
ISMIN = 30
ISMAX = 30
IDHMIN = 126
IDHMAX = 133

ELSEIF (ALT.GE.70.AND.ALT.LT.80)THEN
AMIN = 70
DALT = 10
IMIN = 912
IMAX = 920
ISMIN = 30
ISMAX = 30
IDHMIN = 133
IDHMAX = 135
```

```
ELSEIF (ALT.GE.80.AND.ALT.LT.90)THEN
AMIN = 80
DALT = 10
IMIN = 920
IMAX = 925
ISMIN = 30
ISMAX = 30
IDHMIN = 135
IDHMAX = 136

ELSE
AMIN = ALT
DALT = 1
IMIN = 0
IMAX = 0
ISMIN = 0
ISMAX = 0
IDHMIN = 0
IDHMAX = 0

ENDIF

IF (TIME.GE.12.0.AND.WAZR.GT.0.53)THEN
WAZR=WAZR-PI
ELSEIF(TIME.LT.12.0.AND.WAZR.LT.-0.5)THEN
WAZR=PI+WAZR
ENDIF
WAZ=WAZR*180/PI



IDIR = IMIN+(ALT-AMIN)/DALT*(IMAX-IMIN)

IF (WAZR.GT.-PI/2.AND.WAZR.LT.PI/2)THEN

IVERT = IDIR*COS(ALTR)*COS(WAZR)

ELSE


IVERT = 0

END IF

IS = ISMIN+(ALT-AMIN)/DALT*(ISMAX-ISMIN)

IDH = IDHMIN+(ALT-AMIN)/DALT*(IDHMAX-IDHMIN)
IR = 0.5*0.3*(IDIR*SIN(ALTR)+IDH)

TAIR = (6.45+3.15*COS(HR-PI/4))

RETURN

END
```